STRAIN RELEASE DRIVEN REACTIVITY OF BICYCLOBUTANES AND CYCLOPROPENYL KETONES AND STUDIES TOWARDS UNDERSTANDING THE ROLE OF HELICITY IN SALEN CATALYSIS

by

Natalee Jo-Ann Smith

A dissertation submitted to the Faculty of the University of Delaware in partial fulfillment of the requirements for the degree of Doctor of Philosophy in Chemistry and Biochemistry

Spring 2015

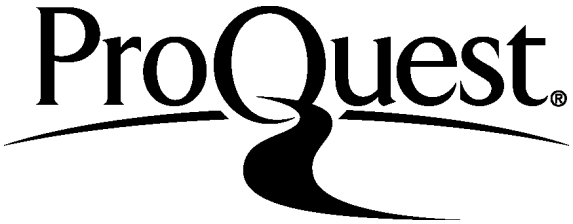

STRAIN RELEASE DRIVEN REACTIVITY OF BICYCLOBUTANES AND CYCLOPROPENYL KETONES AND STUDIES TOWARDS UNDERSTANDING THE ROLE OF HELICITY IN SALEN CATALYSIS

by

Natalee J. Smith

Approved: _____
Murray V. Johnston, Ph.D.
Chair of the Department of Chemistry and Biochemistry

Approved: _____
George H. Watson, Ph.D.
Dean of the College of Arts and Sciences

Approved: _____
James G. Richards, Ph.D.
Vice Provost for Graduate and Professional Education

I certify that I have read this dissertation and that in my opinion it meets the academic and professional standard required by the University as a dissertation for the degree of Doctor of Philosophy.

Signed: _____

Joseph Fox, Ph.D.
Professor in charge of dissertation

I certify that I have read this dissertation and that in my opinion it meets the academic and professional standard required by the University as a dissertation for the degree of Doctor of Philosophy.

Signed: _____

Klaus Theopold, Ph.D.
Member of dissertation committee

I certify that I have read this dissertation and that in my opinion it meets the academic and professional standard required by the University as a dissertation for the degree of Doctor of Philosophy.

Signed: _____

Mary Watson, Ph.D.
Member of dissertation committee

I certify that I have read this dissertation and that in my opinion it meets the academic and professional standard required by the University as a dissertation for the degree of Doctor of Philosophy.

Signed: _____

John Daub, Ph.D.
Member of dissertation committee

ACKNOWLEDGMENTS

There are several people to whom I owe immeasurable debts of gratitude for facilitating the successful completion of my doctoral degree.

To my adviser, Dr Joe Fox, thank you for allowing me to migrate to your research group. Not only have you taught me how to think about chemistry and science as a whole but also how to approach forming sustainable relationships with colleagues. You are an incredible mentor and human being and it has been a pleasure and honor to be a part of your group.

Thanks to the members of my dissertation committee for their advice over the course of my studies. Thank you also for thoroughly reading my thesis and providing detailed feedback.

To my colleagues in the Fox Lab, we've laughed together, sung together - well maybe I just sang all about lab and you tolerated it – we've recognized when we needed a word of encouragement or to be given a little space. I am a better person for having spent the last few years in your company and know that you will go on to do great things.

To the administrative, research and technical staff of the Department of Chemistry and Biochemistry, you are the glue that keeps the department together. Thank you for being patient, attentive and being stellar at your respective jobs.

To the friends I've made outside of the Department of Chemistry and Biochemistry while in Newark, Delaware: my Spokey Speaky and Honey Child loves, thank you for providing me with an outlet that kept me sane through graduate school.

Lastly, I cannot put into very many words how much I love and am grateful for the unwavering support of my family. It has taken a village to raise this young lady and so beginning to name each individual who has been vital to my achievements thus far is impossible. To my parents and siblings, nephews and nieces, your calls, emails, hugs and smiles have sustained me and given me purpose. I love you all and cannot thank you enough.

Finally, Uncle Travert E. A. Spence, this dissertation is dedicated to you. We love and miss you dearly.

TABLE OF CONTENTS

LIST OF TABLES

LIST OF FIGURES

LIST OF SCHEMES

ABSTRACT

My doctoral research in the laboratories of Joseph Fox at the University of Delaware has been multidisciplinary in nature. The results described in this dissertation span across streamlining multistep syntheses, synthetic methods development and exploring chemical biology.

Metal–salen catalysts have emerged as an important class of catalysts in enantioselective synthesis. An ongoing area of interest in the Fox Lab has been to study in detail the mode by which the catalysts, with their chiral, helical organic frameworks impart enantioselectivity to reactions. One of these catalysts was synthesized via a 15 step synthesis and has been used as a probe to understand the mechanistic origin of asymmetric induction in metal-salen catalyzed reactions. As the synthesis of this mechanistic probe was long, I developed a method to streamline the efficiency of the synthesis. These efforts will be discussed in the first chapter.

Chapter two focuses on the development of synthetic methods to allow for the enantioselective bicyclobutanation/homoconjugate addition of a range of heteroatomic nucleophiles as a method for rapidly accessing strereochemically defined cyclobutanes. Optimization of the addition of azides to bicyclobutanes led to the discovery of a new, highly soluble and nucleophilic azide source. Efforts to probe the mechanism of the azide addition reaction are discussed.

Cysteine alkylation represents one of the most broadly useful methods for protein modification, combining the merits of site selectivity with the ability to modify a native protein. Cysteine-modified proteins span a broad range of applications,

including protein-drug conjugation, nuclear medicine, and materials science. Chapter three details studies surrounding the development of a new class of cysteine alkylating agents based on cyclopropenyl ketones. Using strain as a design principle, it was hypothesized that the significant release of strain energy (~27 kcal/mol) upon thiol alkylation would result in an addition reaction that is both fast and irreversible. Results detailed demonstrate that cyclopropenyl ketones are viable alternatives to maleimide reagents, which though widely used are known to form unstable thiol conjugates.

.

Chapter 1

EXAMINING THE ROLE OF HELICITY ON SALEN CATALYSIS

1.1 Introduction

Metal-salen catalysts have proven to be invaluable players in the field of asymmetric catalysis. The term "salen" broadly refers to a family of bisimine compounds having their structure derived from *N*,*N'*-bis(salicylidine)ethylenediamine and are synthesized by the condensation of salicylaldehydes with a 1, 2-diamine (Scheme 1.1). Salen catalysts are obtained through the complexation of salen frameworks with a variety of metals and chirality can be attained through the use of chiral diamines and/or chiral organic frameworks.

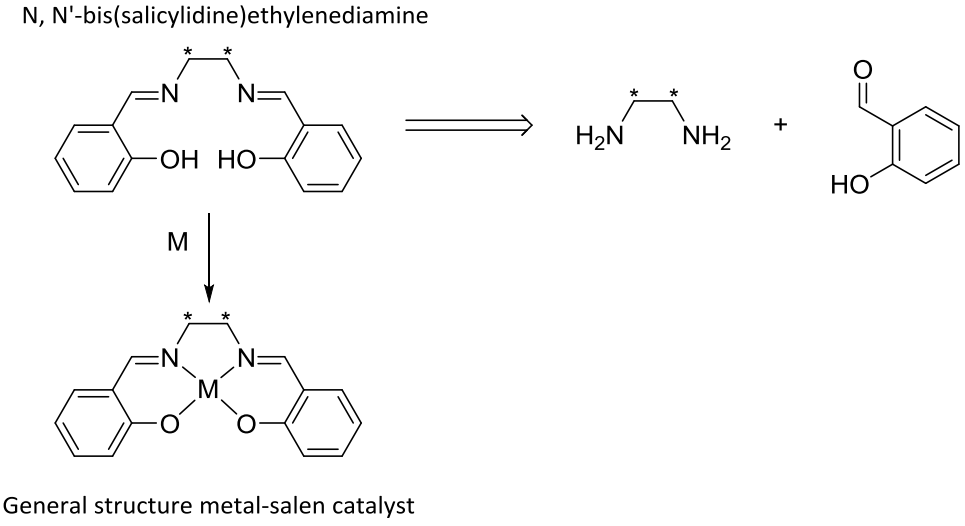

Scheme 1.1: General synthesis of salen ligand and metal-salen catalyst

Seminal work by Jacobsen[1] and Katsuki[2] in 1990, inspired by the preceding report by Kochi[3] in 1986, elegantly demonstrated that chiral manganese (V) salen catalysts (Figure 1.1) were competent in the asymmetric epoxidation of unfunctionalized alkenes.

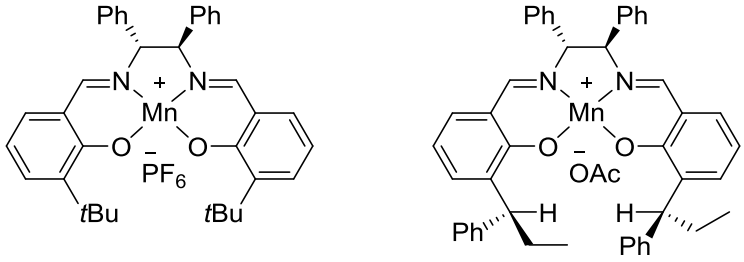

Jacobsen's first reported metal-salen catalyst

Katsuki's first reported metal-salen catalyst

Figure 1.1: First metal-salen catalysts reported to catalyze the asymmetric epoxidation of unfunctionalized alkenes

These communications presented the best solutions, to the date of their reports, to a problem the synthetic community had been grappling with for some time. Further studies on this catalyst framework ushered in an era of not only exciting asymmetric chemical transformations but also fierce debates on the mechanism by which asymmetry is induced by this class of catalysts. The broad reaching transformations achieved using salen catalysts are summarized in Table 1.1[4].

Table 1.1: Summary of metal-salen catalyzed asymmetric transformations. Table reprinted (adapted) with permission from (Carlos Baleizão and Hermenegildo Garcia, *Chemical Reviews* **2006** *106*(9), 3987- 4043 Copyright (2006) American Chemical Society

Entry	Metal	Reaction	ee %
1	Mn	*Alkene epoxidation* 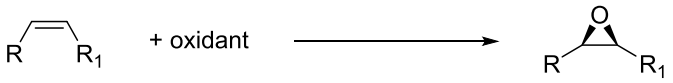	89-92[5]
2	Cu	*Alkene azidirination* 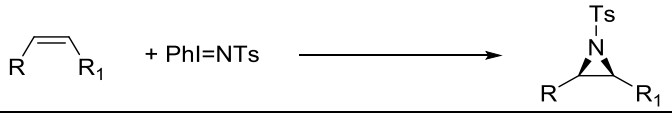	30-98[6]
3	Cr	*Epoxide ring opening* 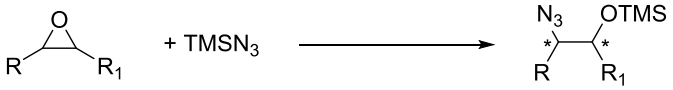	81-95[7]
4	Cr	*Hetero-Diels-Alder* 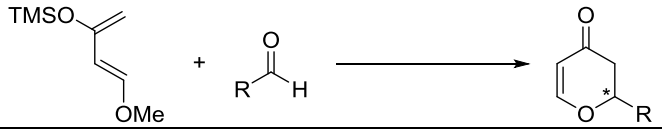	73-93[8]
5	Co	*Epoxide kinetic resolution* 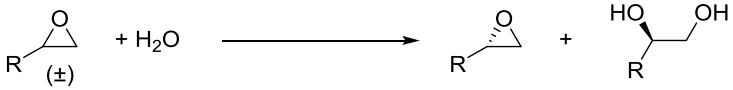	84-98[9]
6	Al	*Conjugate addition of cyanide to α,β-unsaturated amides* 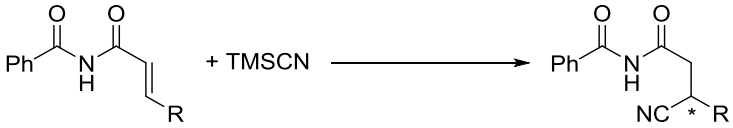	87-98[10]
7	Al	*Strecker reaction* 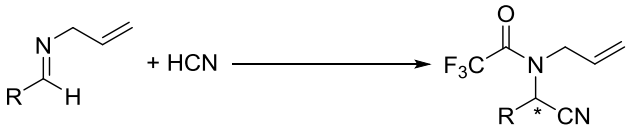	37-95[11]
8	Ru	*Sulfinimidation* 	8-99[12]
9	Ti	*Cyclopropanation* 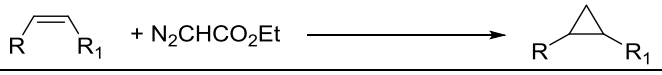	78-99[13]

10	Ti	*Sulfoxidation* 	92-96[14]
11	Zn	*Addition of diethylzinc to aldehydes* 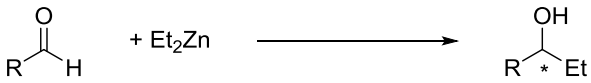	69-91[15]
12	Zn	*Alkyne addition to ketones* 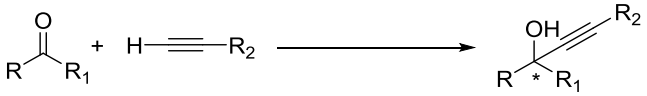	32-81[16]
13	V	*Cyanosilylation of aldehydes* 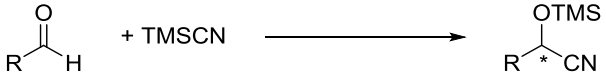	68-95[17]
14	Zr	*Baeyer-Villiger Oxidation* 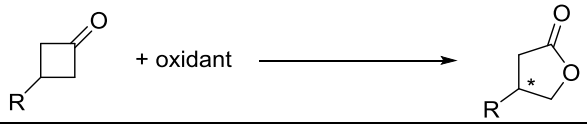	45-99[18]

Any model seeking to explain the induction of asymmetry by salen catalysts needs to bear in mind both the central chirality, that is, the chirality immediately surrounding the metal as provided by a chiral diamine moiety, and the ability of the metal-salen complex to adopt a helical secondary structure. It is postulated that helical chirality plays a key role in asymmetric induction[19] and for some time it was assumed

that the central chirality of the diamine induced a rigid, helical secondary structure. This assumption however, was not explicitly substantiated experimentally. Using nickel salen-based metallofoldamers as tools to probe the relationship between central chirality and secondary structure, the Fox group demonstrated that there is a more complex relationship between central chirality and chiral secondary structure.

Using the 'metallofoldamers' shown in Figure 1.2a, it was demonstrated that *trans*-cyclohexane-1,2-diamine is only a weak director of absolute helicity, as diastereomers of **1**[20] were found to interconvert on the millisecond timescale by variable temperature ^{1}H NMR. By contrast, chiral end groups can very effectively determine the absolute sense of helicity in metal salen-based foldamers (Figure 1.2b). In the case of **2**[21], where the end group directs for an *M*-helix and the diamine directs for a *P*-helix, it is the endgroup that determines the absolute helicity, and the diamine chirality is completely overridden. Similarly, in the smaller metallofoldamer **3**[22], chiral end groups can also override the ability of the central chiral diamine to direct helicity (Figure 1.2c). These findings illustrated that metal salen complexes cannot be viewed as static entities. While ligand helicity may be important in asymmetric catalysis, it is essential to consider the dynamic equilibrium between both helical diastereomers in any model for asymmetric induction involving chiral metal salen complexes.[23]

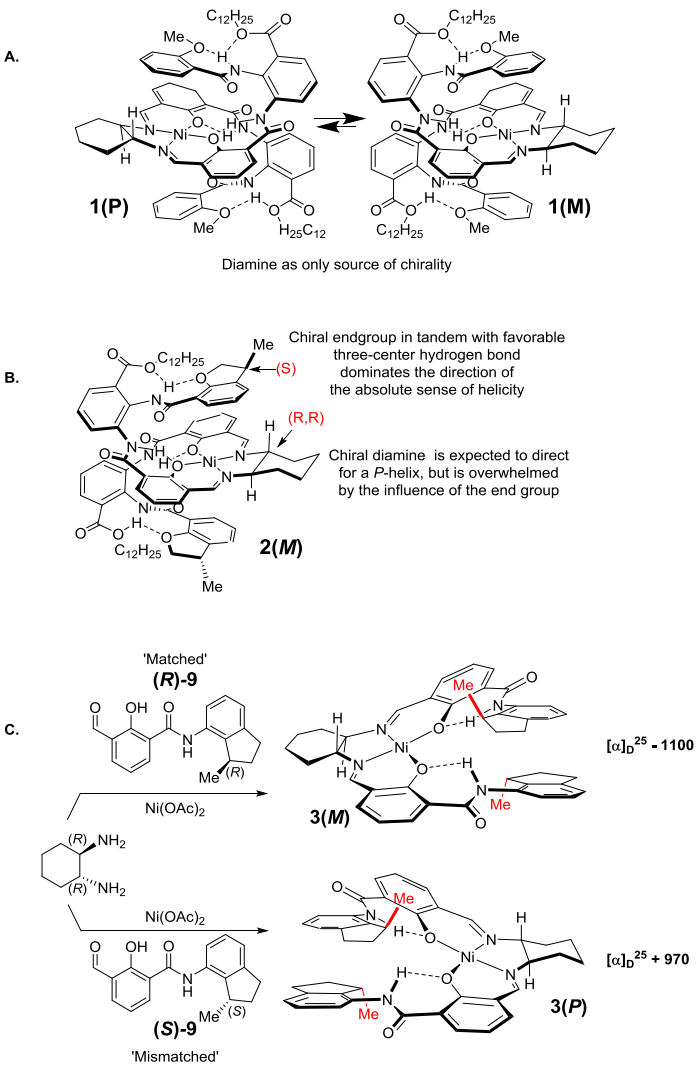

Figure 1.2: (a) For Ni-salen foldamers where *trans*-cyclohexanediamine is the only source for central chirality, both helical diastereomers are in dynamic equilibrium. (b) Chiral endgroups completely override the innate helical directing ability of *trans*-cyclohexanediamine. (c) Minimal endgroups control the sense of absolute helicity even when the helical bias of the endgroup is 'mismatched' relative to that of the central diamine. The term "matched" denotes a complex where both the endgroup and the diamine direct for the same absolute helicity. "Mismatched" refers to a complex where the endgroup and diamine direct for opposing helices

Furthering the interests of the Fox group in probing the mode by which salen catalysts impart asymmetry, James Plampin in his Ph.D studies sought to test the importance of helical chirality in catalytic studies on Rawal's Co-salen catalyzed Diels-Alder reaction[24]. In order to do this, it was necessary to synthesize metallohelicenes **4** and **5** (Scheme 1.2). The helical chirality of compounds **5A** and **5B** is controlled solely by virtue of their end groups irrespective of the stereochemistry of the diamine. Thus, both catalysts were constructed from (*S*, *S*)-cyclohexanediamine, but due to the end group chirality, catalyst **5A** is (*M*)-helical and **5B** is (*P*)-helical. My role in this project was to increase the efficiency of the synthesis of metallohelicenes **5A** and **5B**.

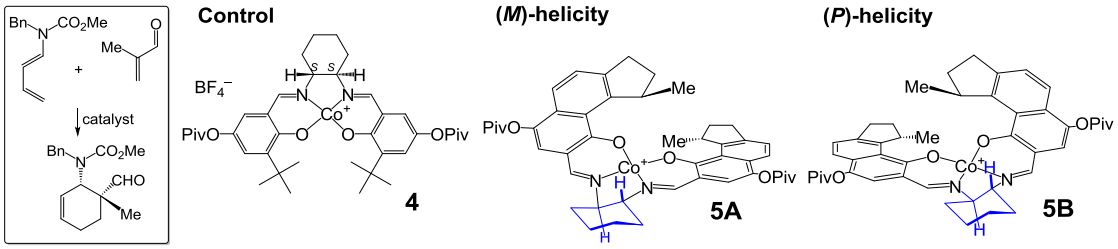

Scheme 1.2: Metallohelicenes used to probe the importance of helical chirality in Rawal's Co-salen catalyzed Diels-Alder reaction.

1.2 Results and Discussion

The synthesis for metallohelicenes **5A** and **5B** developed by Plampin is shown in Scheme 1.3.

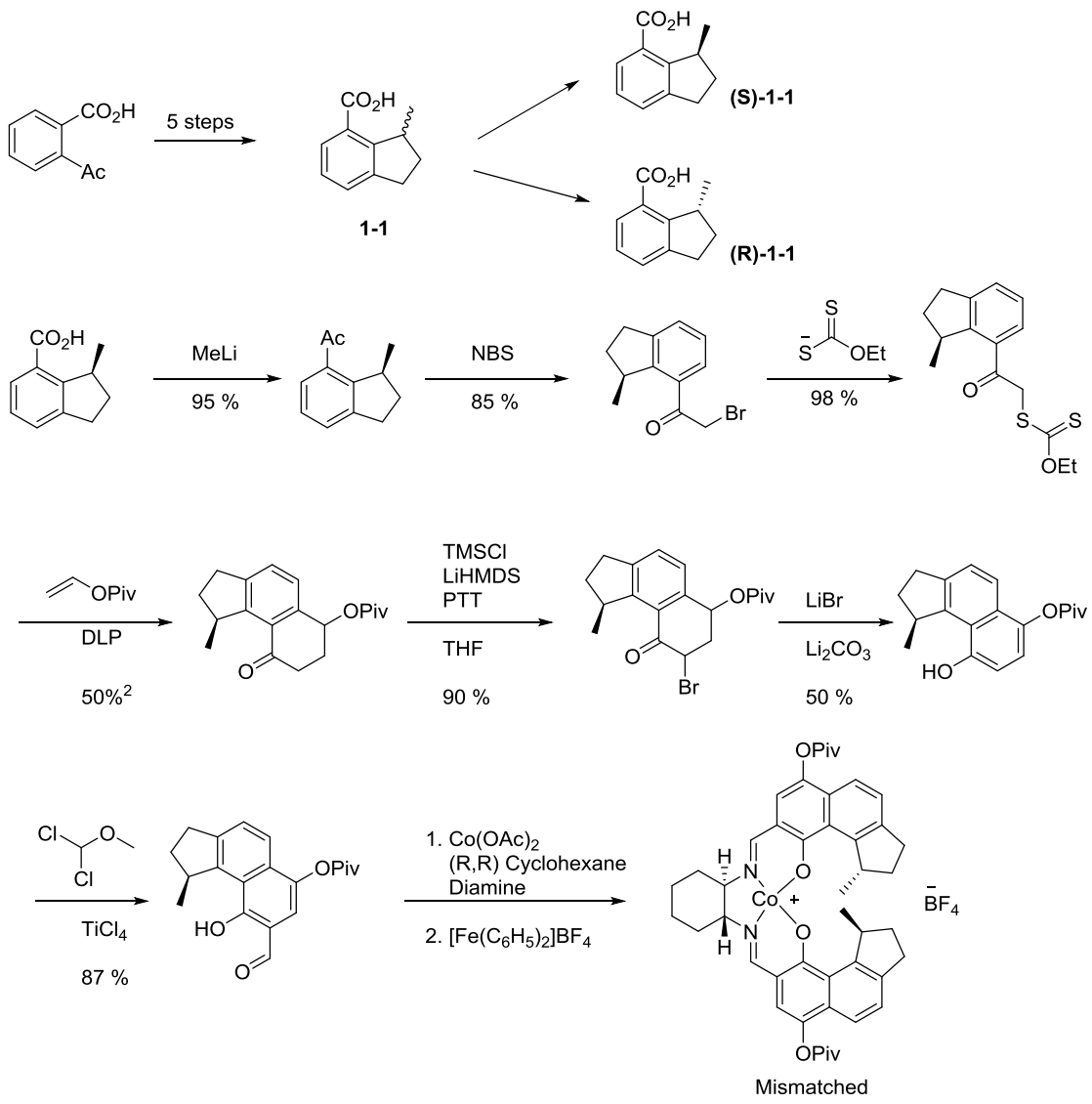

Scheme 1.3: Synthesis of Cobalt helicene **5**

The first generation synthetic route resolved enantiomers of carboxylic acid **1-1** via acid chloride formation and subsequent reaction with the chiral auxiliary (3a*R*-cis)-(+)-3, 3a, 8,81-tetrahydro-2H-indeno[1,2]oxazol-2-one. Diastereomers were separated by HPLC (Scheme 1.4).

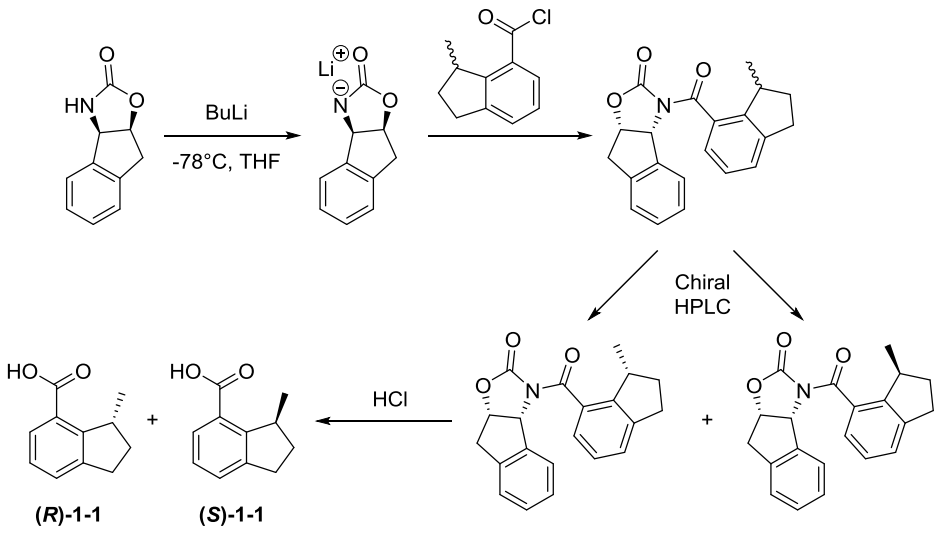

Scheme 1.4: Chiral HPLC resolution of carboxylic acid **1-1**

While this route resolved the carboxylic acid enantiomers, there were limitations including the addition of four steps to the already lengthy synthesis of the desired metallohelicene. The chiral auxiliary, although recoverable, costs $114/gram, and was prohibitively expensive considered in terms of its use this early in a 15 step synthesis and for effecting the chiral resolution of multi-gram quantities of **1-1**. Also explored by Plampin was enantiomer separation by semi-preparative HPLC using a chiral column. This process was a significant bottleneck in the synthesis. It therefore became necessary to identify an alternative option that would result in its enhanced efficiency. Classical resolution was therefore considered as a more scalable option.

Racemic acid **1-1** was synthesized in 5 steps from 2-acetyl benzoic acid using a published sequence[25], as shown in Scheme 1.5.

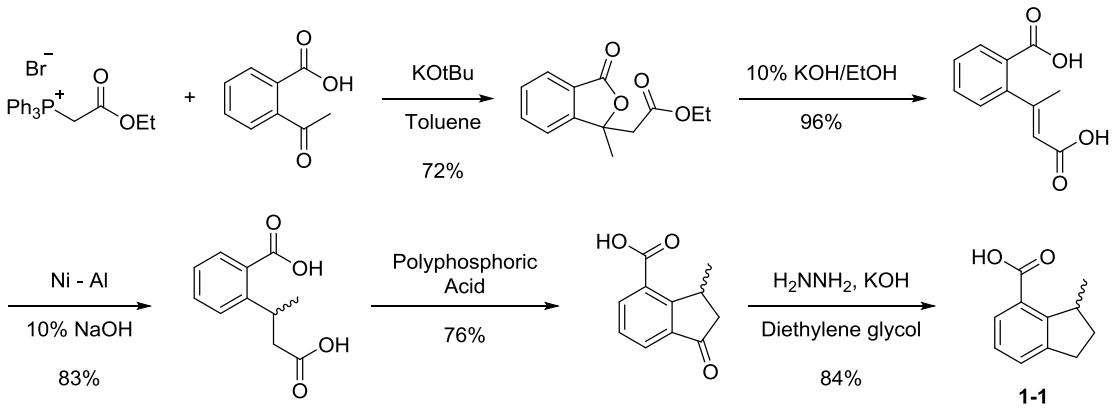

Scheme 1.5: Published[25] synthetic scheme used for the synthesis of carboxylic acid **1-1**

Using a range of chiral bases, I prepared a matrix of crystallization conditions using 7 different bases (Scheme 1.6) and 11 different solvent systems as summarized in Table 1.2. Thus, in 1 dram vials in a 7 x 11 array, the chiral bases were dissolved in the appropriate solvent system, and an equimolar amount of acid **1-1** (0.03 mmol) was added. The mixtures were warmed in an 80 °C water bath to allow for dissolution. The vials were subsequently cooled to room temperature then stored in a – 20 °C freezer for 16 hours to provide opportunity for crystallization. The observation of crystals was considered a "hit". Chiral HPLC analysis was used to assay the enantiomeric ratio of the liberated acid from each hit. Table 1.2 describes the results that were obtained from the screen.

Crystals of diastereomeric salts of **1-1** were observed in seven experiments involving the following bases: brucine, strychnine and (–)-cinchonidine. The most favorable enantiomeric ratios were obtained using brucine in 100% methanol and strychnine in 80% methanol in water. These conditions yielded (+) 72 and () 54 % ee respectively. Gratifyingly, brucine and strychnine formed diastereomeric crystals with

opposite enantiomers of **1-1**. Diastereomeric crystallization was very scalable and bases could easily be recovered and reused. Repeating the crystallization process thrice yielded acid **1-1** in highly enantiomerically enriched form. Thus, three recrystallizations of **1-1** with brucine from methanol yielded (+)-**1-1** in > 99% ee. Likewise, three recrystallizations of **1-1** with strychnine from 80% methanol in water yielded (–)-**1-1** in > 99% ee. In practice, mother liquors from brucine crystallizations, enriched in the levorotatory enantiomer, were recovered and subjected to recrystallization with strychnine. Likewise, mother liquors from strychnine crystallizations were combined and subjected to recrystallization with brucine. In this way, multigram quantities of each enantiomer of **1-1** could be obtained in highly enantiomerically enriched forms.

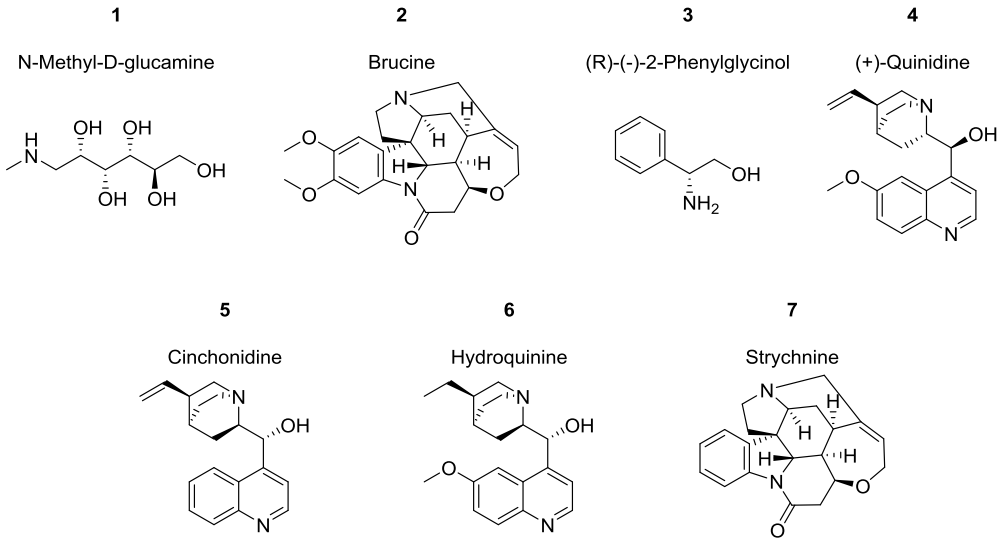

Scheme 1.6: Chiral bases used in homemade classical resolution kit

Table 1.2: Results from '77-well plate' classical resolution screen. Conditions that produced crystals are highlighted in yellow and the numbers listed reflect the enantiomeric excess of **1-1** from the free acid liberated from the diastereomeric salt that crystallized.

	A	**B**	**C**	**D**	**E**	**F**	**G**	**H**	**I**	**J**	**K**
1											
2		(–)4	(–)7	(+)72		(+)8					
3											
4											
5			(+)54				(+)28				
6											
7							(–)54				

Solvent systems: A- 75 % BuOH/H_2O, **B** – EtOH, **C**- 95 % EtOH/H_2O, **D** – MeOH, **E** – 2-PrOH, **F** – 90 % 2-PrOH/H_2O, **G** – 80 % MeOH/H_2O, **H** – H_2O, **I** – 75 % ethylene glycol, **J** – PrOH, **K** – 85 % PrOH

1.3 Conclusion

Classical resolution techniques were used to streamline the 15 step synthesis of metallohelicenes **5A** and **5B**, which have served as a probe for the mechanism of asymmetric induction in chiral metal-salen catalyzed Diels-Alder reactions. Resolution of carboxylic acid **1-1** was achieved by the diastereomeric crystallization with the chiral bases strychnine ($4.18/g) and brucine ($6.02/g) rather than through chiral resolution with (3a*R*-cis)- (+)-3, 3a, 8,81-tetrahydro-2H-indeno[1,2]oxazol-2-one ($114/gram). The improvement on the resolution step of this synthetic route made the process significantly more cost effective, enhanced scalability and improved step economy. With this improved efficiency, Dr Plampin was able to rapidly synthesize Co-salen catalysts **5A** and **5B** (Scheme 1.7) and proceed with his tests on the importance of helical chirality in catalytic studies on Rawal's Co-salen catalyzed

Diels-Alder reaction. As shown in Scheme 1.8, a control reaction with catalyst **4** priceeds in 68% yield and with 86% ee. With the metallohelicenes, it was found that only the (*P*)-helical diastereomer, **5B**, provided the Diels-Alder adduct in high enantioselectivity. These findings demonstrated that helicity plays an important role in catalytic Diels-Alder reactions and also that the absolute sense of chirality may be important.

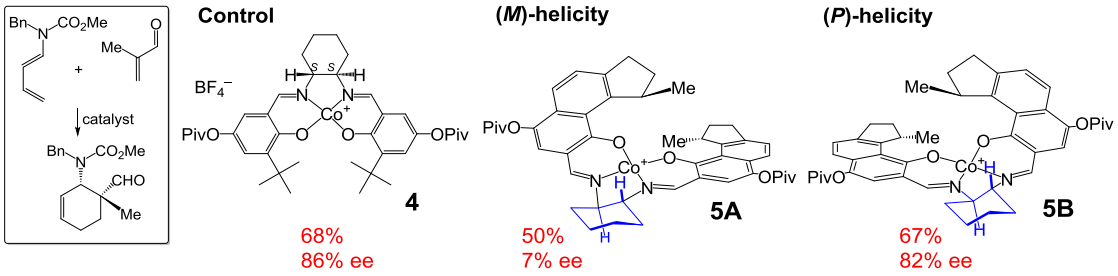

Scheme 1.7: Enantioselective catalysis efficient with (*P*)-diastereomer, but not with the (*M*)-diastereomer**.**

1.4 Experimental Section

General Procedure for Chiral Resolution Assay

A stock solution of carboxylic acid in methylene chloride was portioned into 0.03 mmol aliquots in vials. After allowing for the evaporation of the methylene chloride, 200 µL of a 0.15 M stock solution of chiral base in the respective solvent system was added. If the base was insoluble in a solvent system, it was weighed on a balance and placed into the vial then appropriate solvent system was added. Reaction vials were agitated to allow for vigorous stirring. If the contents were insoluble after agitation the sealed vials were warmed to 80 °C to encourage dissolution. Vials were then cooled to room temperature then stored at 20°C overnight to allow for crystallization. Crystals

which grew overnight were considered ‘hits’. These were washed with cold solvent (whichever solvent effected the crystallization process), acidified with 3 M HCl, extracted with methylene chloride then dried over magnesium sulfate. After filtration and concentration to dryness using a rotary evaporator, crystals were resuspended in a 5% isopropanol in hexanes mixture and assayed via HPLC analysis: (Chiralpak AD 2% 2-propanol in hexanes 1mL/min, 220 nm).

Procedure for large scale resolution of (S)-3-methyl-2,3-dihydro-1H-indene-4-carboxylic acid (*S*)-1-1

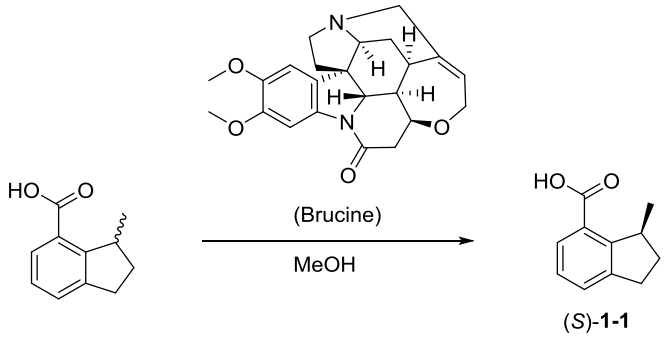

A 250 mL round bottom flask was sequentially charged with racemic 1-methyl-indane-4-carboxylic acid (3.0 g, 17 mmol) and methanol (110 mL). To this solution, brucine-dihydrate (15 g, 34 mmol) was added and the mixture was heated to 90˚C for 1 hour. The solution was allowed to cool to room temperature and then stored in a 20 °C freezer for 16 hours. The precipitated salt was then collected by vacuum filtration, transferred to a 200 mL round bottom flask and 3 M HCl (50 mL) was added. The mixture was allowed to stir for 15 minutes and then extracted thrice with methylene chloride. The combined organic layers were dried over magnesium sulfate, filtered and concentrated to dryness under reduced pressure. The resulting solid was

purified by column chromatography (gradient up to 48% ethyl acetate/hexanes). The product was subjected to two additional crystallizations, each employing two equivalents of brucine-dihydrate, based on the amount obtained from each purification step, to yield enantiomerically pure product. The combined crystallization processes furnished 0.60 g (20 %, 3.4 mmol) of **(*S*)-1-1** as a white solid in > 99% ee. $[\alpha]_D^{23}$ +120 (*c* 0.15, CH_2Cl_2). Spectral data matched published data of rac **1-1**[25].

Procedure for large scale resolution of (S)-3-methyl-2,3-dihydro-1H-indene-4-carboxylic acid (*R*)-1-1

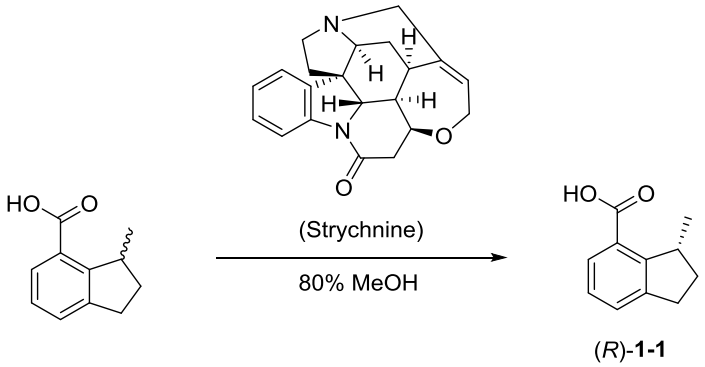

A 250 mL round bottom flask was sequentially charged with racemic 1-methyl-indane-4-carboxylic acid (3.0 g, 17 mmol) and methanol (110 mL). To this solution strychnine (11 g, 34 mmol) was added and the mixture was heated to 80 °C for 1 hour. The solution was allowed to cool to room temperature and then stored in a 20 °C freezer for 16 hours. The precipitated salt was then collected by vacuum filtration, transferred to a 200 mL round bottom flask and 3 M HCl (50 mL) was added. The mixture was allowed to stir for 15 minutes and then extracted thrice with methylene chloride. The combined organic layers were dried over magnesium sulfate, filtered and concentrated to dryness under reduced pressure. The resulting solid was purified by column chromatography (gradient up to 48% ethyl acetate/hexanes). The product was

subjected to two additional crystallizations, each employing two equivalents of strychnine, based on the amount obtained from each purification step, to yield enantiomerically pure product. The combined crystallization processes furnished 0.45 g (015 %, 2.6 mmol) of **(*R*)-1-1** as a white solid in > 99% ee. $[\alpha]_D^{23}$ 120 (*c* 0.15, CH_2Cl_2). Spectral data matched published data of rac **1-1**[25].

REFERENCES

1. Zhang, W.; Loebach, J. L.; Wilson, S. R.; Jacobsen, E. N. *J. Am. Chem. Soc.* **1990**, *112*, 2801.

2. Irie, R.; Noda, K.; Ito, Y.; Matsumoto, N.; Katsuki, T. *Tetrahedron Lett.* **1990**, *31*, 7345.

3. Srinivasan, K.; Michaud, P.; Kochi, J. K. *J. Am. Chem. Soc.* **1986**, *108*, 2309.

4. Baleizão, C.; Garcia, H. *Chem. Rev.* **2006**, *106*, 3987.

5. Jacobsen, E. N.; Zhang, W.; Muci, A. R.; Ecker, J. R.; Deng, L. *J. Am. Chem. Soc.* **1991**, *113*, 7063.

6. Li, Z.; Conser, K. R.; Jacobsen, E. N. *J. Am. Chem. Soc.* **1993**, *115*, 5326.

7. Martinez, L. E.; Leighton, J. L.; Carsten, D. H.; Jacobsen, E. N. *J. Am. Chem. Soc.* **1995**, *117*, 5897.

8. Schaus, S. E.; Brånalt, J.; Jacobsen, E. N. *The Journal of Organic Chemistry* **1998**, *63*, 403.

9. Tokunaga, M.; Larrow, J. F.; Kakiuchi, F.; Jacobsen, E. N. *Science* **1997**, *277*, 936.

10. Sammis, G. M.; Jacobsen, E. N. *J. Am. Chem. Soc.* **2003**, *125*, 4442.

11. Sigman, M. S.; Jacobsen, E. N. *J. Am. Chem. Soc.* **1998**, *120*, 5315.

12. Tamura, Y.; Uchida, T.; Katsuki, T. *Tetrahedron Lett.* **2003**, *44*, 3301.

13. Miller, J. A.; Jin, W.; Nguyen, S. T. *Angew. Chem. Int. Ed.* **2002**, *41*, 2953.

14. Saito, B.; Katsuki, T. *Tetrahedron Lett.* **2001**, *42*, 3873.

15. DiMauro, E. F.; Kozlowski, M. C. *Org. Lett.* **2001**, *3*, 3053.

16. Cozzi, P. G. *Angew. Chem. Int. Ed.* **2003**, *42*, 2895.

17. Belokon, Y. N.; North, M.; Parsons, T. *Org. Lett.* **2000**, *2*, 1617.

18. Watanabe, A.; Uchida, T.; Ito, K.; Katsuki, T. *Tetrahedron Lett.* **2002**, *43*, 4481.

19. (a) Katsuki, T. *Synlett* **2003**, *2003*, 0281; (b) Katsuki, T. *Adv. Synth. Catal.* **2002**, *344*, 131; (c) Katsuki, T. *Chem. Soc. Rev.* **2004**, *33*, 437.

20. Dong, Z.; Yap, G. P. A.; Fox, J. M. *J. Am. Chem. Soc.* **2007**, *129*, 11850.

21. Dong, Z.; Karpowicz, R. J.; Bai, S.; Yap, G. P. A.; Fox, J. M. *J. Am. Chem. Soc.* **2006**, *128*, 14242.

22. Dong, Z.; Plampin, J. N.; Yap, G. P. A.; Fox, J. M. *Org. Lett.* **2010**, *12*, 4002.

23. Dong, Z.; Bai, S.; Yap, G. P. A.; Fox, J. M. *Chem. Commun.* **2011**, *47*, 3781.

24. (a) McGilvra, J. D.; Rawal, V. H. *Synlett* **2004**, *2004*, 2440; (b) Huang, Y.; Iwama, T.; Rawal, V. H. *J. Am. Chem. Soc.* **2002**, *124*, 5950.

25. Rao, G. S. R. S. H., H.K.;, Girija, T.; Bhaskar, K.V *Indian Chemical Society* **1997**, 961.

Chapter 2

ENANTIOSELECTIVE SYNTHESIS OF CYCLOBUTANES VIA SEQUENTIAL RHODIUM-CATALYZED BICYCLOBUTANATION/HOMOCONJUGATE ADDITION OF HETEROATOMIC NUCLEOPHILES

2.1 Introduction

Cyclobutanes are compact and rigid molecular scaffolds that can present molecular functionality in a stereochemically well-defined manner. Dimeric cyclobutanes are prevalent subunits in natural products with diverse biological activity[1] (Figure 2.1).

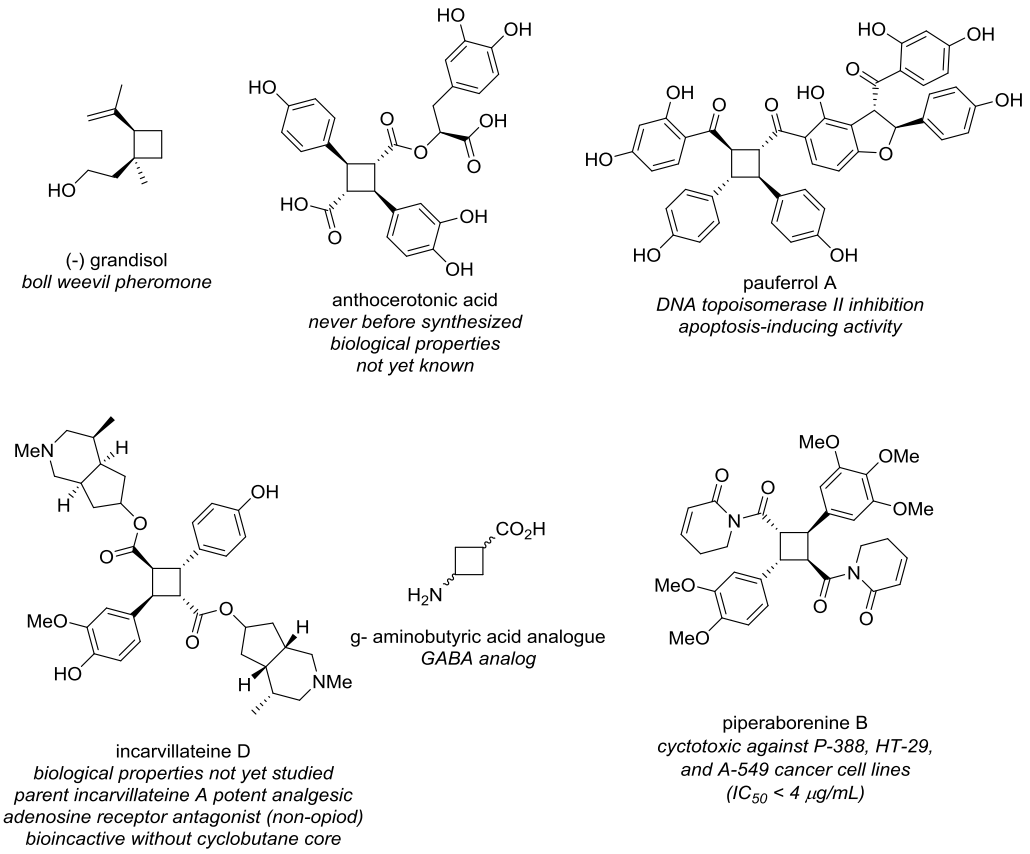

Figure 2.1: Stereochemically rich cyclobutanes exist in nature and have a wide range of biological activity[1a-c]. Several exist whose activity is yet to be determined due to the limited options available for their access synthetically.

One method utilized by Nature to achieve the synthesis of cyclobutanes involves photochemical [2+2] cycloaddition chemistry. In general, the [2+2] photodimerization process gives racemic products and mixtures of homo and heterodimer isomers are obtained unless the reactants are subjected to photocyclization conditions in the solid state[1a,2], are under noncovalent interaction control[3] or as very recently shown by Yoon[4], are engaged through transition metal photocatalysis. Within the synthetic community, a number of approaches have been

taken to furnish functionalized cyclobutanes[5]. These include, but are not limited to photochemical [2+2] cycloadditions[6], photoredox-catalyzed [2+2] cycloadditions[4b,7], cyclobutanone synthesis via ketenes[8], ring expansion of cyclopropylcarbinyl precursors[9] and C-H activation of existing cyclobutanes[6c,6d,10]. Examples of each approach are represented in Table 2.1.

Table 2.1: Approaches to synthesizing functionalized cyclobutanes.

Entry	Reaction	Reference
1	*Photochemical [2+2] addition* 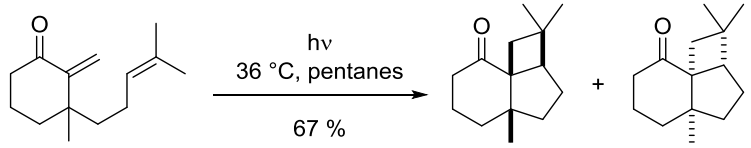 Toward (±)-b-panasinsene	6b
	Catalyzed [2+2] addition 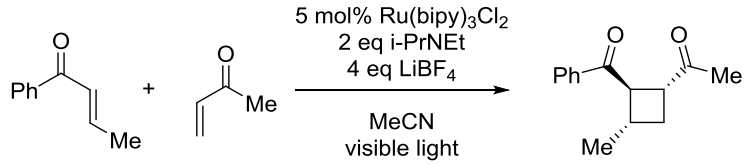 2.5 eq 84 %, > 10:1 dr	4b
	Cyclobutanone access via ketenes 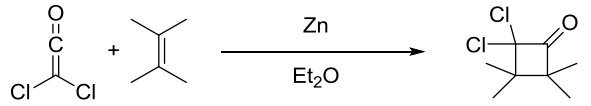 75 %	8b
	Ring expansion of cyclopropylcarbinyl precursors 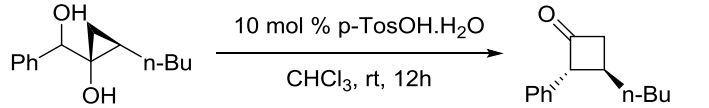 94 %, cis:trans: 1:17	9a

	C-H activation of cyclobutanes 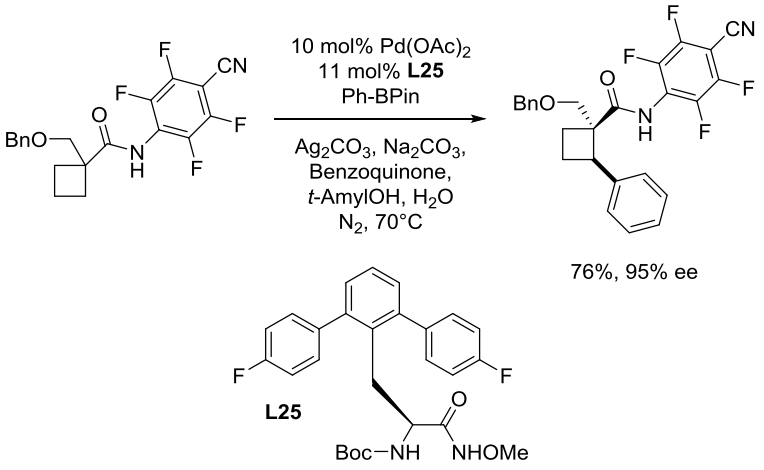 	10

Despite many advances, there remains a need for new methods that allow *rapid* and *enantioselective* construction of densely functionalized cyclobutanes.

Bicyclobutanes (BCBs) are viable precursors of functionalized cyclobutanes. As the smallest possible carbocyclic fused ring system, bicyclobutane has a strain energy (SE) of 63.9 kcal/mol. This high SE and the unusual bonding that must be adopted for the existence of BCB[11] gives rise to unique reactivity. The frontier molecular orbitals of bicyclobutane are dominated by the central bond, which is high in π-character[11-12] and susceptible to stereospecific backside attack by nucleophiles (Figure 2.2).

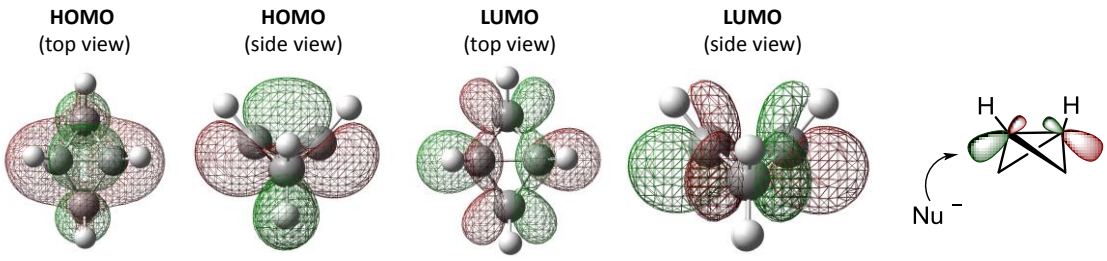

Figure 2.2: Frontier orbitals of bicyclobutanes [B3LYP, 6-31G(d)]

Despite their unique reactivity, since their first reported synthesis in 1959[13], the reactivity of BCBs has largely been under explored. Gaoni, in a series of publications demonstrated that organocuprates[14], and several softer nucleophiles (hydrazoic acid, hydride and phenylselenol)[15] could be added across the polarized central C-C bond of 1- arylsulfonylbicyclobutanes to give functionalized cyclobutanes. Wipf has also shown that BCB derivatives are capable of undergoing catalyst promoted ring expansion reactions[16], formal [2+2] cycloaddition reactions[17], and Alder-ene reactions[18]. Together, these publications showcase the potential of BCBs for synthetic applications. Still, the limited access to bicyclobutanes[13,18c,19] has hindered further exploration into their reactivity. Seminal work by Ganem[20] (Scheme 2.1) demonstrated that 1-carboxylate BCBs could be accessed via rhodium (II) catalyzed cyclization of ethyl α-allyl-α-diazoacetate, however, β-hydride elimination was a significant side reaction.

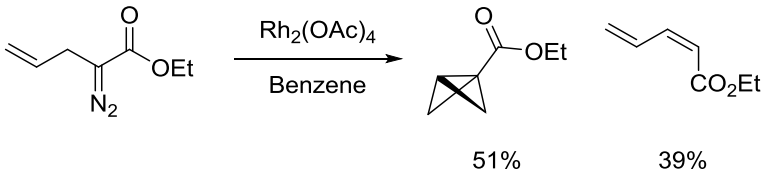

Scheme 2.1: Seminal work by Ganem demonstrating BCB access via carbene insertion into double bonds.

Building on documented efforts known to suppress the undesired β-elimination pathway in rhodium (II) catalyzed transformations of α-allyl-α-diazoacetates[21], the Fox and Davies groups independently reported[22] the enantioselective bicyclobutanation of (*E*)-2-diazo-5-arylpent-4-enoates, which are readily prepared by alkylation of *t*-butyl acetoacetate with the cinnamyl halides and subsequent diazo transfer (Scheme 2.2).

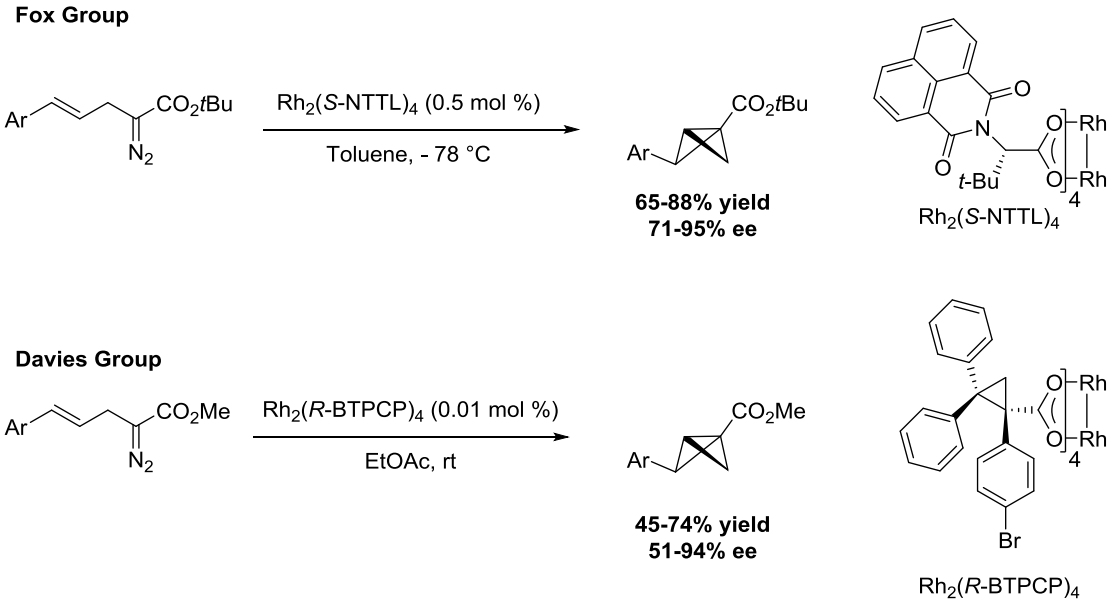

Scheme 2.2: First reports of the rhodium (II) catalyzed enantioselective bicyclobutanation of (*E*)-2-diazo-5-arylpent-4-enoates by the Fox and Davies groups.

As the aim of being able to access bicyclobutanes enantioselectively was to investigate their being precursors for the synthesis of stereodefined cyclobutanes, the Fox lab further investigated the homoconjugate addition of carbon centered nucleophiles across the central C-C bond of the synthesized bicyclobutanecarboxylates. Though bicyclobutanecarboxylic esters were first synthesized in 1959[13], homoconjugation to unsubstituted bicyclobutanecarboxylates had been limited to the addition of thiolate and alkoxide nucleophiles[23], with details surrounding their addition being vague. Fox and coworkers were able to develop conditions for the efficient addition of *in situ* formed organocuprate reagents in a homoconjugate manner to bicyclobutanecaboxylates. Further, they were able to

demonstrate that the enantioselective bicyclobutanation and subsequent homoconjugation reaction could be conducted in a one pot protocol (Scheme 2.3).

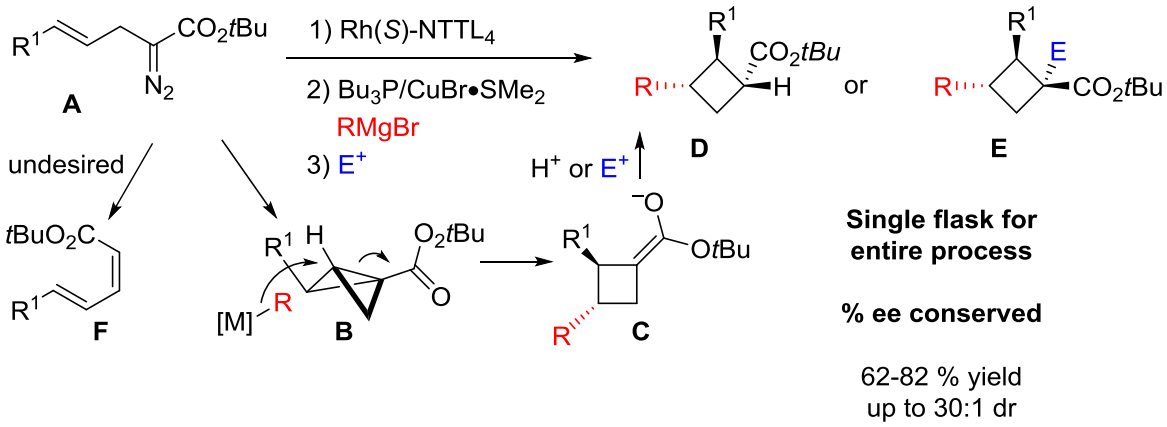

Scheme 2.3: One pot protocol for the enantioselective synthesis of cyclobutanes

Thus, readily prepared α-allyldiazoesters (**A**) (available in 2-3 steps) were treated with the chiral catalyst Rh_2(*S*-NTTL)$_4$ to give bicyclobutane (BCB) **B** under optimized conditions that offer high selectivity over β-hydride elimination product **F**. In the same pot, organomagnesium nucleophiles can be added under Cu-catalyzed conditions to provide homoconjugate **C**. Subsequent protonation under thermodynamic conditions or electrophile quench of the *in situ* formed enolate under kinetic conditions lead to substituted cyclobutanes of structure **D** or **E** respectively in yields of up to 82 %. The enantioselectivity achieved in the bicyclobutanation step was conserved through the homoconjugate addition.

2.2 Results and Discussion

I have developed a system for the extension of the one pot enantioselective bicyclobutanation/homoconjugate addition protocol to the addition of heteroatomic nucleophiles. Single flask procedures were developed for additions of azides, thiols, phenoxides and nitriles and their optimization will be discussed separately below.

2.2.1 Azide Addition

Of note, products of azide addition to bicyclobutanes can serve as precursors to unnatural, conformationally constrained amino acids – compounds with promise for medicinal chemistry as well as peptide design applications

Prior to this work, the addition of azides to arylsulfonyl BCBs in a homoconjugate manner had been described by Gaoni in 1989[15]. There had been no analogous addition to carboxylate substituted BCBs. To achieve azide addition, Gaoni used *in situ* generated tetramethylguanidinium azide (TMGA, $TMGN_3$) in rather forcing conditions: 1 M solution in NMP/DMF, heated to 90 °C for 2 hours. Though TMGA itself is nontoxic and safe to use[24], it is generated from treatment of tetramethylguanidine with the incredibly toxic and explosive hydrazoic acid[25]. In Papa's 1966 preparation of TMGA he stresses the following both in the abstract and body of his publication:

> "Caution must be exercised when working with these compounds since explosion results when heated at a temperature above 50° at atmospheric pressure"

Though this route proved to be a successful approach for the Gaoni group, I decided to investigate azide addition under more mild and safer conditions. Screens were conducted with racemic BCB, compound **2-1** (Table 2.2).

I quickly learned that the addition of azides to BCBs would not be straightforward as the usual sources of azide anions proved unsuccessful under a wide range of reaction conditions screened. Selected results are shown in Table 2.2.

Table 2.2: Optimization of azide addition to **2-1**

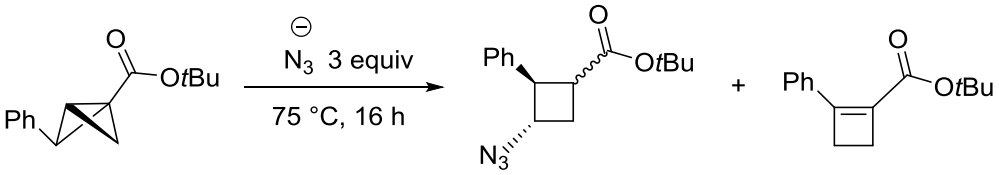

2-1 **2-2** **2-3**

Entry	Azide source	Solvent [**2-1**]	% Yield[b,c] **2-2**	% Yield[b] **2-3**
1	NaN_3	THF [0.2][a]	0	0
2	NaN_3	Toluene [0.2]	0	0
3	NaN_3	DMF [0.2]	25	25
4	NaN_3	DMF [0.1]	34	30
5	NaN_3	DMF [0.05]	60	<5
6	KN_3	DMF [0.05]	25	0-
7	NBu_4N_3	DMF [0.05]	38	15
8	$TMSN_3$[d*]	DMF [0.05]	0[d]	0
9	HN_3 ($TMSN_3$/AcOH/cat DBU[26])	CH_2Cl_2	0	0
10	NaN_3	DMSO [0.05]	16	0
11	NaN_3	HMPA [0.05]	60	0

(a) heated to 66 °C (b) isolated yields were consistent with corrected GC and NMR yields (c) no starting material remaining (SM) at the end of the reaction – highly insoluble presumably polymeric material was observed (d) SM remaining unreacted at the end of the reaction.(GC assay with internal standard)

In initial optimization studies it was found that polar, aprotic solvents were necessary to facilitate the azide addition reaction (Table 2, entries 1 and 2). Reactions were conducted at 75 °C as early studies determined higher temperatures led to the rapid

decomposition of **2-1** to intractable products, and at lower temperatures reactivity was sluggish. Thus, entry 3 in Table 2.2, conducted in DMF [0.2 M), with sodium azide (NaN_3) as the azide source, demonstrated that the desired transformation was possible, yielding 25 % of **2-2**. However these conditions also resulted in the formation a significant quantity, 20 %, of the undesired cyclobutene **2-3** which is presumed to arise from either of two possibilities (Scheme 2.4). The first option to **2-3** results from the elimination of hydrazoic acid from the newly formed **2-2** followed by alkene isomerization to furnish the thermodynamically more favorable conjugated cyclobutene (Pathway A, Scheme 2.2). Alternatively, keto-enol tautomerization of **2-1** would result in the formation of a carbocation at a secondary carbon that would quickly undergo a 1,2-hydride shift to form the more stable tertiary benzylic carbocation. Following this, the enol could collapse into the thermodynamic sink that is cyclobutene **2-3** (Pathway B, Scheme 2.4). However, as this side product was only observed in the presence of an azide source, Pathway A is likely the predominant route leading to the formation of **2-3**.

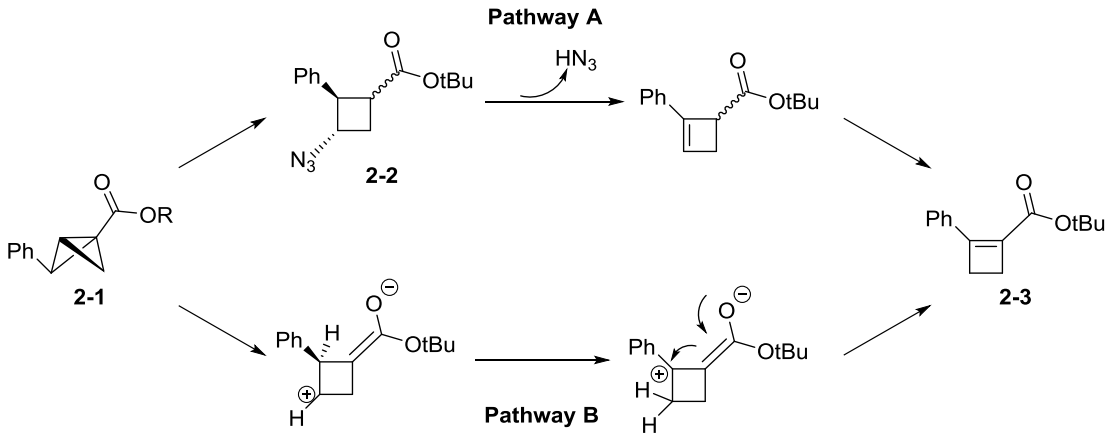

Scheme 2.4: Possible mechanistic pathways for the formation of undesired cyclobutene **2-3**

In an effort to minimize formation of **2-3**, I decided to survey the reaction concentration. Halving the concentration of the reaction to 0.1 M (entry 4), resulted in a marginal increase in yield of the desired **2-2**, 35%, however, it did not suppress the formation of **2-3**. Moving to even more dilute conditions, 0.05 M, proved to be effective in the minimization of **2-3** (entry 5) and also led to a significant increase in the yield of **2-2**, 60%. Having found conditions that suppressed the formation of **2-3**, attentions were shifted to determine parameters which facilitated the more efficient formation of **2-2**. Entry 9 represents efforts to adapt a protocol reported by Miller et al.[26] where the controlled release of hydrazoic acid proved effective in facilitating the addition of azides to α,β-unsaturated carboxylic esters. These conditions or variations thereof were not productive in the BCB system. With the exception of entries 7 – 9, where tetrabutylammonium azide and trimethylsilyl azide were employed, an observation of note was that reactions were heterogeneous in nature – the inorganic azide source largely remained insoluble over the course of the reaction. I regarded this

to be a potential contributor to the limited success in the azide addition reaction. Regardless of the conditions screened using inorganic azides, the yields hovered around 50-60 % at best. As such, I sought to explore the literature for reagents that provided a soluble source of azide. This lead to a report by Thompson and coworkers at Merck Research laboratories[27], where they used the reagent diphenylphosphoryl azide (DPPA) under basic conditions to directly convert optically active, activated alcohols to azides with clean inversion. Under standard Mitsunobu conditions (triphenylphosphine, diethylazodicarboxylate (DEAD) and DPPA) they observed erosion of the ee % on inversion to form the desired azide product. However, they discovered that DPPA in the presence of 1,8-diazabicycloundec-7-ene (DBU) could efficiently serve as both the activator of their alcohol and soluble azide source without the erosion of their starting stereocenter. Mechanistically, the reaction is thought to occur in following manner (Scheme 2.5): the non-nucleophilic, strong *base* DBU deprotonates the alcohol, which can then displace azide from DPPA to form the phosphate **I** and ammonium azide **II**. This activated alcohol is now suited to be displaced by the very soluble azide anion to yield the desired product.

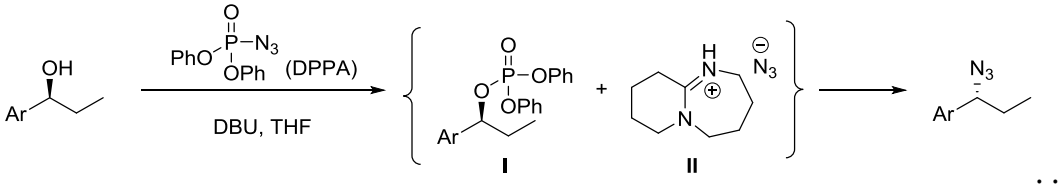

Scheme 2.5: Mechanism of activated alcohol displacement by DPPA and DBU

I sought to apply the reaction conditions discussed in the aforementioned paper to the BCB system with an alteration. The hypothesis was that in the presence of an alcohol additive such as *tert*-butanol where the S_N2 reaction to displace the activated alcohol formed would be unlikely, the soluble azide source generated from DPPA could then productively engage **2-1** in the homoconjugate reaction. Gratifyingly, combining **2-1** with equimolar amounts of DPPA, *tert*-butanol and DBU (3 equiv) in THF (0.25 M) at 50 °C for 16 hours furnished 70% of **2-2** (Scheme 2.6).

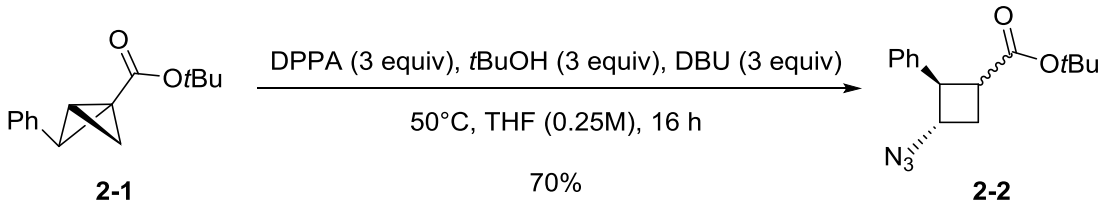

2-1 **2-2**

Scheme 2.6: Mitsunobu type reaction conditions successful in facilitating azide addition to **2-1**

As the long term aim of these additions was for them to be conducted in tandem with bicyclobutanation in a one pot protocol, further optimization led to the discovery that the reaction was also effective in toluene, the solvent that is optimal for BCB formation, with HMPA as a co-solvent at a slightly higher temperature (75 °C). These conditions yielded adduct **2-2** in 75% yield (Table 2.3). With this system, I decided to probe the reaction mechanism of azide addition.

2.2.1.1 Mechanistic Studies

Several control reactions were run and their results are summarized in Table 2.3.

Table 2.3: Control reactions for DPPA-DBU azide addition

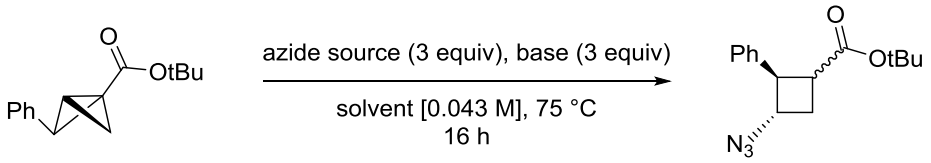

2-1 75% **2-2**

Entry	Azide source	Base	Additive	Solvent	Observations
1	DPPA	DBU	*t*BuOH	Tol	40% yield, 80% conversion
2	DPPA		*t*BuOH	Tol/HMPA	0% conversion
3	DPPA	DBU		Tol/HMPA	75% yield
4	DPPA	DIPEA		Tol/HMPA	**2-1** decomposition
5	DPPA	Et_3N		Tol/HMPA	**2-1** decomposition
6	NaN_3	DBU		Tol/HMPA	0% conversion

While the reaction proceeded in the absence of HMPA (entry 1, Table 2.3), the conversion was only 80% with 40% yield after 16 hours. DBU was found to be essential for the reaction to proceed (entry 2) and a survey of other non-nucleophilic bases confirmed DBU to be the most effective for this transformation (entries 4 and 5). A control experiment using DBU in combination with NaN_3 (entry 6-) did not lead to the formation of product **2-2**. The most unexpected result was that the reaction proceeded equally well in the absence of the alcohol additive (entry 3). This result led me to propose that DBU acts a *nucleophile* toward DPPA to displace the azide anion. In so doing, an ionic DPPA-DBU complex, **2-4**, is formed as a nucleophilic and highly soluble azide source (Scheme 2.7). There are precedents outlining DBU and other

amidine bases serving as proficient nucleophilic agents in various organic transformations[28]. Further, the direct interaction of DBU with diphenyl and dialkyl phosphorochloridates/phosphonates and DBU has been reported[28d-f].

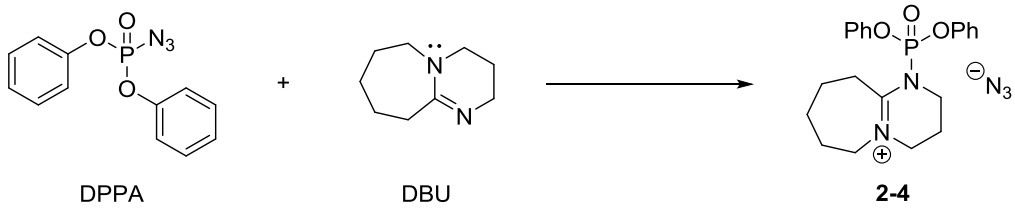

Scheme 2.7: Proposed formation of azide source

ReactIR Studies

The *in situ* monitoring of chemical reactions using FTIR spectroscopy can provide information on reaction kinetics and intermediates and has been a vital tool in both academic and industrial settings[29]. The reaction of bicyclobutanecarboxylates with the DPPA-DBU system is particularly suited to this technique as azido groups can be identified by the strong N_3 asymmetric stretches which occur in the 2100- 2170 cm^{-1} range[30]. Also, the reaction is homogenous, which makes analysis of intermediates and products that much more feasible.

The reaction with IR monitoring was carried out at 0.1 M in DPPA and DBU, 0.2 M in bicyclobutanes **2-1** (Scheme 2.8).-

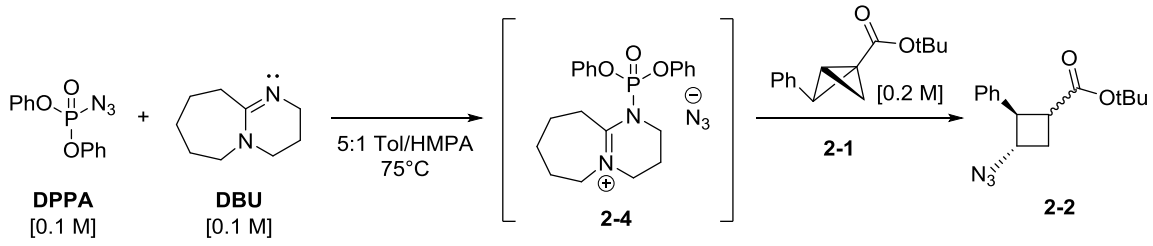

Scheme 2.8: ReactIR experiment

Upon the addition of an equimolar amount of DBU to DPPA at 75 °C, the intensity of the asymmetric azide stretch of DPPA (2170 cm^{-1}) decreases concomitant with the growth of a new peak (2003 cm^{-1}). After 45 minutes, the DPPA is completely consumed and only that of the new azide intermediate is observed (Figure 2.3).

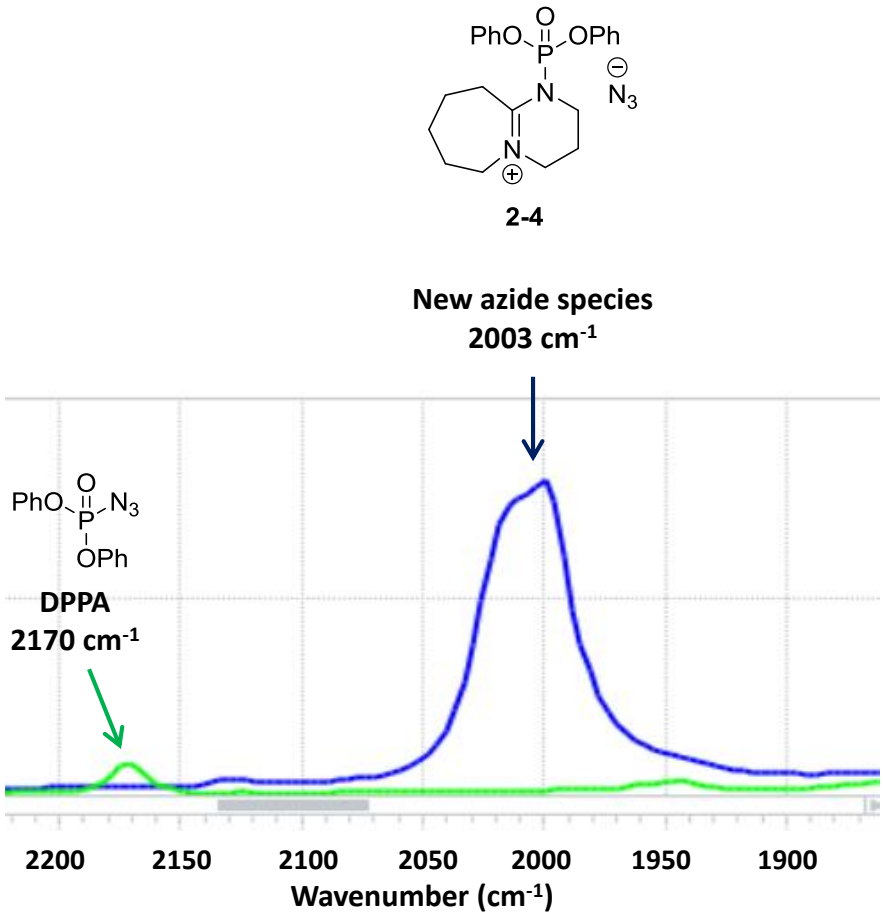

Figure 2.3: IR spectrum before (**green spectrum)** and 45 minutes after DBU addition (**blue spectrum)** to DPPA.

In order to support the proposed formation of ionic azide intermediate **2-4** I synthesized tetrabutylammonium azide (NBu_4N_3) to compare its asymmetrical azide stretch with that of **2-4**. The asymmetrical azide stretch of NBu_4N_3 was found to be 2000 cm^{-1}, which compares quite well with 2003 cm^{-1} of **2-4**.

An excess of **2-1** was then added to the reaction vessel and over the course of 6 hours, the azide stretch of **2-2** (2100 cm^{-1}) increased in intensity while that of the intermediate species simultaneously diminished (Figure 2.4)

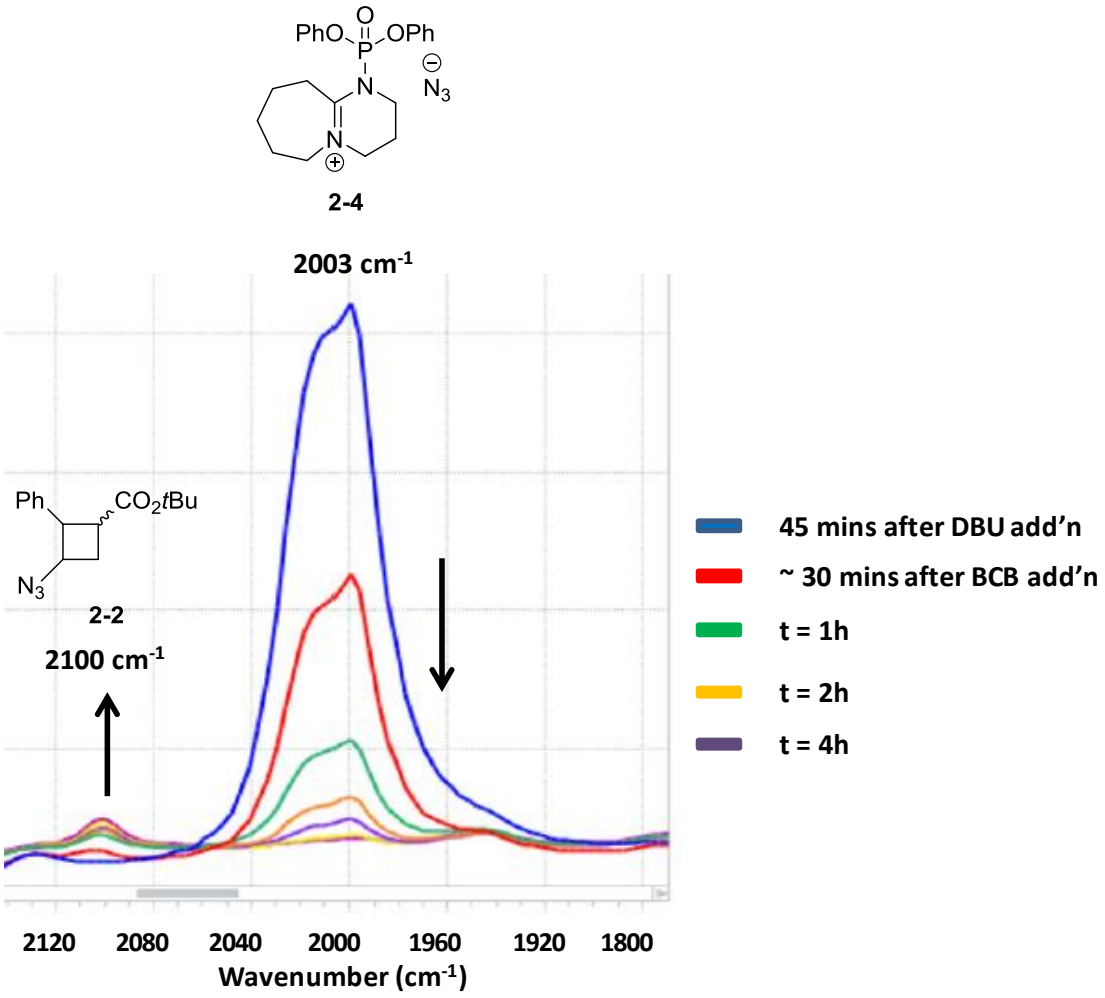

Figure 2.4: As the concentration of the new azide species decreases, the concentration of **2-2** increases. $t_{1/2}$ is approximately 30 minutes under these conditions

NMR Studies

In an analogous experiment, an equimolar amount of DBU was added to DPPA in a 0.1 M, 5:1 solution of toluene-D8/HMPA at 75˚C.

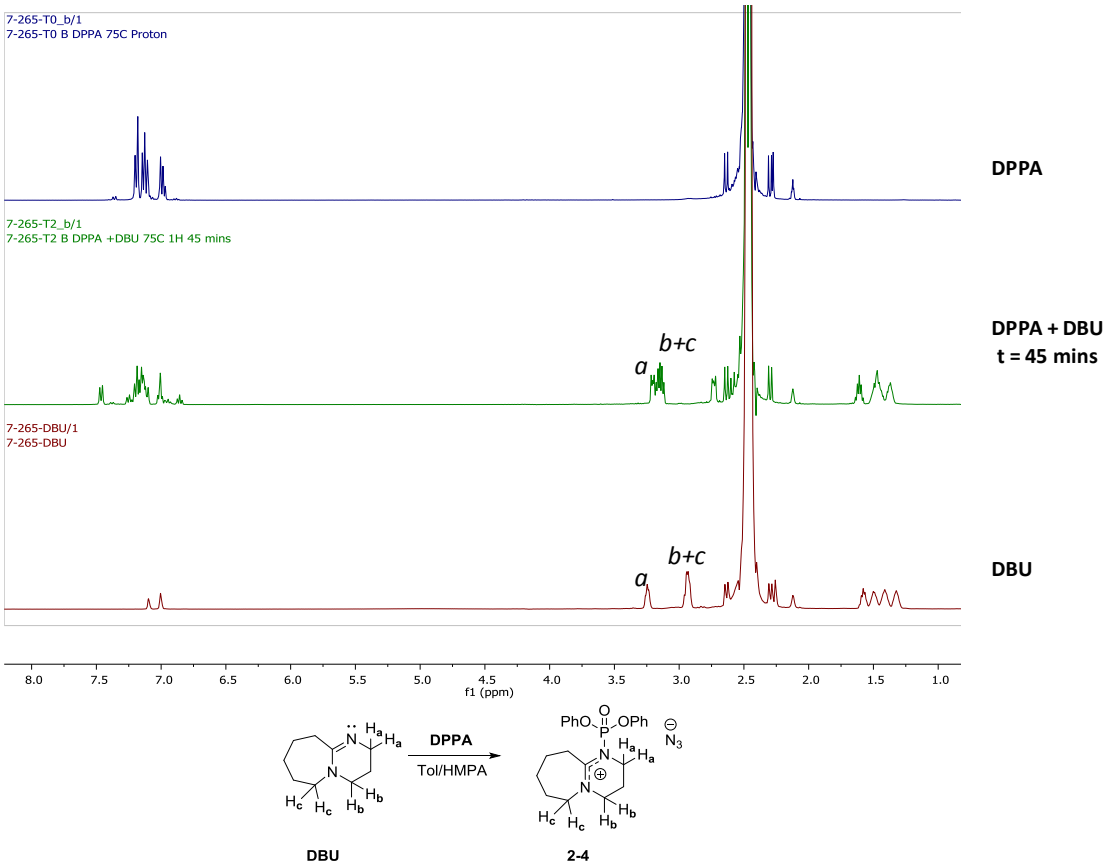

Figure 2.5: (a) ^{1}H NMR showing the formation of a new species on the mixing of DPPA and DBU at 75 °C.

After 45 minutes, there are marked changes in the proton spectra of both reagents (Figure 2.5) the peaks labeled H_a, H_b and H_c. shift to 3.22-3.20 and 3.19-3.12 ppm from 3.26-3.23 and 2.94-2.92 ppm, respectively. The change of chemical shift is consistent with the IR data, and the formation of a new species assigned to structure **2-4**.

<u>High Resolution Mass Spectrometry</u>

A portion of the NMR sample described above was submitted for high resolution mass spectrometry analysis (HR-MS). The exact mass of the cationic

portion of **2-4** was calculated to be 385.1681 g/mol. The found mass was 385.1699 g/mol, providing further support for the formation of the proposed intermediate structure (Figure 2.6)

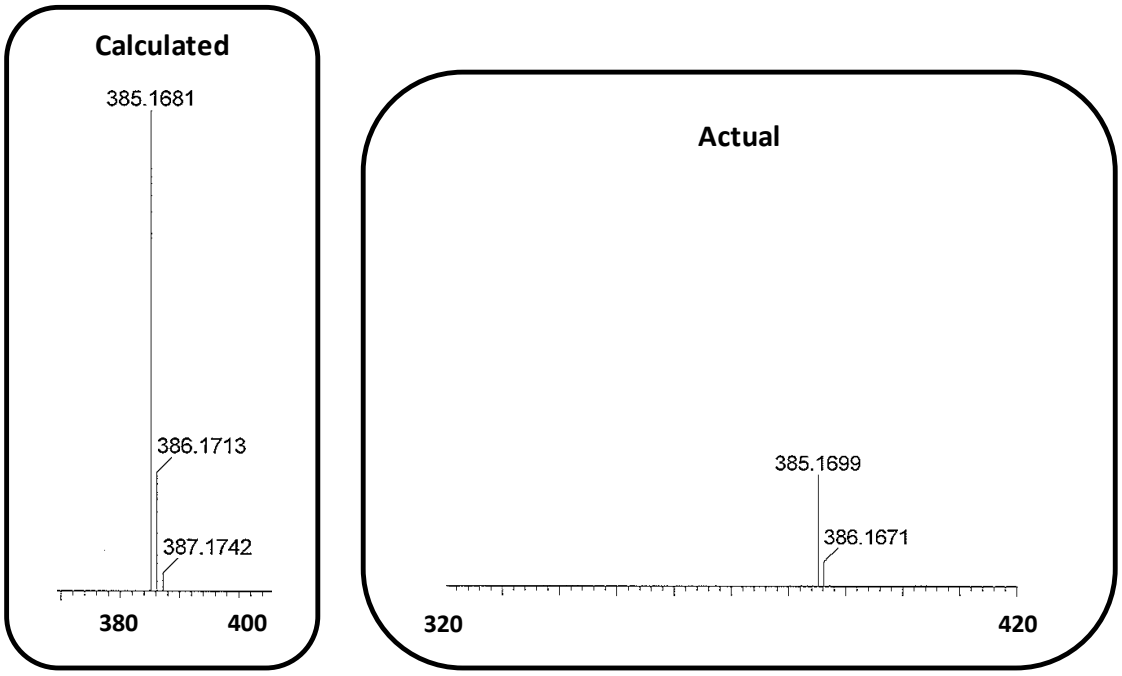

Figure 2.6: HR-MS analysis of DPPA + DBU. Mass of expected adduct observed.

In situ FTIR analysis, NMR and HR-MS studies have together supported the proposed mechanism for the addition of azide to bicyclobutanes using the DPPA-DBU system. Efforts then turned to the investigation of the reaction scope for the one pot synthesis of cyclobutanes azides from *t*-butyl-(*E*)-2-diazo-5-arylpent-4-enoates.

Substrate Scope

The substrates to be described were used for all subsequent homoconjugate additions to be discussed and were known compounds, with the exception of **2-8** whose methyl and not *tert*- butyl ester has been reported. With the minor alteration in the ester group, all substrates were synthesized following published procedures[22a]. The general strategy used for the synthesis of the diazo esters is shown in Scheme 2.9. Diazo esters were synthesized in 4 steps from commercially available cinnamyl esters or cinnamaldehydes (in the case of **2-7**).

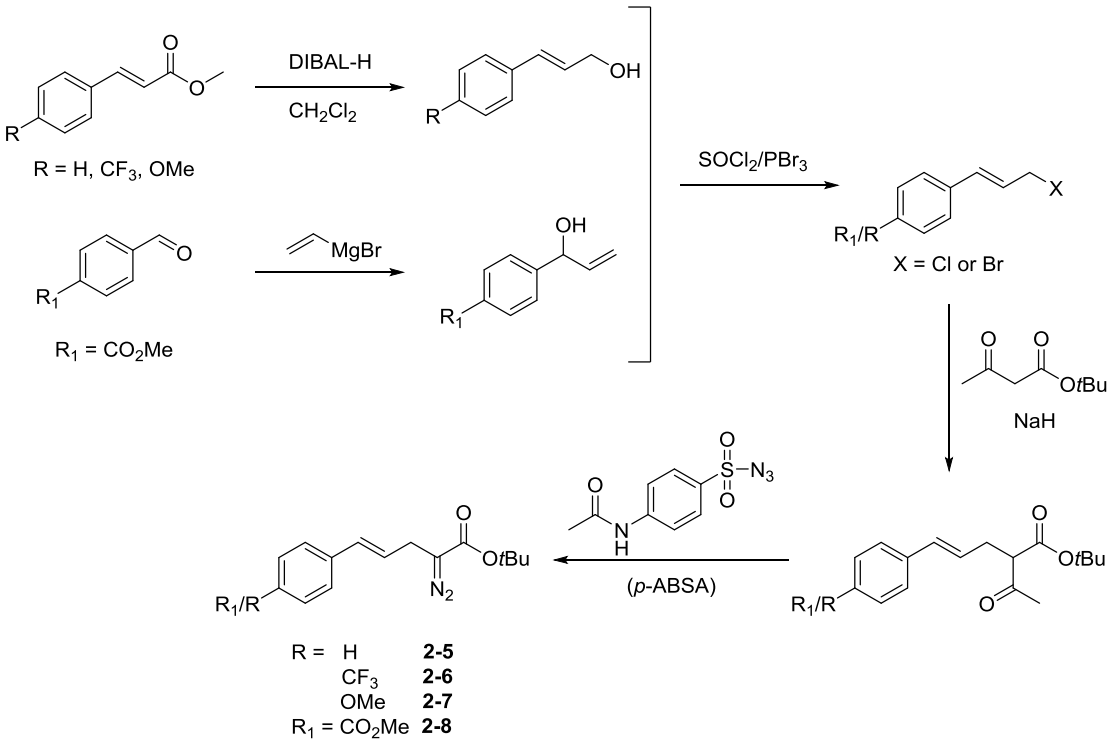

Scheme 2.9: Synthesis of *t*-butyl-(*E*)-2-diazo-5-arylpent-4-enoates.

The enantioselective bicyclobutanation of substrates **2-5** to **2-8** at 78 °C in toluene, catalyzed by Rh_2(*S*-PTTL)$_4$ followed by the subsequent homoconjugate azide addition under optimized conditions, proceeded with good yields (Scheme 2.10). Both electron withdrawing and donating groups present on aryl diazo esters were well tolerated. On aqueous quench, cyclobutanes **2-2** and **2-9** to **2-11** were all obtained as an approximately 1:1 mixture of diastereomers. **2-2**, **2-10** and **2-11** could reproducibly be epimerized to mainly a single diastereomer with good yields (> 80% yields). However under the standard epimerization conditions (potassium *tert*-butoxide (KO*t*Bu, 50 mol % in 0.1 M THF) as well as under others attempted using alternate bases, significant amounts of **2-9** decomposed such that recovery yields ranged from 20 – 45%. The diastereomeric ratio of the recovered **2-9** also varied. The electron withdrawing CF_3 group potentially increases the acidity of the benzylic proton to the point of making its abstraction competitive with the proton alpha to the epimerizable center thereby leading to the elimination of hydrazoic acid trace amounts of cyclobutene were recovered from epimerization attempts.

Consistent with studies reported by Panish et al[22a], the one pot procedure yields tend to be slightly higher than the product of the isolated single steps. Also consistent is the retention of the enantioselectivity obtained in the bicyclobutanation reaction through the homoconjugation step. HPLC analysis was conducted on the major diastereomer of **2-2**. This stereoretention holds true for all subsequent one pot procedures to be discussed.

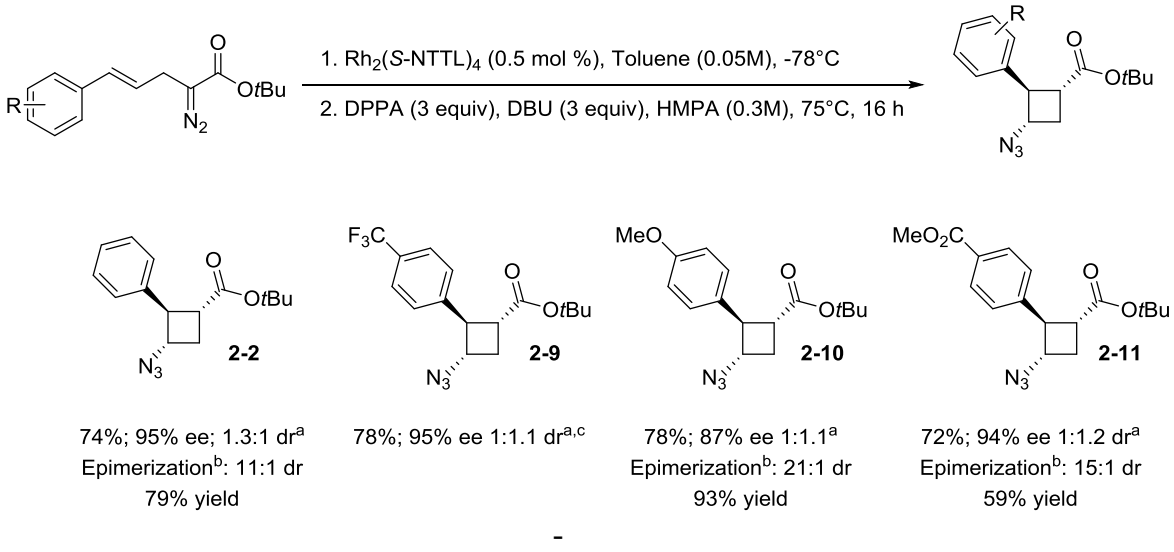

Scheme 2.10: Enantioselective, one flask, multicomponent cyclobutyl-azide synthesis. (a) Determined by ^{1}H NMR analysis (b) Epimerization done in separate experiment using KO*t*Bu (50 mol %) in THF (0.1 M) at r.t. (c) Substrate was not stable under epimerization conditions

2.2.2 Nitrile Addition

With support for the proposed mechanism involved in the addition of azides to BCBs, I investigated whether this mechanism could be harnessed to effect a similar transformation, but with a displaced nitrile anion. Using the commercially available diethyl cyanophosphonate (DEPCN), I screened several conditions, summarized in Table 2.4.

Table 2.4: Optimization of nitrile addition to **2-1**

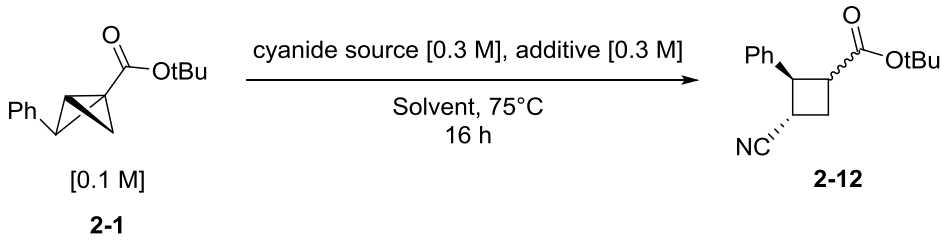

[0.1 M]

2-1

2-12

Entry	Cyanide Source	Additive	Solvent	% Conversion[a]	% **2-12**[a]
1	DEPCN	DBU	Tol/HMPA	34	14
2	DEPCN	DBU	THF/HMPA	70	9
3	DEPCN	DBU	DMF/HMPA	91	9
4	DEPCN	DBU, *t*BuOH	DMF/HMPA	0	0
5	DEPCN	KO*t*Bu	DMF/HMPA	100	75[b]
6	DEPCN	KO*t*Bu	DMF	100	60[b]
8	KCN[c]	-	DMF/HMPA	100	48[b]
9	TMSCN	-	DMF/HMPA	0	0
10	NaCN	-	DMF/HMPA	100	0

(a) Corrected GC values (b) Isolated yield (c) 500g Acros bottle

The optimized conditions determined for azide addition or variations thereof (entries 1-3) were quickly found to be ineffective for the generation of **2-12** in useful yields. While increasing the polarity of the co-solvent resulted in an increased conversion of **2-1**, this was not to the desired product. Ultimately, DBU was found to be minimally effective in liberating cyanide anion to facilitate the formation of **2-12**. Aiming to achieve cyanide liberation under Mitsunobu type conditions, *t*BuOH was added to the reaction (entry 4). However, this approach was unsuccessful. Use of the base potassium KO*t*Bu (entry 5), not only resulted in the full conversion of **2-1** but also afforded **2-12** in good yield, 75%. In the absence of HMPA (entry 6), there was a drop in the yield of **2-12** to 60 %. As with the azide addition reaction, HMPA as a co-

solvent serves to accelerate the rate of addition to **2-1**. In so doing, HMPA minimizes the loss of starting material to unproductive decomposition pathways.

Interestingly, though the displacement of cyanide from DEPCN in effect yields KCN, the use of commercially available KCN (entry 8), resulted in a significantly diminished yield of **2-12** for the single step process, 48%, and was completely ineffective in the one pot protocol, there yielding intractable decomposition products. Potentially, it is the *in situ* generation of a more anhydrous form of KCN that accounts for the superior performance of the DEPCN/KO*t*Bu system. Other sources of cyanide ions screened proved to be unsuccessful in this reaction (entries 9-10).

With the optimized conditions, the substrate scope of the one pot enantioselective bicyclobutanation/homoconjugate nitrile addition protocol was investigated. As DMF/HMPA was found to be the optimal solvent system for nitrile addition, in this one pot protocol, after the bicyclobutanation reaction a solvent swap is conducted simply by removing the toluene *in vacuo* prior to the addition of the cyanide source and base.

As shown in Scheme 2.11, nitrile addition was well tolerated across all substrates studied, ranging from 54 – 80% for the one pot procedure. An additional feature of this reaction is that with the exception of **2-15**, the cyclobutanes obtained after aqueous quench are mainly a single diastereomer.

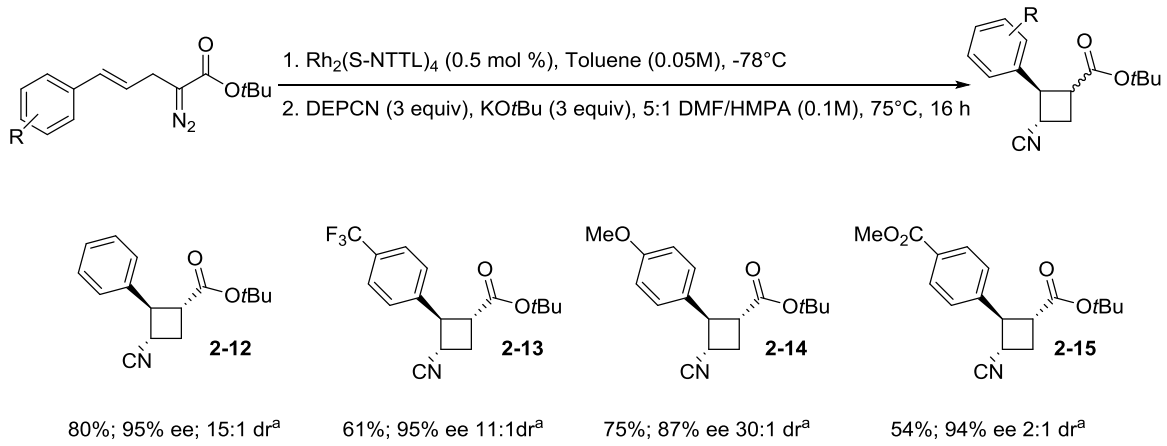

Scheme 2.11: Enantioselective, one flask, multicomponent cyclobutyl-nitrile synthesis. (a) Determined by ^{1}H NMR analysis

2.2.3 Phenoxide Addition

There have been limited reports of the addition of methoxide to carboxylate substituted BCBs[23]. Attempts to adapt the vaguely reported conditions or to investigate a set of conditions for the addition of alkoxides to **2-1** proved unsuccessful.

Thus far, I have described conditions for the addition of moderately soft (N_3^-) and soft ($^-$CN) nucleophiles to bicyclobutanes. Panish has shown that Grignard addition to bicyclobutanes carboxylates requires the addition of catalytic $CuBr{\cdot}SMe_2/PBu_3$, which presumably generates a softer cuprate nucleophile *in situ*[22a]. Phenoxides are considered soft nucleophiles, relative to alkoxides, due to their ability to disperse anionic charge through delocalization. I therefore sought to determine whether this subtle difference could result in productive engagement of phenoxides with the bridgehead C-C bond of BCBs.

Indeed, I was able to determine conditions which allowed for the efficient addition of 4-bromophenol to **2-1** (Table 2.5).

Table 2.5: Optimization of phenoxide addition to **2-1**

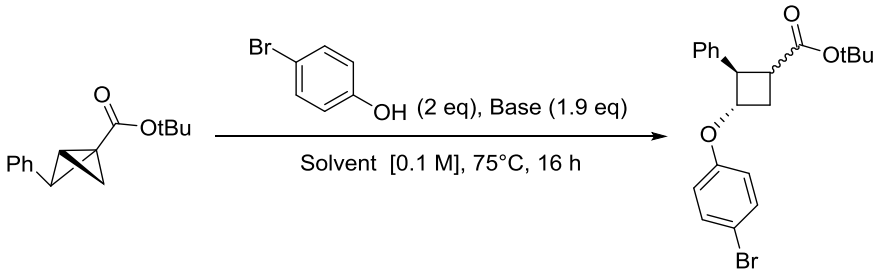

2-1 **2-16**

Entry	Base	Solvent	Observation
1	$Na_{(s)}$	THF	**2-1** decomposition
2	Et_3N or DBU or DIPEA	THF or DMF	no reaction
3	K_2CO_3	THF or DMF	no reaction
4	K_3PO_4	DMF	80 % **2-16**[a]
5	K_3PO_4	DMF/HMPA	85 % **2-16**[a]
6	CsF	DMF/HMPA	75 % **2-16**[a]
7	K_3PO_4	DMF/DMPU	72 % **2-16**[a]

(a) Isolated yield

Neither sodium metal nor non nucleophilic nitrogen bases were able to facilitate the addition of 4-bromophenol to **2-1** (entries 1-4) in THF or DMF as solvents. The only bases able to effect the desired transformation were potassium phosphate (K_3PO_4) and cesium fluoride (CsF) (entries 4-6), with the former being more successful. As is the trend in the addition of nucleophiles previously discussed to **2-1**, HMPA as a co-solvent results in an increased yield: from 80% to 85% (entries 4 vs 5). The less hygroscopic base, CsF is also competent in this reaction, albeit with a slightly diminished yield (75%). Substituting 1,3-dimethyl-3,4,5,6-tetrahydro-2-pyrimidinone (DMPU) into the reaction in lieu of HMPA is possible, but with a slight decrease in overall yield, 72% (entry 7).

Scheme 2.12 describes exploration of the substrate scope of the one pot enantioselective bicyclobutanation/ homoconjugate phenoxide addition protocol. As with the homoconjugate addition of nitriles, the one pot protocol for the addition of phenoxides requires a solvent swap after the bicyclobutanation step. For all substrates, especially **2-20**, where only one diastereomer is obtained, under the described reaction conditions, there is some diastereoselectivity in the initial reaction. Cyclobutanes **2-17** to **2-20** are epimerizable and under the standard conditions, single diastereomers are obtained in good yields. The attenuated yield of the substrate **2-20**, 67% for the phenoxide addition step, is believed to be due to the hydrolysis and subsequent decomposition of the ester moiety under the basic reaction conditions. However, no major side products are isolable or clearly apparent by the analysis of the crude reaction mixture by NMR. Efforts to ameliorate the suspected hydrolysis reaction: lowering reaction temperatures, shortening stirring times and/or using alternate bases proved unsuccessful.

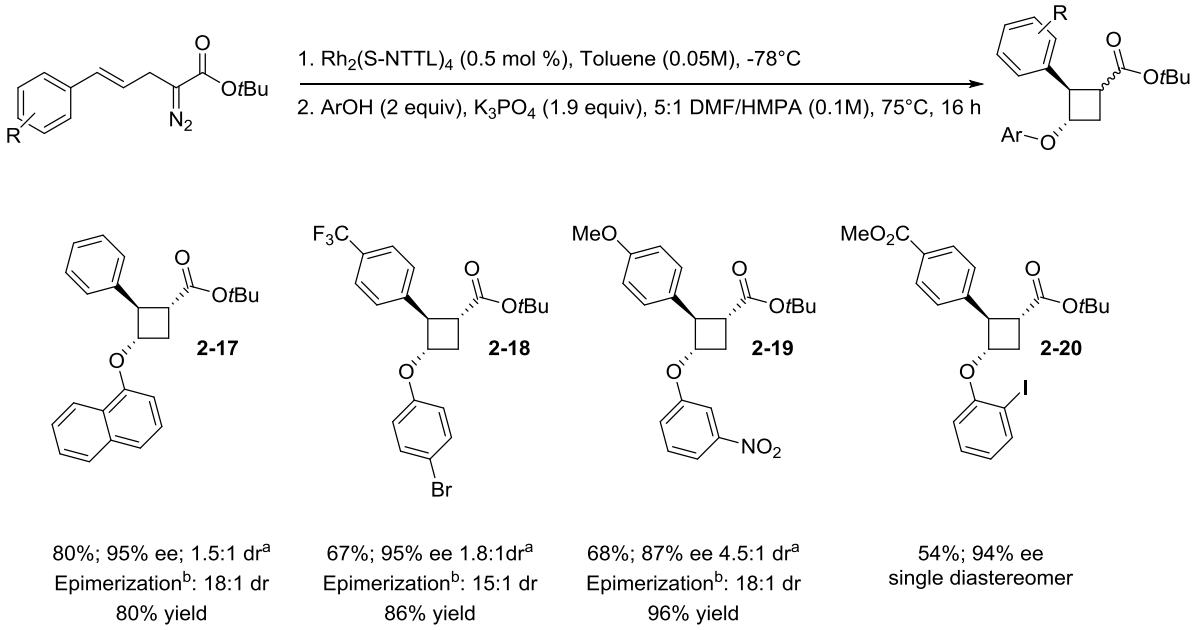

Scheme 2.12: Enantioselective, one flask, multicomponent cyclobutyl-arylether synthesis. (a) Determined by ^{1}H NMR analysis (b) Epimerization done in separate experiment using KO*t*Bu (50 mol %) in THF (0.1 M) at r.t**.**

2.2.4 Thiol Addition

Thiolates are incredibly efficient nucleophiles, and so developing conditions for their addition to bicyclobutanes proved to be fairly straightforward. Efforts are summarized in Table 2.6.

I conducted the thiol addition screen with thiophenol and **2-1**. Interestingly, thiophenol adds to **2-1** even in the absence of a base (entry 1), albeit at a slow rate. Adding the bases Et_3N or K_2CO_3 to the mixture completely arrest the reaction (entries 2 and 3).

Table 2.6: Optimization of thiol addition to **2-1**

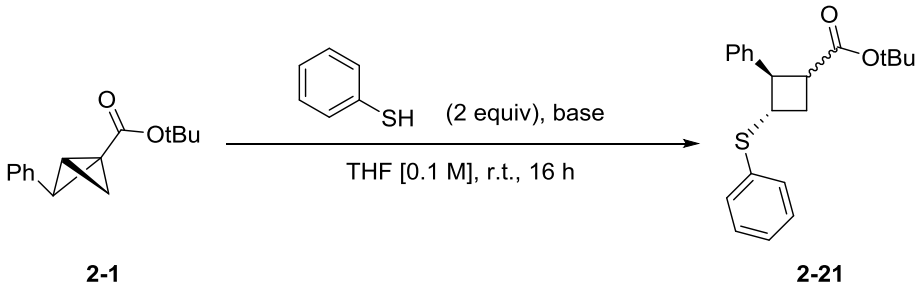

2-1 **2-21**

Entry	Base (eq)	Yield (%) [a]
1	-	50[b]
2	Et_3N (2)	0
3	K_2CO_3 (2)	0
4	KO*t*Bu (2)	64
5	KO*t*Bu (0.2)	87
6	KO*t*Bu (0.2)c	26

(a) Isolated yield (b) Reaction was incomplete after 16 h (c) Conducted in Toluene

KO*t*Bu was found to be the most effective base in this reaction, entry 4, resulting in a 64 % isolated yield of **2-21**. Further, it was found that using catalytic amounts of this base was optimal (entry 5). Toluene was not an effective solvent for this transformation (entry 6) and as such a solvent swap is necessary at the end of the bicyclobutanation reaction prior to the thiol addition, which is still carried out in a single flask.

With the optimized conditions, the substrate scope of the one pot protocol for the enantioselective bicyclobutanation/homoconjugate thiol addition was surveyed (Scheme 2.13).

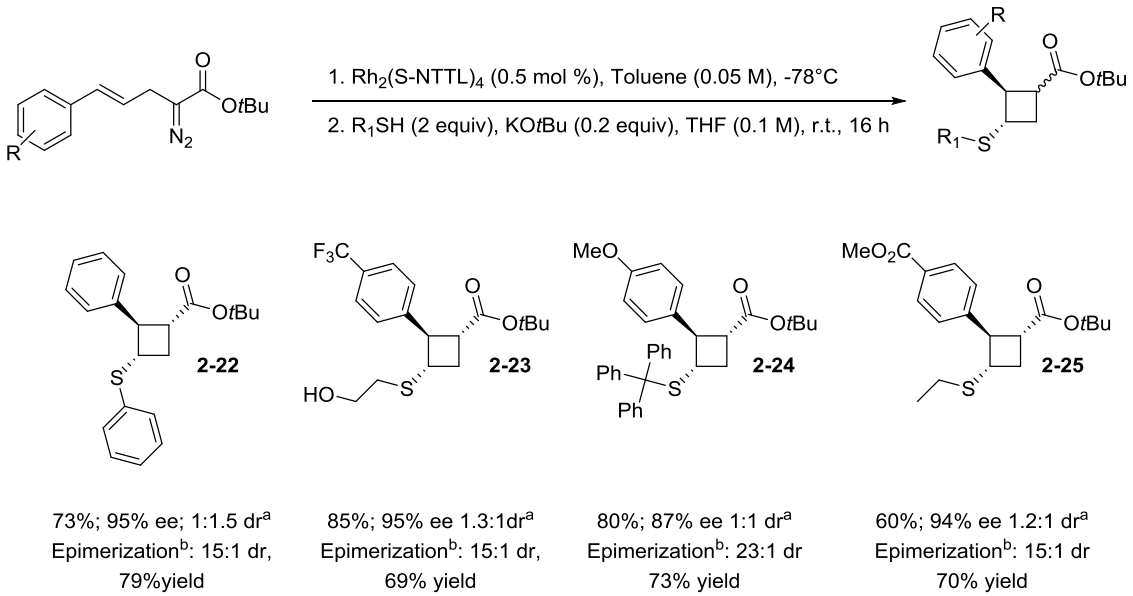

Scheme 2.13: Enantioselective, one flask, multicomponent cyclobutyl-thioether synthesis. (a) Determined by ^{1}H NMR analysis (b) Epimerization done in separate experiment using KO*t*Bu (50 mol %) in THF (0.1 M) at r.t.

The one pot bicyclobutanation/thiolate addition was very efficient across substrates **2-22** to **2-24**, ranging from 60-85% yield . Substrates **2-22** and **2-23** demonstrate that both aryl and alkyl thiols are well tolerated in this transformation and all substrates are readily epimerizable in good yields.

2.2.5 Unsuccessful Nucleophiles

Several other nucleophiles were investigated towards addition to bicyclobutanes. However, I was unable to discern conditions under which the desired transformations were achieved. Scheme 2.14 summarizes the nucleophilic additions attempted.

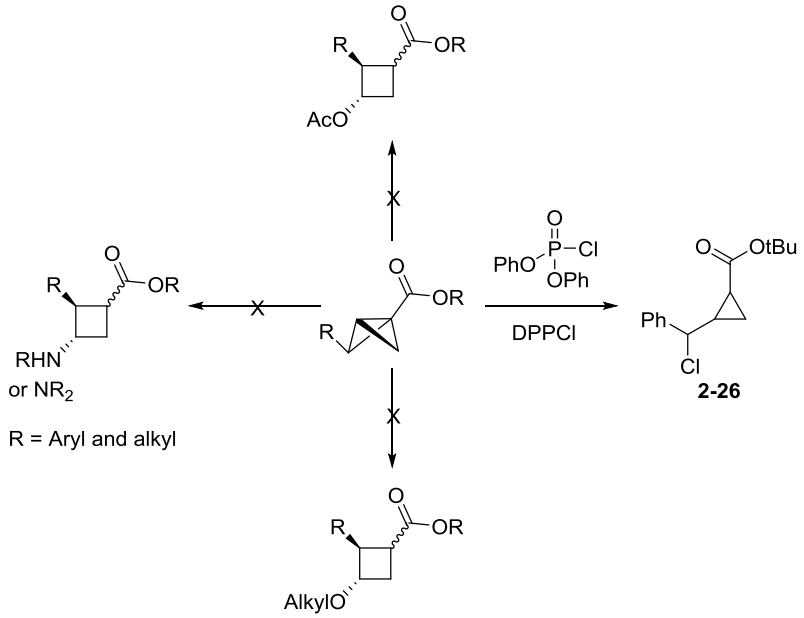

Scheme 2.14: Unsuccessful nucleophiles attempted

Alkoxide and amine based nucleophiles, both considered "hard" nucleophiles, were not successful at the homoconjugation reactions attempted under a wide range of conditions. Attempts to facilitate the addition of acetates across the central BCB bond also proved futile for unapparent reasons. Efforts to elaborate the 'phosphoryl-X' reagent type addition to the addition of the chloride anion using diphenylphosphoryl chloride (DPPCl) were unsuccessful. The major product isolated under an array of reaction conditions screened was cyclopropane **2-26**. Though intriguing mechanistically, this reaction pathway completely obliterates the stereocenter set in the bicyclobutanation step and as such this reaction was not pursued further.

2.2.6 Cyclobutane Substrate Elaboration

Cyclobutane substrates can be further elaborated in a number of ways, two of which are demonstrated in Scheme 2.15. By being able to rapidly assemble densely functionalized, stereochemically defined structures, one can imagine creating a library of these never before enantioselectively accessible organic compounds to screen against biological activity.

The reduction of azide **2-2** proceeded readily to yield the unnatural γ – amino acid **2-27** in 75 %. Also, quenching the *in situ* formed enolate from a 1:1 dr mix of **2-22** with allyl iodide resulted in the formation of cyclobutane **2-28** in good yield, and excellent diastereoselectivity. **2-28** contains a stereodefined quaternary center.

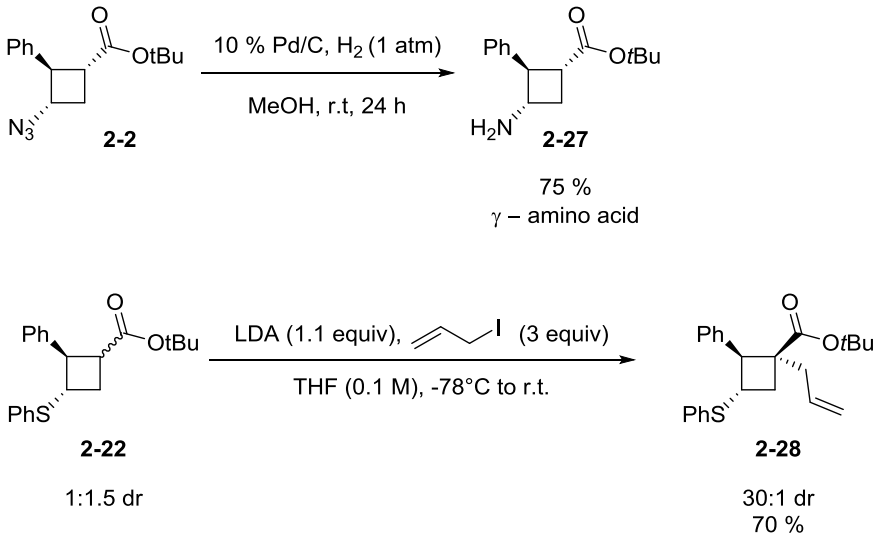

Scheme 2.15: Elaboration of cyclobutane substrates - azide reduction and the formation of a quaternary center through the electrophile quench of an *in situ* formed enolate.

2.3 Conclusion

I have been able to develop single flask procedures for the addition of azides, cyanide, phenoxides and thiols to bicyclobutanes. Further, the protocol for the one pot enantioselective bicyclobutanation/homoconjugate addition of nucleophiles has been expanded to include the addition of heteroatomic nucleophiles. Herein lies the description of a new, soluble and highly nucleophilic azide anion source and some light has been shed on the mode by which it operates.

Cyclobutane assemblies described offer new options for rapidly accessing enantiopure variants of an underexplored class of natural products (Scheme 2.16), a task that once had significant challenges which proved prohibitive to the exploration of their biological activity.

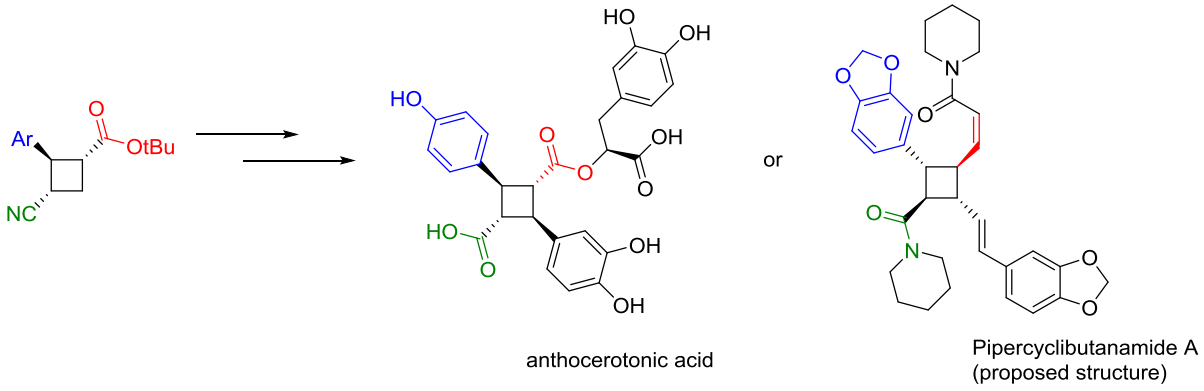

Scheme 2.16: New chemistry offers path to rapidly and efficiently assemble stereodefined cyclobutyl natural products

2.4 Experimental Section

General procedure for cyclobutyl-azide formation

To a flame-dried round bottomed flask was added Rh_2(*S*-NTTL)$_4$ (2 mg, 0.002 mmol, 0.5 mol %). The flask was outfitted with a septum-fitted, gas inlet adapter and evacuated and backfilled with nitrogen three times. Anhydrous toluene was added, and the mixture was stirred under nitrogen at r.t. until the Rh_2(*S*-NTTL)$_4$ had dissolved. The reaction was then cooled in a bath of dry ice/acetone (–78 °C). The appropriate diazoester (1 equiv) was diluted in anhydrous toluene (2 mL) and then added to the reaction flask via syringe pump (1 mL/h) with stirring at –78 °C. After the addition was complete, the reaction was stirred for an additional 10 minutes at –78 °C, and then allowed to warm to RT. A solution of DPPA (3 equiv) in HMPA (1 M with respect to DPPA) was then added followed by the addition of neat DBU (3 equiv). The reaction was warmed to 75 °C and stirred for 16 h. After cooling to room temperature, the reaction was quenched with brine and extracted with EtOAc (3 x 20 mL). The organic layers were collected, dried over magnesium sulfate, filtered and concentrated under reduced pressure. Purification by flash column chromatography (0-4% EtOAc in hexanes) afforded the desired product.

General epimerization procedure

To a 10 mL round bottom flask was added a solution of cyclobutane in THF (0.1 M). KO*t*Bu (50 mol %) was then added and the reaction was stirred at r.t overnight. The reaction was quenched with brine, washed with 1M HCl (10 mL) and extracted Et_2O (3×10 mL). The organic extracts were collected, dried over $MgSO_4$, filtered and concentrated by rotary evaporation. Purification by column chromatography afforded the product.

***tert*-butyl (1*R*,2*R*,3*S*)-3-azido-2-phenylcyclobutane-1-carboxylate** and ***tert*-butyl (1*S*,2*R*,3*S*)-3-azido-2-phenylcyclobutane-1-carboxylate (2-2)**

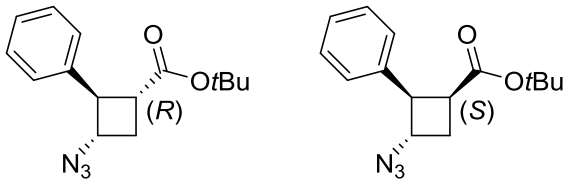

(1*R*)-**2-2** (1*S*)-**2-2**

The general procedure for cyclobutyl-azide formation was followed using *tert*-butyl (*E*)-2-diazo-5-phenylpent-4-enoate (**2-5**, 100 mg, 0.387 mmol). Purification by flash column chromatography using 2% EtOAc in hexanes yielded **2-2** as a pale yellow oil (78 mg, 74% yield, 1:1.3 dr).

The general procedure for epimerization was carried out using the above diastereomers (78 mg, 0.285 mmol), and KO*t*Bu (16.0 mg, 0.143 mmol) in THF (2.90 mL). Flash column chromatography using 2% EtOAc: hexanes furnished ***tert*-butyl (1*R*,2*R*,3*S*)-3-azido-2-phenylcyclobutane-1-carboxylate** as a colorless oil (62 mg, 79% yield, 11:1 dr). $[\alpha]_D^{20}$ +41 (*c* 0.36, $CHCl_3$). FT-IR (NaCl, thin film): 2979, 2098, 1725, 1498, 1449, 1368; 1259, 1238, 1152, 846, 751, 698 HRMS (LIFDI) *m/z*: [M]+ Calcd for $C_{12}H_{19}N_3O_2$ 273.1477; Found 273.1452.

NMR spectral properties assigned to *tert*-butyl (1*R*,2*R*,3*S*)-3-azido-2-phenylcyclobutane-1-carboxylate [(1*R*)-2-2]

^{1}H NMR (400 MHz, $CDCl_3$) δ: 7.42-7.33 (m, 2H), 7.32-7.25 (m, 3H), 3.79 (q, *J* = 8.5 Hz, 1H), 3.71(t, *J* = 9.1 Hz, 1H), 2.87-2.81 (m, 1H), 2.59-2.53 (m, 1H), 2.36-2.28 (m, 1H), 1.49 (s, 9H); ^{13}C NMR (100 MHz, $CDCl_3$) δ: 172.2 (C), 140.0 (C), 128.7 (CH),

127.1 (CH), 126.4 (CH), 81.2 (C), 57.0 (CH), 50.6 (CH), , 38.8 (CH), 29.1 (CH_2), 28.1 (CH_3).

NMR spectral properties assigned to *tert*-butyl (1*S*,2*R*,3*S*)-3-azido-2-phenylcyclobutane-1-carboxylate [(1*S*)-2-2]

^{1}H NMR (400 MHz, $CDCl_3$) δ: 7.42-7.33 (m, 2H), 7.32-7.25 (m, 3H),4.60 (q, *J* = 8.6 Hz, 1H), 3.90 (t, *J* = 10.2 Hz, 1H), 3.36-3.32 (m, 1H), 2.64-2.61 (m, 1H), 2.26-2.21 (m, 1H), 1.09 (s, 9H); ^{13}C NMR (100 MHz, $CDCl_3$) δ: 170.0 (C), 137.4 (C), 128.3 (CH), 127.1 (CH), 127.0 (CH), 80.8 (C), 56.5 (CH), 49.2 (CH), 40.2 (CH), 28.2 (CH_2), 27.6 (CH_3)

***tert*-butyl *(*1*R*,2*R*,3*S*)-3-azido-2-(4-(trifluoromethyl)phenyl)cyclobutane-1-carboxylate and *tert*-butyl *(*1*S*,2*R*,3*S*)-3-azido-2-(4-(trifluoromethyl)phenyl)cyclobutane-1-carboxylate (2-9)**

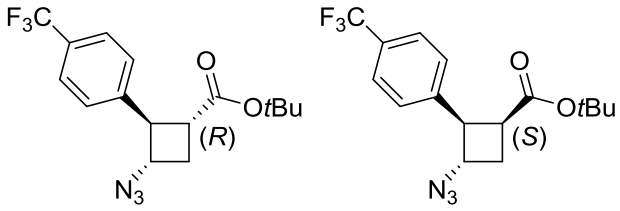

(1*R*)-**2-9** (1*S*)-**2-9**

The general procedure for cyclobutyl-azide formation was followed using *tert*-butyl (*E*)-2-diazo-5-(4-(trifluoromethyl)phenyl)pent-4-enoate (**2-6**, 100 mg, 0.306 mmol). Purification by flash column chromatography using 2% EtOAc in hexanes yielded **2-9** as a pale yellow oil (82 mg, 78% yield, 1:1.1 dr).). FT-IR (NaCl, thin film): 2981, 2101, 1724, 1394, 1369, 1327, 1154, 1127, 1069, 668 HRMS (LIFDI) *m/z*: $[M]^+$ Calcd for $C_{16}H_{18}N_3O_2$ 341.1351; Found 341.1375.

NMR spectral properties assigned to *tert*-butyl *(*1*R*,2*R*,3*S*)-3-azido-2-(4-(trifluoromethyl)phenyl)cyclobutane-1-carboxylate [(1*R*)-2-9]

^{1}H NMR (400 MHz, $CDCl_3$) δ: 7.64-7.59 (m, 2H), 7.42-7.40 (m, 2H), 3.83-3.71 (m, 2H), 2.88-2.81 (m, 1H), 2.65-2.58 (m, 1H), 2.39-2.25 (m, 1H) 1.49 (s, 9H); ^{13}C NMR (100 MHz, $CDCl_3$) δ: 171.7 (C), 144.0 (C), 129.5 (C, q, ^{2}J(CF) = 32 Hz), 126.8 (CH), 125.6 (CH, q, ^{3}J(CF) = 3.8 Hz), 124.1 (C, q, ^{1}J(CF) = 272 Hz), 81.5 (C), 56.8 (CH), 50.3 (CH), 38.6 (CH), 29.2 (CH_2), 28.1 (CH_3); ^{19}F NMR (376 MHz, $CDCl_3$) δ: 62.50

NMR spectral properties assigned to *tert*-butyl *(*1*R*,2*R*,3*S*)-3-azido-2-(4-(trifluoromethyl)phenyl)cyclobutane-1-carboxylate [(1*S*)-2-9]

^{1}H NMR (400 MHz, $CDCl_3$) δ: 7.64-7.59 (m, 2H), 7.42-7.34 (m, 2H), 4.65-4.58 (q, *J* = 8.6 Hz, 2H), 3.95-3.90 (t, *J* = 9.7 Hz, 1H), 3.40-3.35 (m, 1H), 2.65-2.58 (m, 1H), 2.39-2.25 (m, 1H), 1.10 (s, 9H); ^{13}C NMR (100 MHz, $CDCl_3$) δ: 171.7 (C), 141.6 (C), 129.5 (C, q, ^{2}J(CF) = 32 Hz) , 127.5 (CH), 125.3 (CH, q, ^{3}J(CF) = 3.8 Hz), 124.1 (C, q, ^{1}J(CF) = 272 Hz), 81.2 (C), 56.4 (CH), 48.8 (CH), 40.1 (CH), 28.4 (CH_2), 27.6 (CH_3); ^{19}F NMR (376 MHz, $CDCl_3$) δ: 62.55.

***tert*-butyl (1*R*,2*R*,3*S*)-3-azido-2-(4-methoxyphenyl)cyclobutane-1-carboxylate and *tert*-butyl (1*S*,2*R*,3*S*)-3-azido-2-(4-methoxyphenyl)cyclobutane-1-carboxylate (2-10)**

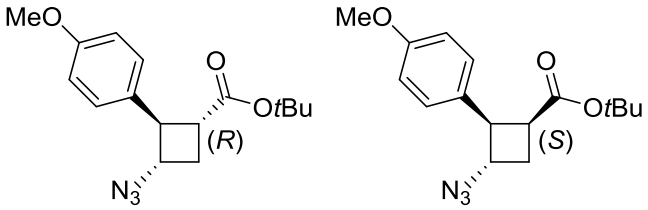

(1*R*)-**3-10** (1*S*)-**3-10**

The general procedure for cyclobutyl-azide formation was followed using *tert*-butyl (*E*)-2-diazo-5-(4-methoxyphenyl)pent-4-enoate (**2-7**, 100 mg, 0.347 mmol). Purification by flash column chromatography using 2% EtOAc in hexanes yielded **2-10** as a yellow oil (82 mg, 78% yield, 1:1.1 dr).

The general procedure for epimerization was carried out using a portion of the above diastereomers (27 mg, 0.09 mmol) and KO*t*Bu (5.0 mg, 0.04 mmol) in THF (1.0 mL). Flash column chromatography using 2% EtOAc: hexanes furnished ***tert*-butyl (1*R*,2*R*,3*S*)-3-azido-2-(4-methoxyphenyl)cyclobutane-1-carboxylate** as a pale yellow oil (25 mg, 93% yield, 21:1 dr based on *tert*- butyl peak integration; 19:1 based on methyl ether peak integration). $[\alpha]_D^{20}$ +30 (*c* 1.0, $CHCl_3$). FT-IR (NaCl, thin film): 2978, 2934, 2099, 1724, 1516, 1252, 1152, 1036, 738, 638 HRMS (LIFDI) *m/z*: $[M]^+$ Calcd for $C_{16}H_{21}N_3O_3$ 303.1583; Found 303.1609.

NMR spectral properties assigned to *tert*-butyl (1*R*,2*R*,3*S*)-3-azido-2-(4-methoxyphenyl)cyclobutane-1-carboxylate [(1*R*)-2-10]

^{1}H NMR (400 MHz, $CDCl_3$) δ:7.21 (d, *J* = 8.6 Hz, 2H), 6.90 (d, *J* = 8.6 Hz, 2H), 3.82 (s, 3H), 3.77-3.71 (m, 1H), 3.62 (t, *J* = 9.1 Hz, 1H), 2.81-2.74 (m, 1H), 2.56-2.50 (m, 1H), 2.32-2.24 (m, 1H), 1.47 (s, 9H); ^{13}C NMR (100 MHz, $CDCl_3$) δ: 172.3 (C), 158.7 (C), 132.1 (C), 127.6 (CH), 114.0 (CH), 81.1 (C), 57.2 (CH), 55.3 (CH_3), 50.2 (CH), 39.2 (CH), 28.9 (CH_2), 28.1 (CH_3)

NMR spectral properties assigned to *tert*-butyl (1*S*,2*R*,3*S*)-3-azido-2-(4-methoxyphenyl)cyclobutane-1-carboxylate [(1*S*)-2-10]

^{1}H NMR (400 MHz, $CDCl_3$) δ: 7.15 (d, *J* = 8.6 Hz, 2H), 6.87 (d, *J* = 8.6 Hz, 2H), 4.54 (q, *J* = 8.7 Hz, 1H), 3.85-3.82 (m, 1H), 3.80 (s, 3H), 3.32-3.28 (m, 1H), 2.63-2.59 (m, 1H), 2.22-2.17 (m, 1H), 1.12 (s, 9H); ^{13}C NMR (100 MHz, $CDCl_3$) δ: 172.1 (C), 158.7 (CH),129.5 (C),128.3 (CH), 113.7 (CH), 80.7 (C), 56.8 (CH), 55.3 (CH_3), 48.7 (CH), 40.4 (CH), 28.0 (CH_2), 27.7 (CH_3)

Methyl-4-((1*R*,2*S*,4*R*)-2-azido-4-(*tert*-butoxycarbonyl)cyclobutyl)benzoate and methyl-4-((1*S*,2*S*,4*R*)-2-azido-4-(*tert*-butoxycarbonyl)cyclobutyl)benzoate (2-11)

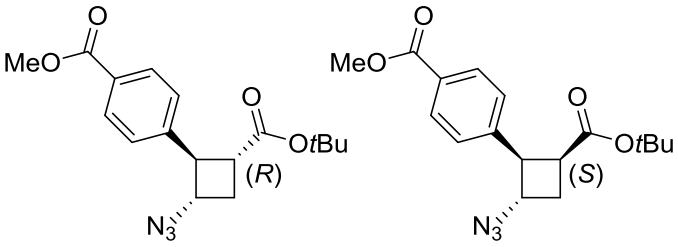

(1*R*)-**3-11** (1*S*)-**3-11**

The general procedure for cyclobutyl-azide formation was followed using methyl *(E)*-4-(5-(*tert*-butoxy)-4-diazo-5-oxopent-1-en-1-yl)benzoate (**2-8**, 100 mg, 0.316 mmol). Purification by flash column chromatography using 2% EtOAc in hexanes yielded **2-11** as a pale yellow oil (75 mg, 72% yield, 1:1.1 dr).

The general procedure for epimerization was carried out using a portion of the above diastereomers (30 mg, 0.09 mmol) and KO*t*Bu (5.0 mg, 0.04 mmol) in THF (1.0 mL). Flash column chromatography using 2% EtOAc: hexanes furnished **methyl 4-((1*R*,2*S*,4*R*)-2-azido-4-(*tert*-butoxycarbonyl)cyclobutyl)benzoate** as a pale yellow oil (22 mg, 75% yield, 15:1 dr). $[\alpha]_D^{20}$ +48 (*c* 0.45, $CHCl_3$). FT-IR (NaCl, thin film):

2979, 2953, 2100, 1724, 1613, 1281, 1153, 1111 HRMS (LIFDI) *m/z*: $[M]^+$ Calcd for $C_{17}H_{21}N_3O_4$ 331.1532; Found 331.1513.

NMR spectral properties assigned to methyl 4-((1*R*,2*S*,4*R*)-2-azido-4-(*tert*-butoxycarbonyl)cyclobutyl)benzoate [(1*R*)-2-11]

^{1}H NMR (600 MHz, $CDCl_3$) δ: 8.03 (d, *J* = 8.2 Hz, 2H), 7.36 (d, *J* = 8.2 Hz, 2H), 3.94 (s, 3H), 3.80 (q, *J* = 8.5 Hz, 1H), 3.73 (t, *J* = 9.2 Hz, 1H), 2.87-2.83 (m, 1H), 2.60-2.55 (m, 1H), 2.37-2.32 (m, 1H), 1.48 (s, 9H); ^{13}C NMR (150 MHz, $CDCl_3$) δ: 171.9 (C), 166.8 (C), 145.1 (C), 130.0 (CH), 129.0 (C), 126.4 (C), 81.4 (C), 56.8 (CH), 52.1 (CH_3), 50.6 (CH), 38.6 (CH), 29.1 (CH_2), 28.1 (CH_3).

NMR spectral properties assigned to methyl 4-((1*S*,2*S*,4*R*)-2-azido-4-(*tert*-butoxycarbonyl)cyclobutyl)benzoate [(1*S*)-2-11]

^{1}H NMR (600 MHz, $CDCl_3$) δ: 8.00 (d, *J* = 8.4 Hz, 2H), 7.30 (d, *J* = 8.4 Hz, 2H), 4.61 (q, *J* = 8.6 Hz, 1H), 3.94 (s, 3H), 3.94-3.90 (m, 1H), 3.39-3.35 (m, 1H), 2.65-2.62 (m, 1H), 2.30-2.25 (m, 1H), 1.10 (s, 9H); ^{13}C NMR (150 MHz, $CDCl_3$) δ: 171.7 (C), 166.8 (C), 142.9 (C), 129.6 (CH), 128.9 (C), 127.1 (CH), 81.1 (C), 56.5 (CH), 52.1 (CH_3), 49.1 (CH), 40.1 (CH), 28.4 (CH_2), 27.7 (CH_3).

General procedure for cyclobutyl-nitrile formation

To a flame-dried round bottomed flask was added Rh_2(*S*-NTTL)$_4$ (2 mg, 0.002 mmol, 0.5 mol %). The flask was outfitted with a septum-fitted, gas inlet adapter and evacuated and backfilled with nitrogen three times. Anhydrous toluene was added, and the mixture was stirred under nitrogen at r.t. until the Rh_2(*S*-NTTL)$_4$ had dissolved.

The reaction was then cooled in a bath of dry ice/acetone (–78 °C). The appropriate diazoester (1.00 equiv) was diluted in anhydrous toluene (2 mL) and then added to the reaction flask via syringe pump (1 mL/h) with stirring at –78 °C. After the addition was complete, the reaction was stirred for an additional 10 minutes at –78 °C, and then allowed to warm to r.t. Toluene was removed *in vacuo* and replaced by a solution of diethyl cyanophosphonate (DEPCN, 3 equiv) in 5:1 mixture of DMF:HMPA (0.1 M). KO*t*Bu (3 equiv) was then added. The reaction was warmed to 75 °C and stirred for 16 h. After cooling to room temperature, the reaction was quenched with brine and extracted with EtOAc (3 x 20 mL). The organic layers were collected, dried over magnesium sulfate, filtered and concentrated under reduced pressure. Purification by flash column chromatography (0-6% EtOAc in hexanes) afforded the desired product.

***tert*-butyl (1*R*,2*R*,3*S*)-3-cyano-2-phenylcyclobutane-1-carboxylate** and ***tert*-butyl (1*S*,2*R*,3*S*)-3-cyano-2-phenylcyclobutane-1-carboxylate (2-12)**

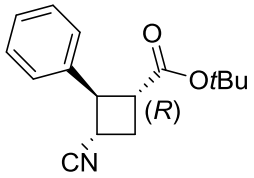

(1*R*)-**2-12**

The general procedure for cyclobutyl-nitrile formation was followed using *tert*-butyl (*E*)-2-diazo-5-phenylpent-4-enoate (**2-5**, 100 mg, 0.387 mmol). Purification by flash column chromatography using 2% EtOAc in hexanes yielded **2-12** as a white solid as a white solid (80 mg, 80% yield, 15:1 dr). mp 112-114 °C. $[\alpha]_D^{20}$ +21 (*c* 1.1, $CHCl_3$). ^1H NMR (400 MHz, $CDCl_3$) δ: 7.40-7.36 (m, 2H), 7.33-7.29 (m, 3H). 4.03 (t, *J* = 9.8

Hz, 1H), 3.17 (q, *J* = 9.5 Hz, 1H), 3.07 (q, *J* = 9.5 Hz, 1H), 2.63-2.57 (m, 2H), 1.48 (s, 9H); ^{13}C NMR (100 MHz, $CDCl_3$) δ: 171.4 (C), 139.5 (C), 128.8 (CH), 127.6 (CH), 126.1 (CH), 120.6 (C), 81.6 (C), 47.7 (CH), 43.4 (CH), 28.0 (CH_3), 26.3 (CH_2), 25.2 (CH). FT-IR (NaCl, thin film) 3003, 2978, 2934, 2238, 1725, 1369, 1242, 1154, 845, 749, 698: HRMS (LIFDI) *m/z*: [M]+ Calcd for $C_{16}H_{19}NO_2$ 257.1416; Found 257.1434

***tert*-butyl (1*R*,2*R*,3*S*)-3-cyano-2-(4-(trifluoromethyl)phenyl)cyclobutane-1-carboxylate** and ***tert*-butyl (1*S*,2*R*,3*S*)-3-cyano-2-(4-(trifluoromethyl)phenyl)cyclobutane-1-carboxylate (2-13)**

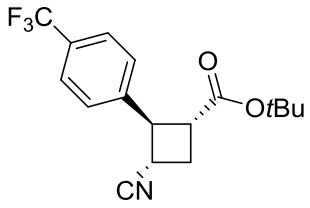

(1*R*)-**2-13**

The general procedure for cyclobutyl-nitrile formation was followed using *tert*-butyl (*E*)-2-diazo-5-(4-(trifluoromethyl)phenyl)pent-4-enoate (**2-6**, 100 mg, 0.306 mmol). Purification by flash column chromatography using 6% EtOAc in hexanes yielded **2-13** as a yellow oil (61 mg, 61% yield, 11:1 dr). The purity by ^{1}H NMR was estimated to be 90%. $[\alpha]_D^{20}$ +6.3 (*c* 1.3, $CHCl_3$). ^{1}H NMR (400 MHz, $CDCl_3$) δ: 7.65 (d, *J* = 8.3 Hz, 2H), 7.42 (d, *J* = 8.0 Hz, 2H), 4.08 (t, *J* = 10.0 Hz, 1H), 3.18 (q, *J* = 9.5 Hz, 1H), 3.08 (q, *J* = 9.5 Hz, 1H), 2.65-2.59 (m, 2H), 1.49 (s, 9H); ^{13}C NMR (100 MHz, $CDCl_3$) δ: 171.0 (C), 143.3 (C), 130.0 (C, q, ^2J(CF) = 33.1 Hz), 126.5 (CH), 125.8 (CH, q, ^3J(CF) = 3.8 Hz), 124.0 (C, q, ^1J(CF) = 272 Hz), 120.2 (C), 82.0 (C), 47.3 (CH), 43.2 (CH), 28.0 (CH_3), 26.4 (CH_2), 24.7 (CH); ^{19}F NMR (376 MHz, $CDCl_3$) δ: -

62.59. FT-IR (NaCl, thin film) 2980, 2935, 2240, 1726, 1620, 1328, 1163, 1126, 1069, 1018, 845: HRMS (LIFDI) *m/z*: [M]+ Calcd for $C_{17}H_{18}F_3NO_2$ 325.1290; Found 325.1264

tert-butyl (1*R*,2*R*,3*S*)-3-cyano-2-(4-methoxyphenyl)cyclobutane-1-carboxylate (2-14)

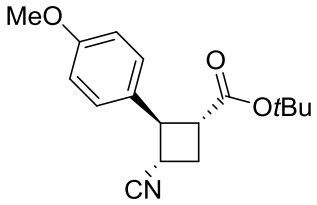

(1*R*)-**2-14**

The general procedure for cyclobutyl-azide formation was followed using *tert*-butyl (*E*)-2-diazo-5-(4-methoxyphenyl)pent-4-enoate (**2-7**, 100 mg, 0.347 mmol). Purification by flash column chromatography using 6% EtOAc in hexanes yielded **2-14** as an off-white solid (74 mg, 75 % yield, 30:1 dr). mp 76-78 °C. $[\alpha]_D^{20}$ +8.7 (*c* 1.8, $CHCl_3$). The purity by ^{1}H NMR was estimated to be 87% ^{1}H NMR (400 MHz, $CDCl_3$) δ: 7.25-7.20 (m, 2H), 6.95-6.89 (m, 2H, 3.95 (t, *J* = 9.8 Hz, 1H), 3.83 (s, 3H), 3.12 (q, *J* = 9.4 Hz, 1H), 3.01 (q, *J* = 9.4 Hz, 1H), 2.56 (t, *J* = 9.5 Hz, 2H), 1.47 (s, 9H); ^{13}C NMR (100 MHz, $CDCl_3$) δ: 171.4 (C), 159.0 (C), 131.5 (C), 127.3 (CH), 120.7 (C), 114.1 (CH), 81.5 (C), 55.3 (CH_3), 47.4 (CH), 43.7 (CH), 28.0 (CH_3), 26.1 (CH_2), 25.5 (CH). FT-IR (NaCl, thin film): 2978, 2237, 1724, 1516, 1253, 1179, 1154, 1034, 738, HRMS (LIFDI) *m/z*: $[M]^+$ Calcd for $C_{17}H_{21}NO_3$ 287.1521; Found 287.1528

methyl 4-((1*R*,2*R*,4*S*)-2-(*tert*-butoxycarbonyl)-4-cyanocyclobutyl)benzoate and **methyl 4-((1*S*,2*R*,4*S*)-2-(*tert*-butoxycarbonyl)-4-cyanocyclobutyl)benzoate (2-15)**

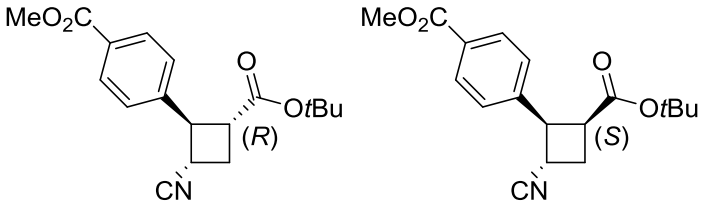

(1*R*)-**2-15** (1*S*)-**2-15**

The general procedure for cyclobutyl-azide formation was followed using methyl *(E)*-4-(5-(*tert*-butoxy)-4-diazo-5-oxopent-1-en-1-yl)benzoate (**2-7**, 100 mg, 0.316 mmol). Purification by flash column chromatography using 2% EtOAc in hexanes yielded **2-15** as a pale yellow oil (53 mg, 54% yield, 2:1 dr). The purity by ^{1}H NMR was estimated to be 85%. FT-IR (NaCl, thin film): 2978, 2239, 1724, 1282, 1154, 1112, 1020, 845, 761 HRMS (LIFDI) *m/z*: $[M]^{+}$ Calcd for $C_{18}H_{21}NO_4$ 315.1471; Found 315.1484

NMR spectral properties assigned to methyl 4-((1*R*,2*R*,4*S*)-2-(*tert*-butoxycarbonyl)-4-cyanocyclobutyl)benzoate [(1*R*)-2-15]

^{1}H NMR (600 MHz, $CDCl_3$) δ: 8.05 (d, *J* = 8.2 Hz, 2H), 7.37 (d, *J* = 8.3 Hz, 2H), 4.07(t, *J* = 10.4 Hz, 1H), 3.94 (s, 3H), 3.18 (q, *J* = 9.5 Hz, 1H), 3.09 (q, *J* = 9.5 Hz, 1H), 2.64-2.58 (m, 2H); ^{13}C NMR (150 MHz, $CDCl_3$) δ: 171.0 (C), 166.59 (C), 144.3 (C), 130.1 (CH), 129.5 (C), 126.1 (CH), 120.2 (C), 81.9 (C), 52.2 (CH_3), 47.6 (C), 43.2 (C), 28.0 (CH_3), 26.4 (CH_2), 25.0 (CH).

NMR spectral properties assigned to methyl 4-((1*S*,2*R*,4*S*)-2-(*tert*-butoxycarbonyl)-4-cyanocyclobutyl)benzoate [(1*S*)-2-15]

^{1}H NMR (600 MHz, $CDCl_3$) δ:8.03 (d, *J* = 8.2 Hz, 2H), 7.27 (d, *J* = 8.4 Hz, 2H), 4.28 (t, *J* = 10.8 Hz, 1H), 3.94 (s, 3H), 3.87-3.82 (m, 1H), 3.50-3.46 (m, 1H), 2.72-2.68 (m, 1H), 2.35-2.55 (m, 1H); ; ^{13}C NMR (100 MHz, $CDCl_3$) δ: 170.8 (C), 166.61 (C), 141.9 (C), 129.7 (CH), 129.4 (C), 126.9 (CH), 81.6 (C), 52.2 (CH_3), 46.1 (CH), 43.5 (CH), 27.6 (CH_3), 25.6 (CH_2), 24.5 (CH).

General procedure for cyclobutyl-aryl ether formation

To a flame-dried round bottomed flask was added Rh_2(*S*-NTTL)$_4$ (2 mg, 0.002 mmol, 0.5 mol %). The flask was outfitted with a septum-fitted, gas inlet adapter and evacuated and backfilled with nitrogen three times. Anhydrous toluene was added, and the mixture was stirred under nitrogen at r.t. until the Rh_2(*S*-NTTL)$_4$ had dissolved. The reaction was then cooled in a bath of dry ice/acetone (–78 °C). The appropriate diazoester (1equiv) was diluted in anhydrous toluene (2 mL, final reaction concentration 0.05 M) and then added to the reaction flask via syringe pump (1 mL/h) with stirring at –78 °C. After the addition was complete, the reaction was stirred for an additional 10 minutes at –78 °C, and then allowed to warm to r.t. Toluene was removed *in vacuo* and replaced by a 5:1 mixture of DMF:HMPA (0.1 M). The appropriate phenol (2 equiv) was added followed by K_3PO_4 (1.9 equiv). The reaction was warmed to 75˚C and stirred for 16 h. After cooling to room temperature, the reaction was quenched with brine and extracted thrice with EtOAc (3 x 20 mL). The organic layers were collected, dried over magnesium sulfate and concentrated under reduced pressure. Purification by flash column chromatography (0-6% EtOAc in hexanes) afforded the desired product.

***tert*-butyl (1*R*,2*R*,3*S*)-3-(naphthalen-1-yloxy)-2-phenylcyclobutane-1-carboxylate and *tert*-butyl (1*S*,2*R*,3*S*)-3-(naphthalen-1-yloxy)-2-phenylcyclobutane-1-carboxylate (2-17)**

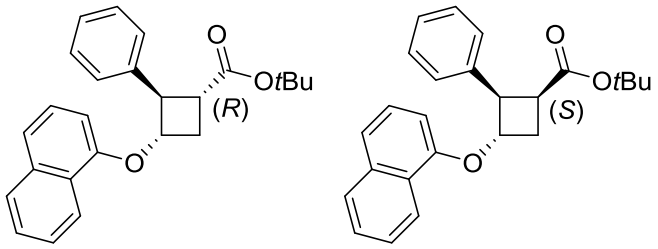

(1*R*)-**2-17** (1*S*)-**2-17**

The general procedure for cyclobutyl-aryl ether formation was followed using *tert*-butyl (*E*)-2-diazo-5-phenylpent-4-enoate (**2-5**, 100 mg, 0.387 mmol), 2-naphthol (112 mg, 0.744 mmol) and K_3PO_4 (160 mg, 0.735 mmol) Purification by flash column chromatography using 2% EtOAc in hexanes yielded **2-17** as a yellow oil (117 mg, 80% yield, 1.5:1 dr).

The general procedure for epimerization was carried out using a portion of the above diastereomers (55 mg, 0.15 mmol) and KO*t*Bu (33 mg, 0.29 mmol) in THF (1.5 mL). Flash column chromatography using 2% EtOAc: hexanes furnished ***tert*-butyl (1*R*,2*R*,3*S*)-3-(naphthalen-1-yloxy)-2-phenylcyclobutane-1-carboxylate** as a yellow oil (44 mg, 80% yield, 18:1 dr). $[\alpha]_D^{20}$ –33 (*c* 1.5, $CHCl_3$). FT-IR (NaCl, thin film) 3060, 2977, 1724, 1629, 1257, 1152, 841, 748: HRMS (LIFDI) *m/z*: [M]+ Calcd for $C_{25}H_{26}O_3$ 374.1882; Found 374.1873

NMR spectral properties assigned to *tert*-butyl (1*R*,2*R*,3*S*)-3-(naphthalen-1-yloxy)-2-phenylcyclobutane-1-carboxylate [(1*R*)-2-17]

^{1}H NMR (400 MHz, $CDCl_3$) δ: 7.76 (t, *J* = 8.8 Hz, 2H), 7.55 (d, *J* = 8.0 Hz, 1H); 7.45-7.34 (m, 7H), 7.15 (dd, *J* = 8.9, 2.5 Hz, 1H), 6.92 (d, *J* = 2.5 Hz, 1H), 4.83-4.77 (m, 1H), 3.95 (t, *J* = 8.1 Hz, 1H), 2.93-2.86 (m, 2H), 2.46-2.39 (m, 1H), 1.50 (s, 9H); ^{13}C NMR (100 MHz, $CDCl_3$) δ: 172.7 (C), 155.1 (C), 140.8 (C), 134.3 (C), 129.5 (CH), 129.0 (C), 128.6 (CH), 127.6 (CH), 127.0 (CH), 126.8 (CH), 126.7 (CH), 126.4 (CH), 123.7(CH), 119.0 (CH), 108.2 (CH), 80.9 (C), 73.6 (CH), 51.7 (CH), 38.0 (CH), 31.4 (CH_2), 28.1 (CH_3).

NMR spectral properties assigned to *tert*-butyl (1*S*,2*R*,3*S*)-3-(naphthalen-1-yloxy)-2-phenylcyclobutane-1-carboxylate [(1*S*)-2-17]

^{1}H NMR (400 MHz, $CDCl_3$) δ: 7.75 (t, *J* = 9.2 Hz, 2H), 7.68 (d, *J* = 8.2 Hz, 1H), 7.54-7.24 (m, 7H), 7.15-7.12 (m, 2H), 5.48 (q, *J* = 7.5 Hz, 1H), 4.17 (dd, *J* = 7.8, 2.7 Hz), 3.50-3.46 (m, 1H), 3.00-2.96 (m, 1H), 2.31-2.26 (m, 1H); ^{13}C NMR (100 MHz, $CDCl_3$) δ: 172.8 (C), 155.1 (C), 137.9 (C), 134.5 (C), 129.5 (CH), 129.0 (C), 128.3 (CH), 127.5 (CH), 126.9 (CH), 126.8 (CH), 126.7 (CH), 126.4 (CH), 123.7 (CH), 119.0 (CH), 107.9 (CH), 80.7 (C), 72.9 (CH), 49.9 (CH), 39.5 (CH), 30.5 (CH_2), 27.7 (CH_3)

***tert*-butyl (1*R*,2*R*,3*S*)-3-(4-bromophenoxy)-2-(4-(trifluoromethyl)phenyl)cyclobutane-1-carboxylate and *tert*-butyl (1*S*,2*R*,3*S*)-3-(4-bromophenoxy)-2-(4-(trifluoromethyl)phenyl)cyclobutane-1-carboxylate (2-18)**

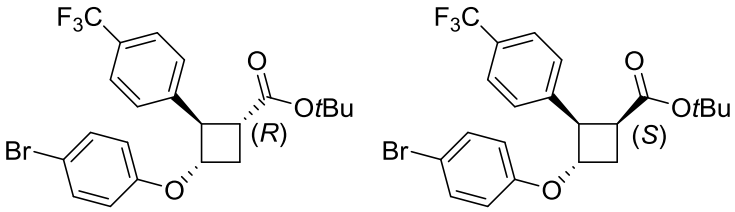

(1*R*)-**2-18** (1*S*)-**2-18**

The general procedure for cyclobutyl-aryl ether formation was followed using *tert*-butyl (*E*)-2-diazo-5-(4-(trifluoromethyl)phenyl)pent-4-enoate (**2-6**, 100 mg, 0.306 mmol), 4-bromophenol (110 mg, 0.636 mmol) and K_3PO_4 (123 mg, 0.581 mmol). Purification by flash column chromatography using 4% EtOAc in hexanes yielded **2-18** as a yellow solid (100 mg, 67% yield, 1.8:1 dr).

The general procedure for epimerization was carried out using a portion of the above diastereomers (91 mg, 0.19 mmol) and KO*t*Bu (11 mg, 0.10 mmol) in THF (1.9 mL). Flash column chromatography using 2% EtOAc: hexanes furnished ***tert*-butyl (1*R*,2*R*, 3*S*)-3-(4-bromophenoxy)-2-(4-(trifluoromethyl)phenyl)cyclobutane-1-carboxylate** as a pale yellow solid (78 mg, 86%, 15:1 dr). mp 102-4 °C. $[\alpha]_D^{20}$ +24 (*c* 1.7, $CHCl_3$). FT-IR (NaCl, thin film): 2979, 1724, 1488, 1326, 1242, 1160, 1125, 1067, 1018, 823 HRMS (LIFDI) *m/z*: $[M]^+$ Calcd for $C_{22}H_{22}BrF_3O_3$ 472.0684; Found 472.0663.

NMR spectral properties assigned to *tert*-butyl (1*R*,2*R*,3*S*)-3-(4-bromophenoxy)-2-(4-(trifluoromethyl)phenyl)cyclobutane-1-carboxylate [(1*R*)-2-18]

^{1}H NMR (400 MHz, $CDCl_3$) δ: 7.61 (d, J = 8.1 Hz, 2H), 7.45 (d, *J* = 8.0 Hz, 2H), 7.36 (d, *J* = 9.3 Hz, 2H), 6.70 (d, *J* = 8.7 Hz , 2H), 4.59 (q, *J* = 7.8 Hz, 1H), 3.93 (t, *J* = 8.7 Hz, 1H), 2.87-2.75 (m, 2H), 2.37-2.30 (m, 1H), 1.49 (s, 9H; ^{13}C NMR (100 MHz, $CDCl_3$) δ:172.2 (C), 156.1 (C), 144.5 (C), 132.4 (CH), 129.3 (C, q, ^2J(CF) = 32.4 Hz),

127.0 (CH), 125.6 (CH, q, ^{3}J(CF) = 3.8 Hz), 124.1 (C, q, ^{1}J(CF) = 272 Hz), 117.1 (CH), 113.6 (C), 81.4 (C), 73.2 (CH), 51.0 (CH), 37.5 (CH), 31.5 (CH_2), 28.1 (CH_3); ^{19}F NMR (376 MHz, $CDCl_3$) δ: 62.4..

NMR spectral properties assigned to *tert*-butyl (1*S*,2*R*,3*S*)-3-(4-bromophenoxy)-2-(4-(trifluoromethyl)phenyl)cyclobutane-1-carboxylate [(1*S*)-2-18]

^{1}H NMR (400 MHz, $CDCl_3$) δ: 7.59 (d, *J* = 8.0 Hz, 2H), 7.40-7.34 (m, 4H), 6.77 (d, *J* = 8.8 Hz, 2H), 5.29 (q, *J* = 7.6 Hz, 1H), 4.12-4.11 (m, 1H), 3.47-3.43 (m, 1H), 2.85-2.75 (m, 1H), 2.26-2.21 (m, 1H), 1.12 (s, 9H); ^{13}C NMR (100 MHz, $CDCl_3$) δ: 172.3 (C), 156.2 (C), 141.9 (C), 132.5 (CH), 129.3 (C, q, ^{2}J(CF) = 32.4 Hz), 127.7 (CH), 125.2 (CH, q, ^{3}J(CF) = 3.8 Hz), 124.1 (C, q, ^{1}J(CF) = 272 Hz), 116.9 (CH), 113.4 (C), 81.2 (C), 72.9 (CH), 49.3 (CH), 39.2 (CH), 30.6 (CH_2), 27.7 (CH_3); ^{19}F NMR (376 MHz, $CDCl_3$) δ: 62.5.

***tert*-butyl (1*R*,2*R*,3*S*)-2-(4-methoxyphenyl)-3-(3-nitrophenoxy)cyclobutane-1-carboxylate and *tert*-butyl (1*R*,2*R*,3*S*)-2-(4-methoxyphenyl)-3-(3-nitrophenoxy)cyclobutane-1-carboxylate (2-19)**

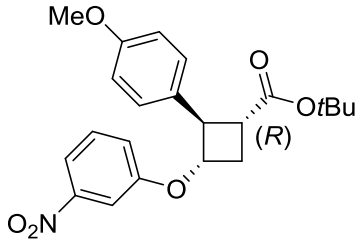

(1*R*)-**2-19**

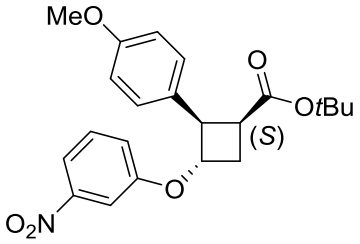

(1*S*)-**2-19**

The general procedure for cyclobutyl-aryl ether formation was followed using *tert*-butyl (*E*)-2-diazo-5-(4-methoxyphenyl)pent-4-enoate (**2-7**, 100 mg, 0.347 mmol), 3-

nitrophenol (97 mg, 0.69 mmol) and K_3PO_4 (140 mg, 0.66 mmol). Purification by flash column chromatography using 5% EtOAc in hexanes yielded **2-19** as a yellow oil (94 mg, 68 % yield, 4.5:1 dr).

The general procedure for epimerization was carried out using a portion of the above diastereomers (47 mg, 0.12 mmol), and KO*t*Bu (7 mg, 0.06 mmol) in THF (1.2 mL). Flash column chromatography using 5% EtOAc: hexanes furnished ***tert*-butyl (1*R*,2*R*,3*S*)-2-(4-methoxyphenyl)-3-(3-nitrophenoxy)cyclobutane-1-carboxylate** as a pale yellow solid (45 mg, 96% yield, 18:1 dr). mp 111 °C. $[\alpha]_D^{20}$ +9.0 (*c* 1.7, $CHCl_3$). FT-IR (NaCl, thin film) 2977, 1723, 1531, 1516, 1351, 1247, 1152, 1036, 815, 737: HRMS (LIFDI) *m/z*: [M]+ Calcd for $C_{25}H_{26}O_3$ 374.1882; Found 374.1873

NMR spectral properties assigned to *tert*-butyl (1*R*,2*R*,3*S*)-2-(4-methoxyphenyl)-3-(3-nitrophenoxy)cyclobutane-1-carboxylate [(1*R*)-2-19]

^{1}H NMR (400 MHz, $CDCl_3$) δ:7.82-7.80 (m, 1H,), 7.60 (t *J* = 2.3 Hz, 1H), 7.39 (t, *J* = 8.2 Hz, 1H), 7.28-7.25 (m, 2H), 7.15-7.12 (m, 1H), 6.91 (d, *J* = 8.6 Hz, 2H), 4.69-4.63 (m, 1H), 3.84-3.80, m, 1H), 3.82 (s, 3H), 2.86-2.78 (m, 2H), 2.35-2.7 (m, 1H), 1.47 (s, 9H);^{13}C NMR (100 MHz, $CDCl_3$) δ:172.3 (C), 158.8 (C), 157.8 (C), 149.1 (C), 132.2 (C), 130.0 (CH), 127.8 (CH), 122.1 (CH), 115.9 (CH), 114.0 (CH), 109.7 (CH), 80.8 (C), 74.3 (CH), 55.2 (CH_3), 51.1 (CH), 38.0 (CH), 30.7 (CH_2), 27.9 (CH_3).

NMR spectral properties assigned to *tert*-butyl (1*S*,2*R*,3*S*)-2-(4-methoxyphenyl)-3-(3-nitrophenoxy)cyclobutane-1-carboxylate [(1*S*)-2-19]

^{1}H NMR (400 MHz, $CDCl_3$) δ: 7.84-7.80 (m, 1H), 7.72-7.70 (m, 1H), 7.43-7.42 (m, 1H), 7.22-7.18 (m, 3H), 6.89-6.87 (m, 2H), 5.33 (q, *J* = 7.6 Hz, 1H), 4.07-4.04 (m,

1H), 3.44-3.40 (m, 1H), 2.92-2.88 (m, 1H), 2.24-2.20 (m, 1H); ^{13}C NMR (100 MHz, $CDCl_3$) δ: 172.5 (C), 158.8 (C), 157.9 (C), 149.2 (C), 130.1 (CH), 129.4 (C), 128.6 (CH), 121.7 (CH), 115.9 (CH), 113.8 (CH), 110.0 (CH), 80.9 (C), 74.0 (CH), 55.4 (CH_3), 49.3 (CH), 39.5 (CH), 30.0 (CH_2), 27.8 (CH_3).

methyl 4-((1*R*,2*R*,4*S*)-2-(*tert*-butoxycarbonyl)-4-(2-iodophenoxy)cyclobutyl)benzoate (2-20)

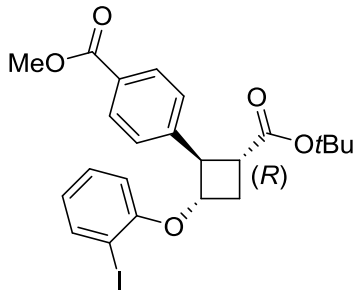

(1*R*)-**2-20**

The general procedure for cyclobutyl-aryl ether formation was followed using methyl *(E)*-4-(5-(*tert*-butoxy)-4-diazo-5-oxopent-1-en-1-yl)benzoate (**2-8**, 100. mg, 0.316 mmol), 2-iodophenol (140 mg, 0.63 mmol) and K_3PO_4 (130. g, 0.600 mmol). Purification by flash column chromatography using 6% EtOAc in hexanes yielded **2-20** as a white solid and a single diastereomer (90 mg, 56 % yield). mp 78-84 °C. The purity by ^{1}H NMR was estimated to be 95%. (Unreacted iodophenol was observed by ^{1}H NMR). $[\alpha]_D^{20}$ +48 (*c* 0.49, $CHCl_3$). **1**H NMR (400 MHz, $CDCl_3$) δ: 8.03 (d, *J* = 8.3 Hz, 2H), 7.79 (dd, *J* = 7.8, 1.6 Hz, 1H), 7.46 (d, *J* = 7.8 Hz, 2H), 7.22-7.18 (m, 1H), 6.73 (td, *J* = 7.7 Hz, 1.2 Hz, 1H), 6.62 (dd, *J* = 8.2, 1.3 Hz, 1H), 4.58 (q, *J* = 7.6 Hz, 1H), 4.05 (t, *J* = 8.6 Hz, 1H), 3.93 (s, 3H), 2.92-2.82 (m, 1H), 2.82-2.76 (m, 1H), 2.50-2.43 (m, 1H), 1.19 (s, 9H); ^{13}C NMR (100 MHz, $CDCl_3$) δ:172.2 (C), 166.9 (C), 156.2

(C), 145.7 (C), 139.7 (CH), 129.9 (CH), 129.4 (CH), 128.8 (C), 126.7 (CH), 123.2 (CH), 113.6 (CH), 87.0 (C), 81.3 (C), 74.8 (CH), 52.1 (CH), 51.5 (CH_3), 37.1 (CH), 31.7 (CH_2), 28.1 (CH_3). FT-IR (NaCl, thin film) 2976, 1722, 1471, 1437, 1279, 1245, 1152: HRMS (LIFDI) *m/z*: [M]+ Calcd for $C_{23}H_{25}IO_5$ 508.0747; Found 508.0740

General procedure for cyclobutyl-thioether formation

To a flame-dried round bottomed flask was added Rh_2(*S*-NTTL)$_4$ (2 mg, 0.002 mmol, 0.5 mol %). The flask was outfitted with a septum-fitted, gas inlet adapter and evacuated and backfilled with nitrogen three times. Anhydrous toluene was added, and the mixture was stirred under nitrogen at r.t. until the Rh_2(*S*-NTTL)$_4$ had dissolved. The reaction was then cooled in a bath of dry ice/acetone (–78 °C). The appropriate diazoester (1 equiv) was diluted in anhydrous toluene (2 mL, final reaction concentration 0.05 M) and then added to the reaction flask via syringe pump (1 mL/h) with stirring at –78 °C. After the addition was complete, the reaction was stirred for an additional 10 minutes at –78 °C, and then allowed to warm to r.t. Toluene was removed *in vacuo* and replaced by a solution of the appropriate thiol (2 equiv) in anhydrous THF (0.1 M). After the addition of KO*t*Bu (0.2 equiv), the reaction was stirred at r.t. for 16 h then concentrated directly on to silica gel. Purification by flash column chromatography (0-50% EtOAc in hexanes) afforded the desired product.

***tert*-butyl (1*R*,2*R*,3*S*)-2-phenyl-3-(phenylthio)cyclobutane-1-carboxylate** and ***tert*-butyl (1*S*,2*R*,3*S*)-2-phenyl-3-(phenylthio)cyclobutane-1-carboxylate (2-22)**

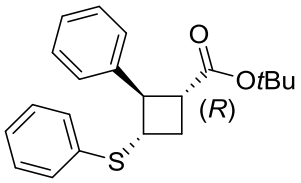

(1*R*)-**2-22**

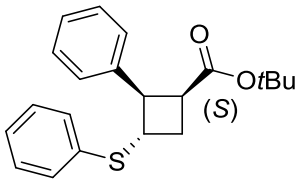

(1*S*)-**2-22**

The general procedure for cyclobutyl-thioether formation was followed using *tert*-butyl (*E*)-2-diazo-5-phenylpent-4-enoate (**2-5**, 100. mg, 0.387 mmol), thiophenol (85 mg, 0.77 mmol) and KO*t*Bu (9 mg, 0.07 mmol). Purification by flash column chromatography using 2% EtOAc in hexanes yielded **2-22** as a pale yellow oil (96 mg, 73 % yield, 1:1.5 dr).

The general procedure for epimerization was carried out using a portion of the above diastereomers (45 mg, 0.13 mmol) and KO*t*Bu (7.4 mg, 0.07 mmol) in THF (1.3 mL). Flash column chromatography using 2% EtOAc in hexanes furnished ***tert*-butyl (1*R*,2*R*,3*S*)-2-phenyl-3-(phenylthio)cyclobutane-1-carboxylate** as a pale yellow oil (40 mg, 89% yield, 15:1 dr). $[\alpha]_D^{20}$ +36 (*c* 0.97, $CHCl_3$). FT-IR (NaCl, thin film) 3060, 2977, 1723, 1147, 740, 697: HRMS (LIFDI) *m/z*: [M]+ Calcd for $C_{21}H_{24}O_2S$ 340.1497; Found 340.1481

NMR spectral properties assigned to *tert*-butyl (1*R*,2*R*,3*S*)-2-phenyl-3-(phenylthio)cyclobutane-1-carboxylate [(1*R*)-2-22]

^{1}H NMR (600 MHz, $CDCl_3$) δ: 7.26-7.19 (m, 6H), 7.16-7.12 (m, 5H), 3.66-3.63 (m, 1H), 3.56 (t, *J* = 9.4 Hz, 1H), 2.93 (q, *J* = 9.2 Hz, 1H), 2.59-2.55 (m, 1H), 2.22-2.17 (q, *J* = 10.0, 1H), 1.33 (s, 9H); ^{13}C NMR (150 MHz, $CDCl_3$) δ: 172.3 (C), 141.2 (C), 134.6 (C), 131.6 (CH), 128.9 (CH), 128.5 (CH), 127.0 (CH), 126.9 (CH), 126.7 (CH), 80.7 (C), 50.5 (CH_3), 44.1 (CH, 42.9 (CH), 31.5 (CH_2), 28.0 (CH_3).

NMR spectral properties assigned to *tert*-butyl (1*S*,2*R*,3*S*)-2-phenyl-3-(phenylthio)cyclobutane-1-carboxylate [(1*S*)-2-22]

^{1}H NMR (600 MHz, $CDCl_3$) δ: 7.36-7.20 (m, 10H), 4.46 (q, *J* = 8.6 Hz, 1H), 3.86 (t, *J* = 9.8 Hz, 1H), 3.48-3.42 (m, 1H), 2.85-2.79 (m, 1H), 2.33-2.16 (m, 1H), 1.07 (s, 9H); ^{13}C NMR (150 MHz, $CDCl_3$) δ: 172.3 (C), 138.4 (C), 134.8 (C), 131.0 (CH), 128.9 (CH), 128.2 (CH), 127.5 (CH), 126.8 (CH), 126.6 (CH), 80.5 (C), 49.1 (CH), 43.2 (CH), 42.5 (CH), 30.2 (CH_2), 27.6 (CH_3).

***tert*-butyl (1*R*,2*R*,3*S*)-3-((2-hydroxyethyl)thio)-2-(4-(trifluoromethyl)phenyl)cyclobutane-1-carboxylate** and ***tert*-butyl (1*S*,2*R*,3*S*)-3-((2-hydroxyethyl)thio)-2-(4-(trifluoromethyl)phenyl)cyclobutane-1-carboxylate (2-23)**

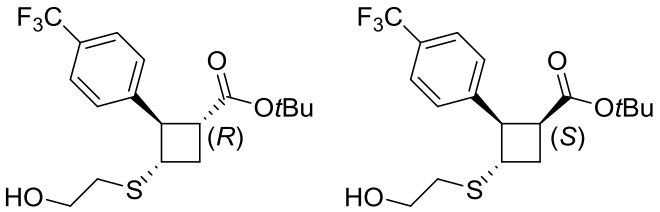

(1*R*)-**2-23** (1*S*)-**2-23**

The general procedure for cyclobutyl-thioether formation was followed using *tert*-butyl (*E*)-2-diazo-5-(4-(trifluoromethyl)phenyl)pent-4-enoate (**2-6**, 100 mg, 0.306 mmol), 2-mercaptoethanol (50 mg, 0.61 mmol) and KO*t*Bu (7.0 mg, 0.06 mmol). Purification by flash column chromatography using a gradient of 0-50% EtOAc in hexanes yielded **2-23** as a pale yellow oil (80 mg, 69% yield, 1.3:1 dr).

The general procedure for epimerization was carried out using a portion of the above diastereomers (35 mg, 0.09 mmol), and KO*t*Bu (5.0 mg, 0.05 mmol) in THF (1.0 mL).

Flash column chromatography using a gradient of 0-50% EtOAc: hexanes furnished ***tert*-butyl (1*R*,2*R*,3*S*)-3-((2-hydroxyethyl)thio)-2-(4-(trifluoromethyl)phenyl)cyclobutane-1-carboxylate** as a pale yellow oil (20 mg, 57%) $[\alpha]_D^{20}$ +19 (*c* 0.64, $CHCl_3$). FT-IR (NaCl, thin film): 3428, 2979, 2933, 1722, 1326, 1163, 1125, 1069, 1018, 845 HRMS (LIFDI) *m/z*: $[M]^+$ Calcd for $C_{18}H_{21}F_3O_3S$ 472.0684; Found 472.0663.

NMR spectral properties assigned to *tert*-butyl (1*R*, 2*R*, 3*S*)-3-((2-hydroxyethyl)thio)-2-(4-(trifluoromethyl)phenyl)cyclobutane-1-carboxylate [(1*R*)-2-23]

^{1}H NMR (400 MHz, $CDCl_3$) δ:7.61(d, *J* = 8.1 Hz, 2H), 7.46 (d, *J* = 7.4 Hz, 2H), 3.74-3.64 (m, 3H), 3.42 (q, *J* = 9.3 Hz, 1H), 3.01 (q, *J* = 8.7 Hz, 1H), 2.79-2.73 (m, 2H), 2.66-2.59 (m, 1H), 2.27 (q, *J* = 9.9 Hz, 1H), 1.90 (bs, OH), 1.46 (s, 9H); ^{13}C NMR (100 MHz, $CDCl_3$) δ:172.1 (C), 145.0 (C), 129.3 (C. q. ^2J(CF) = 33 Hz), 126.9 (CH), 125.5 (CH, q, ^3J(CF) = 3.8 Hz), 121.5 (C. q. ^1J(CF) = 272 Hz), 81.2 (C), 61.2 (CH_2), 51.0 (CH), 42.6 (CH), 41.9 (C), 34.5 (CH_2), 31.4 (CH_2), 28.1 (CH_3); ^{19}F NMR (376 MHz, $CDCl_3$) δ: 62.4

NMR spectral properties assigned to *tert*-butyl (1*S*,2*R*,3*S*)-3-((2-hydroxyethyl)thio)-2-(4-(trifluoromethyl)phenyl)cyclobutane-1-carboxylate [(1*S*)-2-23]

^{1}H NMR (400 MHz, $CDCl_3$) δ: 7.58 (d, *J* = 8.2 Hz, 2H), 7.36 (d, *J* = 8.2 Hz, 2H), 4.15 (q, *J* = 8.8 Hz, 1H), 3.88 (t, *J* = 10.4 Hz, 1H), 3.72-3.64 (m, 2H), 3.49-3.45 (m, 1H), 2.79-2.71 (m, 2H), 2.22 (bs, OH), 2.18-2.15 (m, 1H), 1.06 (s, 9H); ^{13}C NMR (100 MHz, $CDCl_3$) δ: 171.9 (C), 142.6 (C), 129.3 (C. q. ^2J(CF) = 33 Hz), 126.9 (CH), 125.2

(CH. q. ^{3}J(CF) = 3.8 Hz), 121.5 (C. q. ^{1}J(CF) = 272 Hz), 81.2 (C), 61.1 (CH_2), 49.9 (CH), 43.0 (CH), 40.5 (CH), 34.6 (CH_2), 30.2 (CH_2), 27.6 (CH_3); ^{19}F NMR (376 MHz, $CDCl_3$) δ: 62.5.

***tert*-butyl (1*R*,2*R*,3*S*)-2-(4-methoxyphenyl)-3-(tritylthio)cyclobutane-1-carboxylate** and ***tert*-butyl (1*R*,2*R*,3*S*)-2-(4-methoxyphenyl)-3-(tritylthio)cyclobutane-1-carboxylate (2-24)**

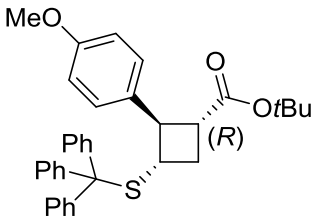

(1*R*)-**2-24**

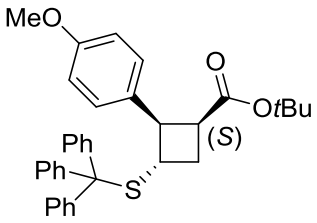

(1*S*)-**2-24**

The general procedure for cyclobutyl-thioether formation was followed using *tert*-butyl (*E*)-2-diazo-5-(4-methoxyphenyl)pent-4-enoate (**2-7**, 100 mg, 0.347 mmol), triphenylmethanethiol (192 mg, 0.694 mmol) and KO*t*Bu (8.0 mg, 0.07 mmol). Purification by flash column chromatography using 4% EtOAc in hexanes yielded **2-19** as a white semi solid (149 mg, 80% yield, 1:1 dr).

The general procedure for epimerization was carried out using a portion of the above diastereomers (60 mg, 0.11 mmol), and KO*t*Bu (7 mg, 0.06 mmol) in THF (1.1 mL). Flash column chromatography using 5% EtOAc in hexanes furnished ***tert*-butyl (1*R*,2*R*,3*S*)-2-(4-methoxyphenyl)-3-(tritylthio)cyclobutane-1-carboxylate** as a white semi-solid (44 mg, 73% yield, 23:1 dr).

$[\alpha]_D^{20}$ 76 (*c* 0.64, $CHCl_3$). FT-IR (NaCl, thin film) 3495, 3058, 2977, 29333, 1722, 1612, 1514, 1445, 1367: HRMS (LIFDI) *m/z*: [M]+ Calcd for $C_{35}H_{36}O_3S$ 536.2385; Found 536.2368

NMR spectral properties assigned to *tert*-butyl (1*R*,2*R*,3*S*)-2-(4-methoxyphenyl)-3-(tritylthio)cyclobutane-1-carboxylate [(1*R*)-2.24]

^{1}H NMR (400 MHz, $CDCl_3$) δ: 7.36-7.29 (m 9H), 7.24-7.19 (m, 8H), 7.12 (d, *J* = 8.7 Hz, 2H), 6.87 (d, *J* = 8.7 Hz, 2H), 3.86 (s, 3H), 3.48 (t, *J* -9.9 Hz, 1H), 2.97-2.90 (m, 1H), 2.64 (q, *J* = 9.4 Hz, 1H), 1.89 (q, *J* = 10.4 Hz, 1H), 1.73-1.67 (m, 1H), 1.39 (s, 9H); ^{13}C NMR (100 MHz, $CDCl_3$) δ: 172.4 (C), 158.6 (C), 144.9 (C), 132.5 (C), 129.6 (CH), 128.4 (CH), 128.0 (CH), 127.9 (CH), 127.8 (CH), 127.3 (CH), 126.6 (CH), 113.7 (CH), 80.5 (C), 67.5 (C), 55.4 (CH_3), 50.4 (CH), 43.7 (CH), 42.6 (CH), 33.5 (CH_2), 28.0 (CH_3).

methyl 4-((1*R*,2*R*,4*S*)-2-(*tert*-butoxycarbonyl)-4-(ethylthio)cyclobutyl)benzoate and **methyl 4-((1*S*,2*R*,4*S*)-2-(*tert*-butoxycarbonyl)-4-(ethylthio)cyclobutyl)benzoate (2-25)**

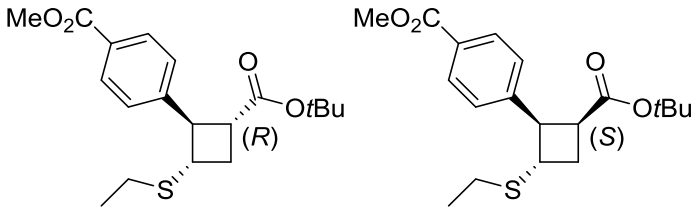

(1*R*)-**2-25** (1*S*)**2-25**

The general procedure for cyclobutyl-thioether formation was followed using methyl *(E)*-4-(5-(*tert*-butoxy)-4-diazo-5-oxopent-1-en-1-yl)benzoate (**2-7**, 100 mg, 0.316

mmol), ethanethiol (46 μL, 0.63 mmol) and KO*t*Bu (7 mg, 0.6 mmol). Purification by flash column chromatography using 6% EtOAc in hexanes yielded **2-25** as a colorless oil (66 mg, 60% yield).

The general procedure for epimerization was carried out using a portion of the above diastereomers (40 mg, 0.11 mmol), and KO*t*Bu (7 mg, 0.06 mmol) in THF (1.1 mL). Flash column chromatography using 5% EtOAc in hexanes furnished **methyl 4-((1*R*, 2*R*, 4*S*)-2-(*tert*-butoxycarbonyl)-4-(ethylthio)cyclobutyl)benzoate** as a colorless oil (28 mg, 70% yield, 11:1 dr). $[\alpha]_D^{20}$ +16 (*c* 1.7, $CHCl_3$). FT-IR (NaCl, thin film) 2977, 1724, 1279, 1148, 1109, 742, 668: HRMS (LIFDI) *m/z*: [M]+ Calcd for $C_{19}H_{26}O_4S$ 350.1552; Found 350.1552

NMR spectral properties assigned methyl 4-((1*R*, 2*R*, 4*S*)-2-(*tert*-butoxycarbonyl)-4-(ethylthio)cyclobutyl)benzoate [(1*R*)-2-25]

^{1}H NMR (600 MHz, $CDCl_3$) δ: 8.01 (d, *J* = 8.4 Hz, 2H), 7.42 (d, *J* = 8.3 Hz, 2H), 3.93 (s, 3H), 3.67 (t, *J* = 9.5 Hz, 1H), 3.44-3.38 (m, 1H), 3.01 (q, *J* = 8.7 Hz, 1H), 2.62-2.54 (m, 3H), 2.31-2.23 (m, 1H), 1.45 (s, 9H), 1.22 (t, *J* = 7.4 Hz, 3H); ^{13}C NMR (150 MHz, $CDCl_3$) δ:172.3 (C), 166.9 (C), 146.7 (C), 129.8 (CH), 128.7 (C), 126.6 (CH), 81.0 (C), 52.1 (CH_3), 51.3 (CH), 42.7 (CH), 41.9 (CH), 30.9 (CH_2), 28.1 (CH_3), 25.0 (CH_2), 15.3 (CH_3).

NMR spectral properties assigned methyl 4-((1*S*, 2*R*, 4*S*)-2-(*tert*-butoxycarbonyl)-4-(ethylthio)cyclobutyl)benzoate [(1*S*)-2-25]

^{1}H NMR (600 MHz, $CDCl_3$) δ: 7.98 (d, *J* = 8.5 Hz, 2H), 7.32 (d, *J* = 8.2 Hz, 2H), 4.13 (q, *J* = 8.9 Hz, 1H), 3.91 (s, 3H), 3.49-3.45 (m, 1H), 2.73-2.69 (m, 1H), 2.60-2.51 (m,

2H), 2.18-2.14 (m, 2H), 1.20 (t, J = 7.4 Hz, 3H); ^{13}C NMR (150 MHz, $CDCl_3$) δ: 172.1 (C), 167.0 (C), 144.3 (C), 129.5 (CH), 128.5 (C), 127.5 (CH), 81.0 (C), 52.1 (CH_3), 50.2 (CH), 43.1 (CH), 40.6 (CH), 30.0 (CH_2), 27.7 (CH_3), 25.4 (CH_2), 15.3 (CH_3).

tert-butyl (1*S*, 3*S*)-1-allyl-2-phenyl-3-(phenylthio)cyclobutane-1-carboxylate (2-25)

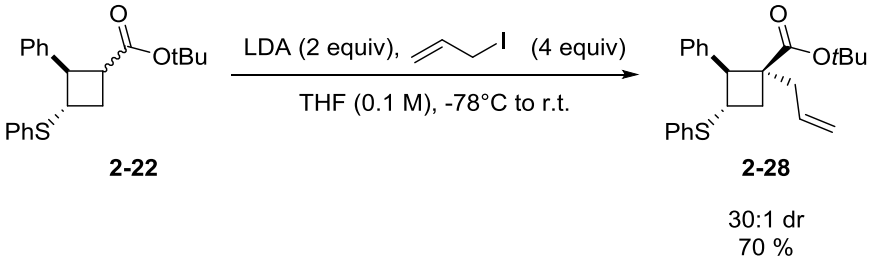

2-22 **2-28**

30:1 dr
70 %

A dry 10 mL round bottom flask was charged with a solution of racemic **2-22** (30 mg, 0.09 mmol) in THF (0.9 mL) and cooled to 78 °C with an acetone/dry ice bath. Lithium diisopropylamide (0.1 mL of a 1.8 M solution in heptane/THF and benzene) was added dropwise and the mixture allowed to stir for 10 minutes. Allyl iodide (0.03 mL, 0.4 mmol, 4 equiv) was then added and the reaction progress monitored by TLC. After *ca* 30 minutes, the reaction was quenched with brine, washed with 1 M HCl (1 x 20 mL), saturated sodium thiosulfate (1 x 20 mL) and then extracted with Et_2O. The organic layers were combined, dried over magnesium sulfate and concentrated to dryness using a rotary evaporator. Purification by column chromatography (4% Et_2O in hexanes) furnished **2-28** as a yellow oil (23 mg, 70% yield, 30:1 dr). ^{1}H NMR (400 MHz, $CDCl_3$) δ: 7.37-7.35 (m, 2H), 7.31-7.28 (m, 5H), 7.26-7.21 (m, 2H), 7.19 (d, J = 8.0 Hz, 2H), 5.59-5.52 (m, 1H), 5.00-4.94 (m, 2H), 4.31(q, J = 8.8 Hz, 1H), 3.52 (d, J = 9.8 Hz, 1H), 3.01 (dd, J = 11.6, 8.4 Hz, 1H), 2.88 (dd, J = 13.8, 6.8 Hz, 1H), 2.38

(dd, 13.8, 7.3 Hz, 1H), 1.95 (dd, 11.6, 8.7 Hz, 1H), 1.04 (s, 9H); ^{13}C NMR (100 MHz, $CDCl_3$) δ:172.2 (C), 138.0 (C), 134.8 (C), 133.3 (CH), 131.3 (CH), 128.9 (CH), 128.2 (CH), 127.4 (CH), 126.9 (CH), 126.7 (CH), 118.0 (CH_2), 80.6 (C), 55.3 (CH), 52.7 (C), 43.7 (CH_2), 39.4 (CH), 35.8 (CH_2), 27.5 (CH_3). FT-IR (NaCl, thin film) 3061, 2977, 2930, 1717, 1367, 1148, 737, 696 HRMS (LIFDI) *m/z*: [M]+ Calcd for $C_{24}H_{28}O_2S$ 380.1810; Found 380.1783

tert-butyl (1*R*,3*S*)-3-amino-2-phenylcyclobutane-1-carboxylate (2-27)

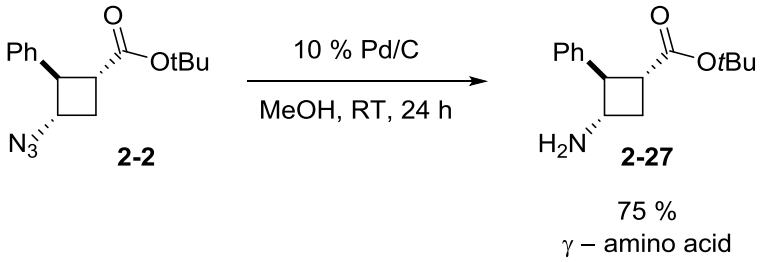

To a 0.125 M methanol solution of racemic **2-2** (50 mg, 0.18 mmol) was added 10% palladium-carbon (10 mg). The reaction was stirred under hydrogen atmosphere (balloon pressure) for 24 h, then filtered through celite and concentrated under reduced pressure. Purification by flash column chromatography using C-2 silica gel[21h] (gradient 0-10% methanol in methylene chloride) furnished **2-27** as a pale yellow solid (34 mg, 75%). mp 175 °C. ^{1}H NMR (600 MHz, CD_3OD) δ: 7.41-7.34 (m, 4H), 7.33-7.30 (m, 1H), 3.92 (q, *J* = 8.7 Hz, 1H), 3.68 (t, *J* = 9.3 Hz, 1H), 3.00 (q, *J* = 9.5Hz, 1H), 2.64-2.58 (m, 1H), 2.27 (q, *J* = 10.3Hz, 1H), 1.45 (s, 9H); ^{13}C NMR (150 MHz, CD_3OD) δ:174.1 (C), 140.6 (C), 130.6 (CH), 129.5 (C), 128.9 (CH), 83.2 (C), 51.7 (CH), 49.1 (CH), 42.7 (CH), 29.1 (CH_2), 29.0 (CH_3). FT-IR (NaCl, thin film) 2978,

1722, 1367, 1158, 736, 697; HRMS (LIFDI) *m/z*: [M]+ Calcd for $C_{15}H_{21}NO_2$ 247.1572; Found 247.1557

tert-butyl (_E_)-2-diazo-5-(4-methoxyphenyl)pent-4-enoate (2-7)

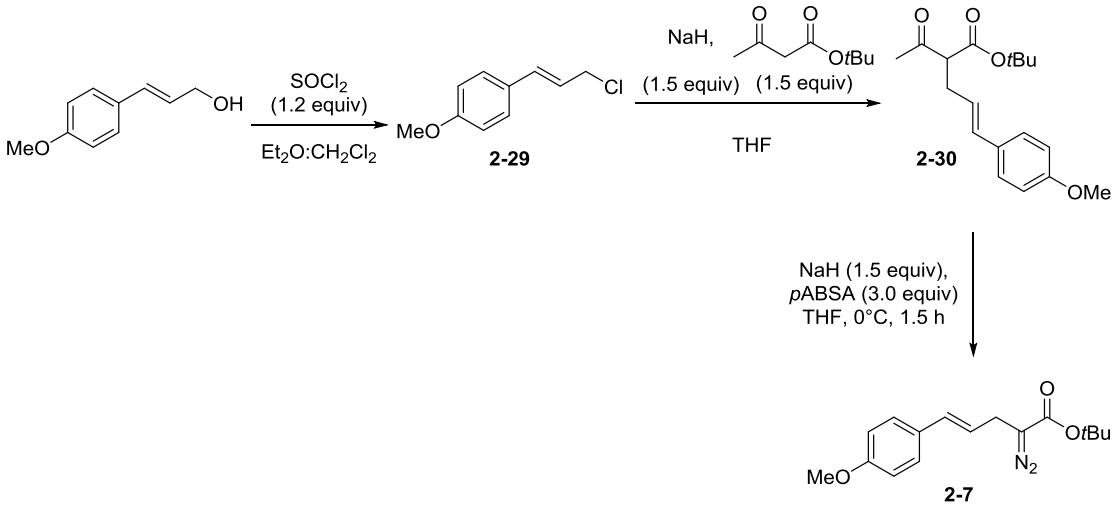

A dry round bottomed flask was charged with a solution of (*E*)-3-(4-methoxyphenyl)prop-2-en-1-ol (2.85 g, 17.5 mmol) in diethyl ether (17.5 mL) and cooled to 0 °C. Methylene chloride (*ca* 5 mL) was added to solubilize the allyl alcohol at the lower temperature. Thionyl chloride (1.5 mL, 21 mmol) was added dropwise and the reaction monitored by TLC for completion. After approximately 2 hours, the reaction was poured carefully onto COLD saturated sodium bicarbonate solution then extracted with diethyl ether. The combined organic layers were washed with saturated sodium bicarbonate solution, water, and brine, dried over $MgSO_4$, filtered and concentrated under reduced pressure. The resulting allyl chloride was used

immediately in the subsequent step without purification as it was to prone to decomposition.

A flame-dried round bottomed flask was charged with a suspension of sodium hydride (1.0 g 60% dispersion in mineral oil, 26 mmol) in THF (15 mL) then cooled to 0 °C. After the slow addition of a solution of *tert*-butylacetoacetate (4.2 g, 26 mmol) in THF (10 mL), the reaction was allowed to warm to room temperature and stirred for approximately 15 minutes before re-cooling to 0 °C. A solution of (*E*)-1-(3-chloroprop-1-en-1-yl)-4-methoxybenzene (3.2 g, 17 mmol) in THF (10 mL was added then the mixture warmed to 50 °C and allowed to stir overnight. Upon completion, the reaction was cooled to room temperature and, diluted with EtOAc and washed with distilled water. The aqueous phase was extracted thrice with EtOAc. The combined organic layers were dried over $MgSO_4$, filtered and concentrated on to silica gel (10 g) under reduced pressure. Flash chromatography though a short silica gel plug (to remove excess *tert*-butylacetoacetate before the subsequent step), gave a crude *tert*-butyl (*E*)-2-acetyl-5-(4-methoxyphenyl)pent-4-enoate as a yellow oil (2.5 g, 47%), which was used in the next step.

A flame-dried round bottomed flask was charged with a suspension of sodium hydride (0.50 g 60% dispersion in mineral oil, 12 mmol) in THF (14 mL) then cooled to 0 °C. After the slow addition of a solution of *tert*-butyl (*E*)-2-acetyl-5-(4-methoxyphenyl)pent-4-enoate from above in THF (10 mL), the reaction was allowed to warm to room temperature and stirred for approximately 15 minutes before re-cooling to 0 °C. A solution of *p*-acetamidobenzenesulfonyl azide (*p*-ABSA, 5.9 g, 25 mmol) in THF (17 mL) was added dropwise. The reaction was complete after the addition *p*-ABSA was complete. The mixture was quenched with 10% NaOH solution

and extracted thrice with EtOAc. The combined organic layers were dried over $MgSO_4$, filtered and concentrated under reduced pressure. Purification via flash column chromatography (gradient from 0-100 % CH_2Cl_2 in hexanes) furnished **2-7** as a yellow oil (1.0 g, 45% yield). ^{1}H NMR (600 MHz, $CDCl_3$) δ: 7.32 (d, *J* = 8.6 Hz, 2H), 6.87 (d, *J* = 8.9 Hz, 2H), 6.45 (d, *J* = 15.8 Hz, 1H), 6.10-6.03 (m, 1H), 3.82 (s, 3H), 3.16 (dd, *J* = 6.9, 1.4 Hz, 2H), 1.51 (s, 9H); ^{13}C NMR (150 MHz, $CDCl_3$) δ:166.5 (C), 159.1 (C), 132.0 (C), 129.6 (CH), 127.4 (CH), 122.0 (CH), 114.0 (CH), 81.3 (C), 55.3 (CH_3), 28.4 (CH_3), 26.8 (CH_2). FT-IR (NaCl, thin film) 2977, 2934, 2837, 208:, 1385, 1512, 1116, 834; HRMS (LIFDI) *m/z*: [M]+ Calcd for $C_{16}H_{20}N_2O_3$ 288.1474; Found 288.1457.

tert-butyl (3*S*)-2-(4-methoxyphenyl)bicyclo[1.1.0]butane-1-carboxylate (2-28)

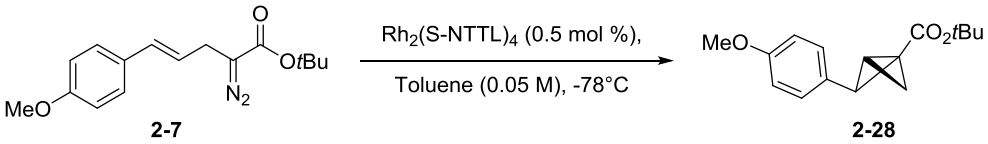

2-7 **2-28**

To a flame-dried round bottomed flask was added Rh_2(*S*-NTTL)$_4$ (1.5 mg, 0.0013 mmol, 0.50 mol %). The flask was evacuated and refilled with nitrogen three times. Anhydrous toluene (3.1 mL) was added and the flask stirred at room temperature until the Rh_2(*S*-NTTL)$_4$ had completely dissolved. The mixture was cooled to –78 °C by a dry ice/acetone bath. *tert*-butyl (*E*)-2-diazo-5-(4-methoxyphenyl)pent-4-enoate, **2-7**, (74 mg, 0.26 mmol) was dissolved in anhydrous toluene (2 mL) and added to the reaction flask via syringe pump at a rate of 1 mL/h. After the addition was complete, the solution was allowed to warm to room temperature. The solvent was subsequently

removed under reduced pressure, and the residue, purified by column chromatography (4% Et_2O: hexanes) furnished **2-28** a colorless oil (52 mg, 77% yield). $[\alpha]_D^{20}$ 20 (*c* 1.0, $CHCl_3$). ^1H NMR (600 MHz, $CDCl_3$) δ: 7.11 (d, *J* = 8.6 Hz, 2H), 6.85 (d, *J* = 8.8 Hz, 2H), 3.73 (s, 3H), 2.63-2.62 (m,1H), 2.35 (d, *J* = 1.8 Hz, 1H), 2.25 (d, *J* = 3.7 Hz, 1H), 1.25 (s, 9H), 1.08-1.07 (m, 1H); ^{13}C NMR (100 MHz, $CDCl_3$) δ:170.8 (C), 158.7 (C), 128.3 (CH), 127.6 (C), 113.3 (CH), 80.4 (C), 55.3 (CH_3), 49.9 (CH), 30.8 (CH_2), 27.8 (CH_3), 18.8 (CH). 16.5 (C). FT-IR (NaCl, thin film) 2976, 2932, 1719, 1512, 1249, 1153, 846: HRMS (LIFDI) *m/z*: [M]+ Calcd for $C_{16}H_{20}O_3S$ 260.1412; Found 260.1394. HPLC analysis: (CHIRALCEL IA column 0.1% 2-propanol in hexanes, 1mL/min, 220 nm, 85 % ee.

In situ FTIR Experiment

In situ FTIR experiments were performed using a Mettler Toledo ReactIR system (ReactIR10 with AgX 6mm x 1.5 m Fibre (Silver Halide), Liquid N_2 MCT Detector and SiComp probe). A SiComp probe was used because the area of interest to be examined extended above 2000 cm^{-1} (asymmetrical azide stretching). IR spectra were recorded every 2 minutes at 8 cm^{-1} resolution, and spectral data were collected over the 2800 - 660 cm^{-1} range. The *in situ* FTIR experiment was performed in a three-neck flask. DPPA (36 mg, 0.13 mmol) was dissolved in a 5:1 solution of toluene:HMPA (1.0 mL) and warmed to 75˚C. DBU (0.02 mL, 0.13 mmol) was added neat and the reaction was allowed to stir for 1 h. A solution of **2-1** (60 mg, 0.26 mmol) in a 5:1 toluene:HPMA (0.30 mL) was then added and the reaction allowed to stir for 8 hours.

REFERENCES

1. (a) Dembitsky, V. *Journal of Natural Medicines* **2008**, *62*, 1; (b) Nozaki, H.; Hayashi, K.-i.; Kido, M.; Kakumoto, K.; Ikeda, S.; Matsuura, N.; Tani, H.; Takaoka, D.; Iinuma, M.; Akao, Y. *Tetrahedron Lett.* **2007**, *48*, 8290; (c) Sergeiko, A.; Poroikov, V. V.; Hanuš, L. O.; Dembitsky, V. M. *The Open Medicinal Chemistry Journal* **2008**, *2*, 26; (d) Allan, R. D.; Curtis, D. R.; Headley, P. M.; Johnston, G. A. R.; Kennedy, S. M. E.; Lodge, D.; Twitchin, B. *Neurochem. Res.* **1980**, *5*, 393.

2. Cohen, M. D.; Schmidt, G. M. J.; Sonntag, F. I. *Journal of the Chemical Society (Resumed)* **1964**, 2000.

3. (a) Ito, Y.; Kitada, T.; Horiguchi, M. *Tetrahedron* **2003**, *59*, 7323; (b) Feldman, K. S.; Campbell, R. F. *The Journal of Organic Chemistry* **1995**, *60*, 1924.

4. (a) Du, J.; Skubi, K. L.; Schultz, D. M.; Yoon, T. P. *Science* **2014**, *344*, 392; (b) Du, J.; Yoon, T. P. *J. Am. Chem. Soc.* **2009**, *131*, 14604.

5. Lee-Ruff, E.; Mladenova, G. *Chem. Rev.* **2003**, *103*, 1449.

6. (a) Bach, R. D.; Dmitrenko, O. *J. Am. Chem. Soc.* **2004**, *126*, 4444; (b) Bach, T.; Hehn, J. P. *Angew. Chem. Int. Ed.* **2011**, *50*, 1000; (c) Gutekunst, W. R.; Baran, P. S. *The Journal of Organic Chemistry* **2014**, *79*, 2430; (d) Gutekunst, W. R.; Gianatassio, R.; Baran, P. S. *Angew. Chem. Int. Ed.* **2012**, *51*, 7507.

7. (a) Tyson, E. L.; Farney, E. P.; Yoon, T. P. *Org. Lett.* **2012**, *14*, 1110; (b) Canales, E.; Corey, E. J. *J. Am. Chem. Soc.* **2007**, *129*, 12686; (c) Albrecht, Ł.; Dickmeiss, G.; Acosta, F. C.; Rodríguez-Escrich, C.; Davis, R. L.; Jørgensen, K. A. *J. Am. Chem. Soc.* **2012**, *134*, 2543; (d) Qi, L.-W.; Yang, Y.; Gui, Y.-Y.; Zhang, Y.; Chen, F.; Tian, F.; Peng, L.; Wang, L.-X. *Org. Lett.* **2014**, *16*, 6436.

8. (a) T. Brady, W. *Tetrahedron* **1981**, *37*, 2949; (b) Bak, D. A.; Brady, W. T. *The Journal of Organic Chemistry* **1979**, *44*, 107.

9. (a) Hussain, M. M.; Li, H.; Hussain, N.; Ureña, M.; Carroll, P. J.; Walsh, P. J. *J. Am. Chem. Soc.* **2009**, *131*, 6516; (b) Hiroi, K.; Nakamura, H.; Anzai, T. *J. Am. Chem. Soc.* **1987**, *109*, 1249; (c) Nemoto, H. I., H.; Mori, M.; Fujita, S.; Fukumoto, K. *Heterocycles* **1990**, *31*, 1237; (d) Kleinbeck, F.; Toste, F. D. *J. Am. Chem. Soc.* **2009**, *131*, 9178.

10. Xiao, K.-J.; Lin, D. W.; Miura, M.; Zhu, R.-Y.; Gong, W.; Wasa, M.; Yu, J.-Q. *J. Am. Chem. Soc.* **2014**, *136*, 8138.

11. Pomerantz, M.; Abrahamson, E. W. *J. Am. Chem. Soc.* **1966**, *88*, 3970.

12. (a) Wiberg, K. B.; Lampman, G. M.; Ciula, R. P.; Connor, D. S.; Schertler, P.; Lavanish, J. *Tetrahedron* **1965**, *21*, 2749; (b) Schulman, J. M.; Newton, M. D. *J. Am. Chem. Soc.* **1974**, *96*, 6295.

13. Wiberg, K. B.; Ciula, R. P. *J. Am. Chem. Soc.* **1959**, *81*, 5261.

14. (a) Gaoni, Y. *Tetrahedron Lett.* **1982**, *23*, 5215; (b) Gaoni, Y.; Tomazic, A.; Potgieter, E. *The Journal of Organic Chemistry* **1985**, *50*, 2943.

15. Gaoni, Y. *Tetrahedron* **1989**, *45*, 2819.

16. Walczak, M. A. A.; Wipf, P. *J. Am. Chem. Soc.* **2008**, *130*, 6924.

17. Wipf, P.; Walczak, M. A. A. *Angew. Chem. Int. Ed.* **2006**, *45*, 4172.

18. (a) Ueda, M.; Walczak, M. A. A.; Wipf, P. *Tetrahedron Lett.* **2008**, *49*, 5986; (b) Walczak, M. A. A.; Shin, B.-k.; Wipf, P.; Saxena, S. *Organic & Biomolecular Chemistry* **2009**, *7*, 2363; (c) Wipf, P.; Stephenson, C. R. J.; Okumura, K. *J. Am. Chem. Soc.* **2003**, *125*, 14694.

19. (a) Bayless, J.; Friedman, L.; Smith, J. A.; Cook, F. B.; Shechter, H. *J. Am. Chem. Soc.* **1965**, *87*, 661; (b) Wiberg, K. B.; Dailey, W. P.; Walker, F. H.; Waddell, S. T.; Crocker, L. S.; Newton, M. *J. Am. Chem. Soc.* **1985**, *107*, 7247.

20. Ikota, N.; Takamura, N.; Young, S. D.; Ganem, B. *Tetrahedron Lett.* **1981**, *22*, 4163.

21. (a) Goto, T.; Takeda, K.; Shimada, N.; Nambu, H.; Anada, M.; Shiro, M.; Ando, K.; Hashimoto, S. *Angew. Chem. Int. Ed.* **2011**, *50*, 6803; (b) Boruta, D. T.; Dmitrenko, O.; Yap, G. P. A.; Fox, J. M. *Chemical Science* **2012**, *3*, 1589; (c) DeAngelis, A.; Dmitrenko, O.; Yap, G. P. A.; Fox, J. M. *J. Am. Chem. Soc.* **2009**, *131*, 7230; (d) DeAngelis, A.; Panne, P.; Yap, G. P. A.; Fox, J. M. *The Journal of Organic Chemistry* **2008**, *73*, 1435; (e) DeAngelis, A.; Shurtleff, V. W.; Dmitrenko, O.; Fox, J. M. *J. Am. Chem. Soc.* **2011**, *133*, 1650; (f) DeAngelis, A.; Taylor, M. T.; Fox, J. M. *J. Am. Chem. Soc.* **2009**, *131*, 1101; (g) Panne, P.; DeAngelis, A.; Fox, J. M. *Org. Lett.* **2008**, *10*, 2987; (h) Panne, P.; Fox, J. M. *J. Am. Chem. Soc.* **2007**, *129*, 22.

22. (a) Panish, R.; Chintala, S. R.; Boruta, D. T.; Fang, Y.; Taylor, M. T.; Fox, J. M. *J. Am. Chem. Soc.* **2013**, *135*, 9283; (b) Qin, C.; Davies, H. M. L. *Org. Lett.* **2013**, *15*, 310.

23. (a) Hoz, S.; Azran, C.; Sella, A. *J. Am. Chem. Soc.* **1996**, *118*, 5456; (b) Razin, V. V. V., V.A.; Blinkov, I.E. *Russ. J. Org. Chem* **1993**, 759.

24. Błaszczyk, R. *Synlett* **2008**, *2008*, 299.

25. Papa, A. J. *The Journal of Organic Chemistry* **1966**, *31*, 1426.

26. Guerin, D. J.; Horstmann, T. E.; Miller, S. J. *Org. Lett.* **1999**, *1*, 1107.

27. Thompson, A. S.; Humphrey, G. R.; DeMarco, A. M.; Mathre, D. J.; Grabowski, E. J. J. *The Journal of Organic Chemistry* **1993**, *58*, 5886.

28. (a) K. Aggarwal, V.; Mereu, A. *Chem. Commun.* **1999**, 2311; (b) Ghosh, N. *Synlett* **2004**, *2004*, 574; (c) Johnson, M. G.; Foglesong, R. J. *Tetrahedron Lett.* **1997**, *38*, 7003; (d) Kers, A.; Kers, I.; Stawinski, J. *Journal of the Chemical Society, Perkin Transactions 2* **1999**, 2071; (e) Kers, A. S., Jacek; Dembkowski, Leszek; Kraszewski, Adam *Tetrahedron* **1997**, *53*, 12691; (f) Reed, R.; Réau, R.; Dahan, F.; Bertrand, G. *Angewandte Chemie International Edition in English* **1993**, *32*, 399.

29. (a) Aggarwal, V. K.; Sheldon, C. G.; Macdonald, G. J.; Martin, W. P. *J. Am. Chem. Soc.* **2002**, *124*, 10300; (b) Connolly, T. J.; Hansen, E. C.; MacEwan, M. F. *Organic Process Research & Development* **2010**, *14*, 466.

30. Lieber, E.; Rao, C. N. R.; Chao, T. S.; Hoffman, C. W. W. *Anal. Chem.* **1957**, *29*, 916.

Chapter 3

STRAIN RELEASE DRIVEN REACTIVITY OF CYCLOPROPENYL KETONES: A STRATEGY FOR THE FAST, IRREVERSIBLE MODIFICATION OF CYSTEINES

3.1 Introduction

The covalent modification of proteins via bioconjugation is a powerful tool used to probe and influence protein interactions and function[1]. Protein modification has far reaching applications in the fields of chemistry, medicine and biology: from determining protein composition[2], to providing a means to selectively deliver biologically active therapeutics[3], to enabling the *in situ* monitoring of cellular events[4]. There are several requirements for a chemical reaction to find utility in the field of bioconjugation. The reaction should be selective toward the residue of interest in the presence of the diverse chemical functionality found in proteins. Also important is that the reaction should display high efficiency and rapid kinetics at 25˚C - 37˚C, thereby facilitating rapid labeling under convenient conditions that avoid the necessity of using excess labeling reagent at high concentration. A recent and successful approach to selective protein bioconjugation reactions has been the development of bioorthogonal labeling chemistry where an unnatural chemical handle that is inert to the biological milieu is incorporated into the protein of interest. This chemical handle reacts selectively with a reaction partner that is introduced at a later time-point. The more readily recognizable reactions in the field of bioorthogonal chemistry are the Staudinger ligation reaction[5], copper catalyzed[6] and copper-free[7] iterations of "click"

chemistry – the Huigsen 1,3-dipolar cycloaddtion between azide and alkyne, and tetrazine ligation[8] – the inverse demand Diels-Alder reaction between *trans*-cyclooctenes and tetrazines first described by the Fox group (Table 3.1). Note that strain release driven reactions have become increasingly attractive actors in bioconjugation chemistry as the kinetics associated are typically rapid, easily tunable and adducts formed are generally stable in biological systems. While bioorthogonal chemistry represents a powerful tool for protein science, for many applications the modification of native residues is still preferred due to the simplicity and inexpensive nature of this approach.

Table 3.1: Select examples of bioorthogonal reactions

Copper Catalyzed azide-alkyne coupling (CuAAC)[6] 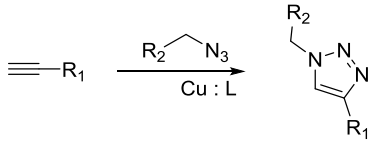	*Copper-Free Strain promoted azide-alkyne coupling reaction (SPAAC)[7a]* 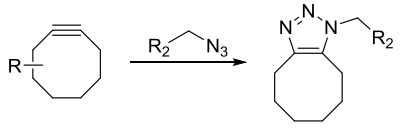
Staudinger Ligation[5] 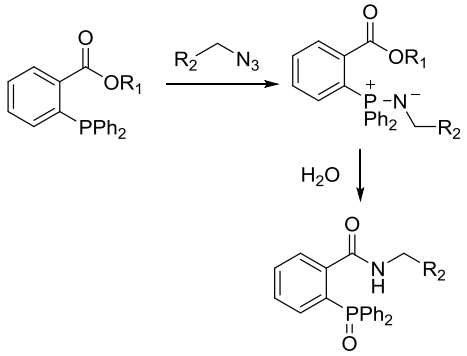	*Tetrazine Ligation[8a]* 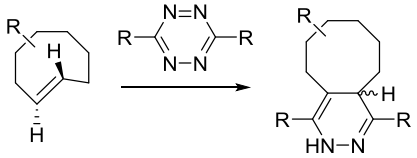

Nature routinely covalently modifies proteinogenic amino acids as a way of modulating various signaling mechanisms[9]. In mimicry of nature, selective bioconjugation reactions provide a chemical way of probing or perturbing function and various biological processes. By far, the leading candidates for covalent modification have been cysteines and lysines, with cysteine modification offering a number of advantages. The low natural abundance of cysteine (1.2 %)[10] makes it possible to modify cysteines with more precision than is possible with lysine modification. Also, standard protocols exist for the site-directed mutagenesis of cysteines into predetermined positions in proteins of interest[11]. When not directly involved in catalysis, cysteines are known to play a significant role in defining the three dimensional structure of proteins through the formation of disulfide bonds. Further, the relatively low pKa of the sulfhydryl group coupled with the strong nucleophilicity of the thiolate anion allow for facile conjugation reactions.

A vast amount of work has been done in developing various reagents capable of selectively modifying cysteines[1-2,12]. Approaches have included oxidative elimination of cysteines[13] to dehydroalanines followed by the conjugate addition of variously substituted thiols, alkylation of maleimides[14], α-halocarbonyls[15] or electron deficient oxanorbornadienes[16], disulfide formation, desulfurization[17], thiol-ene reactions promoted by light or chemical radical initiators[18], conjugate addition to electron deficient alkynes[19], metal mediated modification[20] or most recently, through a nucleophilic aromatic substitution reaction[21]. A list of methods used for cysteine modification is presented in Table 3.2.

Table 3.2: Selected examples of methods employed in the modification of cysteines

Entry	Reaction
1	*Oxidative elimination* 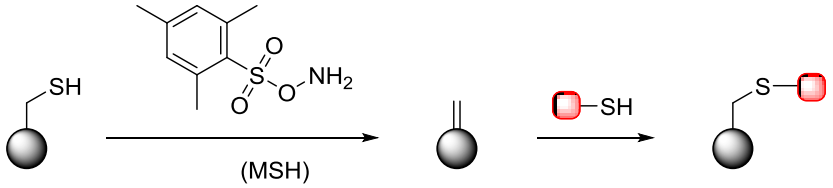
2	*Alkylation* 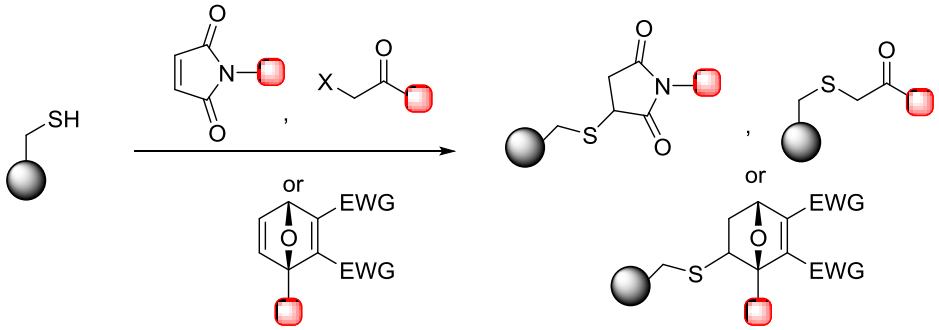
3	*Disulfide formation* 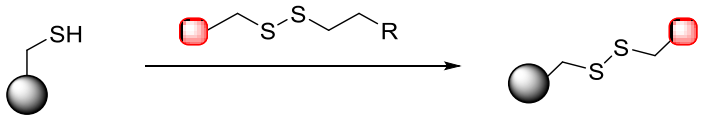
4	*Metal mediated reactions* 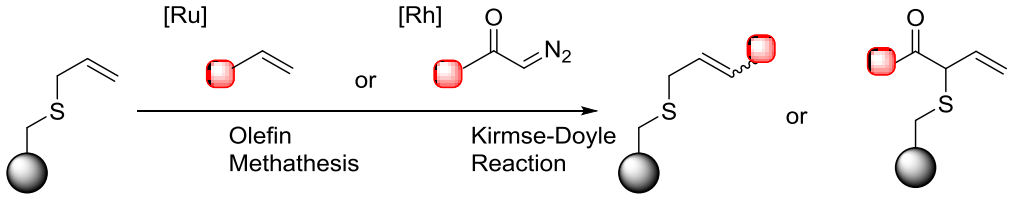
5	*Desulfurization* 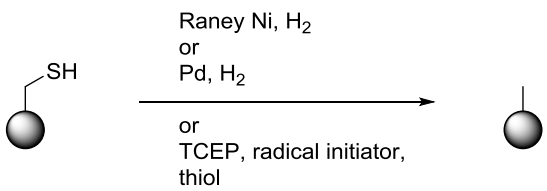

6	*Nucleophilic Aromatic Substitution* 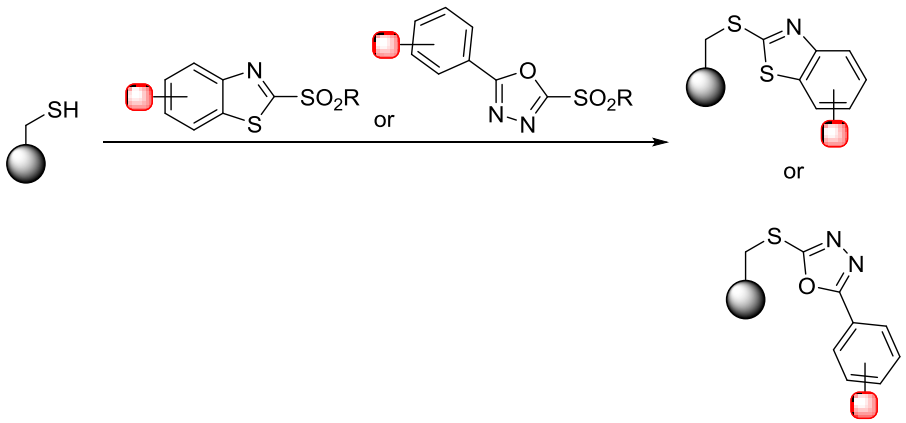
7	*Conjugate Addition to electron deficient alkynes* 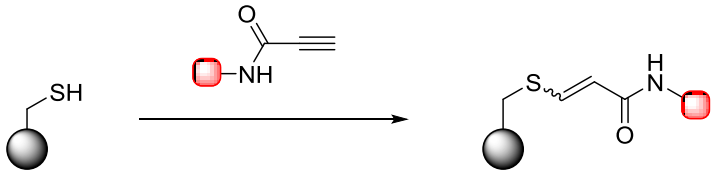
8.	*Thiol-ene reaction* 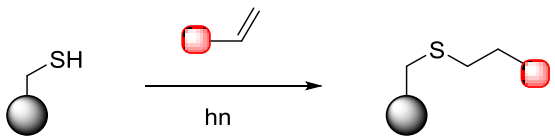

Despite the collection of options available for the modification of cysteines, alkylation remains the preferred route. The most frequently used alkylating agengts are α-haloacetamides and maleimides, which employ two different reaction modes: S_N2 displacement and conjugate addition to an α,β-unsaturated carbonyl compound, respectively. Both options yield thioethers. α-Halocarbonyl compounds have been reported as alkylating agents of cysteines as early as the 1930s[15] and are still utilized

in that capacity[22]. Thiols are irreversibly added to these alkylating agents and due to their small size and polar moieties they are extremely water soluble, which allows for the preparation of quite concentrated solutions. This is important as the second order rate constant for the alkylation of thiols to α-halocarbonyls ranges from 10^{-1} to 10^{1} $M^{-1}s^{-1}$[23]. Under pseudo first-order conditions, α-halocarbonyl alkylations generally require high concentration (mM) in order to be effective within a short timeframe. An additional disadvantage to using α-halocarbonyl reagents is that they often require elevated pH levels (pH 8-9) for reactions to proceed efficiently[24]. At these pHs not only is the denaturation of some proteins possible, but there may also be deprotonation of other reactive sidechains thereby reducing the labeling specificity. Finally, there have been reports of α-halocarbonyl variants that are sensitive to light[23], which can complicate the handling of more complex derivatives.

Currently, the most attractive reagents for the modification of cysteine residues on proteins are maleimides. The conjugate addition reactions of maleimides are highly selective for cysteine modification and proceed efficiently under physiological conditions, with second order rate constants of up to 10^{4} $M^{-1}s^{-1}$ [25]. Functionalized maleimides can be prepared readily, enabling their use in a broad range of applications. A limitation of maleimide-based protein modifications is the stability of the adducts that are formed. The succinimide is susceptible to hydrolysis[14a,26] and more significantly, the retro conjugate addition reaction also occurs under physiological conditions[22,27]. Because the conjugate addition is thermodynamically favorable, the reversibility of the conjugate addition is typically a non-issue in the absence of competing thiols. However, in the biological context, the concentrations of competing thiols can be higher than the thiol of interest, and accordingly can

'scavenge' maleimides from the protein of interest. This is especially true in the intracellular context, where the concentration of glutathione is in the millimolar range[28]. Indeed, the retro-thiol/maleimide conjugate addition has been pursued as the basis for biomaterial designs and drug release applications[29]. However, in instances where a stable thioether linkage is needed, such as for use as linkers in antibody drug conjugates (ADCs)[3], maleimides have documented limitations. Recent studies by Santi et al. have sought to improve the stability of maleimide thioethers by increasing their propensity to hydrolyze[26], as the ring opened variant does not participate in the retro conjugate addition chemistry (Scheme 3.1).

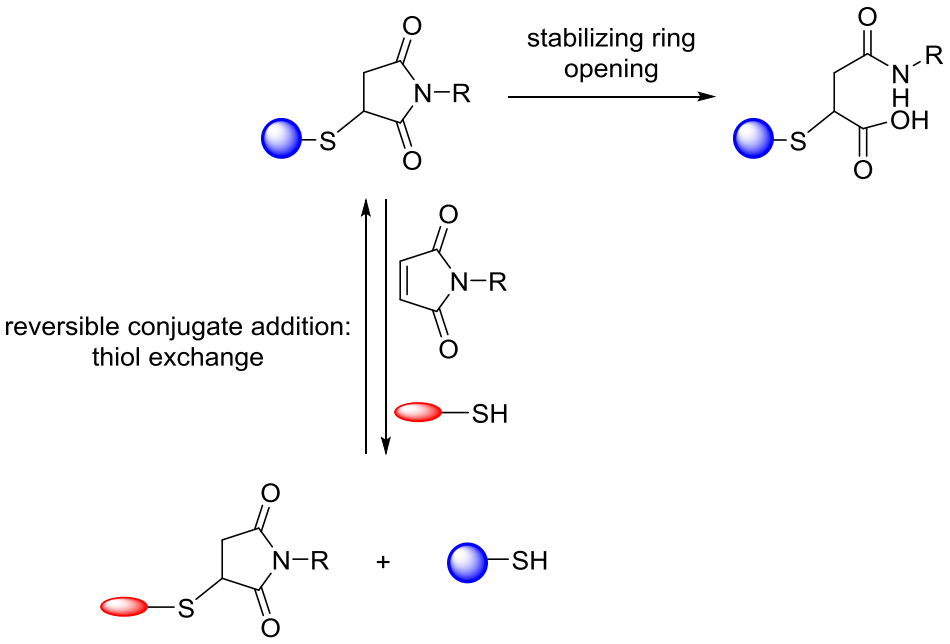

Scheme 3.1: Stabilization of maleimide-thioether linkages by accelerating maleimide hydrolysis. Ring opened variant does not undergo retro conjugate addition reaction.

In their study, substituting electron withdrawing groups on to the *N*-substituent of the maleimide accelerated their hydrolysis up to 500 fold, whereas substituting electron donating groups did the opposite. Taft σ* values, a polar substituent constant used to describe the way a substituent influences a reaction through polar effects, were used to explain their observations, where a larger Taft σ* value correlated to greater hydrolytic acceleration. While it is argued that inductively withdrawing effects might accelerate both the retro conjugate addition and succinimide hydrolysis, they found that the retro conjugate addition was less sensitive to those effects. Moreover, they suggest that for ADC application purposes, the hydrolysis reaction would preferably be performed first, in the absence of competing thiols before *in vivo* administration. While this work presents a viable solution to the maleimide thioether reversibility issue, some effort has to be invested in engineering the maleimide linker with the "goldilocks" set of properties to suit each ADC.

Using an entirely different approach, the work of Barbas et al.[21] has shown that a different structural class of molecules can be considered as stable cysteine modifiers (entry 6, Table 3.2). Drawing inspiration from the recent publication of Zhang and Baez et al.[30] who described methylsulfonylbenzothiazole (MSBT) as being a selective protein thiol blocking agent, Barbas et al. sought to investigate whether a broader range of heteroatomic sulfones could also be useful. The mode of reaction of these thiol modifying agents is entirely different than had been previously explored. They found that a modified version of the Julia-Kocienski olefination reagent (Figure 3.1a) selectively reacted with cysteines in aqueous buffer containing organic cosolvents. The adducts were more stable than their maleimide counterparts under acidic, basic and reducing conditions. Although rate constants for the cysteine modification were

not reported, the rate of reaction appears similar to α-haloacetamide alkylation (reactivity within 60 min at 11 mM in 1:1 THF/PBS at 25˚C). Another limitation of these reagents is that they are bulky and hydrophobic in nature.

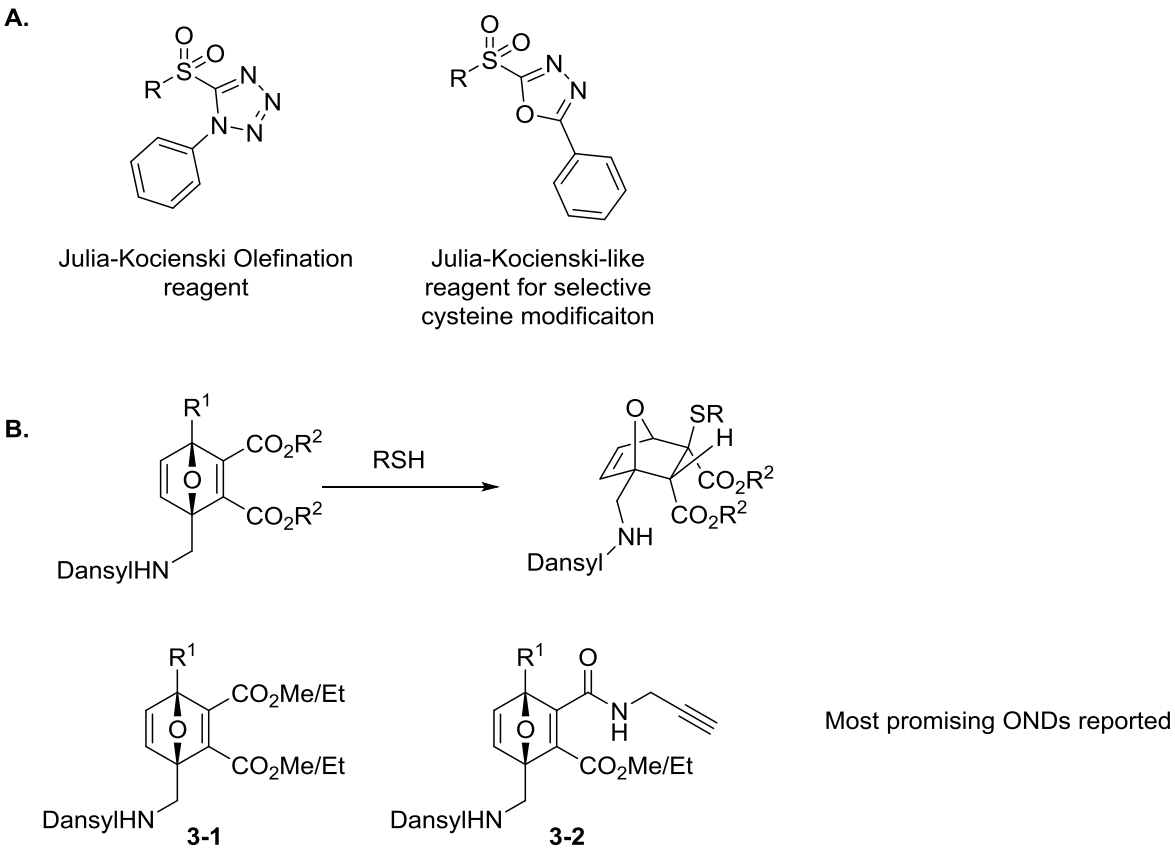

Figure 3.1: (a) Julia-Kocienski type reagent used for stable and selective cysteine modification (b) Electron deficient oxanorbornadienes ONDs as thiol alkylating agents

Finn and coworkers have described the use of electron deficient oxanorbornadienes (ONDs) as thiol-selective alkylating agents[16] with second order

rate constants for glutathione alkylation ranging from 40 – 200 $M^{-1}s^{-1}$ at pH 7 (25 ˚C) (Figure 3.1b). There are however a few limitations to using ONDs as alkylating agents. Experiments conducted necessitated the use of 10 % DMSO solution of ONDs in buffer, which indicates the level of hydrophobicity related with the reagents. The authors noted that the reactivity of ONDs is significantly attenuated (*ca* 600 times less reactive with glutathione) when R^2 = H. This is significant as the most promising ONDs presented (**3-1** and **3-2**, Figure3.1b) both contain an ester functionality, which under physiological conditions will very likely hydrolyze. Further, OND adducts are prone to decomposition via a retro Diels-Alder reaction. The half-life of the decomposition of mercaptoethanol-OND adducts ranged from 10 hours to 24 days at 25˚C incubations in pH 7, 10 % DMSO/phosphate buffer. Presumably, these rates would increase at physiologically relevant temperatures. Though adding to the pool of small molecules available for the selective alkylation of thiols, ONDs are perhaps most suited towards applications where the tunable degradation of thiol linkers are desired[27].

The use of maleimides continues to be pervasive in thiol modification protocols. The aforementioned limitations as well as the surprising lack of alternatives dictate that there exists a need for the continued engineering of small molecules to serve as robust, viable alternatives. To this end, I have developed a new class of cysteine alkylating agents based on cyclopropenyl ketones. While the use of cyclopropenes in bioorthogonal reactions with tetrazines and tetrazoles has been documented recently[31], the use of cyclopropenyl ketones has not been described. Based on prior work where cyclopropenyl ketones were found to serve as very reactive and selective dienophiles[32], we hypothesized that for the hetero-Michael

addition, as with the Diels-Alder chemistry, the significant strain release energy (~27 kcal/mol)[33] upon alkylation should render the reaction both fast and irreversible. Additionally, cyclopropenyl ketones are small (MW 168 g/mol), bifunctional and allow for simple attachment of pendant groups via amide bond construction based on *N*-hydroxysuccinimide (NHS)-ester chemistry (Scheme 3.2.).

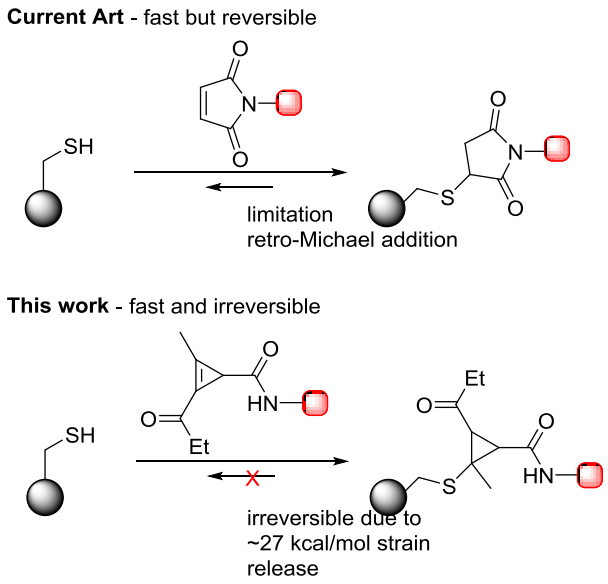

Scheme 3.2: Strain release driven cysteine modification

3.2 Results and Discussion

3.2.1 Synthesis of Cyclopropenyl Ketones

In order to maximize the viability of cyclopropenyl ketones as bioconjugation tools, I sought to synthesize a cyclopropenyl ketone that would be small, readily handled and stored and stable enough in aqueous media to allow for selective conjugation to thiols. To that end, the cyclopropenyl ketones were prepared in 5-6

easily scalable steps starting from 2-methylcycloprop-2-enecarboxylic acid, **3-3**, obtained from the rhodium catalyzed cyclopropenation of propyne. Adding propanal to the dianion of **3-3** furnished an intermediate alkenol **3-4**, which after work up was either esterified to the methyl ester with diazomethane then oxidized to the cyclopropenyl ketone **3-5** or purified and treated with *N*-hydroxysuccinimide to yield an activated ester, **3-6**, whose subsequent reaction with an amine of choice then oxidation would yield cyclopropenyl ketone **3-7** (Scheme 3.3).

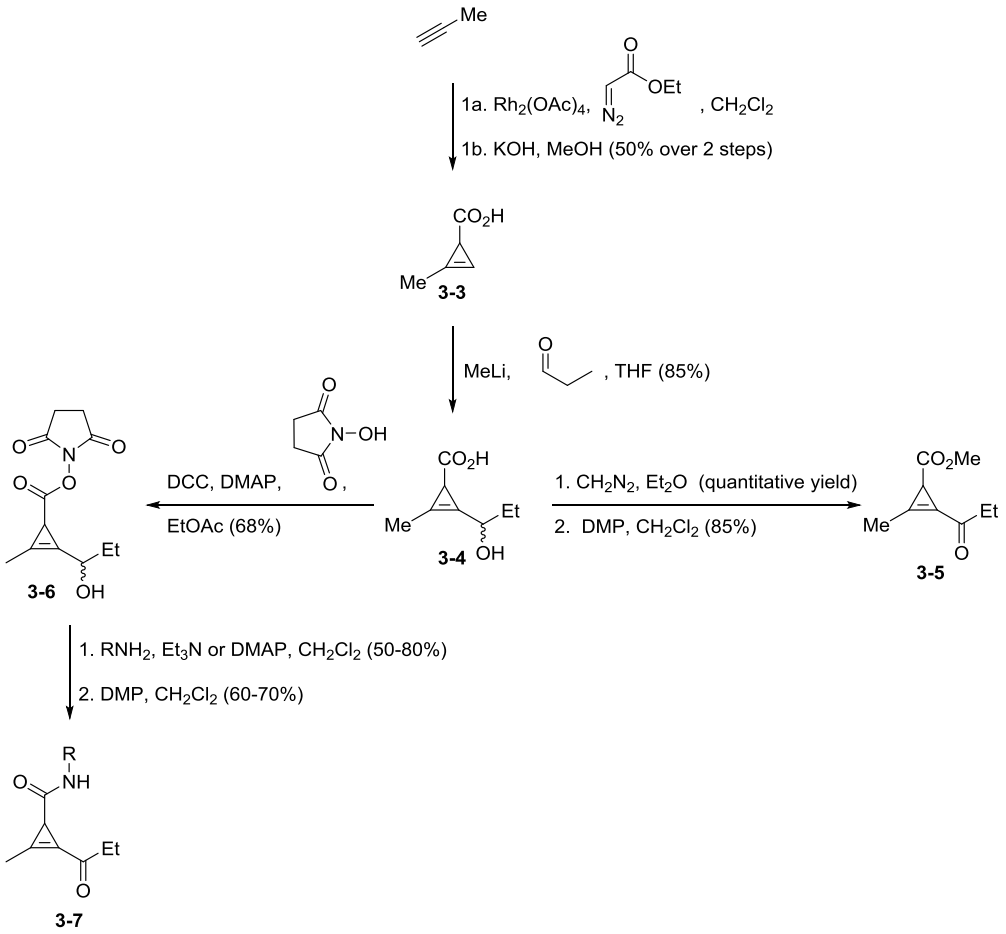

Scheme 3.3: Synthesis of cyclopropenyl ketones used in experiments

3.2.2 Preliminary cyclopropenyl ketone evaluations

Aware of the enhanced electrophilicity of cyclopropenyl ketones[32], I assessed the stability by ^{1}H NMR, of a 20 mM solution of **3-8** in 9:1 D_2O/CD_3OD (Figure 3.2) before evaluating their potential for use as bioconjugation reaction tools. The study indicates that water and/or methanol slowly add to cyclopropenyl ketone **3-8** over time. The half-life for the addition of these nucleophiles to **3-8** at room temperature is approximately 6 hours, which is tolerable as conjugation reactions with the more nucleophilic thiolate anion should proceed at a much faster rate.

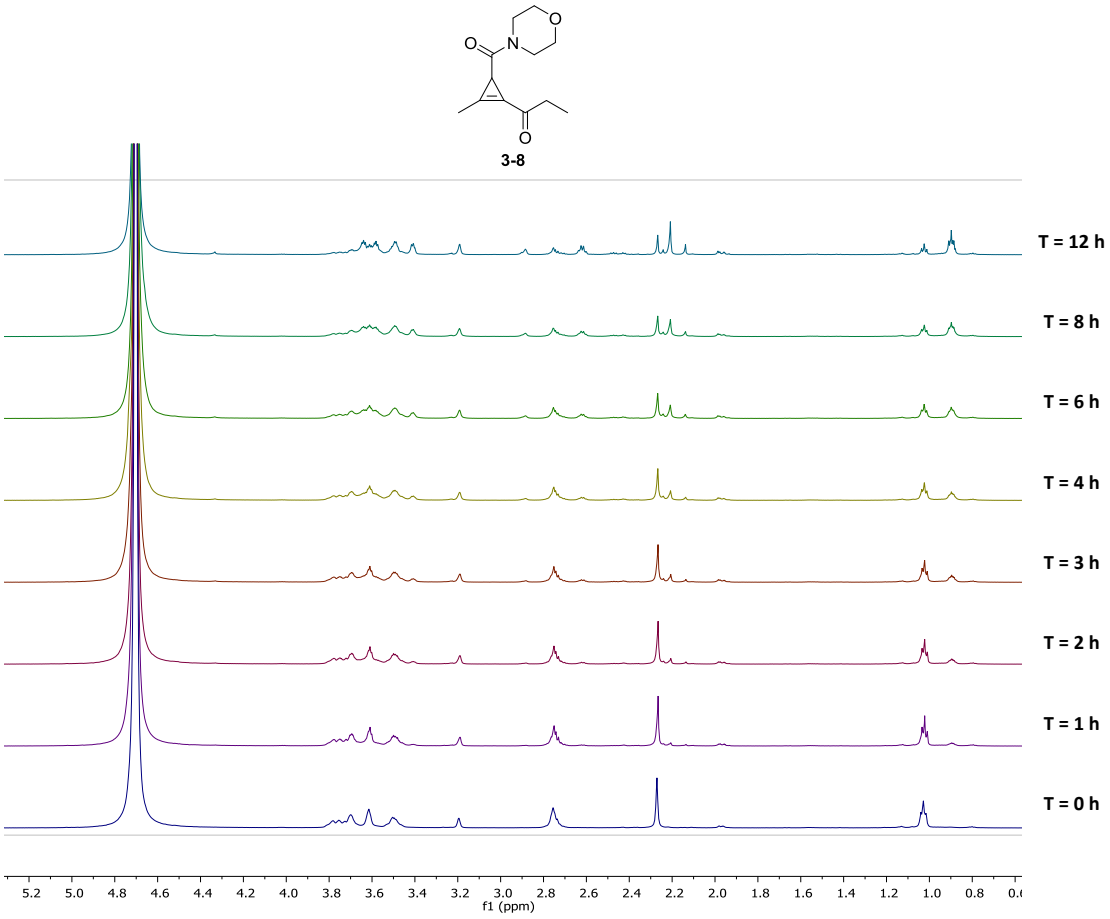

Figure 3.2: Assessment of the stability of **3-8** in 9:1 D_2O/CD_3OD via ^{1}H NMR

Also evaluated was the efficiency of small molecule thiol additions to **3-8** (Scheme 3.4). Addition reactions of mercaptophenylacetic acid (MPA) and the slightly less reactive β-mercaptoethanol (β-ME) to **3-8**, conducted in methanol, with catalytic *N*, *N*-diisopropylethylamine (DIPEA) in the case of the addition of β-ME, proceeded with quantitative NMR yields. Due to the extremely polar nature of these compounds, purification proved difficult and this is reflected in the isolated yields of adducts **3-9** and **3-10**.

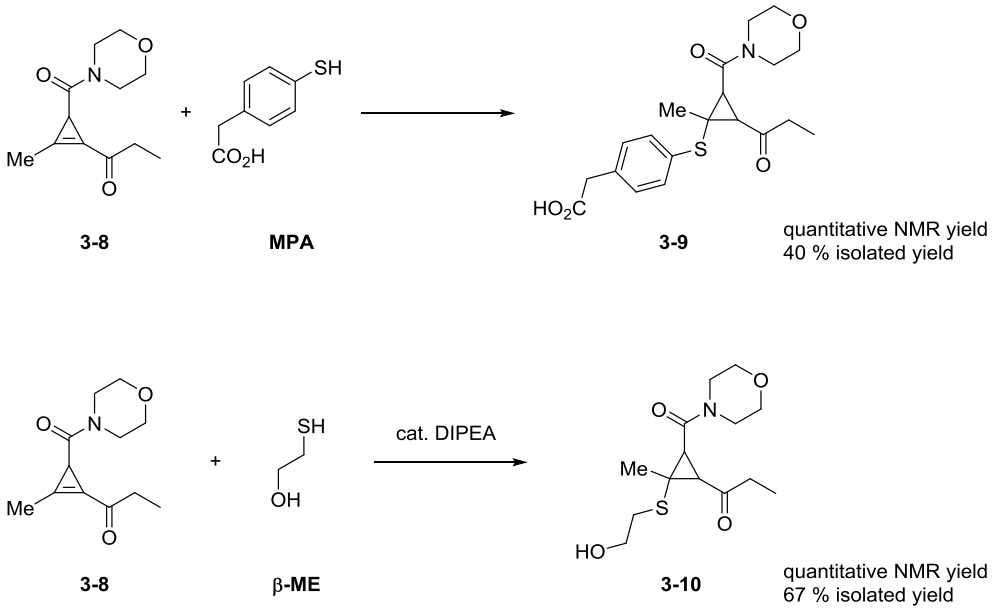

Scheme 3.4: Reactivity of **3-8** with small molecule thiols

I then embarked on determining whether cyclopropenyl ketones satisfy criteria necessary to be considered viable bioconjugation reagents. These results will be discussed under three main headings: specificity/selectivity; kinetic studies and stability of conjugates formed.

3.2.3 Specificity/Selectivity

For small molecules to be successful bioconjugation tools they should selectively tag a functional group of interest. In the case of cyclopropenyl ketones, a concern could be side reactivity with the numerous nucleophiles that exist in the biological milieu. In order to demonstrate the specificity of cyclopropenyl ketones toward reaction with thiol groups, I chose to examine the conjugation of the protein Thioredoxin (Trx) to **3-5** (Figure 3.3). Trx is a redox active protein of approximately 11.7 kDa that contains a single disulfide bond. The reduction of this disulfide bond unmasks two thiol residues, which can react with electrophiles such as *N*-ethylmaleimide and potentially cyclopropenyl ketone **3-5**. However, Trx also contains other reactive side chains such as lysines which can potentially react with electrophile **3-5**. To test for the ability of **3-5** to selectively tag the cysteine residues of Trx without lysine modification, I tested the reactivity of **3-5** toward the oxidized (disulfide) and reduced (dithiol) forms of Trx that was expressed and purified by Colin Thorpe (University of Delaware) according to a published procedure[34]. Trx can be ionized readily by ESI-MS: the raw MS spectrum and the deconvoluted spectrum are shown in Figure 3.3a. As shown in Figure 3.3b, Trx (final conc 10 μM) in pH 6 acetate buffer was reduced by tris(hydroxypropyl)phosphine (THP, final conc 50 μM) for 12 h, and subsequently treated with **3-5** (final conc 500 μM) and aliquots analyzed by ESI-MS after 10 minutes. Labeling of $Trx_{reduced}$ was observed to give an adduct with *m/z* 11994, corresponding to the addition of two cyclopropenyl ketones **3-5** to the Trx core. In an otherwise identical experiment where the reduction step with THP was omitted, no labeling of the protein was observed. These observations support that the labeling of Trx takes place selectively at the cysteine residues and that lysines do not react with **3-5** under these experimental conditions (Figure 3.3c)

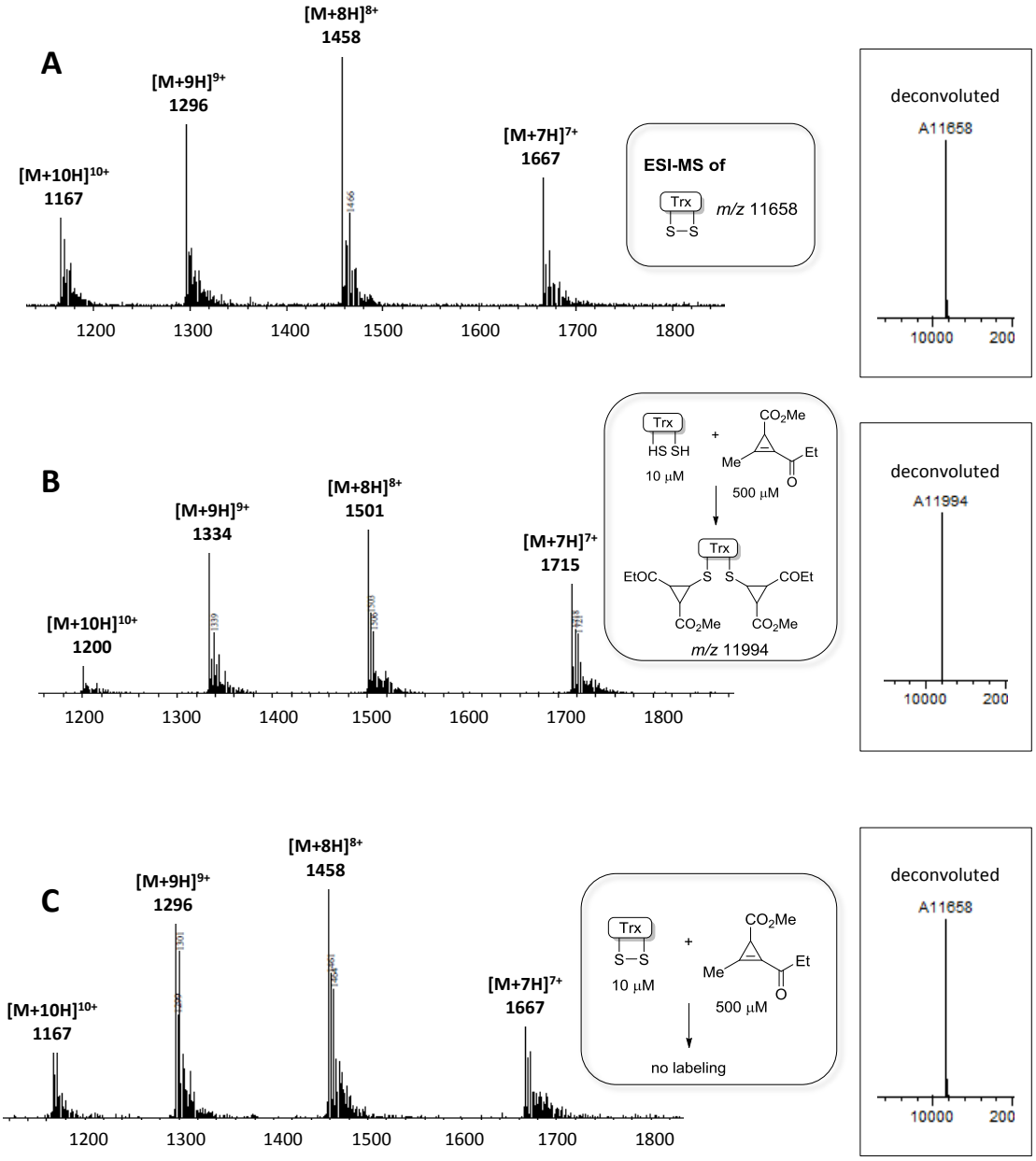

Figure 3.3: Protein labeling by cyclopropenyl ketone **3-5** is selective for cysteine modification (a) ESI-MS of Trx. The raw mass spectrum was deconvoluted using the MagTran software package. (b) Double labeling is observed by ESI-MS for Trx (10 μM) that had been reduced by THP (50 μM) and subsequently reacted with **3-5** (500 μM) for 10 min. (c) No labeling is observed by ESI-MS when Trx (10 μM) is directly incubated with **3-5** (500 μM) for 10 min.

The experiments above outline that it was possible to use **3-5** to label 10 μM Trx selectively without over alkylation. It was also possible to carry out the labeling under preparative conditions (0.9 mM Trx; 5.2 mM **3-5**) with equivalent results.

Having demonstrated that the addition of thiols to cyclopropenyl ketones in the presence of competing nucleophiles is specific, the next logical step was to measure the rate constant for a model reaction. The kinetics of the addition of thiols to cyclopropenyl ketone was evaluated using the tripeptide glutathione (GSH), which has one cysteine residue. An initial competition experiment was conducted using equimolar amounts of **3-5** (0.5 mM) and *N*-ethylmaleimide (NEM, 0.5 mM) and a limiting amount of GSH (50 μM). The crude reaction products were assayed using ESI-MS, and adducts of both NEM and **3-5** were observed. This result qualitatively suggested that the cyclopropenyl ketone reagent is able to compete with the highly reactive NEM as an alkylating agent (Figure 3.4).

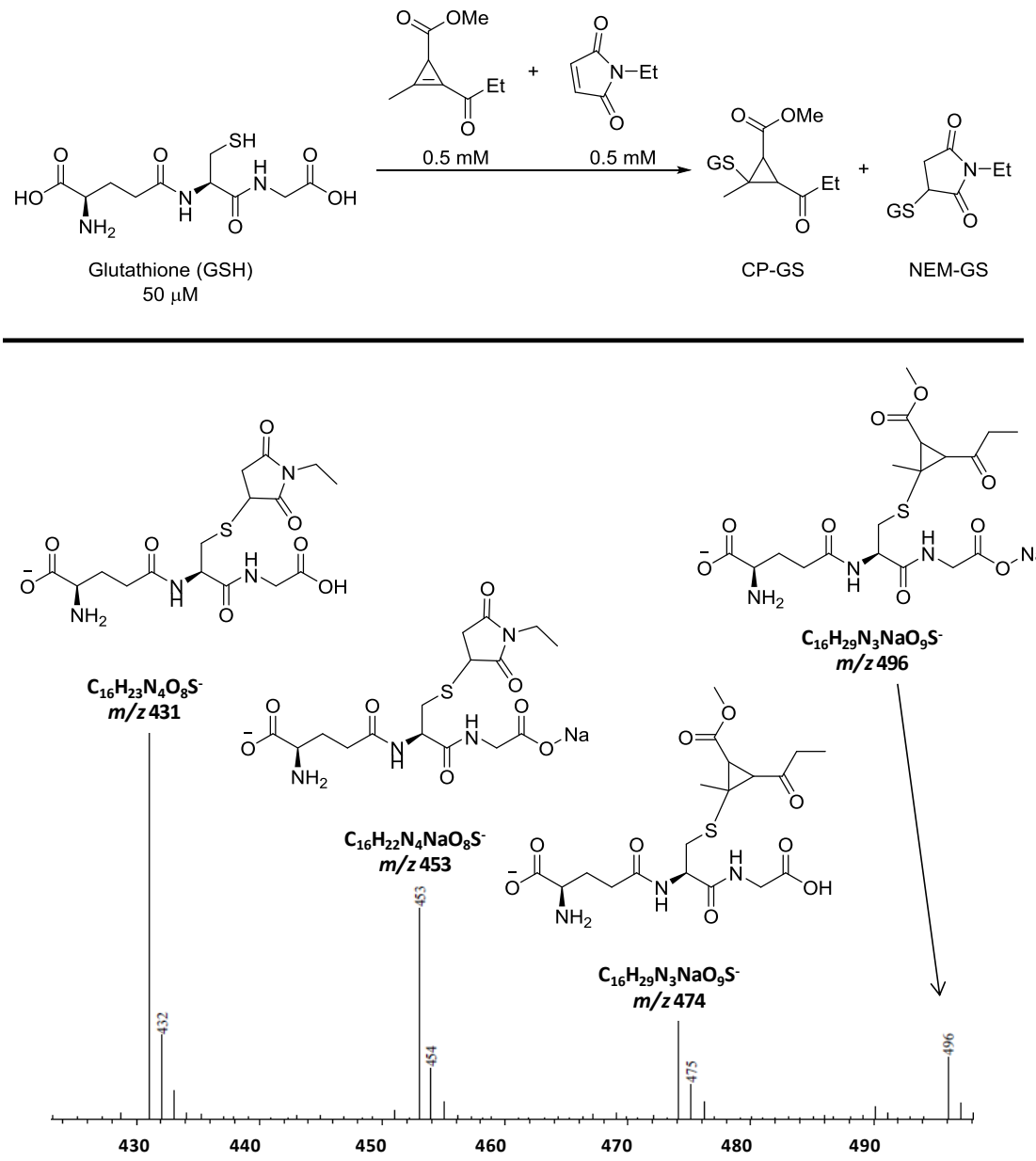

Figure 3.4: Competition experiment between NEM and **3-5** for GSH. ESI-MS in positive mode shows that alkylation by **3-5** competes with NEM.

Experiments were conducted in order to measure the second order rate constant for the conjugation of GSH to cyclopropenyl ketone **3-5**. It was possible to monitor the reaction of **3-5** and GSH by UV-vis spectroscopy. Displayed in Figure 3.5a are the UV

spectra for the reaction between 50 μM **3-5** and 50 μM GSH at pH 7.4 in 50 mM phosphate buffer with 1mM EDTA, containing 0.5 % MeOH. The reaction progress was marked by the disappearance of the intense absorption maximum of **3-5** at 252 nm with $\varepsilon = 4600\ M^{-1}cm^{-1}$, and the appearance of a less intense maximum at 272 nm with $\varepsilon = 2000\ M^{-1}cm^{-1}$. To accurately measure the rate constant for the addition of GSH to **3-5**, stopped flow kinetics experiments were performed under pseudo first order conditions with monitoring at 252 nm at room temperature, in pH 7.4 in 50 mM phosphate buffer with 1mM EDTA and containing 0.5 % MeOH. Upon mixing, the concentrations of the reactants were 0.25 and 2.5 mM respectively and the k_{obs}, determined by nonlinear regression analysis of the data points were found to be 1.12 s^{-1} (Figure 3.5b). The second order rate constant was calculated to be 448 ± 1 $M^{-1}s^{-1}$. For perspective, the second order rate constant of reaction between *N*-phenylmaleimide and GSH was found to be 8680 ± 80 $M^{-1}s^{-1}$ by Thorpe et al[25b] and that of cysteine with bromoacetamide in pH 8.4 buffer is 5.6 $M^{-1}s^{-1}$ [23].

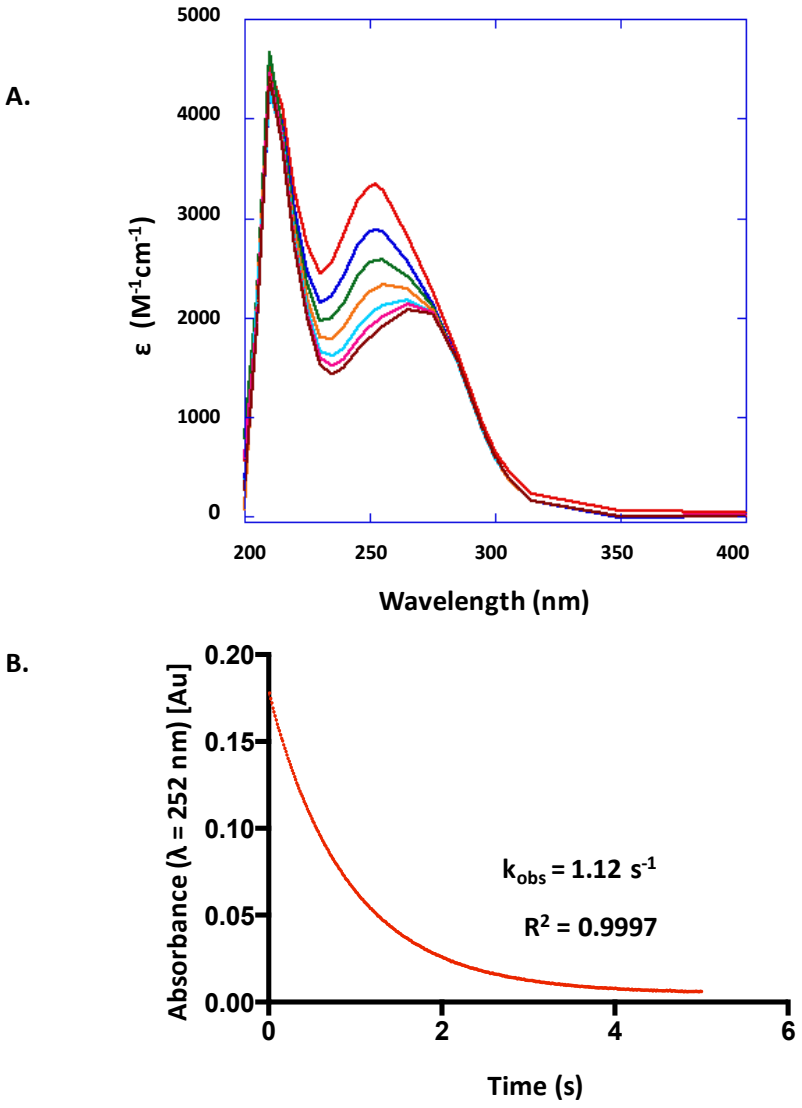

Figure 3.5: (a). UV-vis spectroscopy was used to monitor the reaction between 50 μM **3-5** and 50 μM GSH at pH 7.5 in 50 mM phosphate buffer with 1mM EDTA containing 0.5 % MeOH. Enone **3-5** has an absorption maximum at 252 nm ($\varepsilon = 4600\ M^{-1}cm^{-1}$), and the conjugate has a maximum at 272 nm (with $\varepsilon = 2000\ M^{-1}cm^{-1}$). (b) Stopped flow kinetics experiments were used to measure the rate of the reaction between **3-5** (0.25 mM) and GSH (2.5 mM) at 25 °C in pH 7.5, 50 mM phosphate buffer with 1mM EDTA containing 0.5 % MeOH. Based on k_{obs} 1.12 s^{-1}, the second order rate constant was calculated to be 448 ± 1 $M^{-1}s^{-1}$

3.2.4 Stability Studies

The addition of thiols to maleimides is a reversible process[22,26-27]. In addition, the stability of adducts formed between thiols and maleimides is further compromised by the eventual hydrolysis of maleimides under physiologically relevant conditions (Figure 3.6). In 2011, Baldwin and Kiick studied the kinetics associated with the degradation of various maleimide thiol adducts in the presence of an excess of glutathione at biologically relevant concentrations. The aim of their work was to investigate the viability of maleimide-thiol linkages as being agents for controlled drug release.

Specifically, Baldwin and Kiick described a HPLC study demonstrating that conjugates **1** underwent elimination reactions upon incubation with GSH at 37˚C, over the course of 6 days to give rise to glutathione adducts **3**. Of the adducts studied, the mercaptophenylacetic acid (MPA) adduct was expected to be more labile than alkylthiol conjugates. The pKa of MPA (6.6[35]) is significantly lower than those of the alkylthiols that were studies: *N*-acetylcysteine has a pKa of 9.5[36], and 3-mercaptopropionic acid has a pKa of 10.3[37]. Indeed, it was observed that **1a** (0.1 mM) eliminated MPA in the presence of GSH (10 mM) to form adduct **3a** with $t_{1/2}$ = 19 h. Other thiol conjugates showed less rapid release and their kinetics were more complicated by competing hydrolysis of the maleimide adduct **2**.

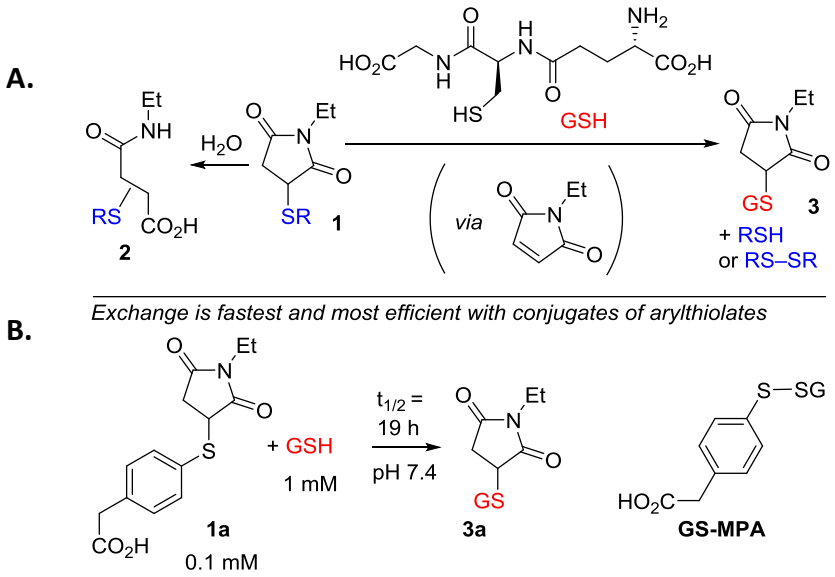

Figure 3.6: **(**a) Maleimide-thiol adducts are unstable due to retro-conjugate addition and hydrolysis. In the presence of GSH, conjugate **1** can eliminate and add glutathione to give conjugate **3**. (b) Maleimide conjugates of arylthiolates undergo rapid elimination. Compound **1a** eliminates mercaptophenylacetic acid in the presence of GSH to give conjugate **3a** with a half-life of 19 h. Analogous reactions of alkylthiol conjugates (**1**, R = $CH_2CH_2CO_2H$ or R = $CH_2C(NHAc)CO_2H$) are slower and are complicated by hydrolysis to **2**

Because arylthiolate conjugates are known to be more labile than those of alkylthiolates, I chose the former to study in the cyclopropenyl ketone system. I rationalized that if the cyclopropenyl ketone-arylthiolate conjugates were stable, it would demonstrate the robustness of the cyclopropenyl ketone bioconjugation method

I sought to test the stability of the cyclopropenyl ketone–MPA conjugate **3-9** in the presence of glutathione. Compound **3-9** was prepared as described in Scheme 3.4 .As shown in Scheme 3.5, the elimination of MPA would lead to the transient formation of cyclopropenyl ketone **3-8**, which would be expected to add GSH.

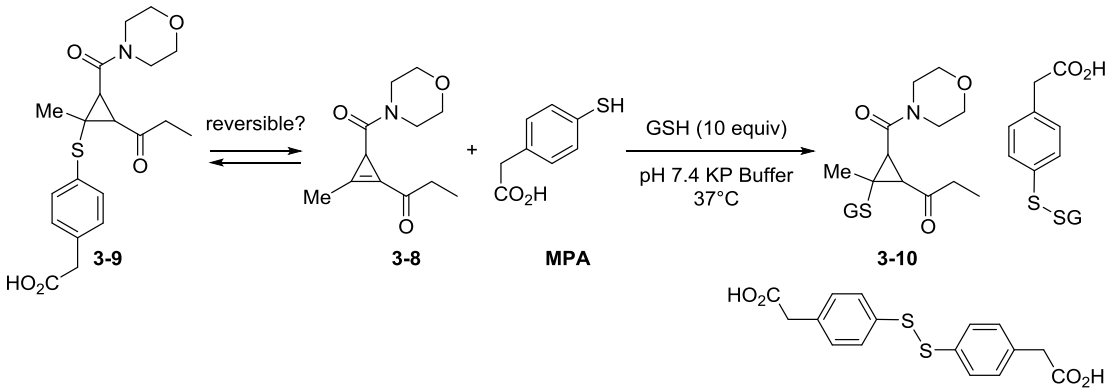

Scheme 3.5. Thiol elimination/GSH conjugate addition of **3-9** could lead to **3-10** via intermediate **3-8** if conjugate addition to cyclopropenyl ketones is reversible.

Indeed, in a control experiment where the crude reaction products resulting from combining **3-8** (0.2 mM) with a 10:1 mixture of GSH/MPA (2 mM, 0.2 mM respectively) are assayed 10 minutes after mixing using ESI-MS, masses corresponding to the adducts of GSH (*m/z* 531) and MPA (*m/z* 392) were observed (Figure 3.7).

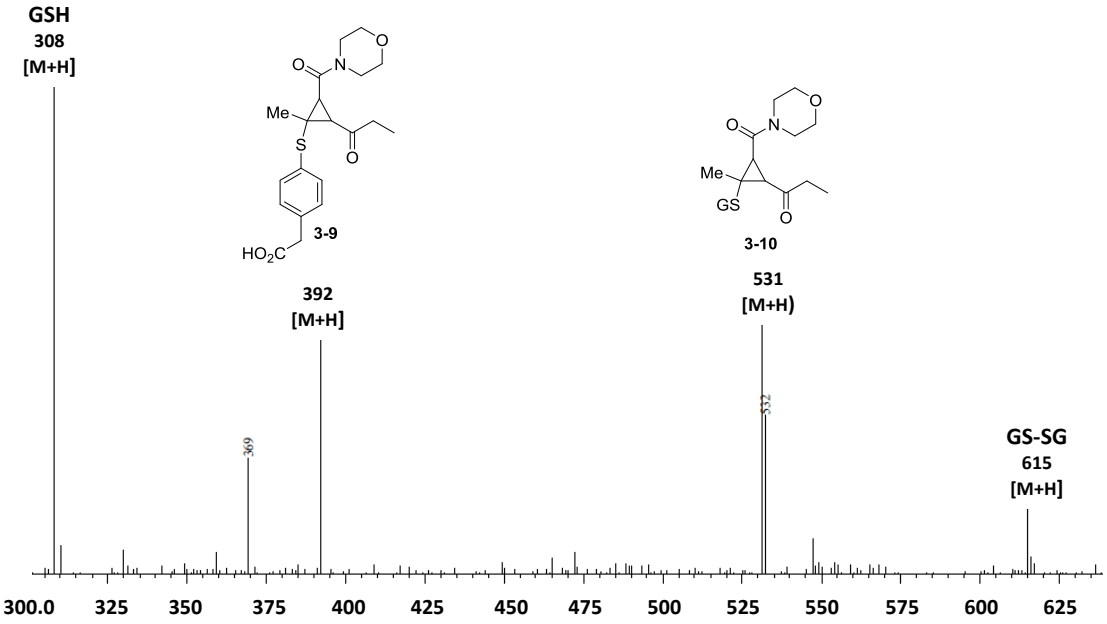

Figure 3.7: Reacting **3-8** with a 10:1 mixture of GSH:MPA demonstrates that should **3-8** be liberated during the course of the incubation study **3-9** should be observed.

Morpholinamide **3-9** (0.2 mM) was incubated at physiologically relevant conditions (37˚C, pH 7.4 50 mM phosphate buffer with 1 mM EDTA) in the presence of GSH (2 mM) and samples were taken periodically and assayed by HPLC. The peaks observed were integrated to determine the stability of the adduct over time. We found that unlike the maleimide-MPA adduct described in the studies by Baldwin and Kiick, adduct **3-9** remained intact for up to 55 hours after incubation (Figure 3.8).

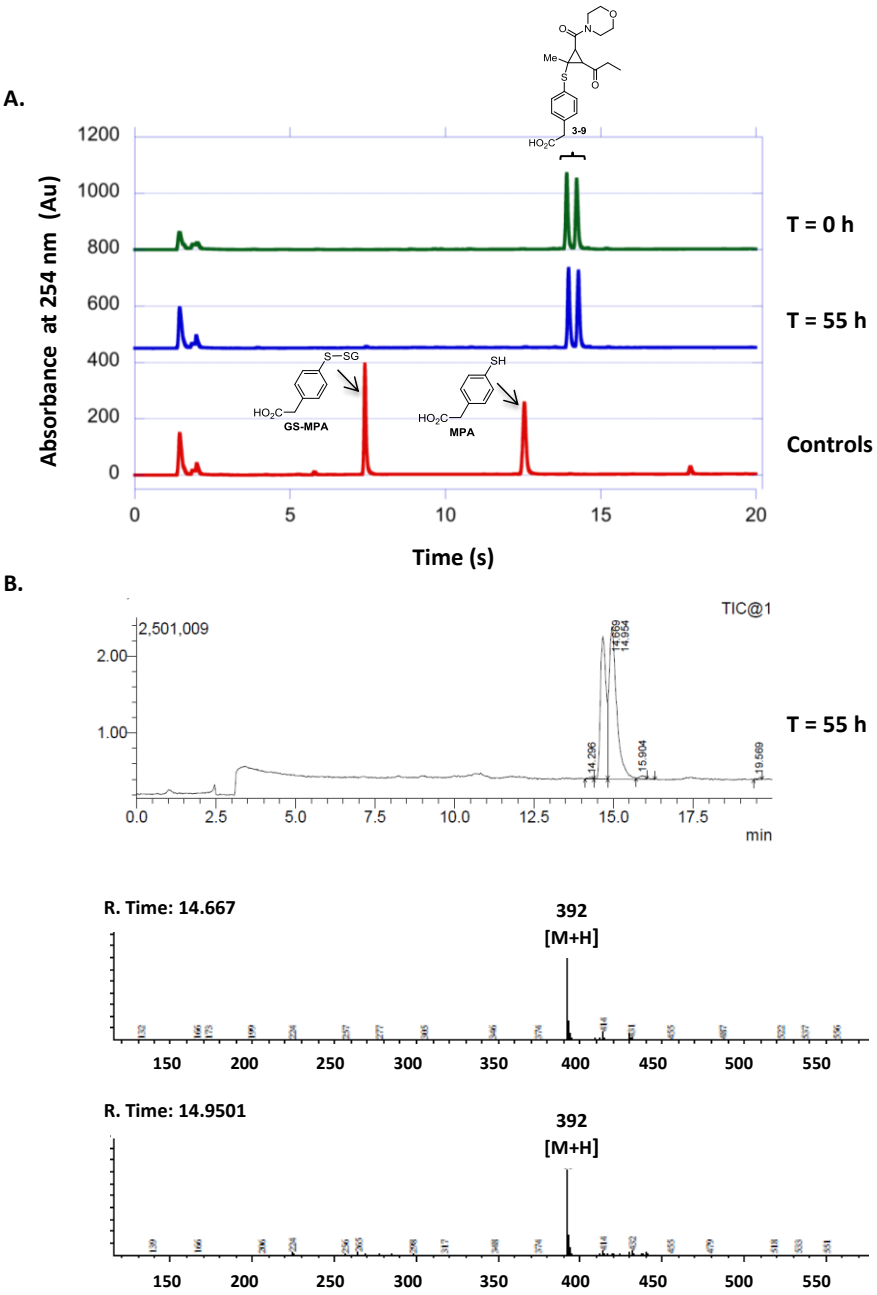

Figure 3.8: (a) Shown are HPLC traces of stability of **3-9** (0.2 mM) in pH 7.4, 50 mM phosphate buffer with 1 mM EDTA incubated with GSH (2 mM) at 37˚C over a period of 55h. The peak area for the diastereomers of **3-9**, remains the same over time. (b) LCMS spectrum of T = 55 h confirms that **3-9** remains intact under these conditions.

I also evaluated the stability of **3-9** in human plasma. **3-9** (40 μL of a 10 mM stock solution) was incubated in human plasma (1960 μL) at 37˚C over a period of 8 days. Periodically, 250 μL aliquots were removed and subjected to centrifugal filtration to allow for large protein removal, and the filtrate obtained assayed by HPLC. At t = 0, there are no peaks after 3 min in human plasma. For human plasma containing **3-9** (0.2 mM), a mixture of diastereomers, two peaks (14.1 min, labeled *a*; 14.4 min, labeled *b*) are detected. The area of *a* was 608 mAu and the area of *b* was 664 mAu. After 8 days, the two samples were again assayed and both contained a small peak (labeled *c*) assignable to background reactivity in plasma. For human plasma containing **3-9**, the area of peak *a*, was 605 mAu, which is 99% of the area measured at t = 0. Likewise, the area of peak *b* was 608 mAu, which is 92% of the area measured at t = 0. From these observations it can be deduced that 95% of compound **3-9** was unchanged after incubation in human plasma at 37C for 8 days (Figure 3.9).

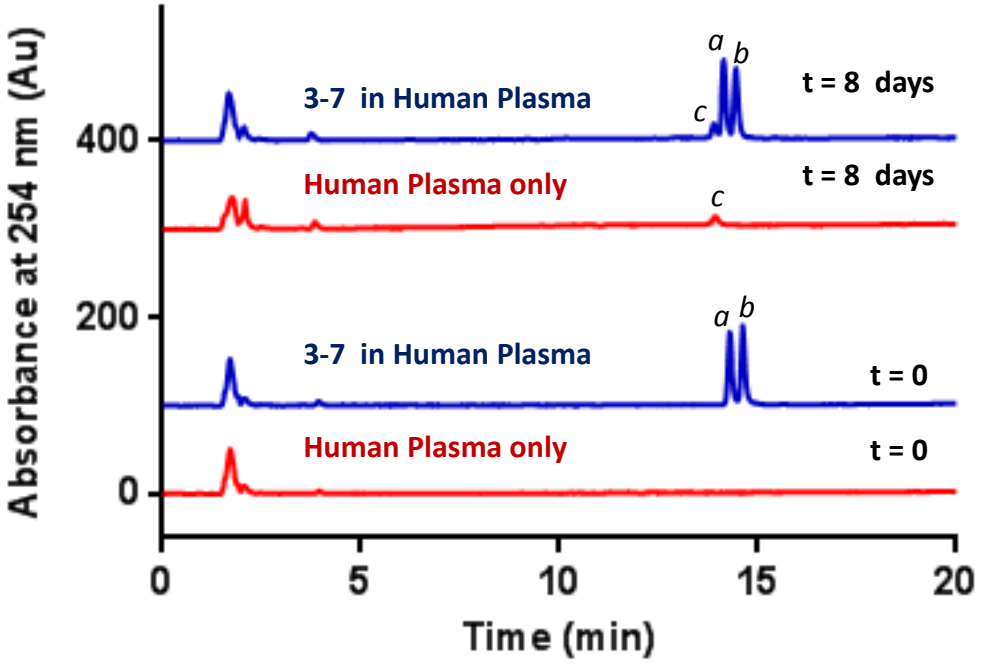

Figure 3.9: HPLC with detection at 254 nm was used to monitor the stability of **3-9** (0.2 mM) incubated in human plasma at 37˚C over a period of 8 days.

In light of the results obtained in studies conducted, cyclopropenyl ketones can be a considered as viable thiol alkylating reagents, providing a remedy to the instability associated with the widely used maleimide based technology while maintaining robust reactivity.

3.3 Applications of cyclopropenyl ketones as thiol alkylating agents

One anticipated application of cyclopropenyl ketones will be as the linkage chemistry for antibody drug conjugation. The field of protein-drug conjugates has in recent years become one of great interest and one with immense value especially as it relates to targeted cancer treatment. One of the main pitfalls of earlier generation

therapeutics is that of discerning between target and non-target cells within a system. ADCs comprise of 3 components: the monoclonal antibody (mAB), the linker and the drug. The mAB will ideally bind specifically with an antigen that is overexpressed on compromised cells, thereby allowing for the targeted drug delivery. This allows for the utilization of significantly more potent drugs than could be used in earlier treatments as surrounding, healthy cells can remain uncompromised. There are currently a few ADCs on the market and several others in different stages of clinical trials[3], which utilize maleimide-thiol linker chemistry (there are several inter-chain disulfides present in the mAbs). Given the increased potency of drugs being administered using ADCs, the need to have linkers that are stable in varying degrees of reducing environments and for extended periods within a biological system is great. Currently, a major pharmaceutical company is evaluating whether cyclopropenyl ketones can form the basis of new linkage chemistry for antibody-drug conjugation

Another application for cyclopropenyl ketones will be as crosslinkers for the formation of stable hydrogels materials for 3-D cell culture applications. Of the various 'click' chemistries, perhaps no reaction has greater impact than the thiol-ene reaction on the fields of materials science and polymer chemistry. As a point of nomenclature, the term "thiol-ene" is generally used in polymer/materials literature to describe additions of thiols to alkenes regardless of reaction mechanism, including conjugate addition reactions of thiols to maleimides and other conjugate acceptors.

Hydrogels are 3-D polymer networks which are able to retain water in their swollen state which can be chemically crosslinked through covalent bonds, non-chemically crosslinked though non-covalent interactions, or a combination of both[38]. The ability of hydrogels to retain large amounts of water, while being largely

chemically inert, results in properties that mimic biological tissue and which lead to a high level of biocompatibility. An early example of hydrogels being applied in the biomedical field occurred in the 1960s, when some of the first contact lenses were described[39]. The properties of a hydrogel can be controlled by the chemical nature of the polymer framework and as such a wide range of chemistries have been employed to push the boundaries of hydrogel possibilities. Linker chemistries have included, but have not been limited to free radical polymerization, reactions between isocyanates and alcohols, condensation reactions, Michael addition, click chemistry, native chemical ligation, tetrazine ligation and enzymatic reactions[40]. As in bioconjugation chemistry, maleimides are widely utilized in the field of biomaterials. A current collaboration with the Kloxin group in the Department of Materials Science and Engineering, here at the University of Delaware has been to evaluate the viability of crosslinked cyclopropenyl ketones as crosslinkers for hydrogel formation, with applications to *in vivo* cell culture (Scheme 3.6).

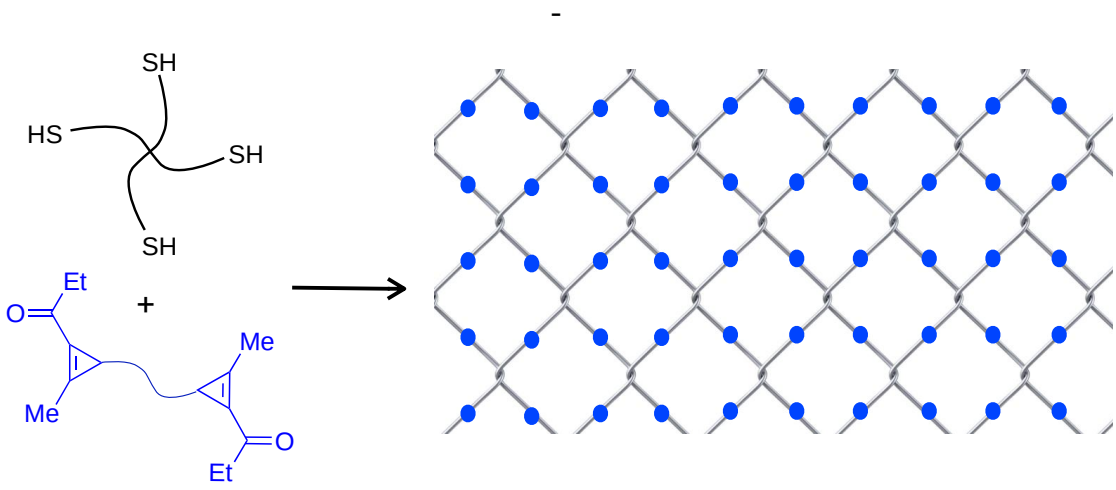

Scheme 3.6: Hydrogel formation with cyclopropenyl ketones and polyfunctional thiol crosslinker.

Synthesis of cyclopropenyl ketone crosslinker

Bisfuctionalized cyclopropenyl ketone cross linkers were synthesized by reacting NHS ester **3-10** with O, O'-bis(2-aminoethyl)octadecaethylene, PEG_{18} Diamine, followed by oxidation of the resulting alkenol with Dess Martin Periodinane (Scheme 3.7). For each set of polymerization experiments conducted, crosslinkers were prepared freshly due to known, slow reactivity with water (Figure 3.2).

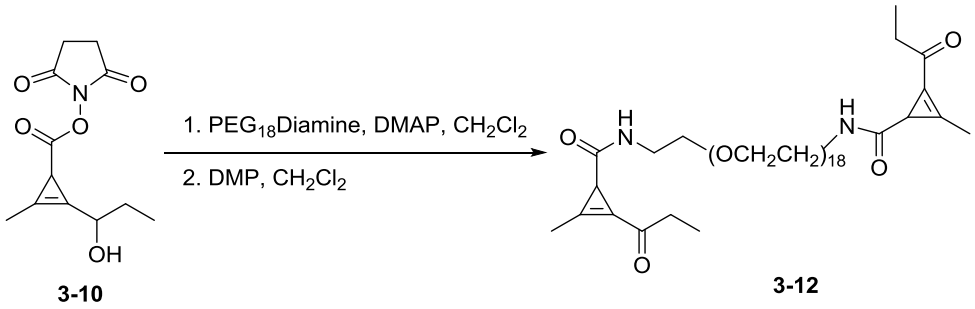

Scheme 3.7: Synthesis of biscyclopropenyl ketone cross linker.

Hydrogel formation

On mixing stoichiometric amounts of biscyclopropenyl ketone **3-11** (~1 kDa) and a PEG-tetra-thiol crosslinker (20 kDa) in PBS buffer, the gelpoint is reached within 30 seconds, which is faster than the initial rheological measurement could be reported by my collaborator, Lisa Sawicki (Figure 3.10).

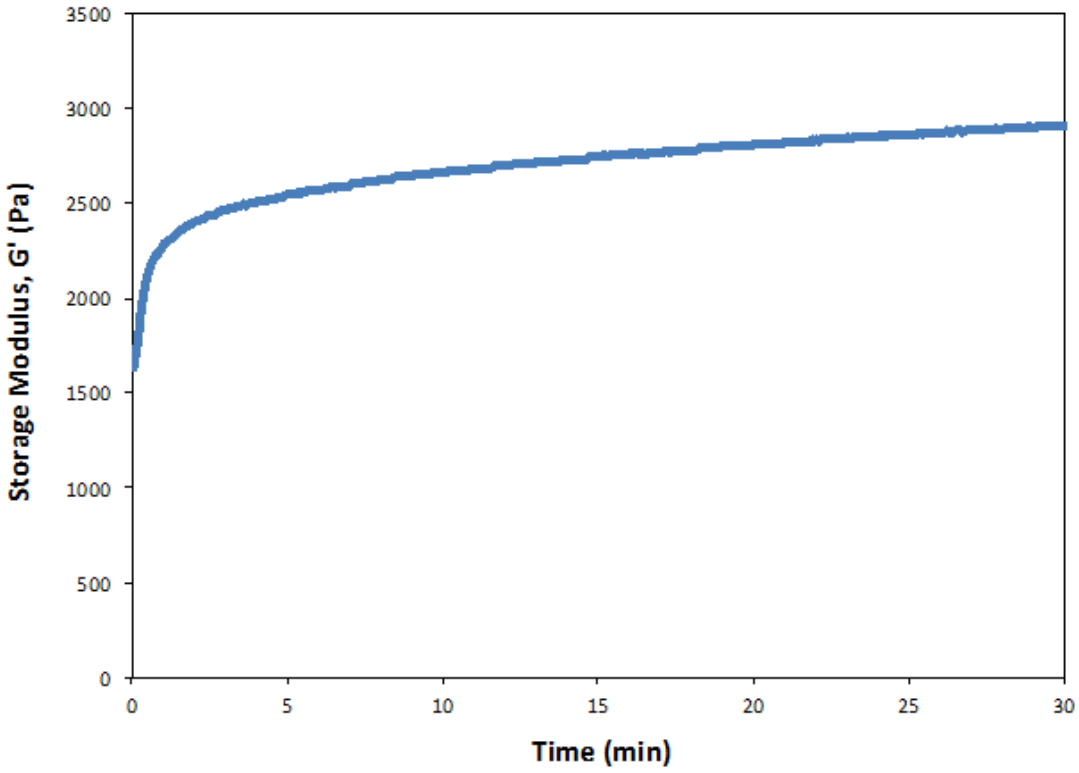

Figure 3.10: Hydrogel formation between 1kDa biscyclopropenyl ketone **3-12** and 20kDa PEG tetra-thiol linker is fast with the gelpoint being reached in prior to 30 seconds.

Further, initial experiments show that cyclopropenyl ketone derived hydrogels incubated in PBS containing 10 mM GSH are stable rheologically for up to 6 days. These data contrast studies reported by Baldwin and Kiick demonstrating the degradation of maleimide based hydrogels in reducing environments[41]. Experimentation in this area is ongoing.

3.4 Conclusion

I have developed a new class of cysteine alkylating agents based on cyclopropenyl ketones. These reagents are fast, selectively target thiols and form stable adducts on reaction. Studies towards utility in the biopharmaceutical and materials science arenas are currently being undertaken.

3.5 Experimental Section

methyl 2-methyl-3-propionylcycloprop-2-ene-1-carboxylate (3-5)

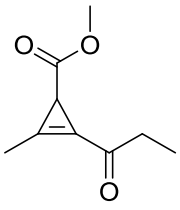

3-5 was prepared by following a published procedure for which I am a coauthor[32].

2,5-dioxopyrrolidin-1-yl 2-(1-hydroxypropyl)-3-methylcycloprop-2-ene-1-carboxylate (3-6)

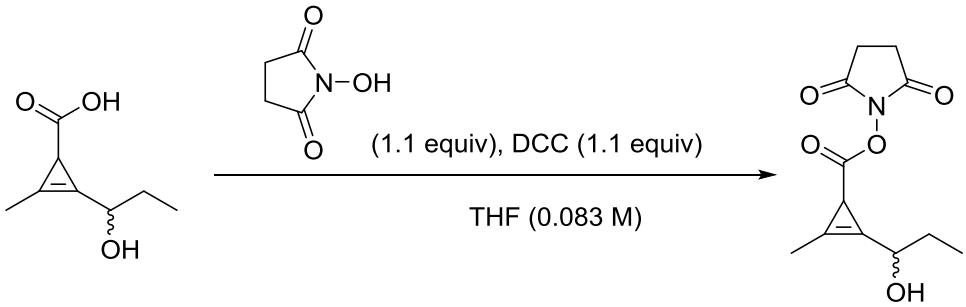

3-6

To a solution of 2-(1-hydroxypropyl)-3-methylcycloprop-2-ene-1-carboxylic acid [32](1.0 g, 6.4 mmol) in anhydrous THF (77 mL, 0.083M), *N*, *N*'-dicyclohexylcarbodiimide (1.4 g, 7.0 mmol) and *N*-hydroxysuccinimide (810 mg, 7.0 mmol) were added. The mixture was allowed to stir at r.t. for 18 h and then filtered through celite. The celite was rinsed with THF and silica gel (5 g) was added to the filtrate, which was then concentrated to dryness on the rotary evaporator. Column chromatography (gradient from 0 - 50 % ethyl acetate in hexanes) furnished the product **3-6** (1.1 g, 4.4 mmol, 68%) as a yellow oil. The diastereomer ratio was 1.1:1 by ^{1}H NMR analysis. ^{1}H NMR ($CDCl_3$, 600 MHz, δ): 4.59 (t, *J* = 6.4 Hz, 0.5H), 4.54 (t, *J* = 6.4 Hz, 0.5H), 3.06 (bs, OH), 2.80 (bs, 4H), 2.38 (d, *J* = 4.2 Hz, 1H), 2.17 (s, 3H), 1.81-1.73 (m, 2H), 1.00-0.95 (m, 3H); ^{13}C NMR ($CDCl_3$, 100 MHz, δ): 170.9 (C), 170.8 (C), 169.8 (broad, C, 2 carbons), 106.8 (C), 106.6 (C), 103.1 (C), 67.9 (CH), 67.3 (CH), 29.0 (CH_2), 28.2 (CH_2), 25.6 (CH_2, 2 carbons), 20.4 (CH), 20.0 (CH), 9.82 (CH_3), 9.80 (CH_3), 9.50 (CH_3), 9.46 (CH_3); FT-IR (NaCl, thin film, cm^{-1}): 3467, 2970, 2879, 1770, 1736, 1431, 1372,1210, 1067; LIFDI MS *m/z* [M +] Calcd for $C_{12}H_{15}NO_5$ 253.0950, Found 253.092

(2-(1-hydroxypropyl)-3-methylcycloprop-2-en-1-yl)(morpholino)methanone (3-11)

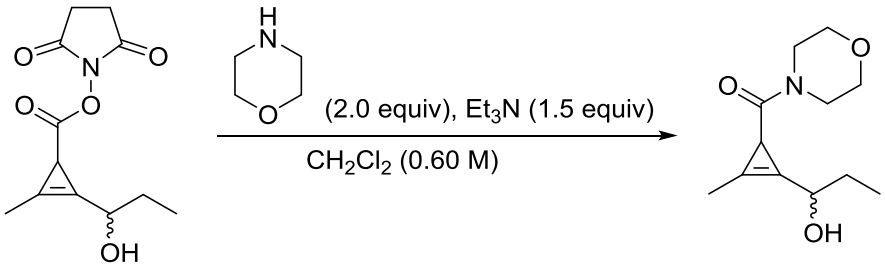

3-6 **3-11**

To a dry round bottom flask charged with a solution of **3-6** (700 mg, 2.76 mmol) in CH_2Cl_2 (2.3 mL) was added a solution of morpholine (481 mg, 5.53 mmol) in CH_2Cl_2 (2.2 mL). Et_3N was added via syringe (0.60 mL, 4.2 mmol) at r.t. The reaction turned cloudy after 5 minutes and was complete after 15 minutes by TLC monitoring. Silica gel (3 g) was then added, and the mixture concentrated to dryness using a rotary evaporator. Column chromatography (gradient from 10-100% ethyl acetate in hexanes) furnished **3-11** (500 mg, 81% yield) as a pale orange oil. The diastereomer ratio was 1.1:1 by ^{1}H NMR analysis. ^{1}H NMR ($CDCl_3$, 600 MHz, δ): 4.71 (t, *J* = 6.7 Hz, 0.5H), 4.42 (t, *J* = 6.7 Hz, 0.5H), 4.23 (bs, OH), 3.70 (bs, 7H), 3.57 (bs, 1H), 2.35 (s, 1H), 2.12 (s, 3H), 1.88-1.78 (m, 1H), 1.77-1.73 (m, 0.5H), 1.64-1.58 (m, 0.5H), 1.04 (t, *J* = 7.6 Hz, 1.4H), 0.90 (t, *J* = 7.6 Hz, 1.6H); ^{13}C NMR ($CDCl_3$, 100 MHz, δ): 175.0 (C), 174.9 (C), 108.7 (C), 107.9 (C), 104.8 (C), 104.4 (C), 67.9 (CH), 66.9 (CH_2, 2 carbons), 66.3 (CH), 46.1 (CH_2), 42.5 (CH_2), 29.8 (CH_2), 28.3 (CH_2), 22.9 (CH), 21.8 (CH), 10.5 (CH_3), 10.3 (CH_3), 9.6 (CH_3), 9.5 (CH_3); FT-IR (NaCl, thin film, cm^{-1}): 3382, 2964, 2921, 2855, 1894, 1613, 1437, 1236, 1115, 1046, 1019, 974, 853, 573; LIFDI MS *m/z* [M +] calcd for $C_{12}H_{19}NO_3$ 225.1365, found 225.1353.

1-(2-methyl-3-(morpholine-4-carbonyl)cycloprop-1-en-1-yl)propan-1-one (3-8)

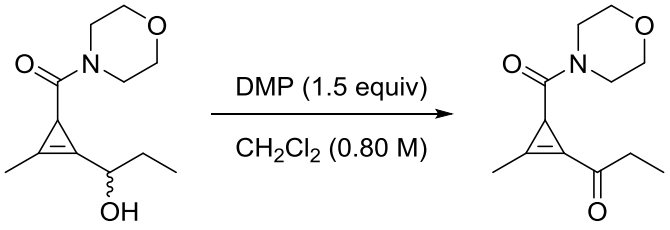

3-11 **3-8**

To a solution of **3-11** (300 mg, 1.30 mmol) in CH_2Cl_2 (1.7 mL, 0.80 M) was added Dess Martin Periodinane, DMP, (850 mg, 2.00 mmol) in one portion. After 30 minutes, the reaction was filtered through celite and the filtrate concentrated onto C-2 silica gel prepared as described below. Column chromatography (slow gradient from 0-80% ethyl acetate in toluene) furnished **3-8** (214 mg, 72%) as a pale yellow oil. Residual toluene peaks are observable in the ^{1}H NMR spectrum at 7.20 and 2.37 ppm. ^{1}H NMR ($CDCl_3$, 400 MHz, δ): 3.92- 3.89 (m, 1H), 3.80-3.62 (m, 6H) 3.50-3.44 (m, 1H), 2.81-2.74 (m, 2H), 2.58 (s, 1H), 2.44 (d, *J* = 2.1 Hz, 3H), 1.19 (td, *J* = 7.4, 2.3 Hz, 3H); ^{13}C NMR ($CDCl_3$, 100 MHz, δ): 192.1 (C), 171.5 (C), 122.4 (C), 105.2 (C), 66.90 (CH_2), 66.86 (CH_2), 46.1 (CH_2), 42.3 (CH_2), 36.6 (CH_2), 22.6 (CH), 11.9 (CH_3), 7.9 (CH_3); FT-IR (NaCl, thin film, cm^{-1}): 2973, 2856, 1849, 1679, 1637, 1457, 1436, 1270, 1236, 1115, 1036. LIFDI MS *m/z* [M +] calcd for $C_{12}H_{17}NO_3$ 223.1208, found 223.1196.

(NB. In some cases after column chromatography, solid DMP byproduct was observed. This could be removed by re-suspending the material in toluene, filtering through celite, rinsing the filtered solid with ethyl acetate and concentrating the filtrate to furnish pure material.)

C-2 Silica Gel Preparation[42]

Flash silica gel (100 g, SiliaFlash ® F60, 40-63 μm (230-400 mesh)) was suspended in 200 mL of dry chloroform in a round bottomed flask under a N_2 atmosphere. The flask was chilled by an ice bath. Ethyltrichlorosilane (5.1 g, 31 mmol) was added via syringe. After the addition was completed, the flask was closed and shaken vigorously to mix (HCl is formed). The mixture was allowed to sit at rt with occasional shaking

until the next day (suspension becomes yellow). The silica gel was filtered on a Buchner funnel and washed twice with 200 mL portions of chloroform and three times with 200 mL portions of methanol. The silica gel was transferred to a round bottomed flask, and was dried by heating (40°C oil bath) under vacuum.

2-(4-((1-methyl-2-(morpholine-4-carbonyl)-3-propionylcyclopropyl)thio)phenyl)acetic acid (3-9)

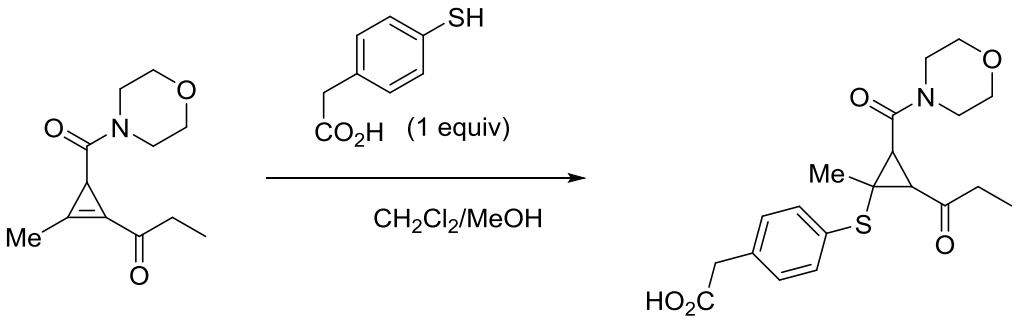

3-8 **3-9**

To a solution of **3-8** (100 mg, 0.45 mmol) in MeOH (0.5 mL, 0.9 M) was added a solution of 4-mercaptophenylacetic acid (75 mg, 0.45 mmol) in MeOH (0.5 mL, 0.9 M). After 15 minutes, silica gel (0.5 g) was added, and the mixture concentrated to dryness using a rotary evaporator. Column chromatography (gradient from 10-100% ethyl acetate in hexanes) furnished **3-9** as a pale yellow oil (68 mg, 0.17 mmol, 40% isolated yield, quantitative ^{1}H NMR yield) as a mixture of diastereomers. ^{1}H NMR ($CDCl_3$, 400 MHz, δ): 7.33-7.32 (d, *J*=8.0 Hz, 0.9H), 7.29 (d, *J*= 8.0 Hz, 1H), 7.20-7.17 (m, 2H), 3.69-3.59 (m, 2H), 3.55 (s, 2H), 3.53-3.40 (m, 2H), 3.37-3.31 (m, 2H), 3.29-3.25 (m, 1H), 3.18-3.14 (m, 1H), 2.83 (d, *J* = 6.1 Hz, 0.5H), 2.71 (d, *J* = 6.1Hz, 0.6H), 2.64-2.57 (m, 1H), 2.51-2.44 (m, 1.4H), 2.35 (d, *J* =9.7Hz, 0.5H), 1.6 (s, 1H), 1.49 (s, 1.6H), 1.03-0.99 (m, 3H); ^{13}C NMR ($CDCl_3$, 100 MHz, δ): 205.8 (C), 204.3

(C), 176.4 (C), 176.0 (C), 165.9 (C), 165.4 (C), 133.7 (C), 133.4 (CH), 133.0 (C), 132.0 (C), 130.3 (CH), 130.2 (CH), 129.9 (CH), 66.89 (CH_2), 66.85 (CH_2), 66.80 (CH_2),66.5 (CH_2), 45.9 (CH_2), 42.6 (CH_2), 42.0 (CH_2), 40.5 (CH), 40.50 (CH_2), 40.47 (CH_2), 38.3 (C), 38.6 (CH), 38.0 (CH_2), 37.9 (CH_2), 35.4 (CH), 34.3 (C), 33.4 (CH), 22.3 (CH_3), 17.0 (CH_3), 7.8 (CH_3); FT-IR3 (NaCl, thin film, cm^{-1}): 3056, 2974, 2927, 1733, 1702, 1615, 1610, 1458, 1439, 1406, 1384,1233, 1116, 732=5; LIFDI *m/z:* [M]+ calcd for $C_{20}H_{25}NO_5S$ 391.1453, found 391.1537.

***N,N'*-(3,6,9,12,15,18,21,24,27,30,33,36,39,42,45,48,51,54,57-nonadecaoxanonapentacontane-1,59-diyl)bis(2-(1-hydroxypropyl)-3-methylcycloprop-2-ene-1-carboxamide) (3-12)**

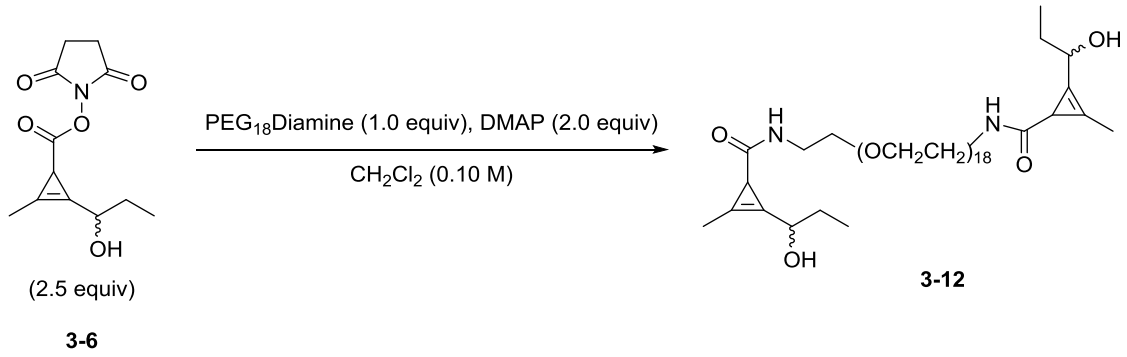

To a dry round bottom flask charged with a solution of O, O'-bis(2-aminoethyl)octadecaethylene, PEG_{18} Diamine (113 mg, 0.13 mmol) in CH_2Cl_2 (1.3 mL), 4-dimethylaminopyridine (31 mg, 0.26 mmol) was added and the mixture stirred for 15 minutes. A solution of **3-6** (80 mg, 0.32 mmol) in CH_2Cl_2 (1.3 mL) was then added, the reaction was allowed to stir at room temperature overnight and then concentrated to dryness onto C-2 silica gel using a rotary evaporator. Column chromatography (gradient from 0-10% methanol in dichloromethane) furnished **3-12**

(70 mg, 0.06 mmol, 46% yield) as a colorless oil. The diastereomer ratio was 1.3:1 by ^{1}H NMR analysis. ^{1}H NMR ($CDCl_3$, 400 MHz, δ): 6.37 (s, NH), 4.66-4.63 (t, *J* = 6.5 Hz, 0.6H), 4.49-4.47 (t, *J* = 6.5 Hz, 0.4H), 3.78-3.62 (m, 40 H), 3.57-3.49 (m, 3H), 3.45-3.40 (m, 1H), 2.55 (bs, OH), 2.13 (s, 3H), 2.11 (s, 1H), 1.85-1.71 (m, 2H), 1.71-1.65 (m, 1H), 1.04-1.02 (t, *J* = 7.7 Hz, 1 H), 0.95-0.93 (t, *J* = 7.7 Hz, 2H) ; ^{13}C NMR ($CDCl_3$, 100 MHz, δ):192.4 (C), 172.4 (C), 122.9 (C), 105.9 (C), 77.2 (CH_2), 70.6 (CH_2), 70.5 (CH_2), 69.9 (CH_2), 39.3 (CH_2), 36.8 (CH_2), 26.3 (CH), 11.9 (CH_3), 7.8 (CH_3); FT-IR (NaCl, thin film, cm^{-1}): 3314, 2870, 1625, 1539, 1457, 1350, 1300, 1250, 1110; LIFDI MS *m/z* [M+Na] calcd for $C_{56}H_{104}N_2O_{23}$ 1195.6928 found 1195.6914

***N*,*N*'-(3,6,9,12,15,18,21,24,27,30,33,36,39,42,45,48,51,54,57-nonadecaoxanonapentacontane-1,59-diyl)bis(2-methyl-3-propionylcycloprop-2-ene-1-carboxamide) (3-13)**

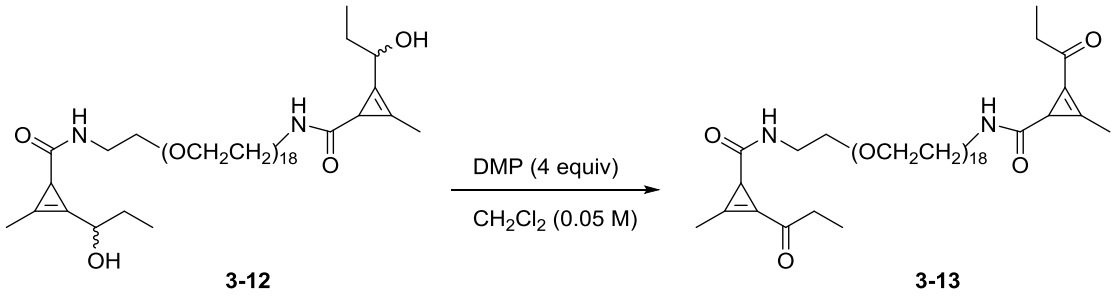

To a solution of **3-12** (55 mg, 0.05 mmol) in CH_2Cl_2 (1 mL, 0.05M) was added Dess Martin Periodinane, DMP, (50 mg, 0.12 mmol) in one portion. After 30 minutes, the reaction was diluted with 0.5 mL hexanes, filtered through celite and the filtrate was concentrated onto C-2 silica gel prepared as described above. Column chromatography (gradient from 0-8% methanol in dichloromethane) furnished **3-13** (35 mg, 0.03

mmol, 60%) as a colorless oil. ^{1}H NMR ($CDCl_3$, 400 MHz, δ): 6.31(s, NH), 3.66-3.43 (m, 41H), 2.83-2.71 (m, 2H), 2.37 (s, 2H), 2.34 (s, 1H), 1.18-1.14 (t, *J* = 7.3 Hz, 3H; ^{13}C NMR (CD_2Cl_2, 90 MHz, δ): 192.1 (C), 172.1 (C), 123.1 (C), 105.8 (C), 70.5 (CH_2), 70.4 (CH_2), 70.2 (CH_2), 69.8 (CH_2), 39.3 (CH_2), 36.7 (CH_2), 26.1 (CH), 11.5 (CH_3), 7.6 (CH_3); FT-IR (neat, cm^{-1}): 2870, 1625, 1539, 1457, 1350, 1300, 1250, 1110; LIFDI MS *m/z* [M +Na] calcd for $C_{56}H_{100}N_2O_{23}$ 1192.6615, found 1192.6620

Protein labeling experiment

To Thioredoxin (Trx, 5 μL of a 1 mM stock solution in H_2O) in 420 μL pH 6 acetate buffer was added aqueous tris(hydroxypropyl)phosphine (THP, 25 μL of a 1 mM stock solution in H_2O). After 12 h, **3-5** (50 μL of a 5 mM stock solution in methanol) was added. The final concentrations were Trx (10 μM), THP (50 μM) and **3-5** (500 μM). Within 10 minutes of addition, ESI-MS analysis in the positive mode (Shimadzu LCMS-2020) indicated double alkylation of Trx (deconvoluted *m/z* 11998).

Preparative Protein Labeling

40 μL of a 1 mM Thioredoxin (Trx) solution in pH 6 acetate buffer was added to aqueous tris(hydroxypropyl)phosphine (THP) (4 μL of a 100 mM stock solution in H_2O). After 2 h, **3-5** (2.4 μL of a 100 mM solution in methanol) was added. The final concentrations were: Trx (0.87 mM), THP (8.7 mM), **3-5** (5.2 mM). Within 10 minutes of the addition, ESI-MS analysis (Shimadzu LCMS-2020) in the positive mode indicated double alkylation of Trx. The doubly alkylated $Trx_{(alkylated)}$ was purified via gravity filtration through a PD-10 desalting column.

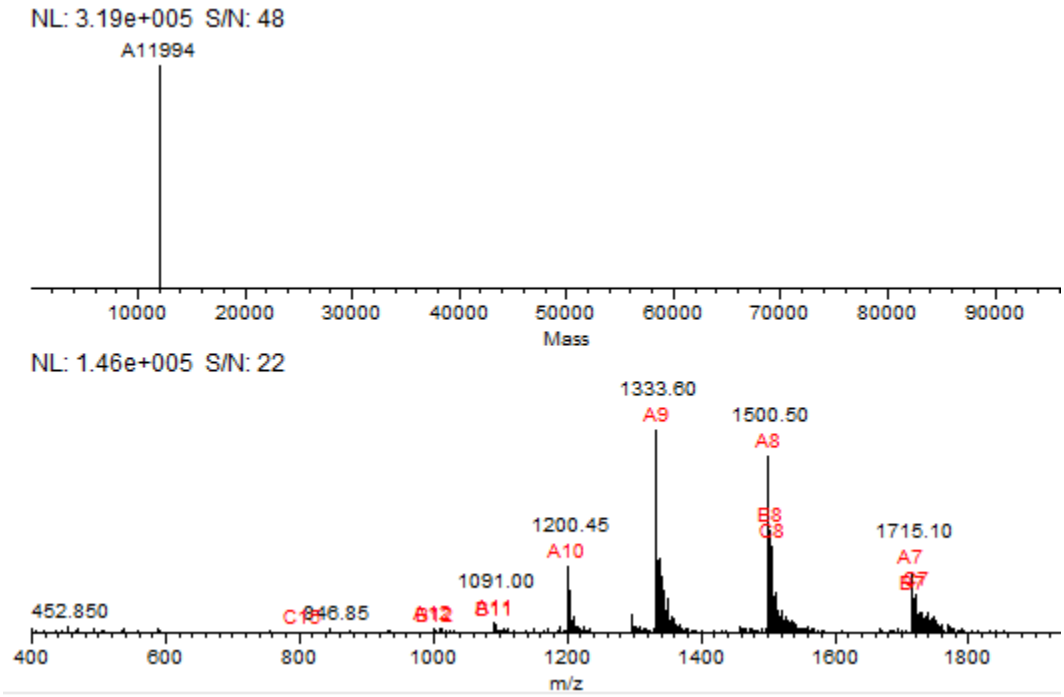

Figure 3.11: (Top) Decovoluted ESI-MS using MagTran software program (Bottom) Raw ESI-MS data.

LCMS Competition Experiment

To GSH, (25 µL of a 1mM stock solution in pH 6 acetate buffer) in 450 µL pH 6 acetate buffer was added a freshly made 1:1 mixture of **3-5** and NEM (25 µL of a 10 mM stock solution in pH 6 acetate buffer). Final concentrations were GSH (50 µM) and 1:1 mixture of **3-5**/NEM (500 µM). Within 10 minutes of the addition, mass spectrometry analysis using a Shimadzu LCMS-2020, operating under negative electrospray ionization (ESI) mode identified adducts of both NEM and **3-5** as present in the crude mixture (*m/z* [M-H] 431 and 474 respectively).

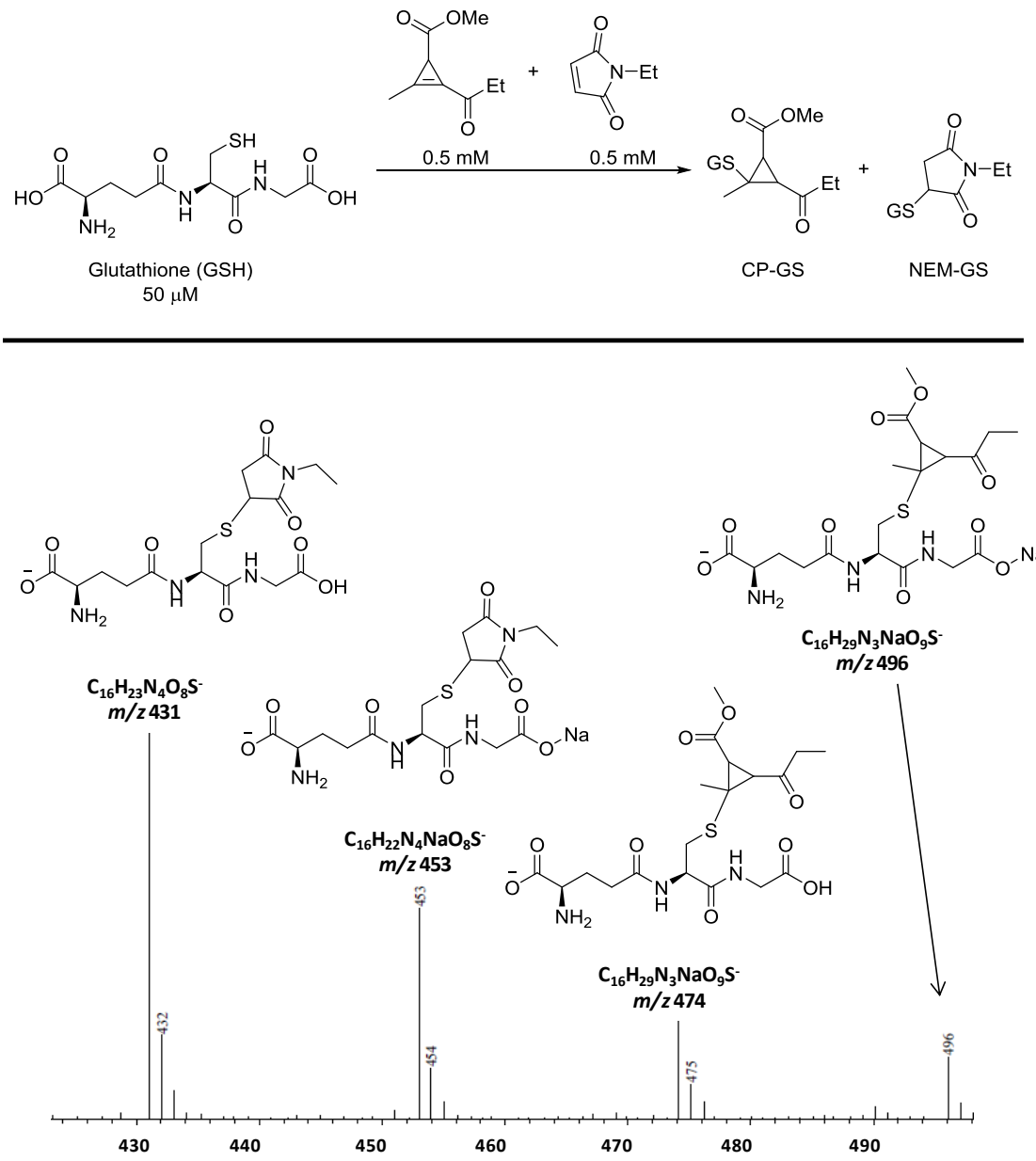

Figure 3.12: Competition experiment between NEM and **3-5** for GSH. ESI-MS in positive mode shows that alkylation by **3-5** competes with NEM.

UV/Vis kinetics analysis under second order conditions

To a 2 mL cuvette with 1970 μL pH 7.4 phosphate buffer with 1 mM EDTA was added GSH (20 μL of a 5 mM stock solution in pH 7.4 phosphate buffer with 1 mM EDTA). **3-5** (10 μL of a 10 mM stock solution in methanol) was then added and the contents of the cuvette mixed thoroughly. UV/Vis spectra were manually collected on a Hewlett Packard 8452A Diode Array Spectrophotometer approximately every 10 seconds and the reaction progress was marked by the disappearance of the intense absorption maximum of **3-5** at 252 nm with $\varepsilon = 4600\ M^{-1}cm^{-1}$, and the appearance of a less intense maximum at 272 nm with $\varepsilon = 2000\ M^{-1}cm^{-1}$. Data was recorded at 25˚C. The $t_{1/2}$ was found to be approximately 35 seconds. A second order rate constant of $570\ M^{-1}s^{-1}$ was calculated.

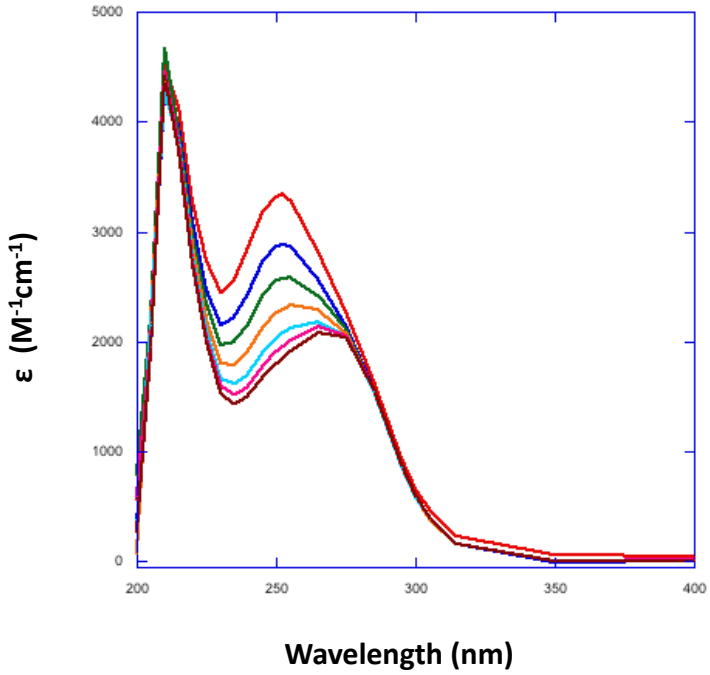

Figure 3.13: UV-vis spectroscopy was used to monitor the reaction between 50 μM **3-5** and 50 μM GSH at pH 7.5 in 50 mM phosphate buffer with 1mM EDTA containing 0.5 % MeOH. Enone **3-5** has an absorption maximum at 252 nm (ε = 4600 $M^{-1}cm^{-1}$), and the conjugate has a maximum at 272 nm (with ε = 2000 $M^{-1}cm^{-1}$).

Kinetic analysis of the reaction between 3-5 and GSH under pseudo first order conditions

The reaction between **3-5** and glutathione (GSH) was measured under pseudo-first order conditions with 10 equivalents of GSH in pH 7.4, 50 mM phosphate buffer with 1mM EDTA by following the exponential decay of **3-5** at 252 nm over time using an SX 18MV-R stopped-flow spectrophotometer (Applied Photophysics Ltd.). Solutions were prepared for **3-5** and GSH (0.5 mM and 5 mM respectively, in pH 7.4, 50 mM phosphate buffer with 1mM EDTA), and thermostated in the syringes of the spectrophotometer before measuring. An equal volume of each was mixed by the

stopped-flow device, resulting in a final concentration of 0.25 mM **3-5** and 2.5 mM GSH. Data was recorded for 0.1-5 seconds and performed in triplicate at 298 K. The k_{obs} was determined by nonlinear regression analysis of the data points using Prism software (v. 6.00, GraphPad Software Inc.). The average k_{obs} for three separate runs conducted in triplicate was 1.12 s^{-1} and the average second order rate constant was calculated to be 448 ± 1 $M^{-1}s^{-1}$.

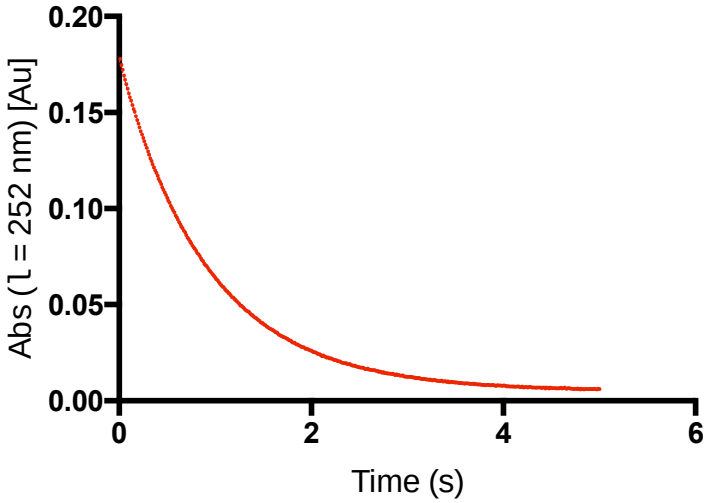

Figure 3.14: Stopped flow kinetics experiments were used to measure the rate of the reaction between **3-5** (0.25 mM) and GSH (2.5 mM) at 25 °C in pH 7.5, 50 mM phosphate buffer with 1mM EDTA containing 0.5 % MeOH. Based on k_{obs} 1.12 s^{-1}, the second order rate constant was calculated to be 448 ± 1 $M^{-1}s^{-1}$

HPLC Stability studies

Evaluating the stability of cyclopropenyl ketone thiol adducts in reducing conditions and in human plasma

Control experiment: 3-8 (30 μL of a 10 mM stock solution in methanol) was added to 120 μL of a 10:1 mixture of GSH (20 mM) and MPA (2 mM) in pH 6 acetate buffer. Within 10 minutes of the addition, mass spectrometry analysis using a Shimadzu LCMS-2020, operating under positive electrospray ionization (+ESI) mode was conducted. Masses corresponding to adducts of both GSH and MPA were observed (*m/z* [M+H] 531 and 392 respectively).

Cyclopropenyl ketone thiol adduct stability in reducing conditions study

To a 245 μL solution of **3-9** (5 μL of a 10 mM stock solution in MeOH in 240 μL of pH 7.4 50 mM phosphate buffer with 1 mM EDTA), was added GSH (5 μL of a 100 mM stock solution in pH 7.4 50 mM phosphate buffer with 1 mM EDTA). Final concentrations were **3-9** (0.2 mM) and GSH (2 mM). Samples were incubated at 37˚C and removed periodically for reverse phase HPLC analysis (254 nm) on a HP 1090 Series .system equipped with an analytical Halo C18 (7.5 x 3.0 mm, 2.7 μL) column. A linear gradient from 10 % to 100 % solvent B was run over 32 min at 0.2 mL/min, where solvent A is 0.1 % formic acid in water and solvent B is 0.1 % formic acid in acetonitrile . Areas of the peaks attributed to **3-9** were integrated in each sample taken to calculate stability. The identities of the compounds present in each peak were determined by LC-MS analysis using a Shimadzu LCMS-2020, operating under

positive electrospray ionization (+ESI) mode, connected to an LC-20AD (Shimadzu, Kyoto, Japan).

Cyclopropenyl ketone thiol adduct stability in human serum study

3-9 (40 μL of a 10 mM stock solution in methanol) was incubated in human serum (from human male AB plasma, USA origin, sterile-filtered, procured from Sigma-Aldrich) (1960 μL) at 37˚C over a period of 8 days. Periodically, 250 μL aliquots were removed and subjected to centrifugal filtration using an Amicon Ultra – 0.5 Centrifugal Filter Unit with Ultracel – 10 membrane to allow for large protein removal, and the filtrate obtained assayed by HPLC using the same conditions as described in the previous stability study. The peaks corresponding to **3-9** were integrated to determine the stability of the adduct over time.

REFERENCES

1. Chalker, J. M.; Bernardes, G. J. L.; Lin, Y. A.; Davis, B. G. *Chemistry – An Asian Journal* **2009**, *4*, 630.

2. Glazer, A. N. *Annu. Rev. Biochem* **1970**, *39*, 101.

3. Alley, S. C.; Okeley, N. M.; Senter, P. D. *Curr. Opin. Chem. Biol.* **2010**, *14*, 529.

4. Wu, Z.; Liu, S.; Hassink, M.; Nair, I.; Park, R.; Li, L.; Todorov, I.; Fox, J. M.; Li, Z.; Shively, J. E.; Conti, P. S.; Kandeel, F. *Journal of Nuclear Medicine* **2013**, *54*, 244.

5. Saxon, E.; Bertozzi, C. R. *Science* **2000**, *287*, 2007.

6. Rostovtsev, V. V.; Green, L. G.; Fokin, V. V.; Sharpless, K. B. *Angew. Chem. Int. Ed.* **2002**, *41*, 2596.

7. (a) Ning, X.; Guo, J.; Wolfert, M. A.; Boons, G.-J. *Angew. Chem. Int. Ed.* **2008**, *47*, 2253; (b) Agard, N. J.; Prescher, J. A.; Bertozzi, C. R. *J. Am. Chem. Soc.* **2004**, *126*, 15046; (c) Jewett, J. C.; Sletten, E. M.; Bertozzi, C. R. *J. Am. Chem. Soc.* **2010**, *132*, 3688.

8. (a) Blackman, M. L.; Royzen, M.; Fox, J. M. *J. Am. Chem. Soc.* **2008**, *130*, 13518; (b) Taylor, M. T.; Blackman, M. L.; Dmitrenko, O.; Fox, J. M. *J. Am. Chem. Soc.* **2011**, *133*, 9646.

9. Li, Z.; Wang, Y.; Yao, Q.; Justice, N. B.; Ahn, T.-H.; Xu, D.; Hettich, R. L.; Banfield, J. F.; Pan, C. *Nat Commun* **2014**, *5*.

10. Bartlett, G. J.; Porter, C. T.; Borkakoti, N.; Thornton, J. M. *J. Mol. Biol.* **2002**, *324*, 105.

11. He, J.; Quiocho, F. *Science* **1991**, *251*, 1479.

12. (a) Baslé, E.; Joubert, N.; Pucheault, M. *Chemistry & Biology* **2010**, *17*, 213; (b) Cohen, L. A. *Annu. Rev. Biochem* **1968**, *37*, 695; (c) Sletten, E. M.; Bertozzi, C. R. *Angew. Chem. Int. Ed.* **2009**, *48*, 6974.

13. (a) Bernardes, G. J. L.; Chalker, J. M.; Errey, J. C.; Davis, B. G. *J. Am. Chem. Soc.* **2008**, *130*, 5052; (b) Matsuo, J.-i.; Kozai, T.; Ishibashi, H. *Org. Lett.* **2006**, *8*, 6095.

14. (a) Gregory, J. D. *J. Am. Chem. Soc.* **1955**, *77*, 3922; (b) Kim, Y.; Ho, S. O.; Gassman, N. R.; Korlann, Y.; Landorf, E. V.; Collart, F. R.; Weiss, S. *Bioconjugate Chem.* **2008**, *19*, 786.

15. Goddard, D. R.; Michaelis, L. *J. Biol. Chem.* **1935**, *112*, 361.

16. Hong, V.; Kislukhin, A. A.; Finn, M. G. *J. Am. Chem. Soc.* **2009**, *131*, 9986.

17. Rademann, J. *Angew. Chem. Int. Ed.* **2004**, *43*, 4554.

18. Campos, L. M.; Killops, K. L.; Sakai, R.; Paulusse, J. M. J.; Damiron, D.; Drockenmuller, E.; Messmore, B. W.; Hawker, C. J. *Macromolecules* **2008**, *41*, 7063.

19. Shiu, H.-Y.; Chan, T.-C.; Ho, C.-M.; Liu, Y.; Wong, M.-K.; Che, C.-M. *Chemistry – A European Journal* **2009**, *15*, 3839.

20. (a) Crich, D.; Zou, Y.; Brebion, F. *The Journal of Organic Chemistry* **2006**, *71*, 9172; (b) Lin, Y. A.; Chalker, J. M.; Davis, B. G. *ChemBioChem* **2009**, *10*, 959.

21. Toda, N.; Asano, S.; Barbas, C. F. *Angew. Chem. Int. Ed.* **2013**, *52*, 12592.

22. Alley, S. C.; Benjamin, D. R.; Jeffrey, S. C.; Okeley, N. M.; Meyer, D. L.; Sanderson, R. J.; Senter, P. D. *Bioconjugate Chem.* **2008**, *19*, 759.

23. Lundblad, R. L. *Chemical Reagents for Protein Modification (4th Edition)*; CRC Press: Boca Raton, FL, USA, 2014.

24. G Biosciences a Geno Technology, I. http://www.gbiosciences.com/PDF/Protocol/FOCUS_Protein_Reduction_Alkylation.pdf, 2012.

25. (a) Singh, R. *Bioconjugate Chem.* **1994**, *5*, 348; (b)Sapra, A.; Thorpe, C. *J. Am. Chem. Soc.* **2013**, *135*, 2415.

26. Fontaine, S. D.; Reid, R.; Robinson, L.; Ashley, G. W.; Santi, D. V. *Bioconjugate Chem.* **2014**.

27. Baldwin, A. D.; Kiick, K. L. *Bioconjugate Chem.* **2011**, *22*, 1946.

28. Hwang, C.; Sinskey, A.; Lodish, H. *Science* **1992**, *257*, 1496.

29. Kharkar, P. M.; Kiick, K. L.; Kloxin, A. M. *Chem. Soc. Rev.* **2013**, *42*, 7335.

30. Zhang, D.; Devarie-Baez, N. O.; Li, Q.; Lancaster, J. R.; Xian, M. *Org. Lett.* **2012**, *14*, 3396.

31. Patterson, D. M.; Nazarova, L. A.; Xie, B.; Kamber, D. N.; Prescher, J. A. *J. Am. Chem. Soc.* **2012**, *134*, 18638.

32. Fisher, L. A.; Smith, N. J.; Fox, J. M. *The Journal of Organic Chemistry* **2013**, *78*, 3342.

33. Bach, R. D.; Dmitrenko, O. *J. Am. Chem. Soc.* **2004**, *126*, 4444.

34. Codding, J. A.; Israel, B. A.; Thorpe, C. *Biochemistry* **2012**, *51*, 4226.

35. DeCollo, T. V.; Lees, W. J. *The Journal of Organic Chemistry* **2001**, *66*, 4244.

36. Harman, B.; Sóvágó, I. *Inorg. Chim. Acta* **1983**, *80*, 75.

37. Danehy, J. P.; Noel, C. J. *J. Am. Chem. Soc.* **1960**, *82*, 2511.

38. Peppas, N. A.; Khare, A. R. *Advanced Drug Delivery Reviews* **1993**, *11*, 1.

39. O. Wichterle, D. L. *Nature* **1960**, *185*, 117.

40. Buwalda, S. J.; Boere, K. W. M.; Dijkstra, P. J.; Feijen, J.; Vermonden, T.; Hennink, W. E. *J. Controlled Release* **2014**, *190*, 254.

41. Baldwin, A. D.; Kiick, K. L. *Polymer Chemistry* **2013**, *4*, 133.

42. Panne, P.; Fox, J. M. *J. Am. Chem. Soc.* **2007**, *129*, 22.

Appendix

Appendix A

CHROMATOGRAPHY DATA FOR CHAPTER 1

Data for Table 1.2 Entry 2B: (Brucine/ EtOH)

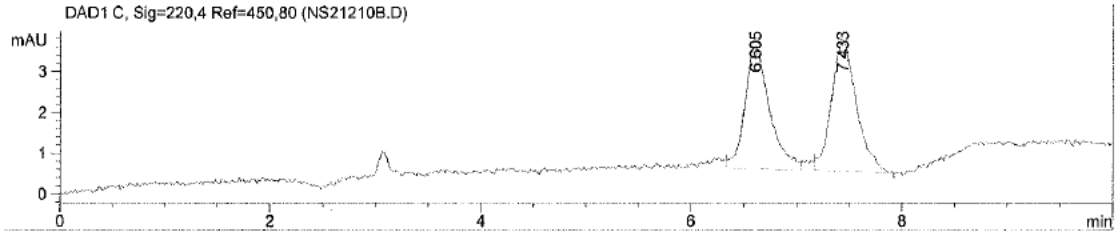

Signal 3: DAD1 C, Sig=220,4 Ref=450,80

Peak #	RetTime [min]	Type	Width [min]	Area [mAU*s]	Height [mAU]	Area %
1	6.605	BB	0.2494	49.49147	3.00978	47.9815
2	7.433	BP	0.2522	53.65561	3.21674	52.0185

Data for Table 1.2 Entry 2C: (Brucine/95 % EtOH)

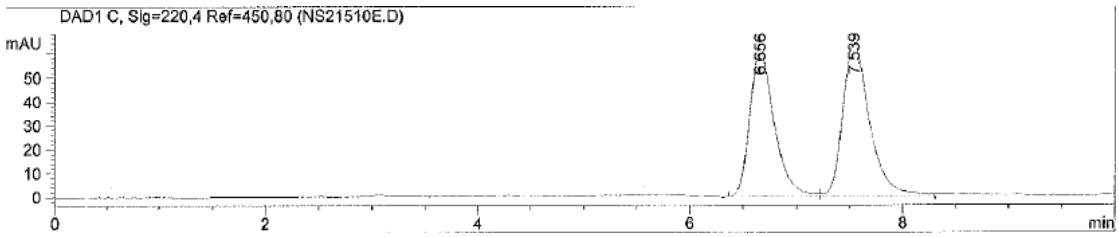

Signal 3: DAD1 C, Sig=220,4 Ref=450,80

Peak #	RetTime [min]	Type	Width [min]	Area [mAU*s]	Height [mAU]	Area %
1	6.656	PV	0.2421	984.11304	61.16604	46.4389
2	7.539	VV	0.2624	1135.04419	64.64677	53.5611

Data for Table 1.2 Entry 2D: (Brucine/MeOH)

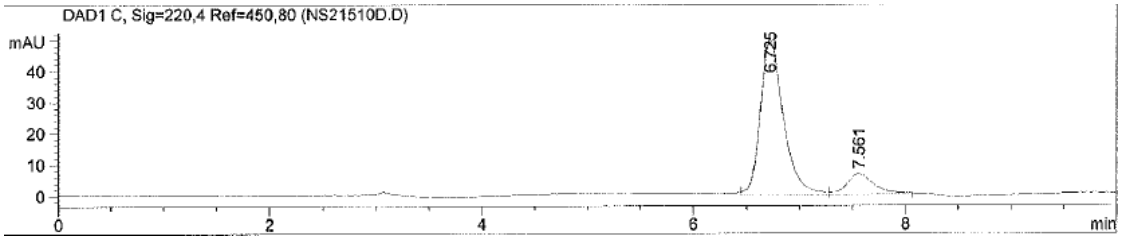

Signal 3: DAD1 C, Sig=220,4 Ref=450,80

Peak #	RetTime [min]	Type	Width [min]	Area [mAU*s]	Height [mAU]	Area %
1	6.725	BV	0.2342	751.88599	49.67424	86.1207
2	7.561	VB	0.2688	121.17467	6.69389	13.8793

Data for Table 1.2 Entry 2F: (Brucine/90 % 2-PrOH)

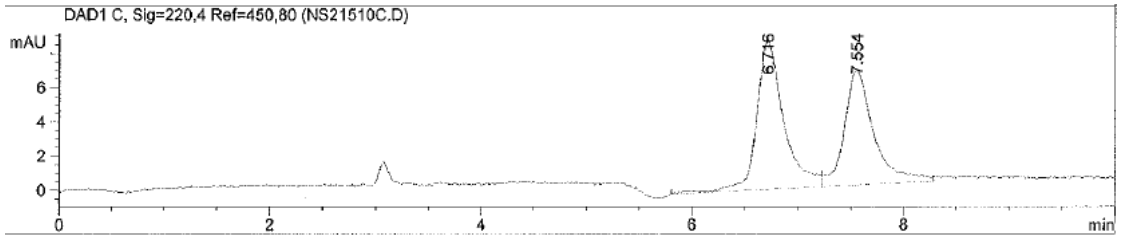

Signal 3: DAD1 C, Sig=220,4 Ref=450,80

Peak #	RetTime [min]	Type	Width [min]	Area [mAU*s]	Height [mAU]	Area %
1	6.716	PV	0.2653	154.48907	8.67617	54.0763
2	7.554	VB	0.2933	131.19807	6.67479	45.9237

Data for Table 1.2 Entry 5C: (Cinchonidine/95 % EtOH)

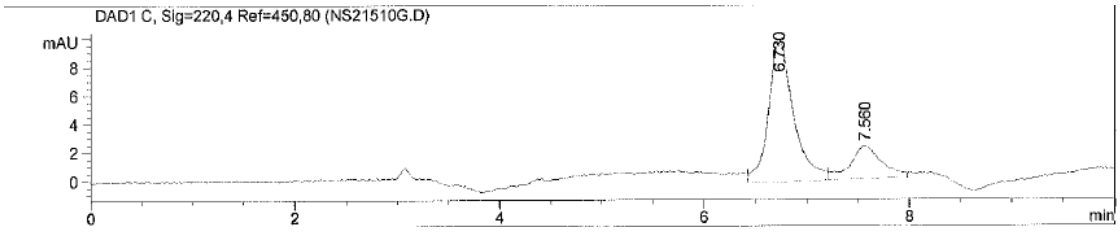

Signal 3: DAD1 C, Sig=220,4 Ref=450,80

Peak #	RetTime [min]	Type	Width [min]	Area [mAU*s]	Height [mAU]	Area %
1	6.730	VV	0.2359	169.44576	10.00726	77.1336
2	7.560	VV	0.2679	50.23246	2.32628	22.8664

Data for Table 1.2 Entry 5G: (Cinchonidine/80 % MeOH)

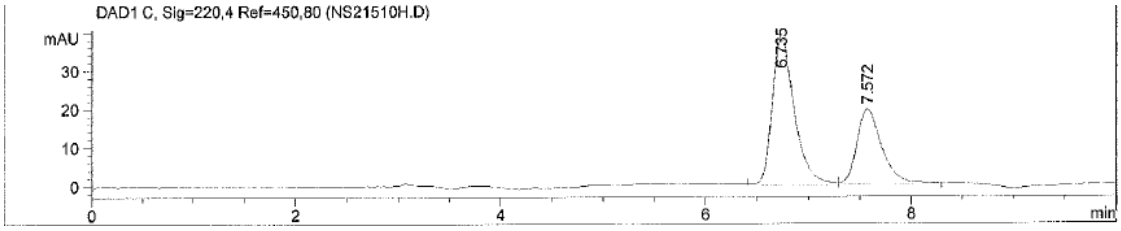

Signal 3: DAD1 C, Sig=220,4 Ref=450,80

Peak #	RetTime [min]	Type	Width [min]	Area [mAU*s]	Height [mAU]	Area %
1	6.735	VV	0.2233	586.75360	39.05057	63.8366
2	7.572	VB	0.2521	332.39536	19.61633	36.1634

-

Data for Table 1.2 Entry 7G: (Strychnine/80 % MeOH)

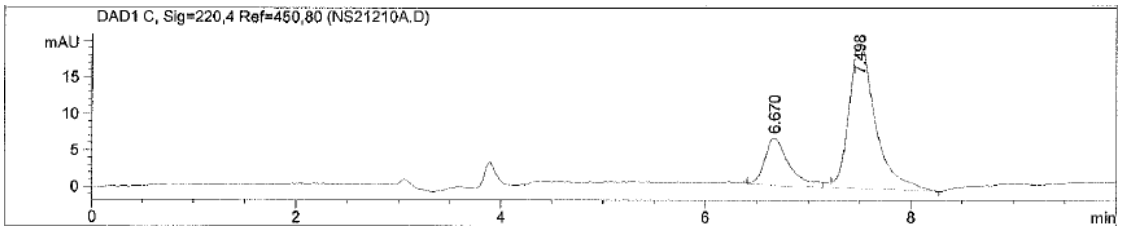

Signal 3: DAD1 C, Sig=220,4 Ref=450,80

Peak #	RetTime [min]	Type	Width [min]	Area [mAU*s]	Height [mAU]	Area %
1	6.670	BB	0.2509	107.81818	6.50829	23.1358
2	7.498	BP	0.2662	358.20450	20.03333	76.8642

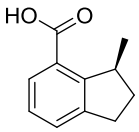

(*S*)-**1-1**

(S)-3-methyl-2,3-dihydro-1H-indene-4-carboxylic acid (*S*)-1-1

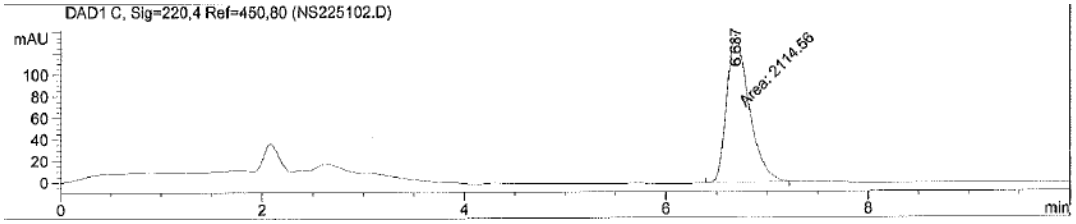

Signal 3: DAD1 C, Sig=220,4 Ref=450,80

Peak #	RetTime [min]	Type	Width [min]	Area [mAU*s]	Height [mAU]	Area %
1	6.798	MM	0.2639	2545.80688	160.78911	100.0000

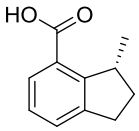

(*R*)-**1-1**

***(R)*-3-methyl-2,3-dihydro-1H-indene-4-carboxylic acid (*R*)-1-1**

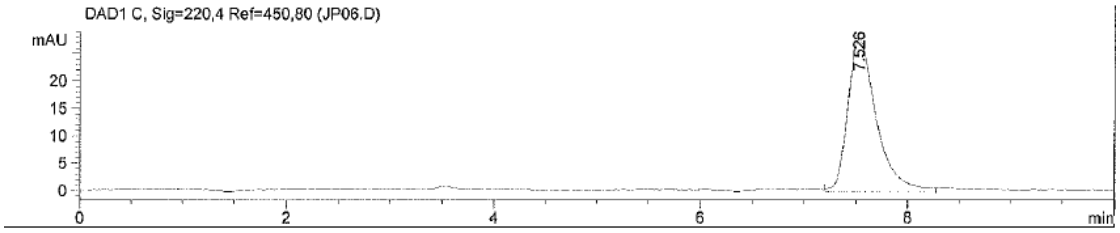

Signal 3: DAD1 C, Sig=220,4 Ref=450,80

Peak #	RetTime [min]	Type	Width [min]	Area [mAU*s]	Height [mAU]	Area %
1	7.526	BV	0.2691	536.85663	27.93003	100.0000

Appendix B

SPECTRAL AND CHROMATOGRAPHY DATA FOR CHAPTER 2

^{1}H NMR (400 MHz, $CDCl_3$)

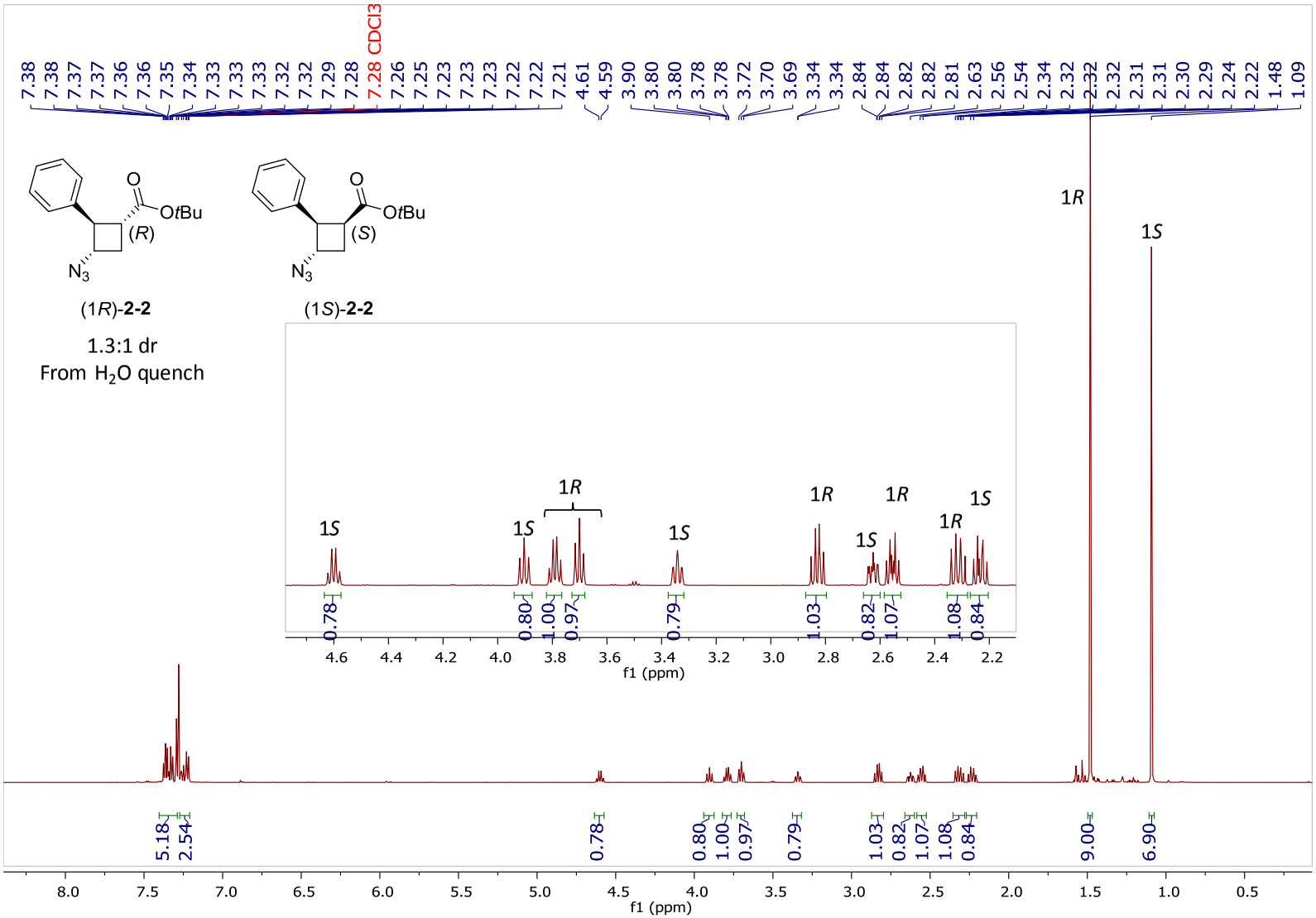

^{13}C NMR (100 MHz, $CDCl_3$)

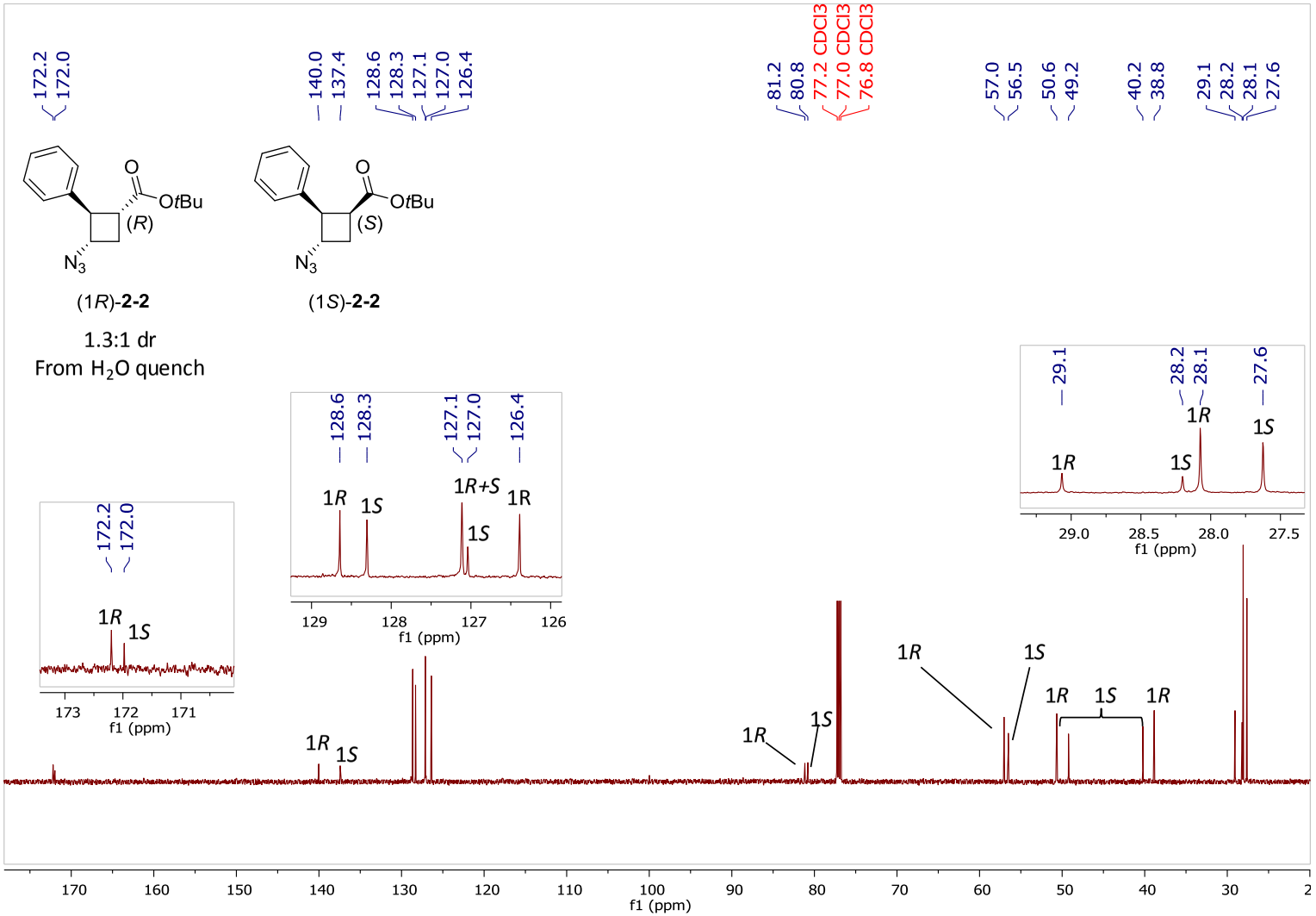

^{1}H NMR (400 MHz, $CDCl_3$)

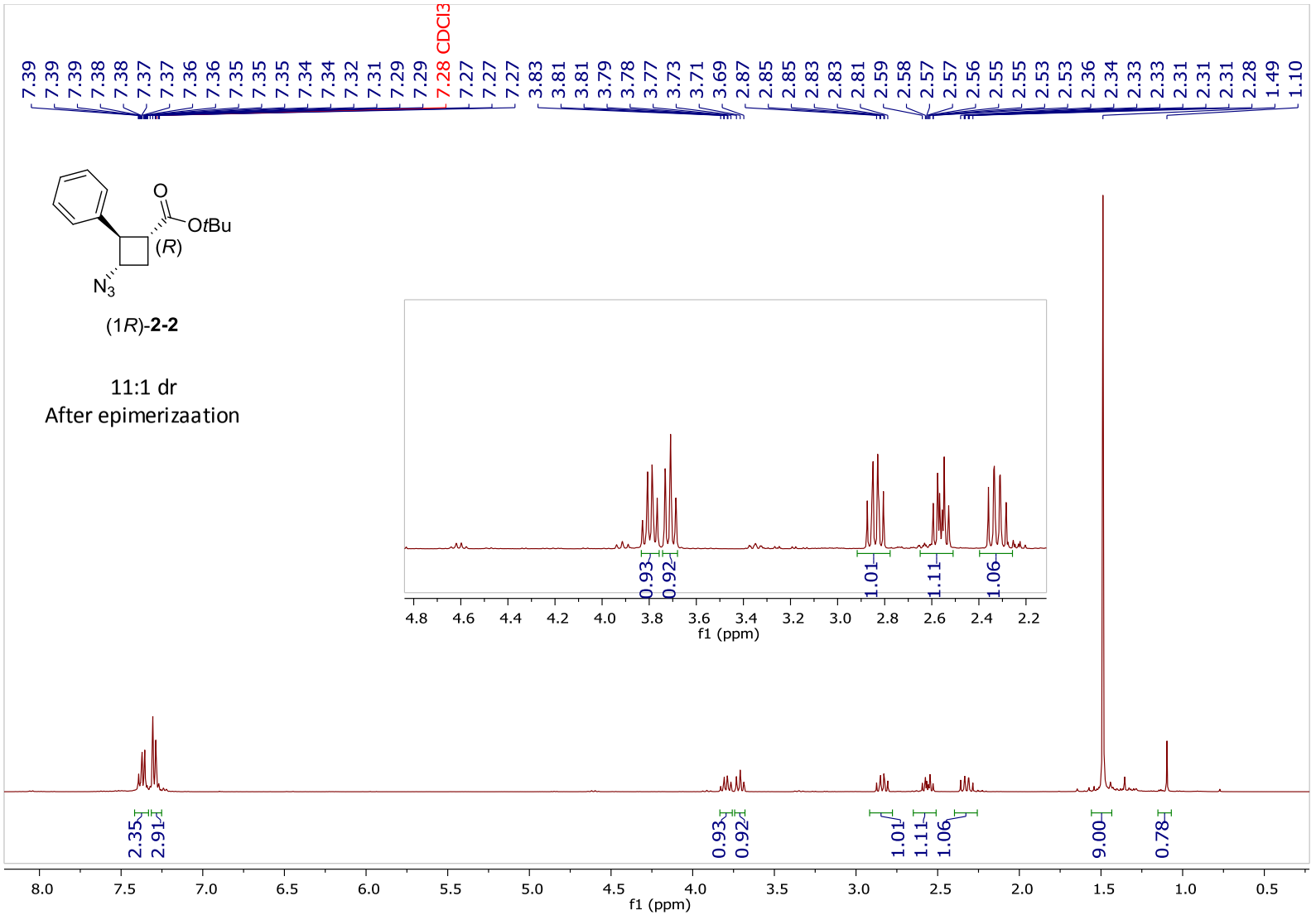

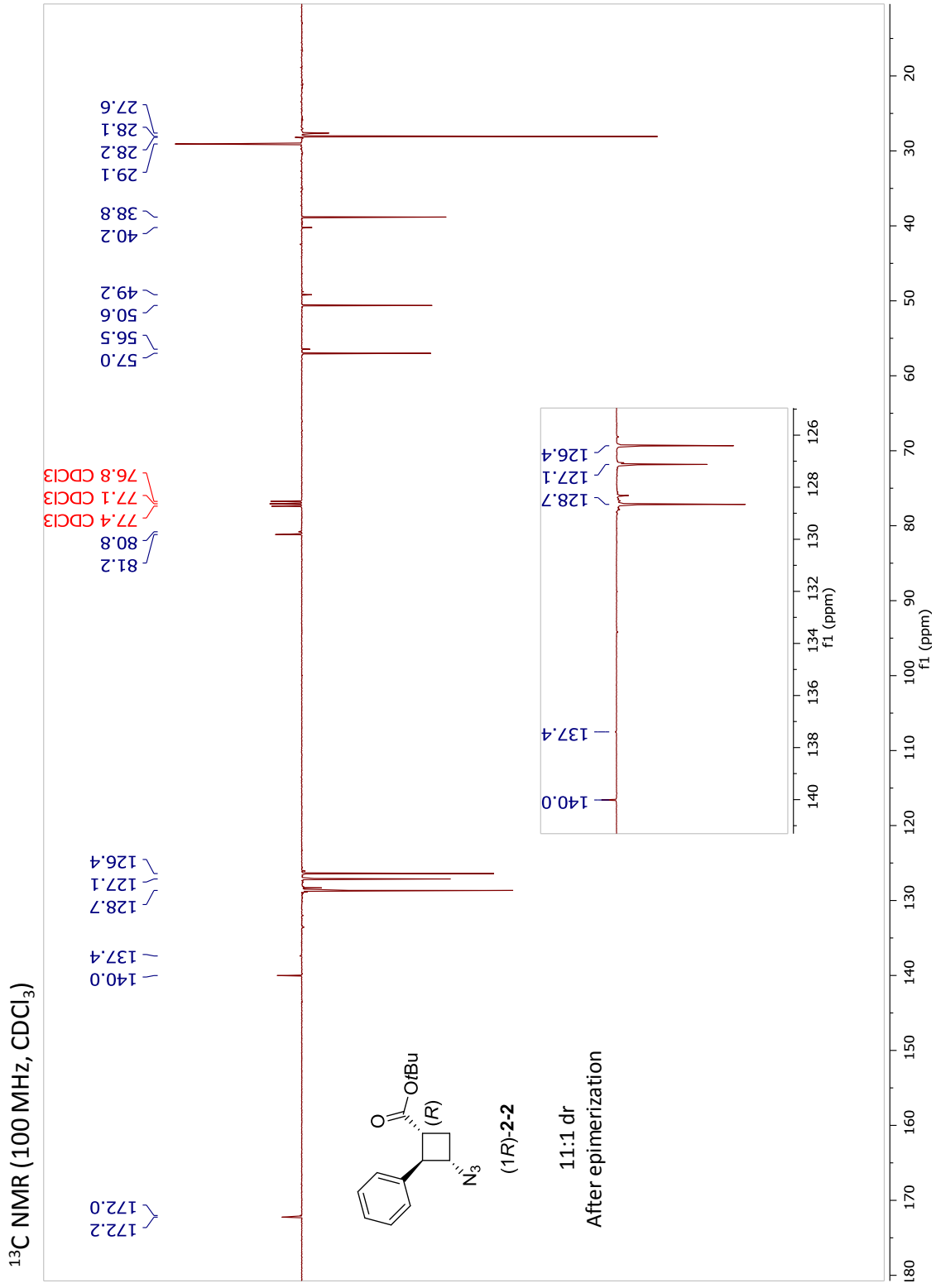
^{13}C NMR (100 MHz, CDCl$_3$)
172.2
172.0
140.0
137.4
128.7
127.1
126.4
81.2
80.8
77.4 CDCl3
77.1 CDCl3
76.8 CDCl3
57.0
56.5
50.6
49.2
40.2
38.8
29.1
28.2
28.1
27.6
O
OtBu
(R)
N3
(1R)-2-2
11:1 dr
After epimerization
f1 (ppm)

^{1}H NMR (400 MHz, $CDCl_3$)

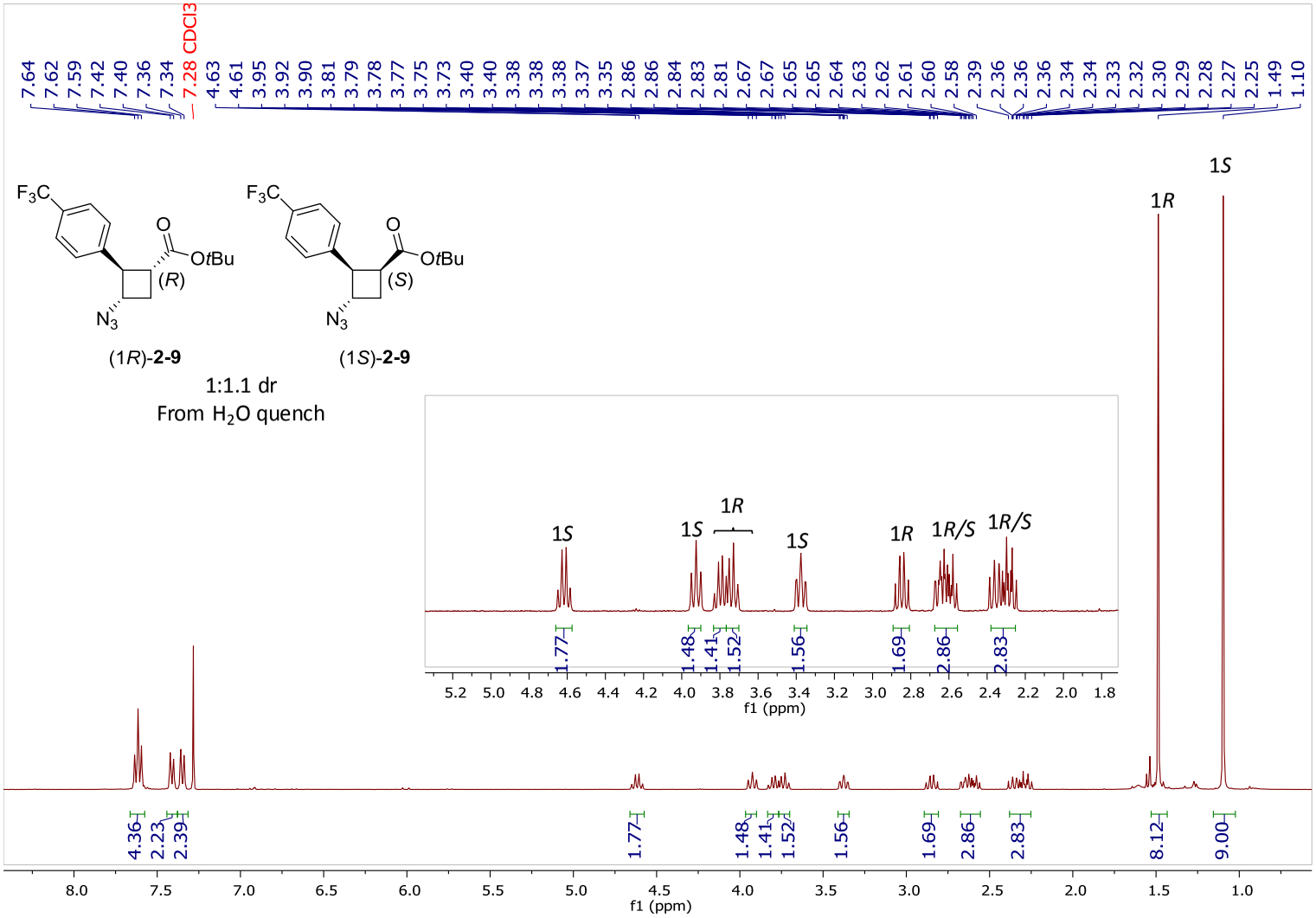

^{13}C NMR (100 MHz, $CDCl_3$)

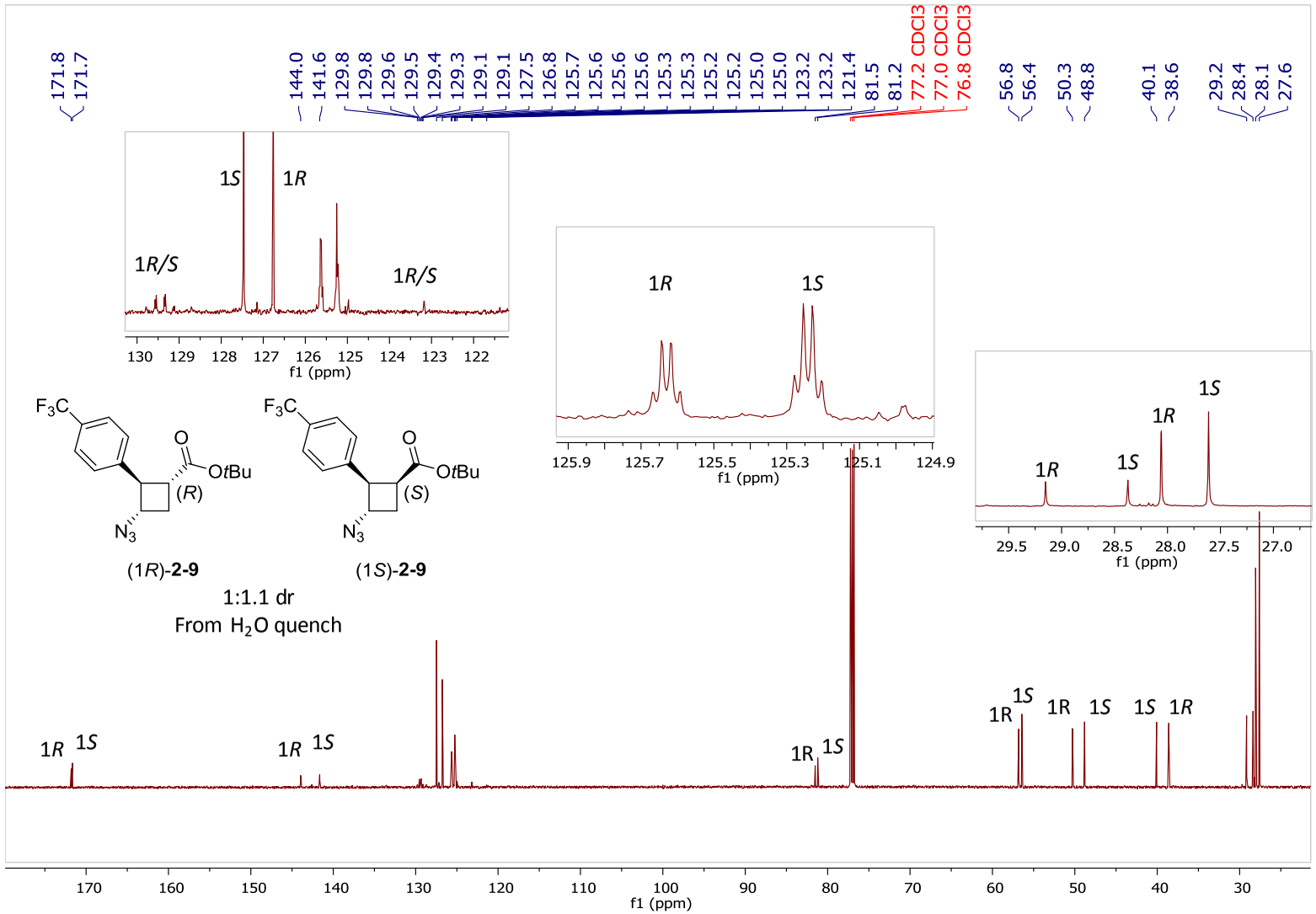

^{19}F NMR (376 MHz, $CDCl_3$)

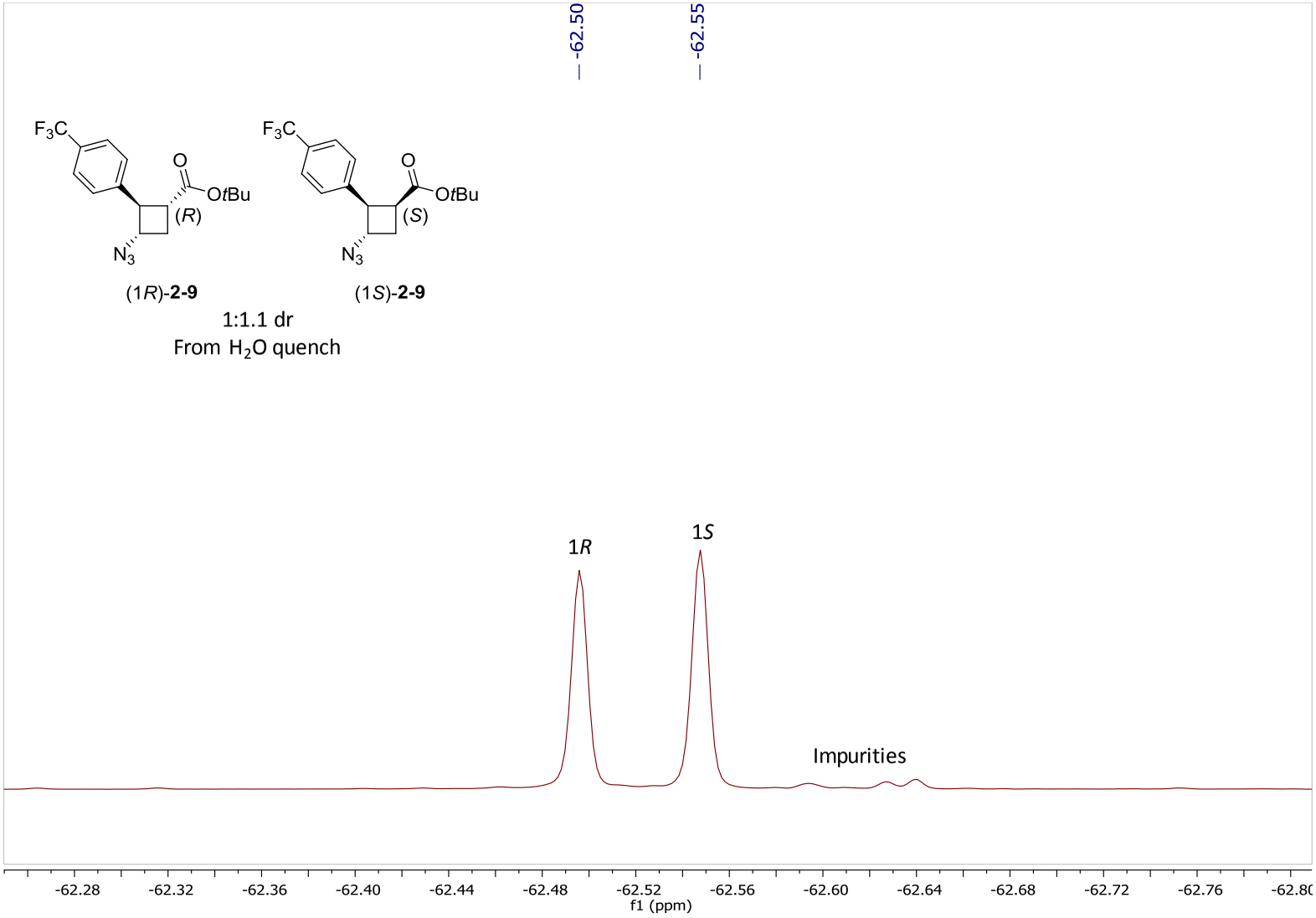

^{1}H NMR (400 MHz, $CDCl_3$)

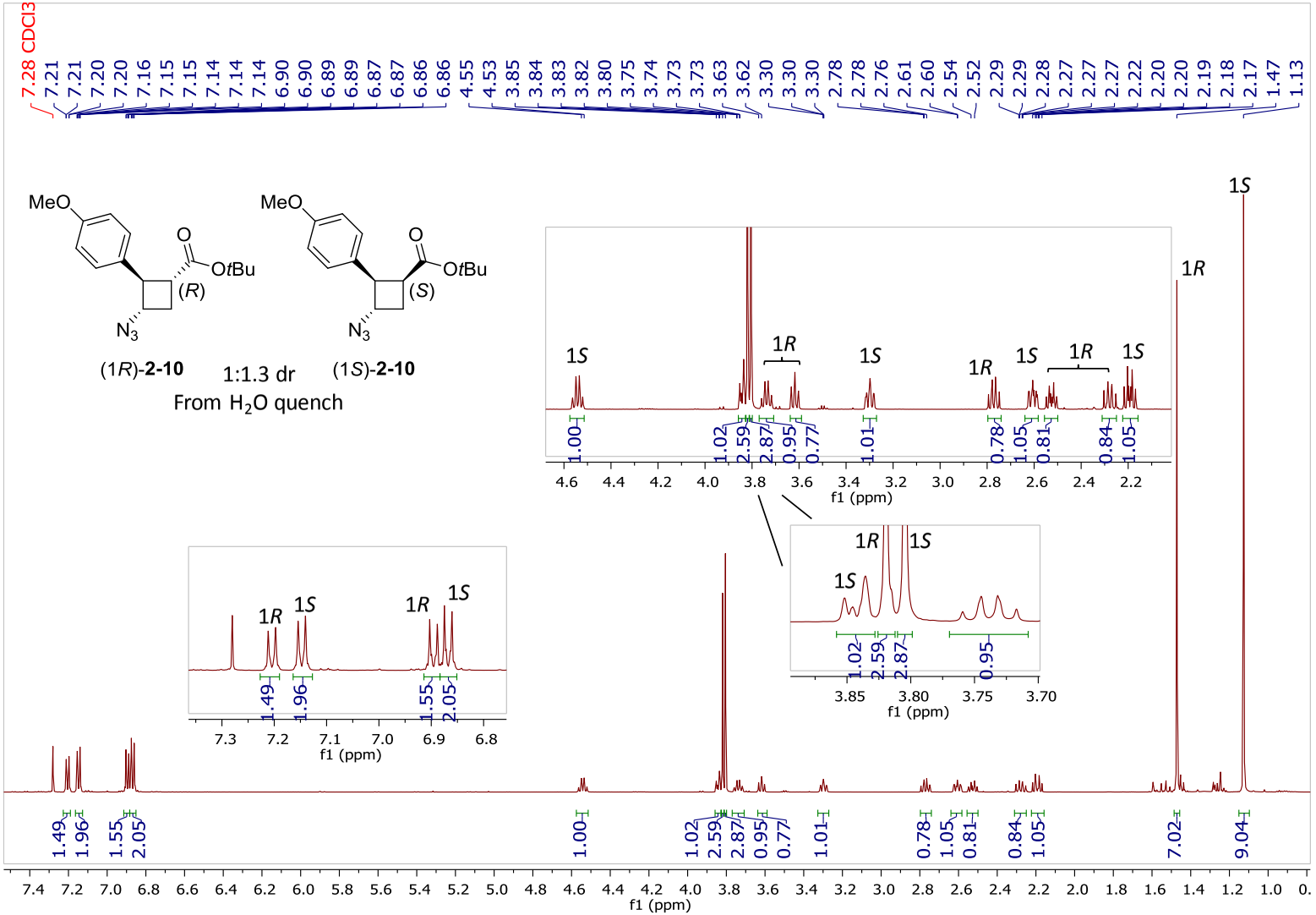

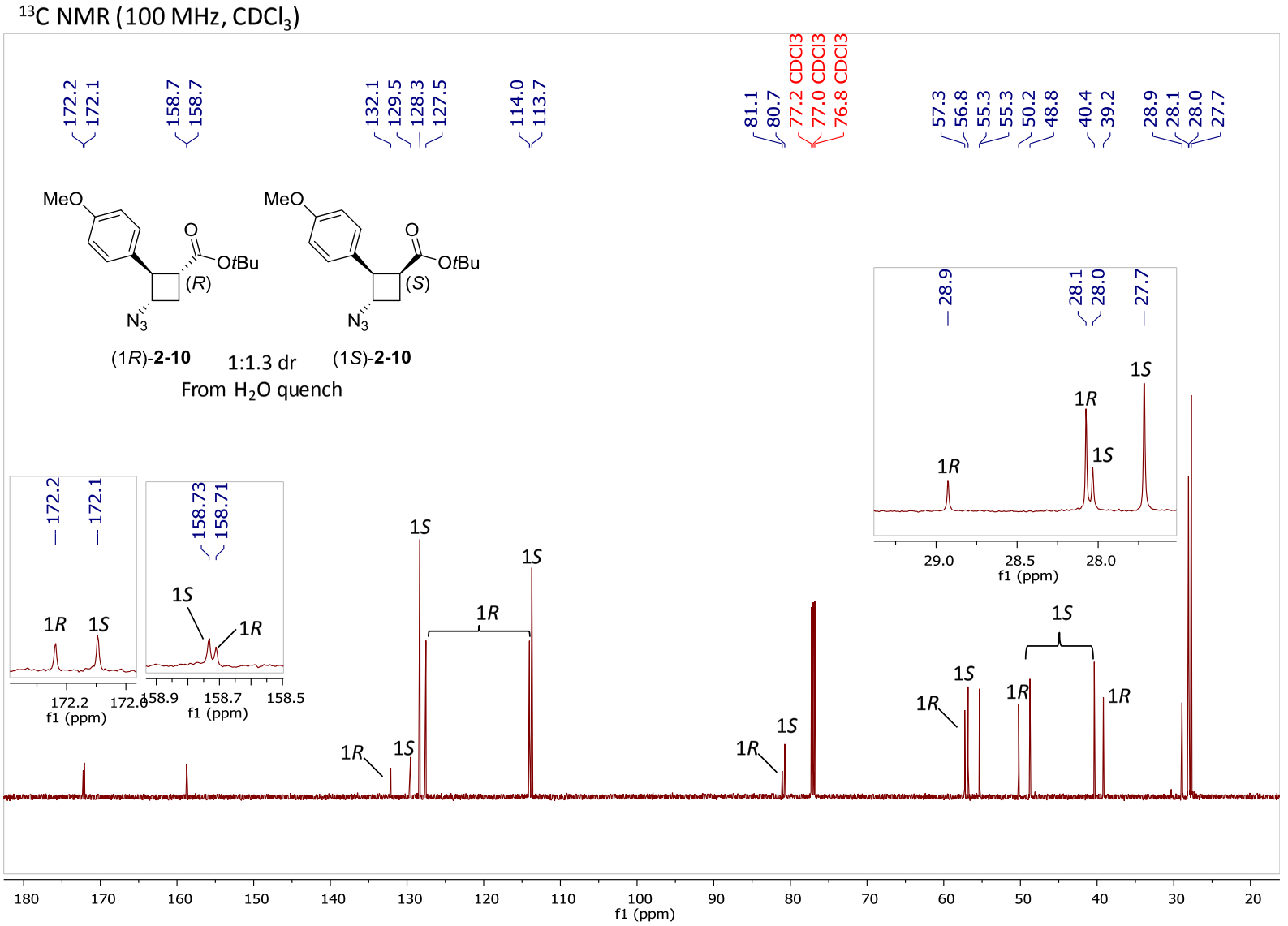
13C NMR (100 MHz, CDCl3)
172.2
172.1
158.7
158.7
132.1
129.5
128.3
127.5
114.0
113.7
81.1
80.7
77.2 CDCl3
77.0 CDCl3
76.8 CDCl3
57.3
56.8
55.3
55.3
50.2
48.8
40.4
39.2
28.9
28.1
28.0
27.7
MeO
OtBu
(R)
N3
(1R)-2-10
1:1.3 dr
From H2O quench
MeO
OtBu
(S)
N3
(1S)-2-10
1R
1S
f1 (ppm)

^{1}H NMR (400 MHz, $CDCl_3$)

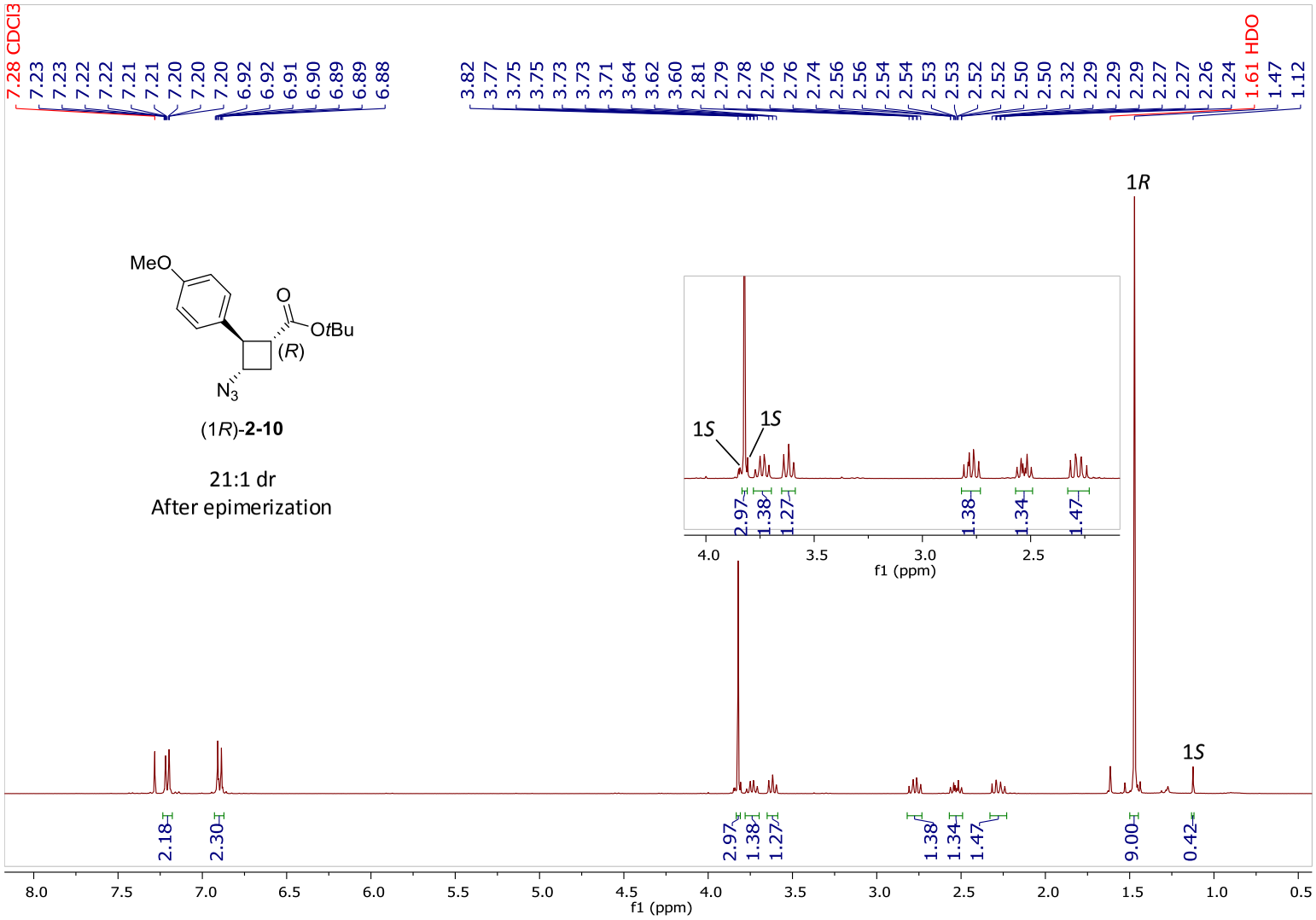

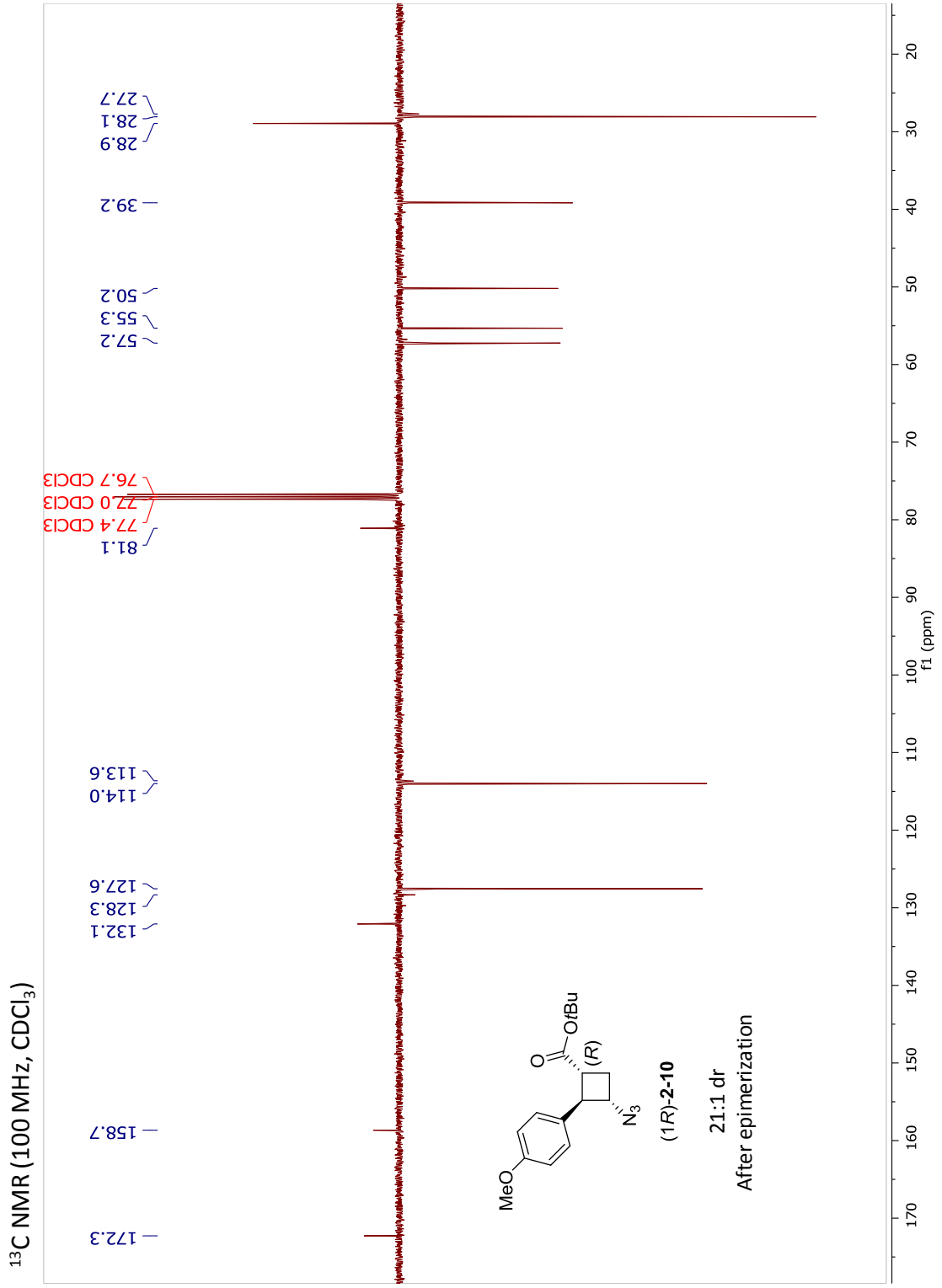
^{13}C NMR (100 MHz, $CDCl_3$)
172.3
158.7
132.1
128.3
127.6
114.0
113.6
81.1
77.4 CDCl3
77.0 CDCl3
76.7 CDCl3
57.2
55.3
50.2
39.2
28.9
28.1
27.7
MeO
O
OtBu
(R)
N_3
(1R)-2-10
21:1 dr
After epimerization
f1 (ppm)

^{1}H NMR (400 MHz, $CDCl_3$)

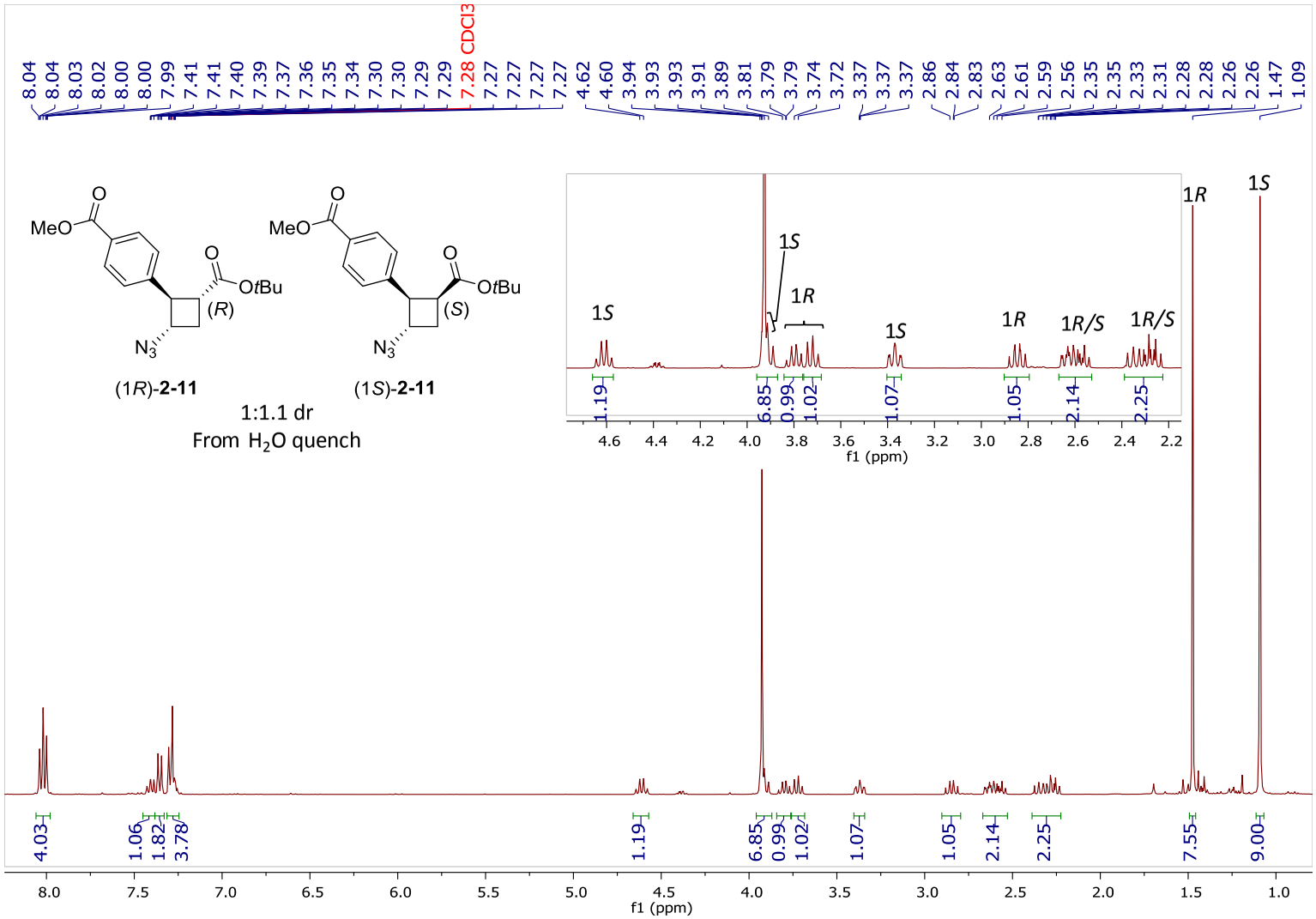

^{13}C NMR (100 MHz, $CDCl_3$)

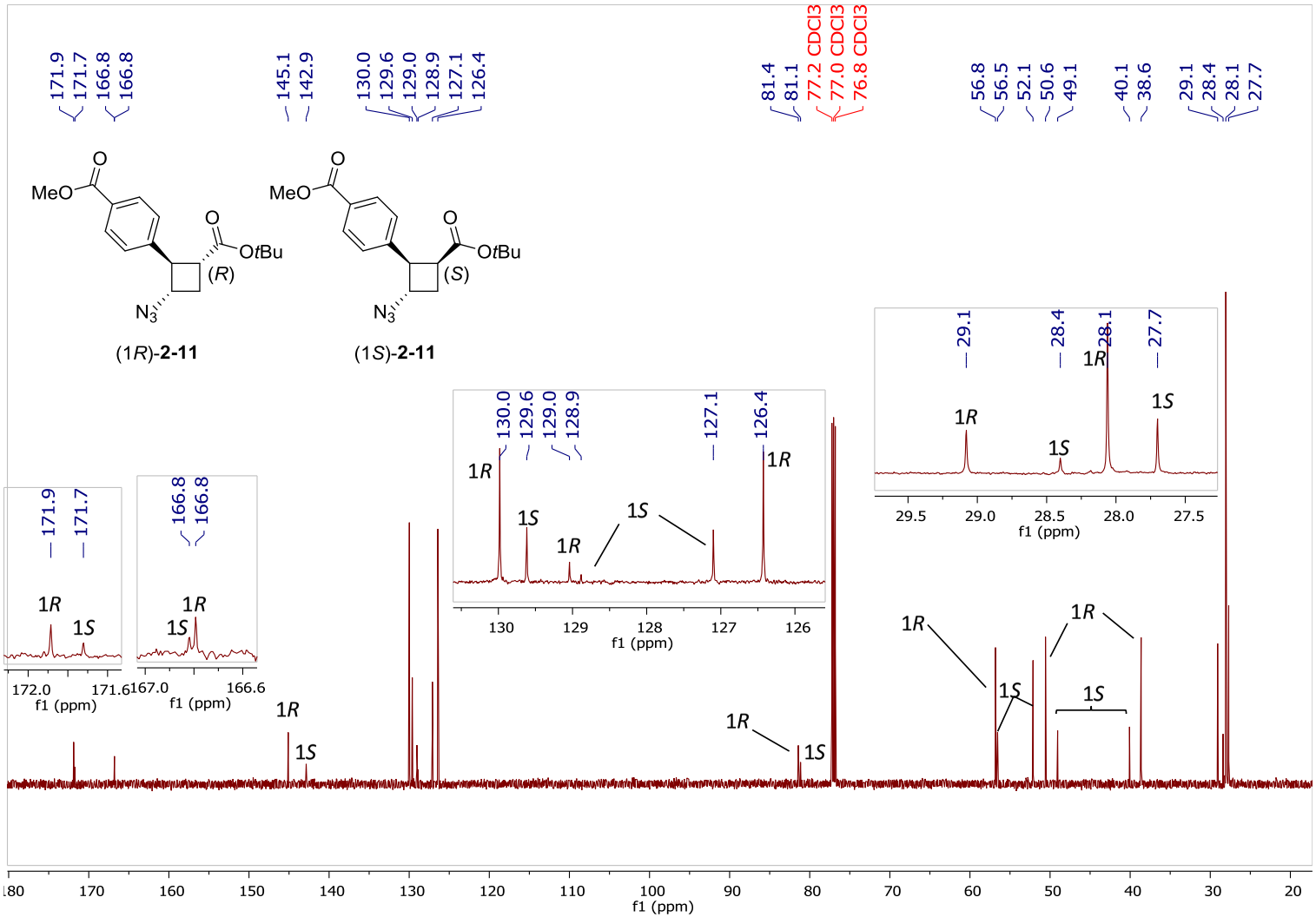

^{1}H NMR (400 MHz, $CDCl_3$)

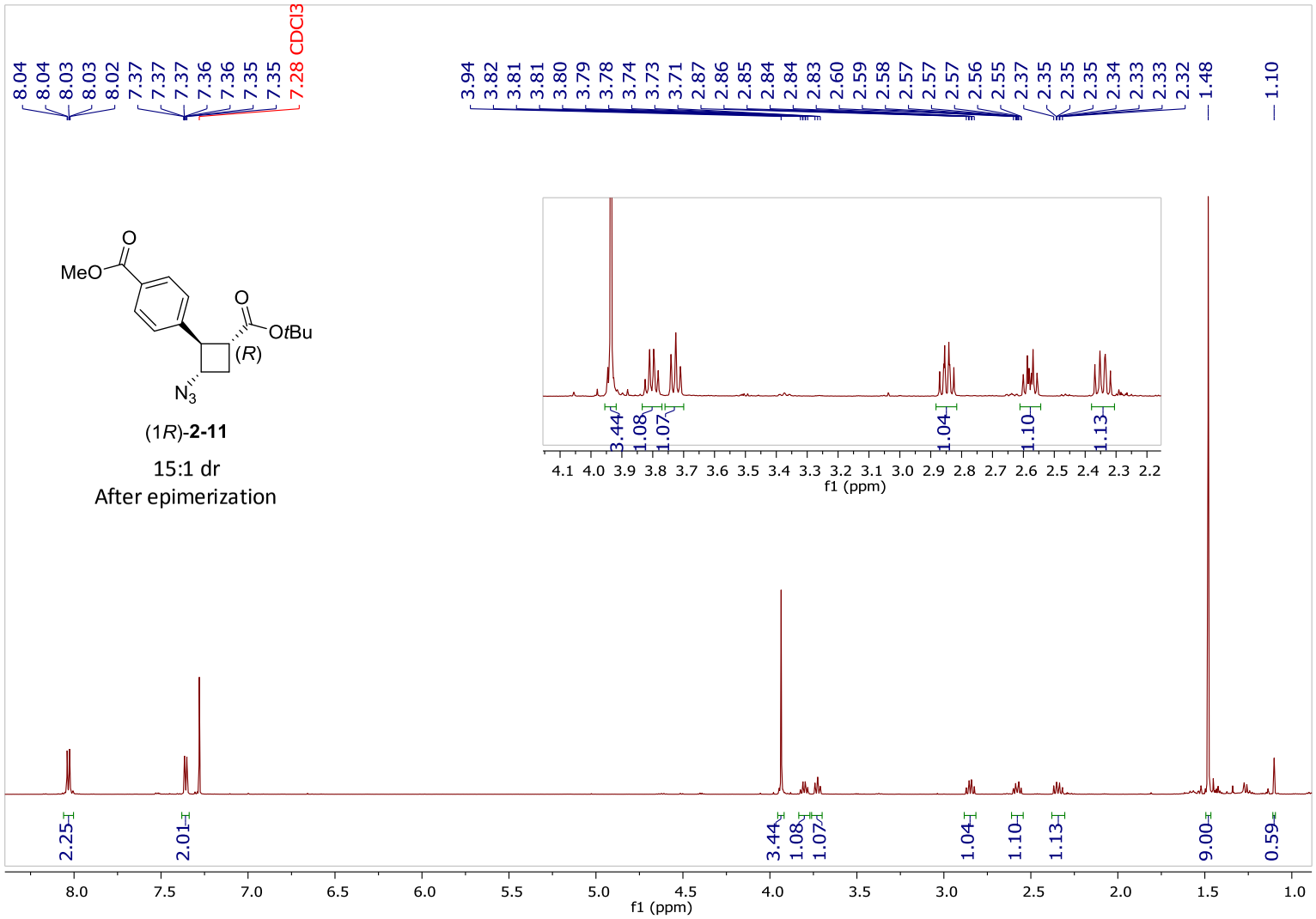

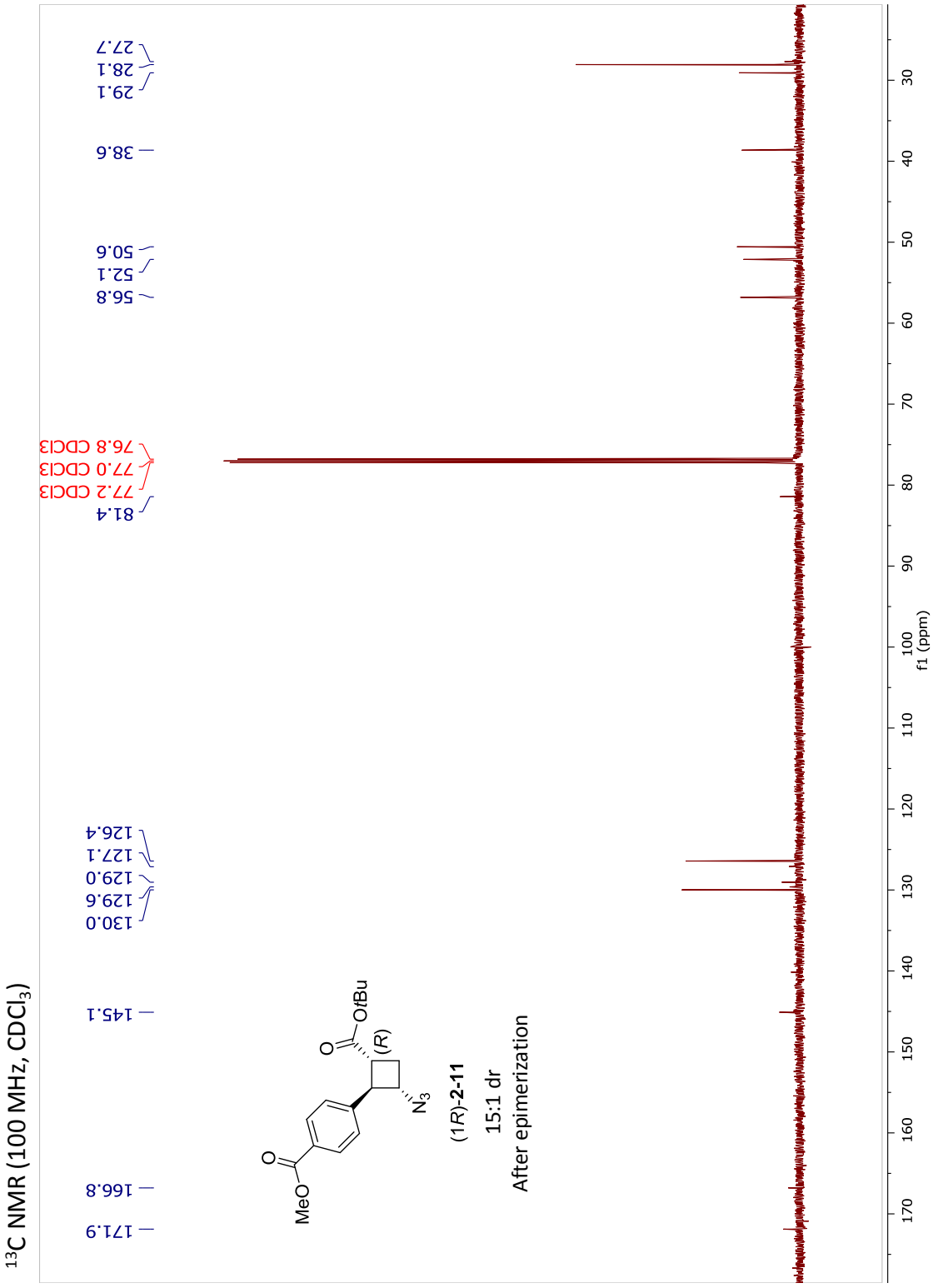
^{13}C NMR (100 MHz, $CDCl_3$)
171.9
166.8
145.1
130.0
129.6
129.0
127.1
126.4
81.4
77.2 CDCl3
77.0 CDCl3
76.8 CDCl3
56.8
52.1
50.6
38.6
29.1
28.1
27.7
MeO
O
O
OtBu
(R)
N_3
(1R)-2-11
15:1 dr
After epimerization
f1 (ppm)

^{1}H NMR (400 MHz, $CDCl_3$)

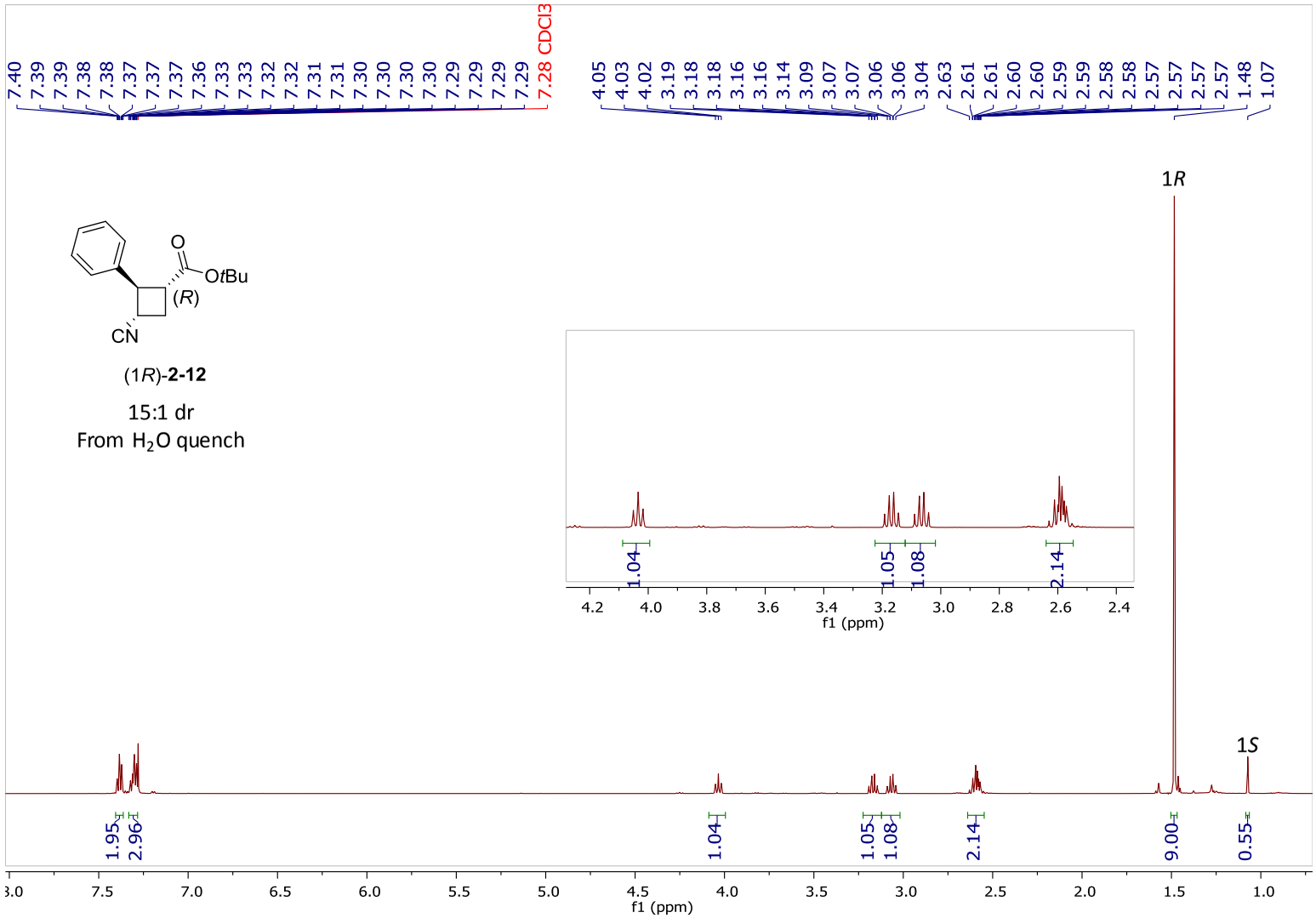

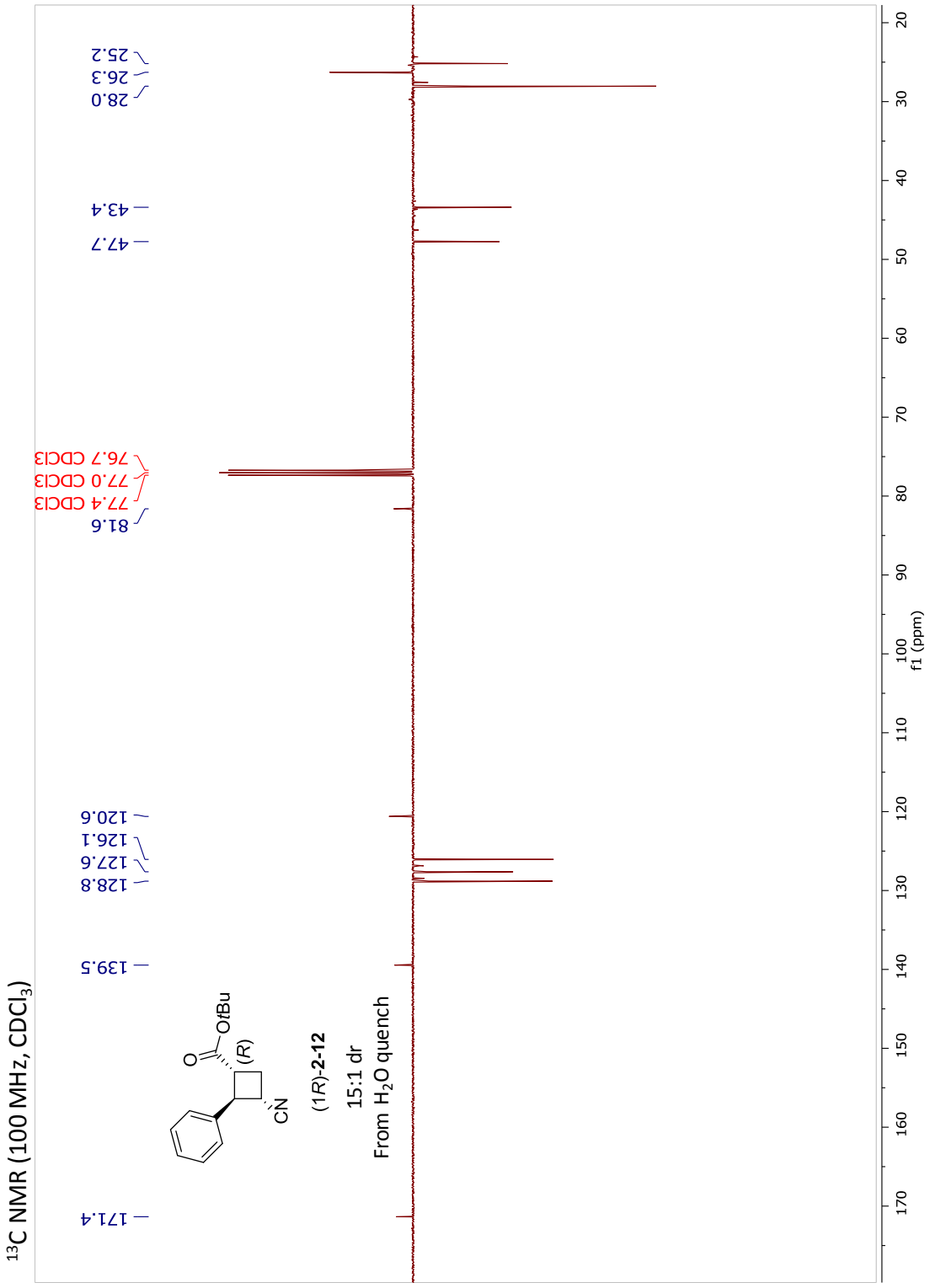
^{13}C NMR (100 MHz, CDCl$_3$)
171.4
139.5
128.8
127.6
126.1
120.6
81.6
77.4 CDCl3
77.0 CDCl3
76.7 CDCl3
47.7
43.4
28.0
26.3
25.2
O
OtBu
(R)
CN
(1R)-2-12
15:1 dr
From H2O quench
20
30
40
50
60
70
80
90
100
110
120
130
140
150
160
170
f1 (ppm)

^{1}H NMR (400 MHz, $CDCl_3$); Purity is estimated to be 90%

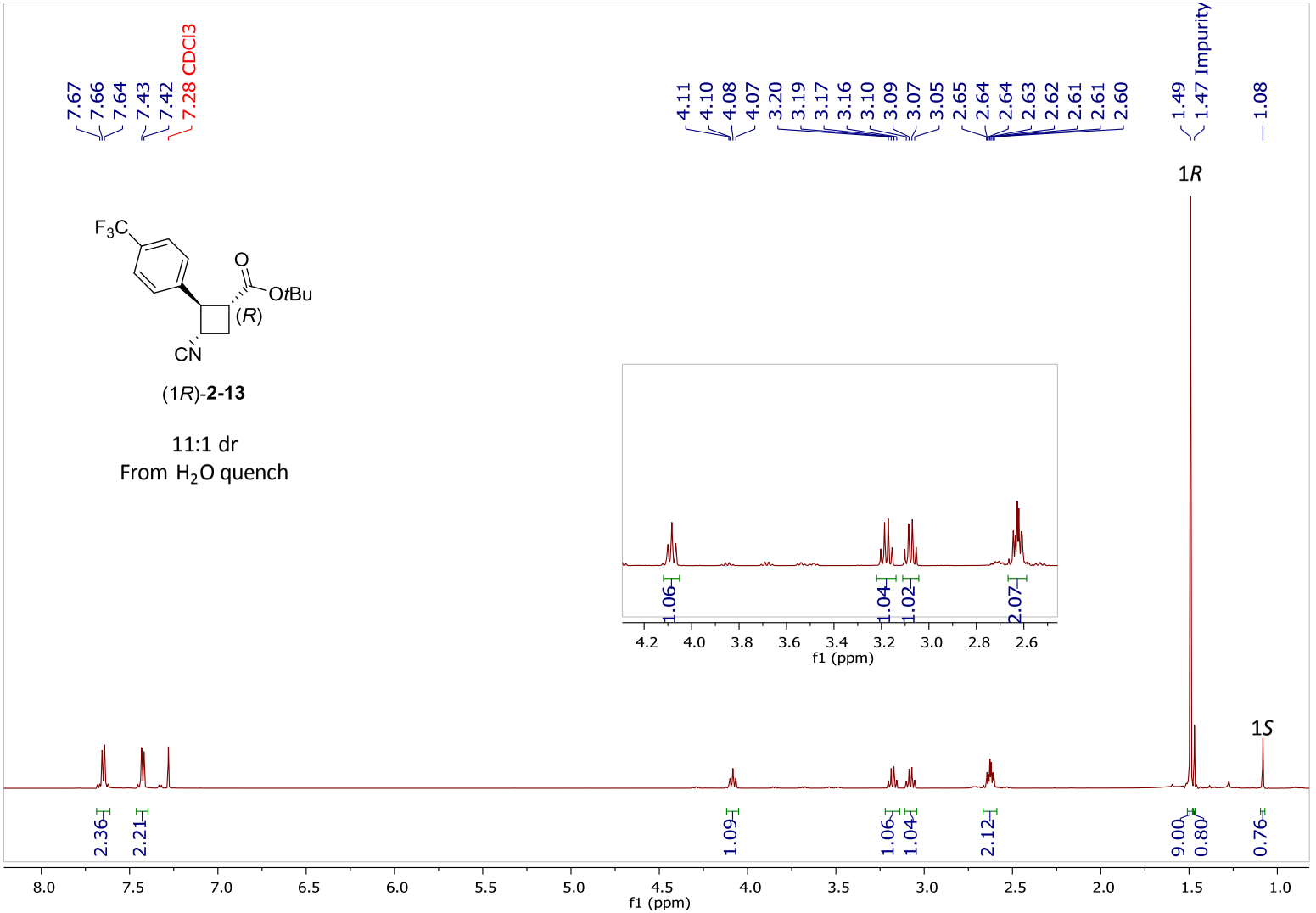

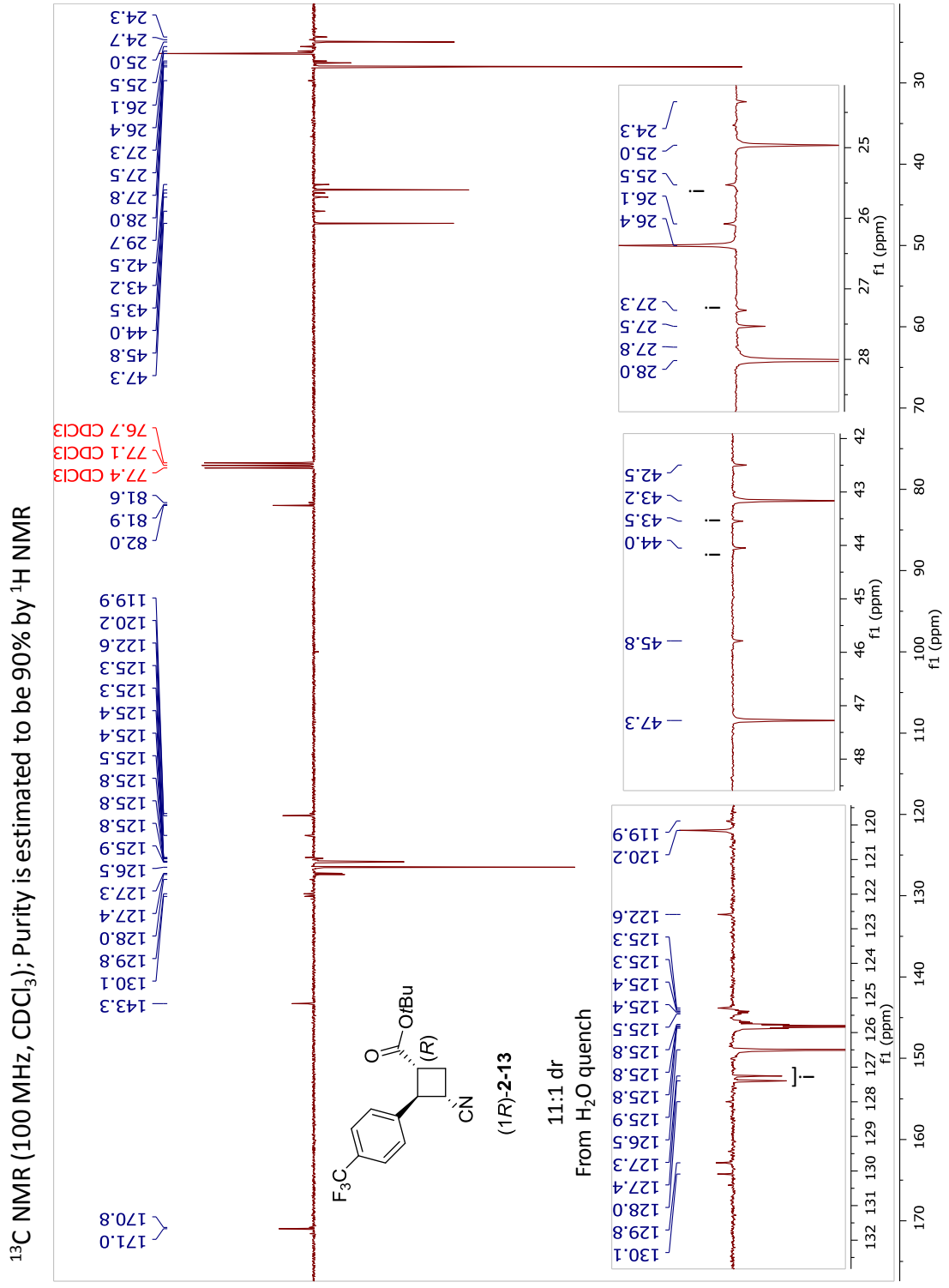
13C NMR (100 MHz, CDCl3); Purity is estimated to be 90% by 1H NMR
(1R)-2-13
11:1 dr
From H2O quench
F3C
O
OtBu
(R)
CN
f1 (ppm)

^{19}F NMR (376 MHz, $CDCl_3$); Purity estimated to be 90%

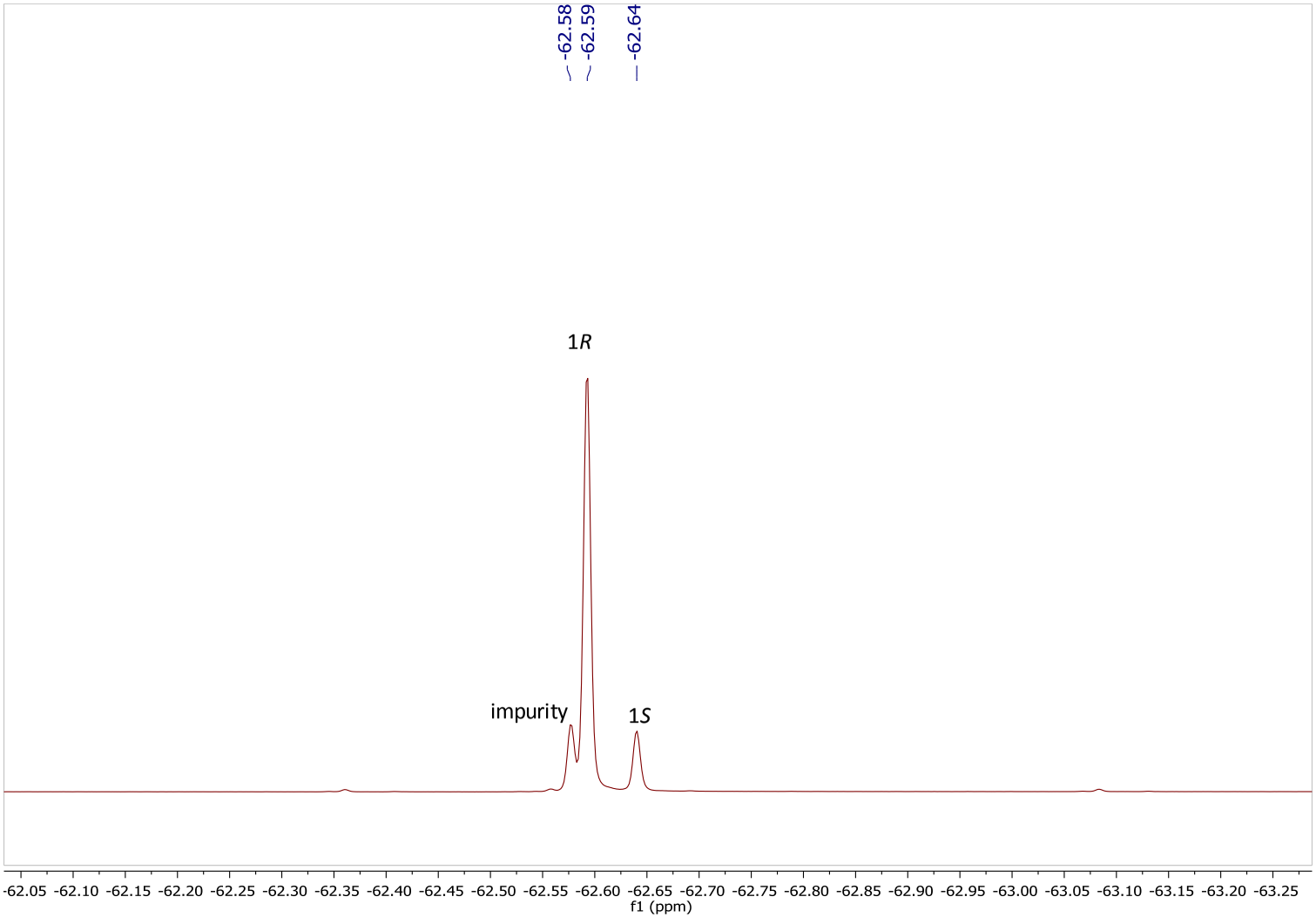

^{1}H NMR (400 MHz, $CDCl_3$); Purity is estimated to be 87%

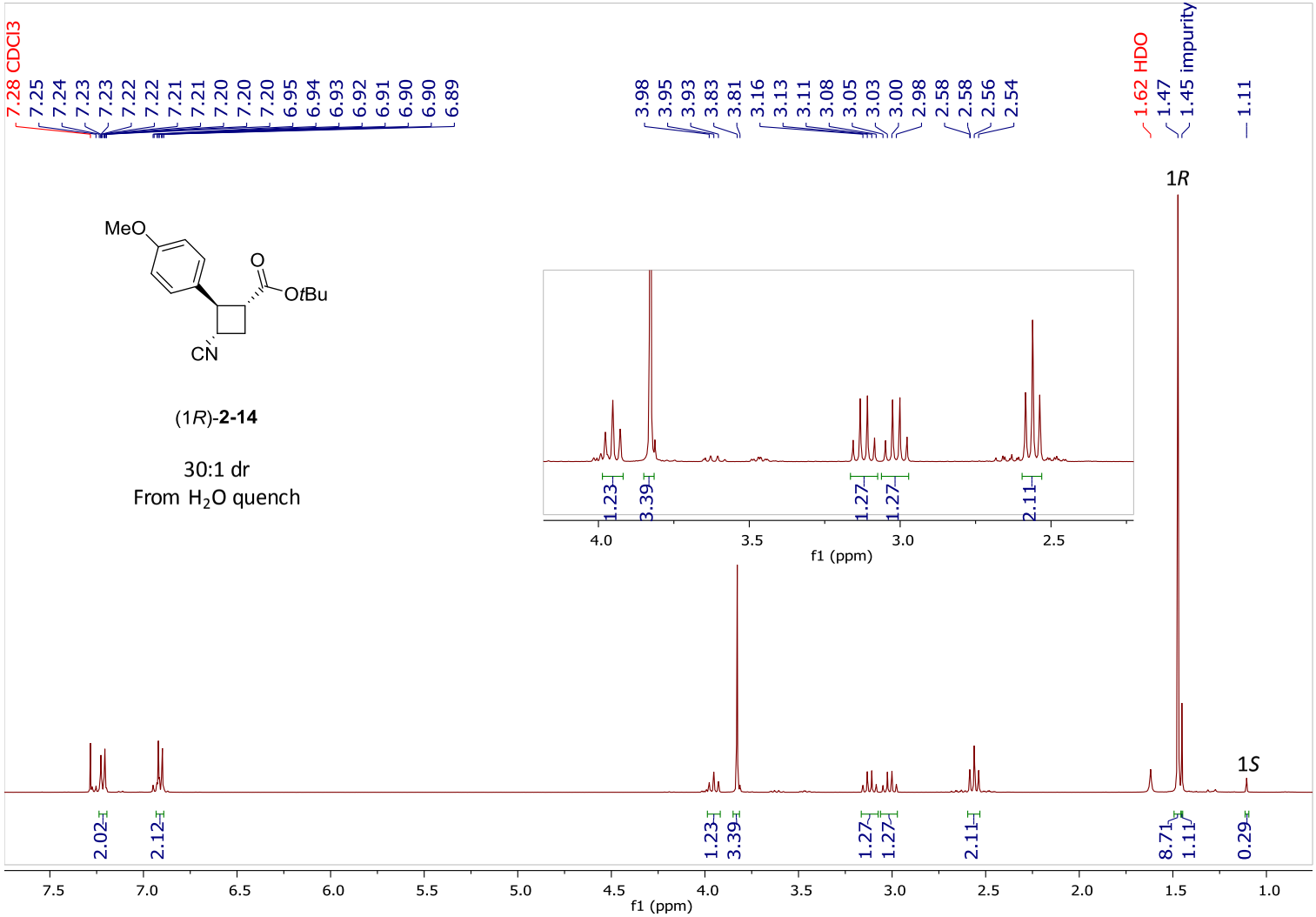

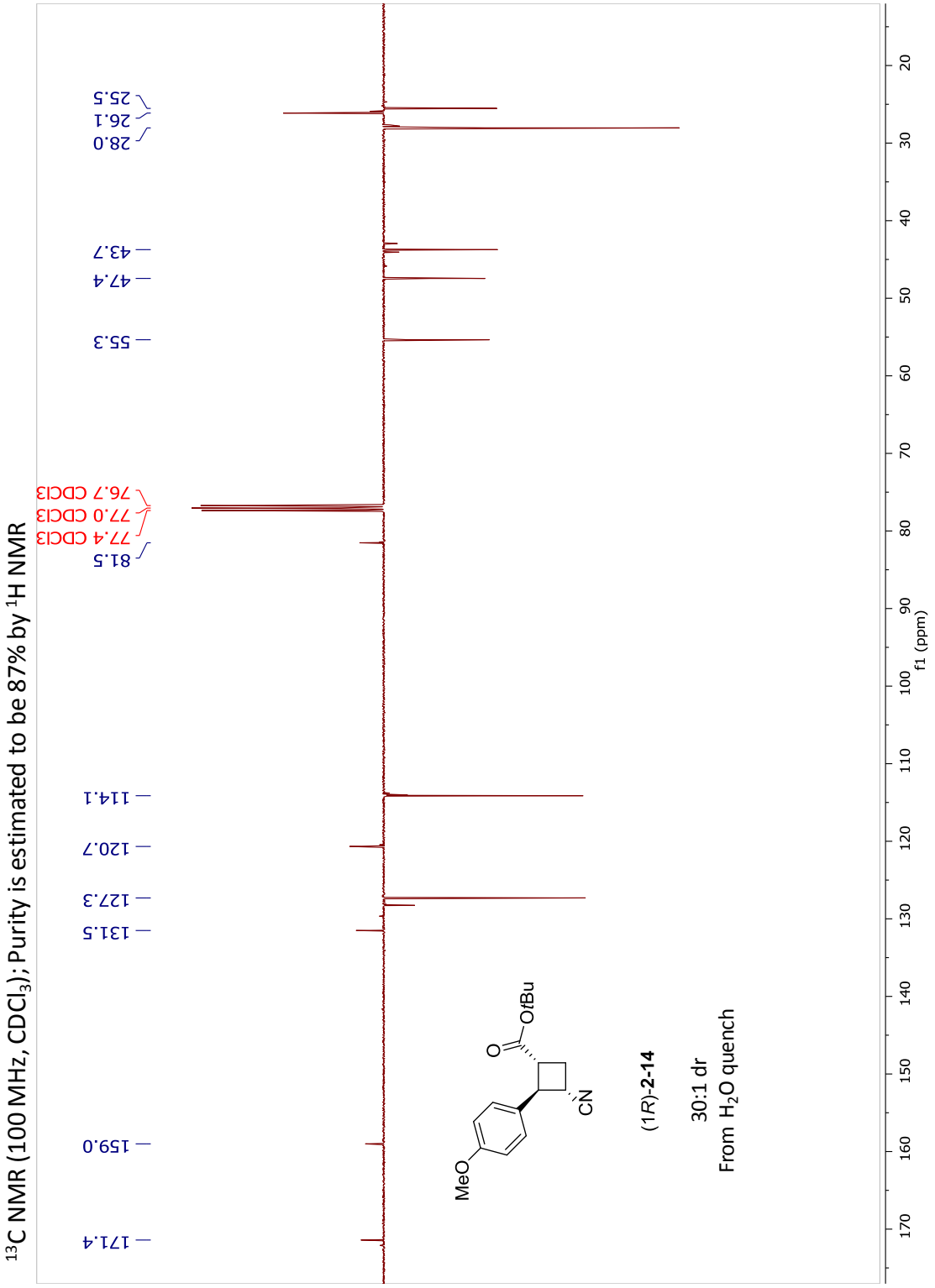
^{13}C NMR (100 MHz, $CDCl_3$); Purity is estimated to be 87% by ^{1}H NMR
171.4
159.0
131.5
127.3
120.7
114.1
81.5
77.4 CDCl3
77.0 CDCl3
76.7 CDCl3
55.3
47.4
43.7
28.0
26.1
25.5
MeO
CN
O
OtBu
(1R)-2-14
30:1 dr
From H_2O quench
f1 (ppm)

^{1}H NMR (400 MHz, $CDCl_3$); Purity is estimated to be 85%

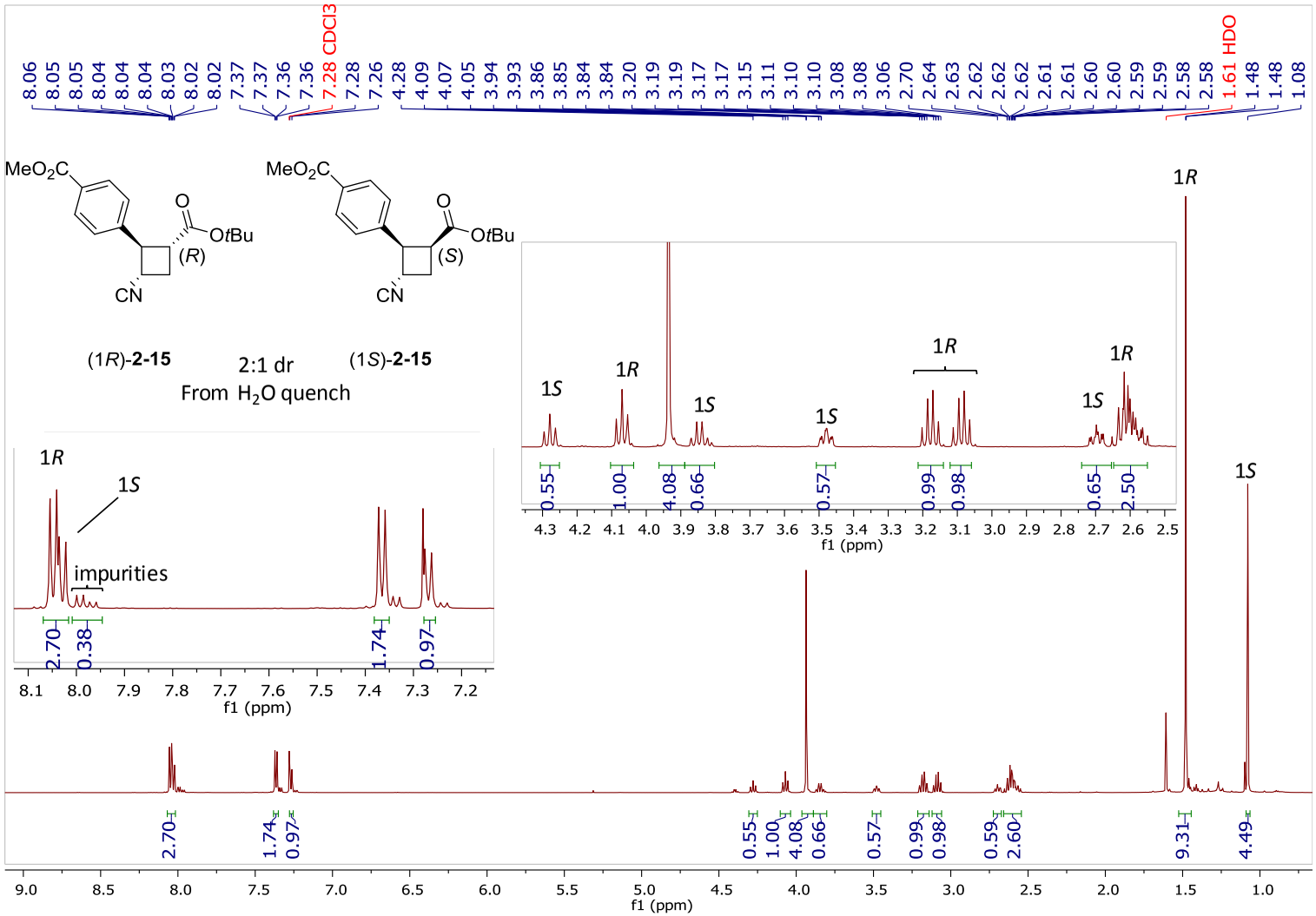

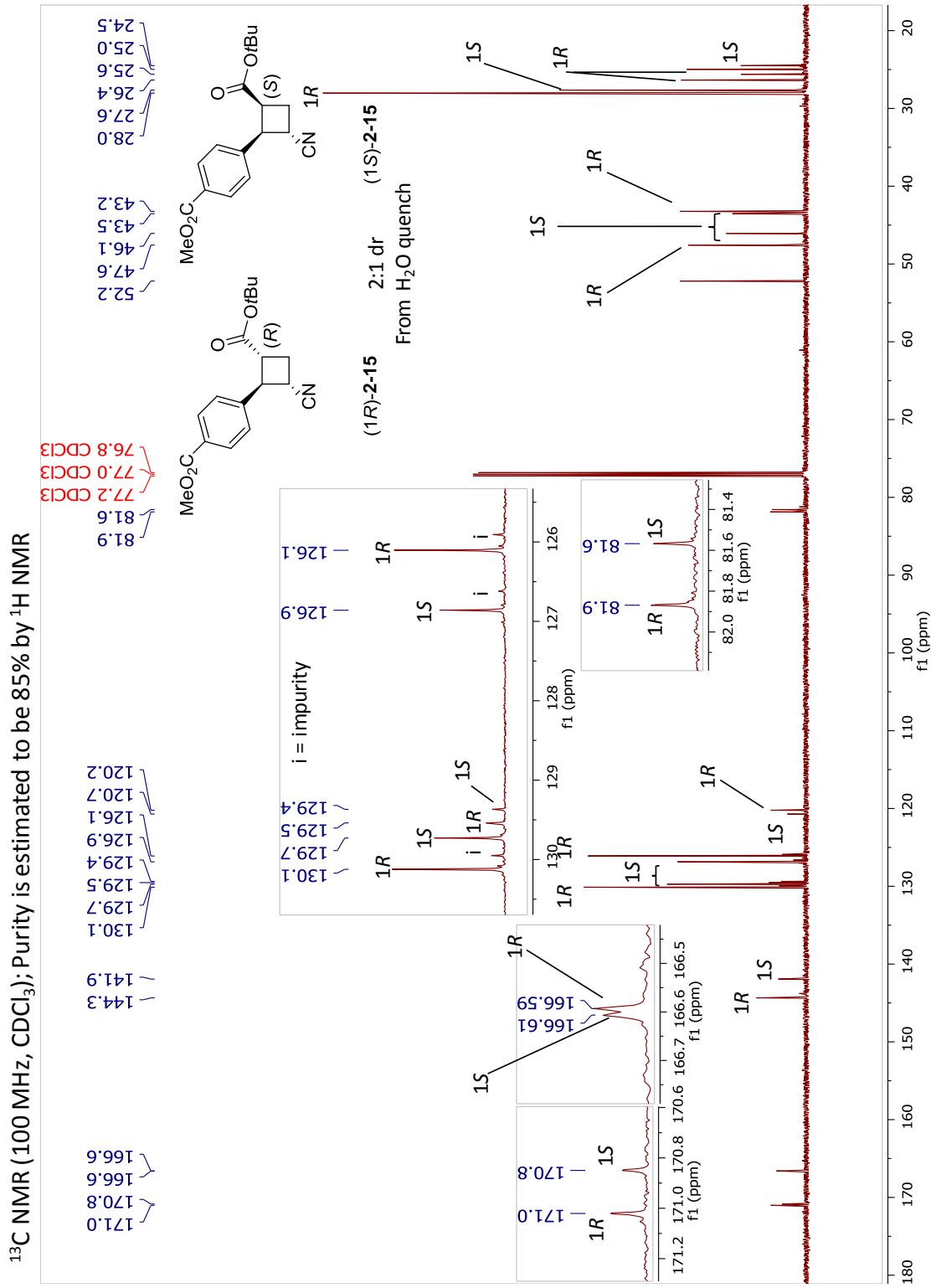
13C NMR (100 MHz, CDCl3); Purity is estimated to be 85% by 1H NMR
(1R)-2-15
2:1 dr
From H2O quench
(1S)-2-15
i = impurity
MeO2C
OtBu
CN
(R)
(S)
1R
1S
f1 (ppm)

^{1}H NMR (400 MHz, $CDCl_3$)

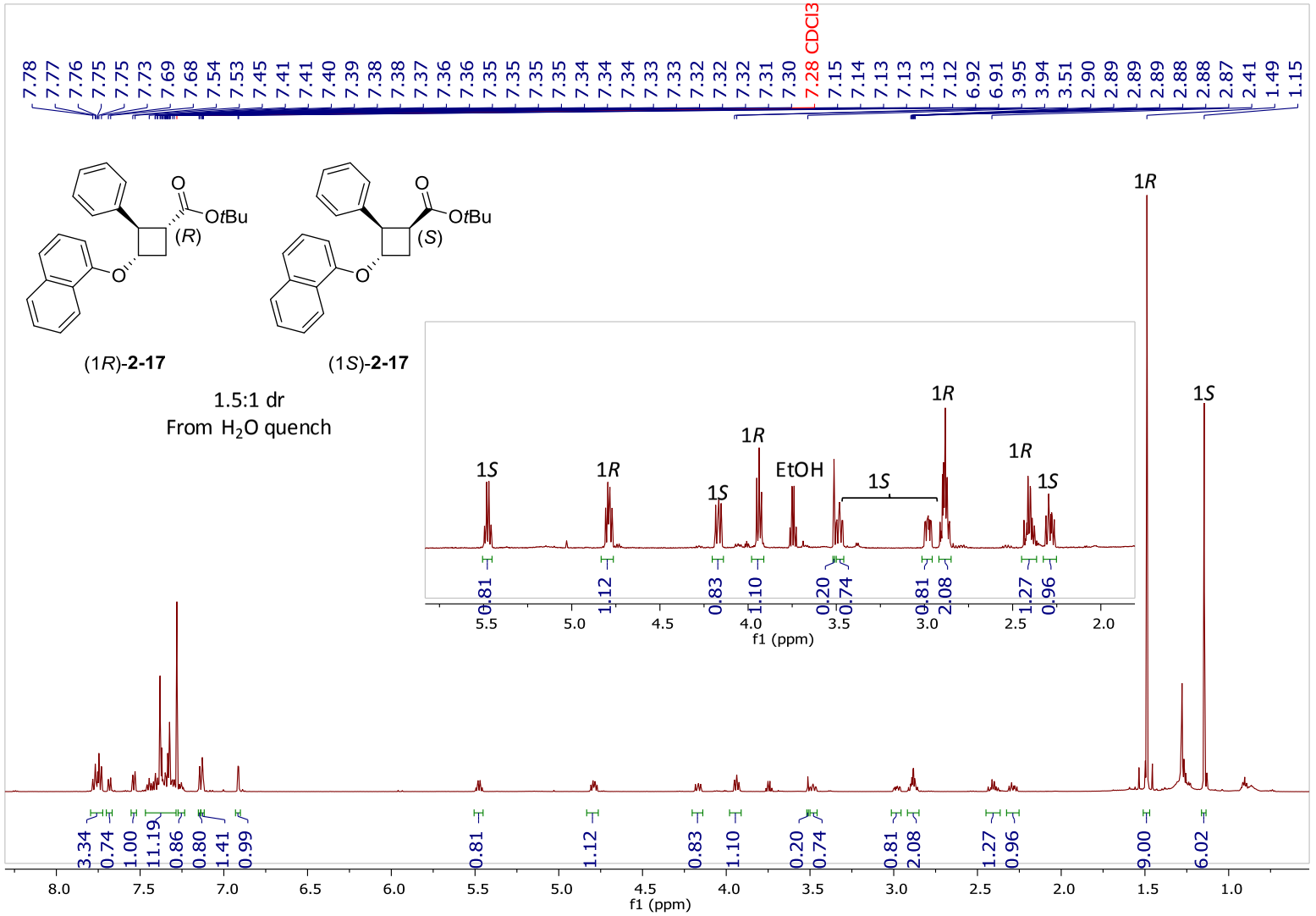

^{13}C NMR (100 MHz, $CDCl_3$)

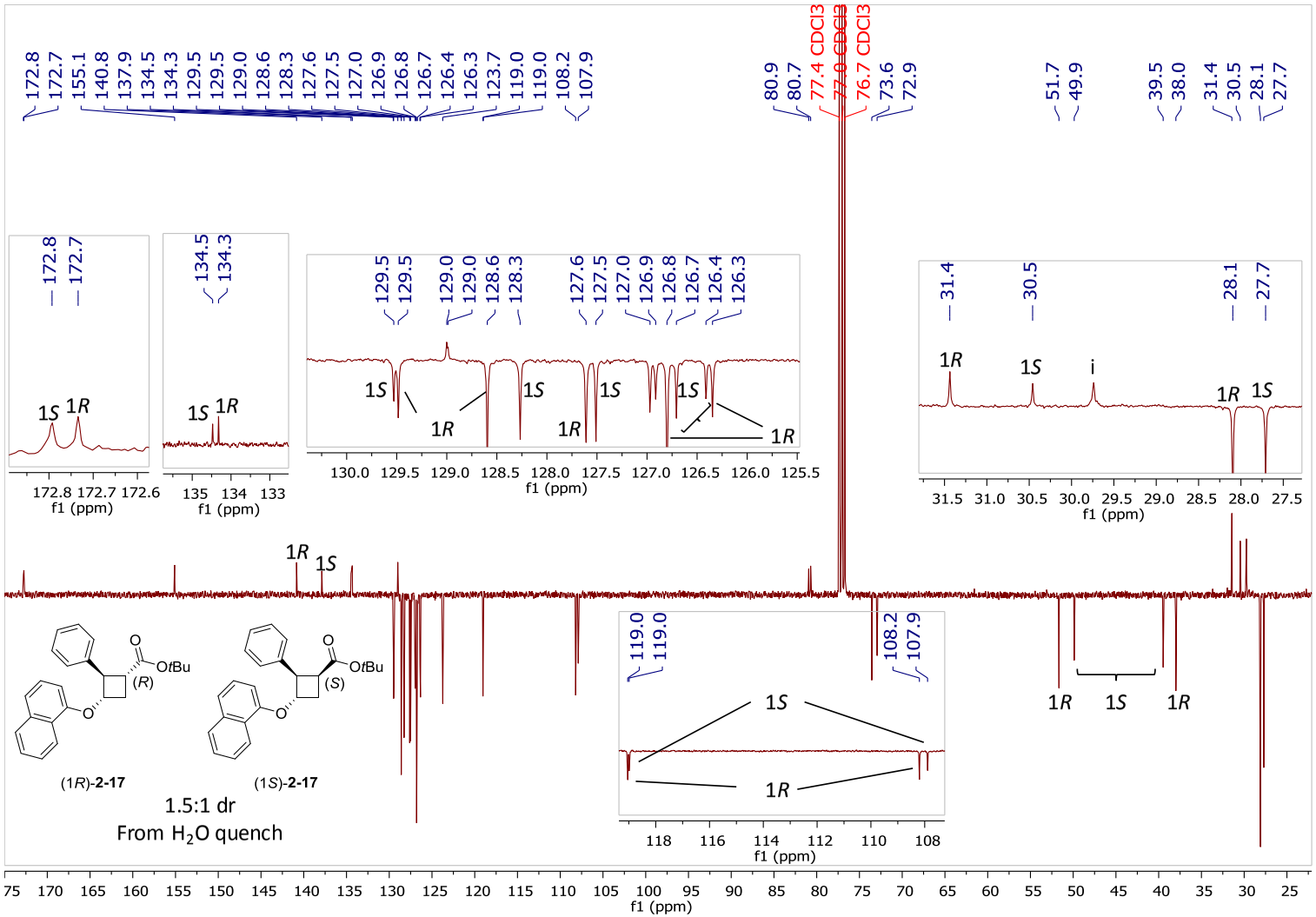

^{1}H NMR (400 MHz, $CDCl_3$)

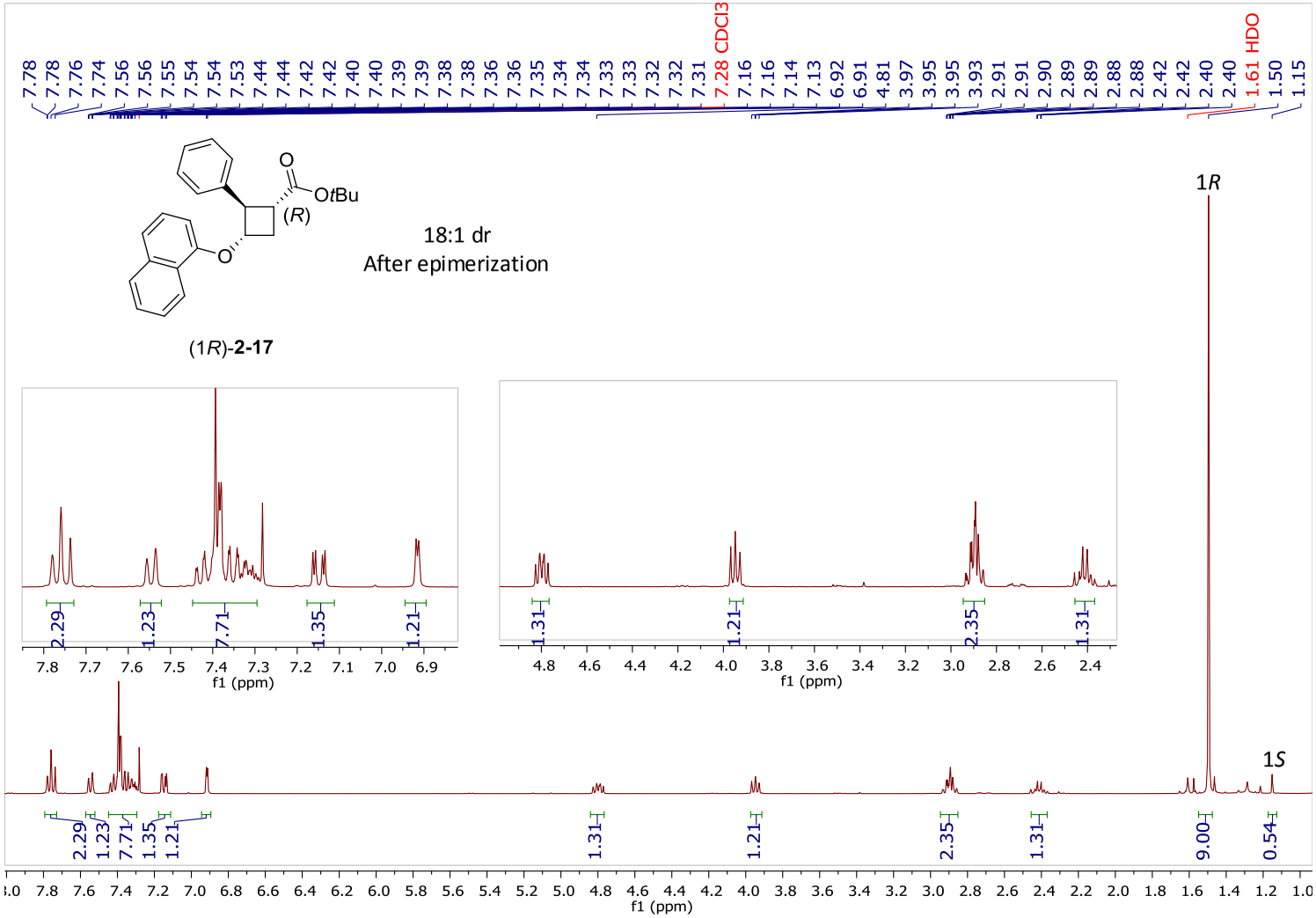

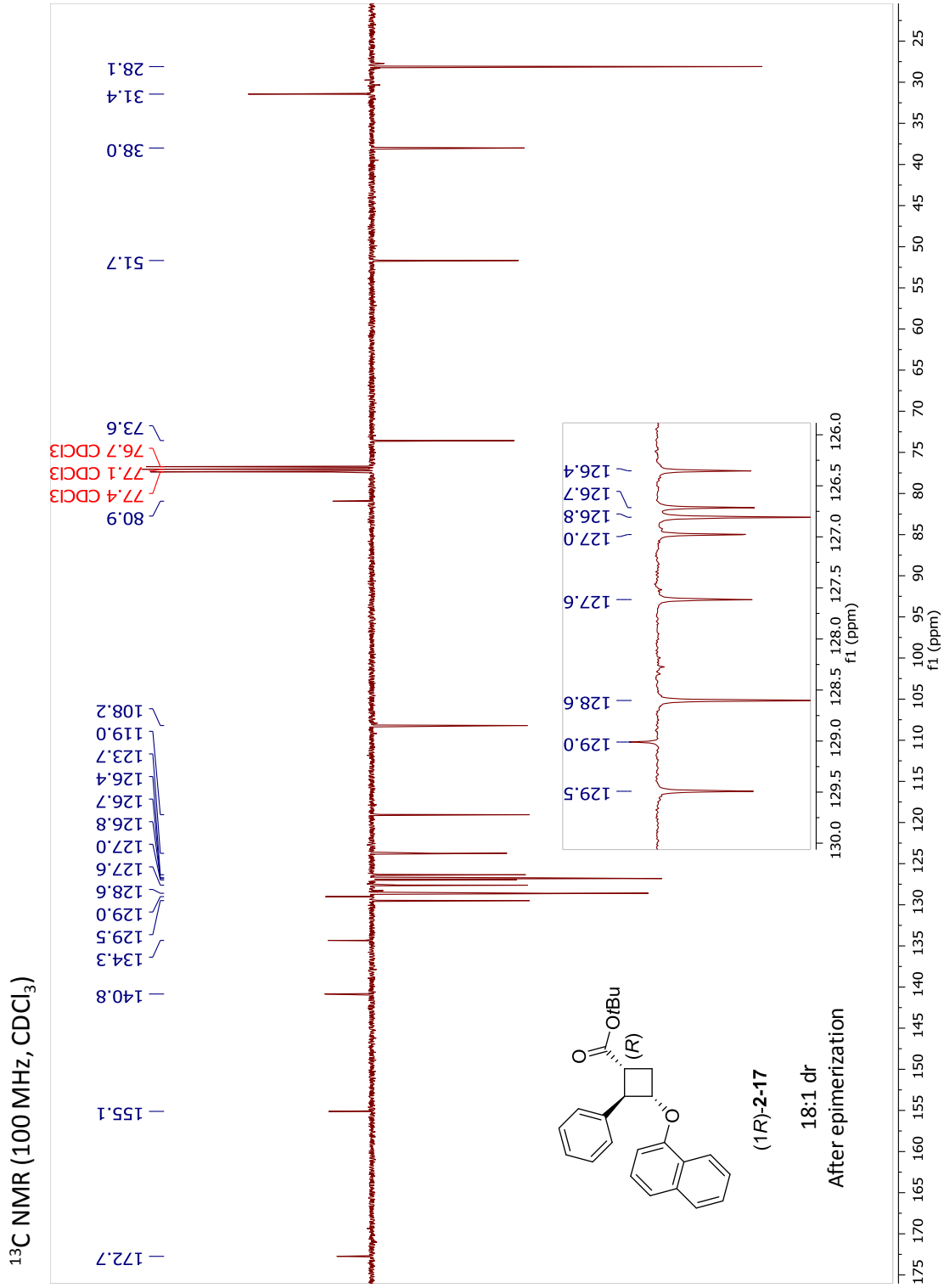
^{13}C NMR (100 MHz, $CDCl_3$)
172.7
155.1
140.8
134.3
129.5
129.0
128.6
127.6
127.0
126.8
126.7
126.4
123.7
119.0
108.2
80.9
77.4 CDCl3
77.1 CDCl3
76.7 CDCl3
73.6
51.7
38.0
31.4
28.1
129.5
129.0
128.6
127.6
127.0
126.8
126.7
126.4
f1 (ppm)
O
OtBu
(R)
O
(1R)-2-17
18:1 dr
After epimerization
f1 (ppm)

^{1}H NMR (400 MHz, $CDCl_3$)

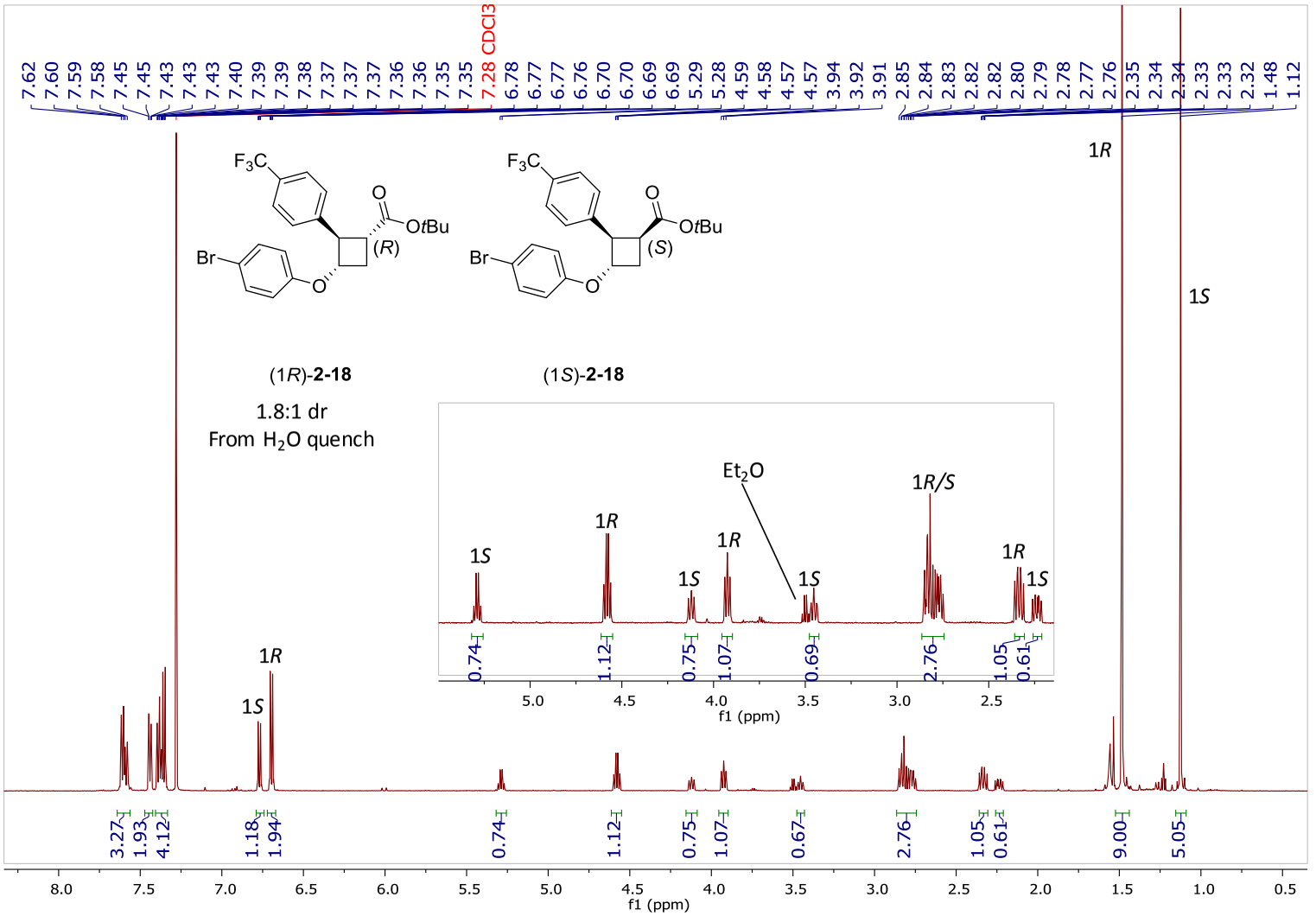

^{13}C NMR (100 MHz, $CDCl_3$)

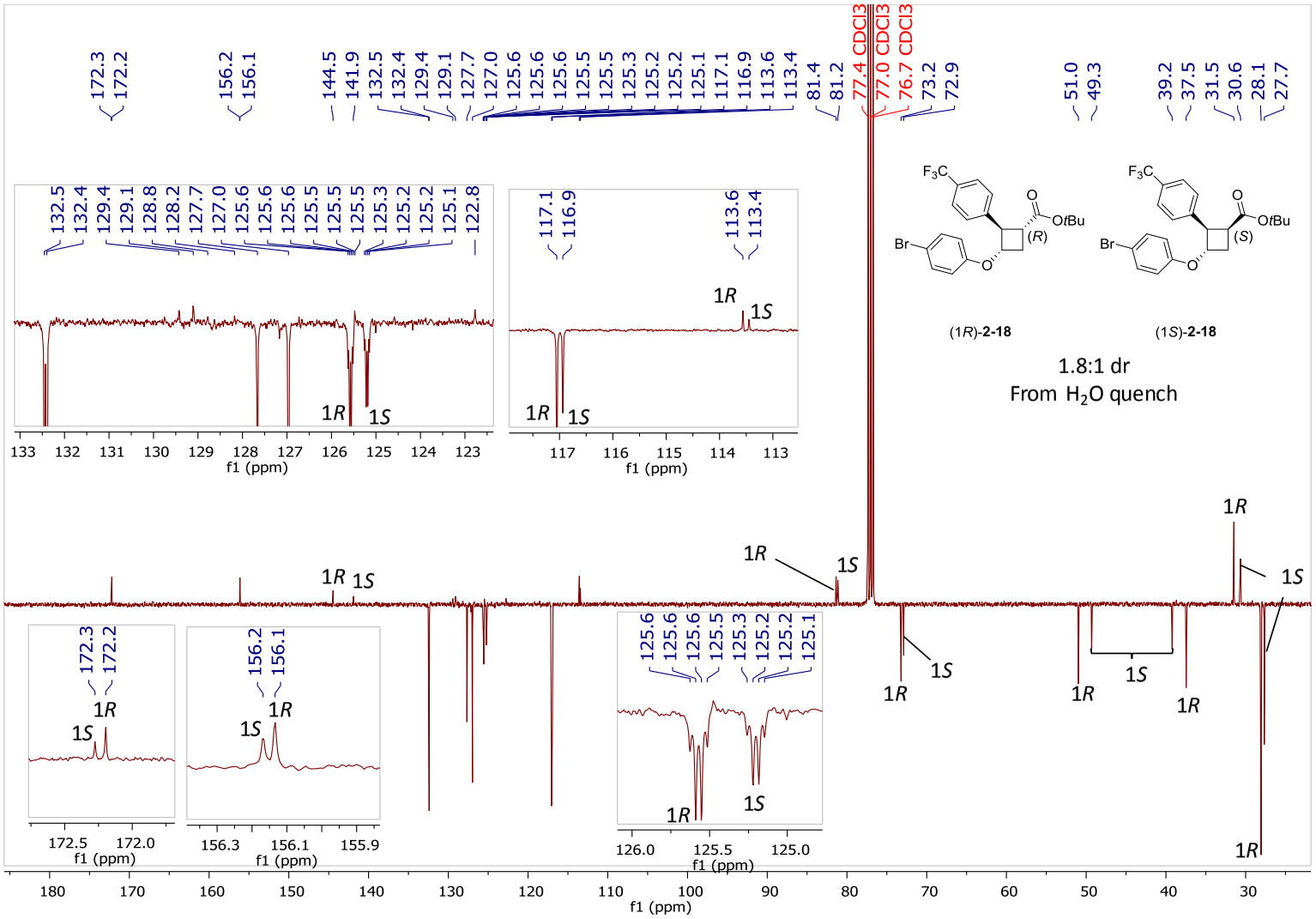

^{1}H NMR (400 MHz, $CDCl_3$)

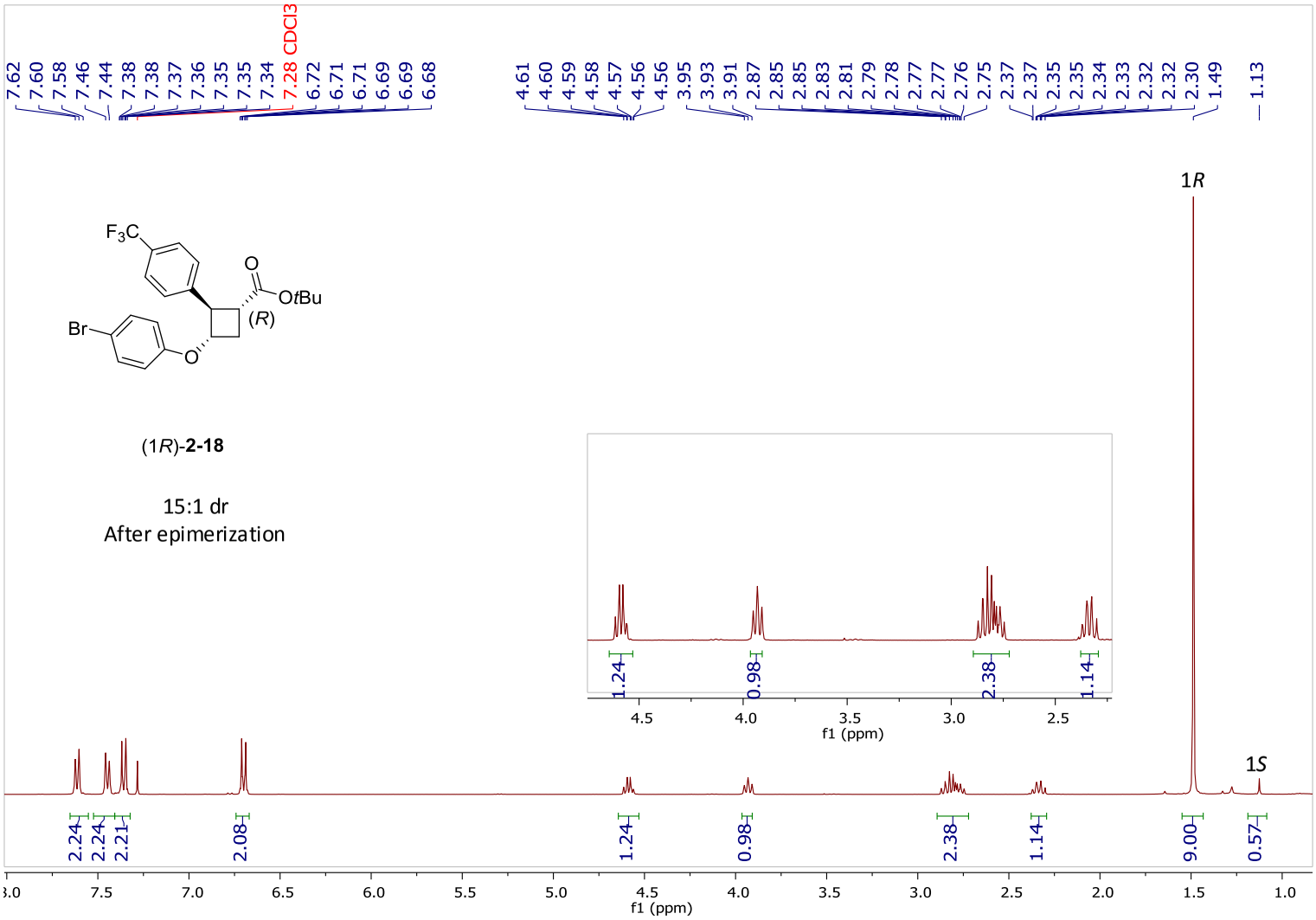

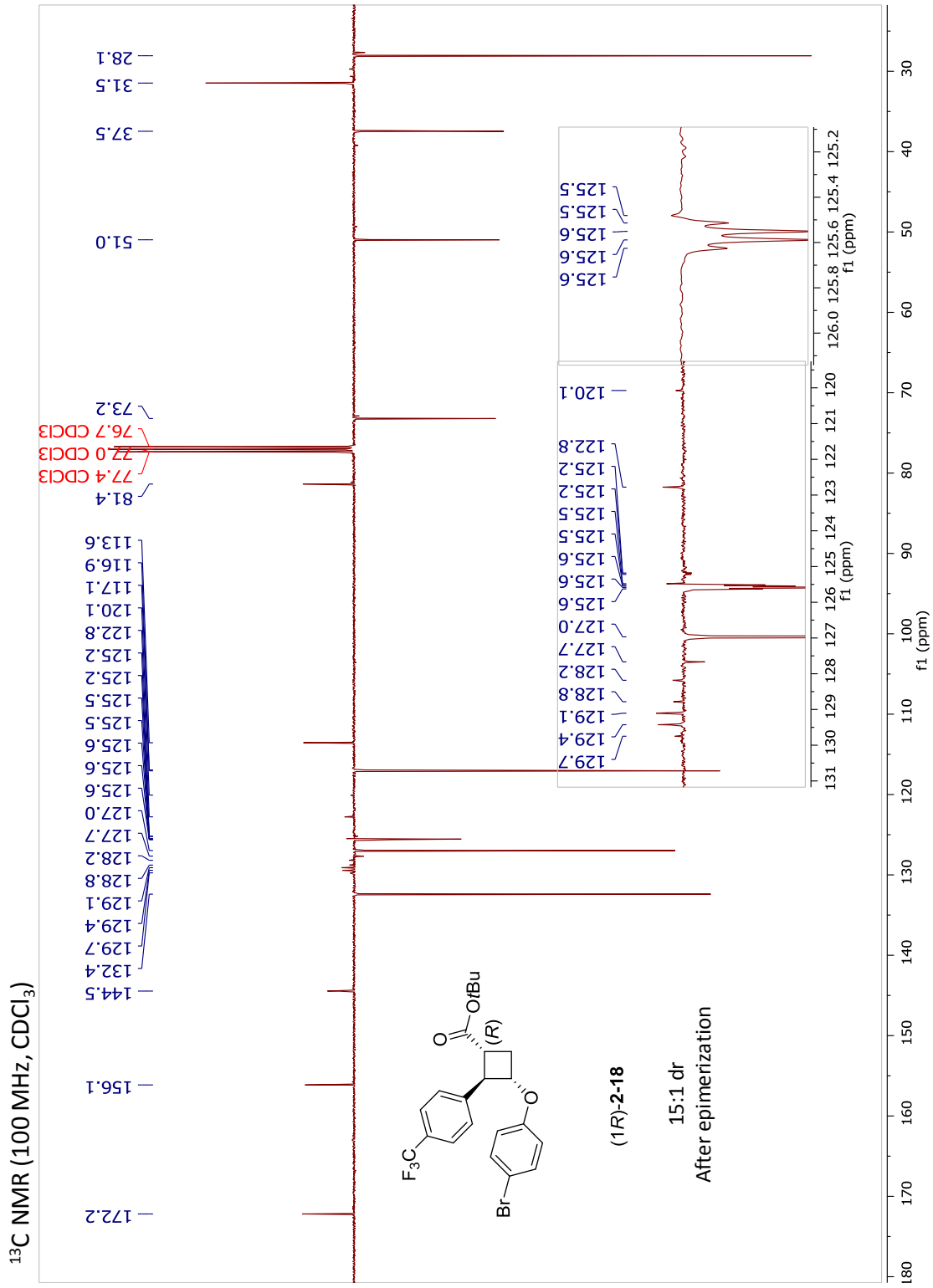
^{13}C NMR (100 MHz, $CDCl_3$)
172.2
156.1
144.5
132.4
129.7
129.4
129.1
128.8
128.2
127.7
127.0
125.6
125.6
125.6
125.5
125.5
125.2
125.2
122.8
120.1
117.1
116.9
113.6
81.4
77.4 CDCl3
77.0 CDCl3
76.7 CDCl3
73.2
51.0
37.5
31.5
28.1
OtBu
O
(R)
O
F_3C
Br
(1R)-2-18
15:1 dr
After epimerization
f1 (ppm)

^{19}F NMR (376 MHz, $CDCl_3$)

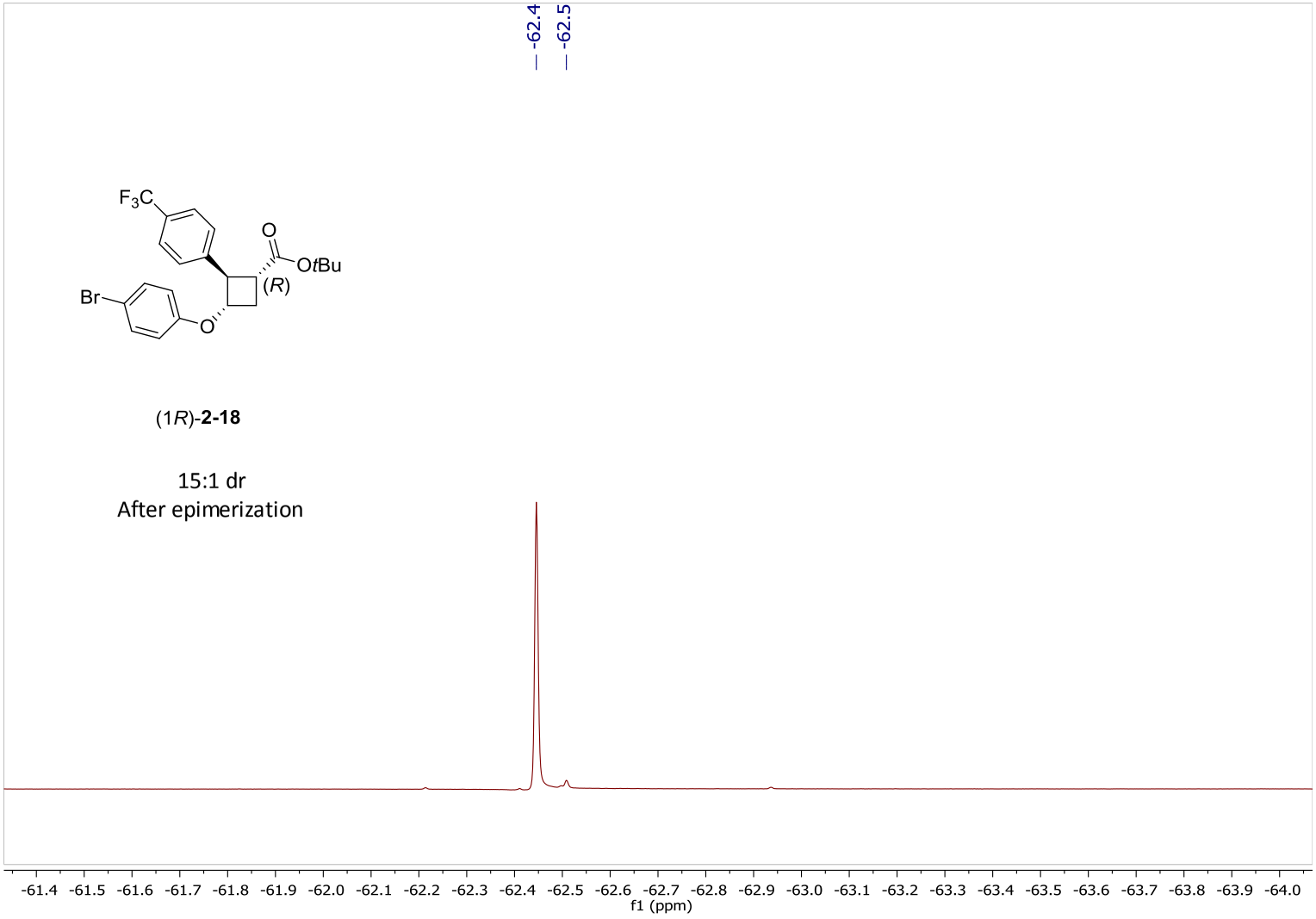

^{1}H NMR (400 MHz, $CDCl_3$)

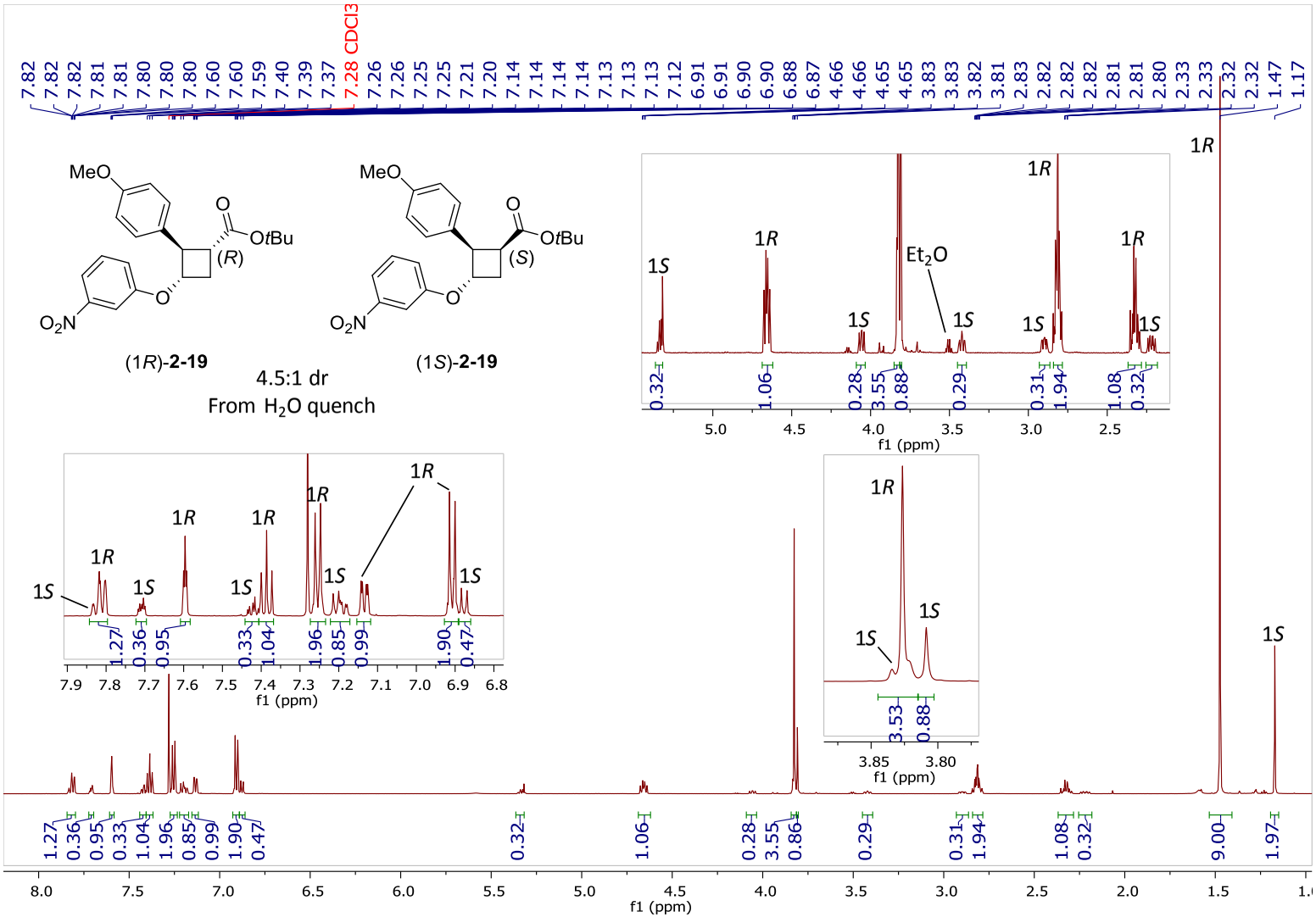

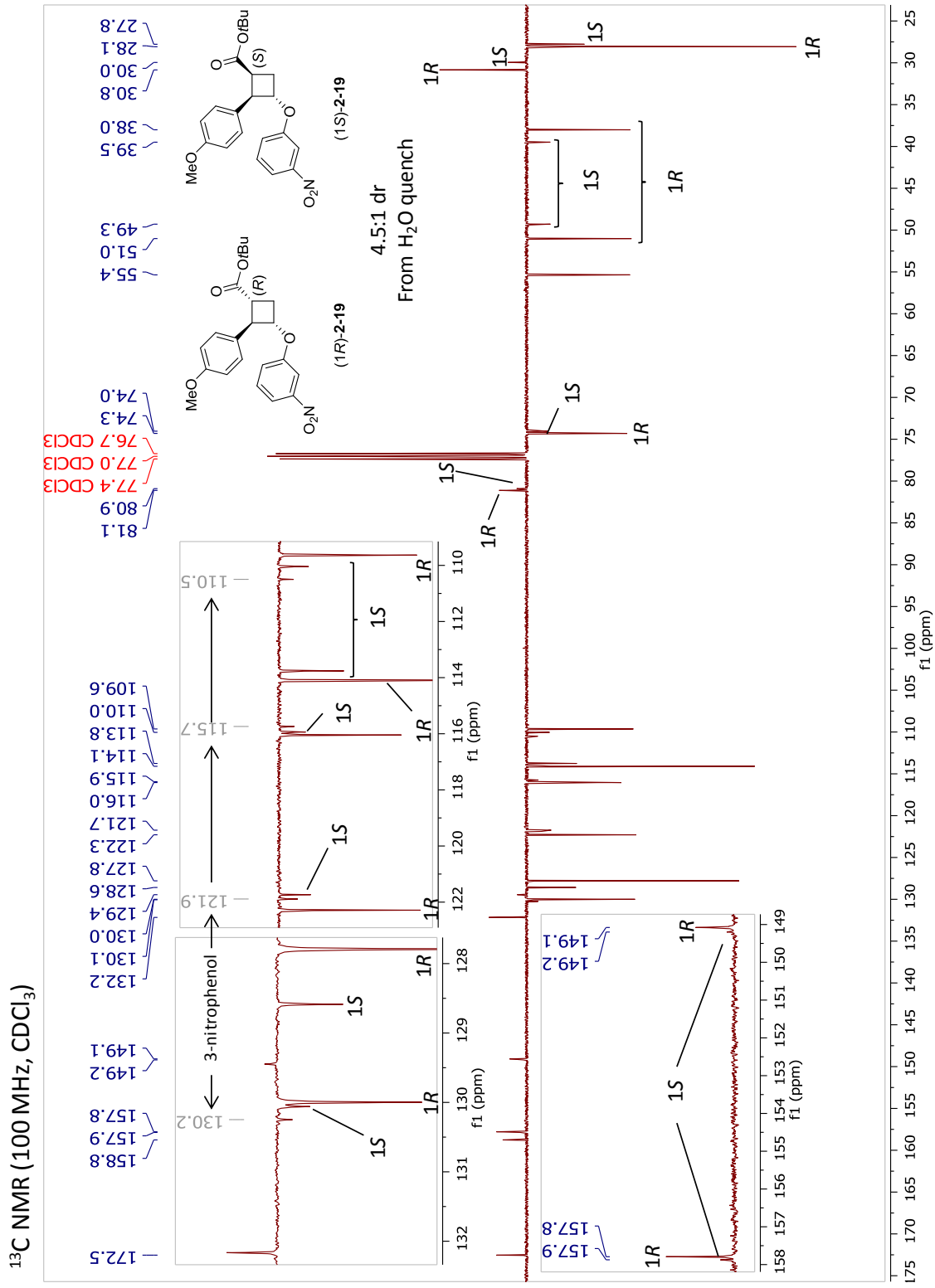
13C NMR (100 MHz, CDCl3)
4.5:1 dr
From H2O quench
(1S)-2-19
(1R)-2-19
3-nitrophenol
1S
1R
f1 (ppm)

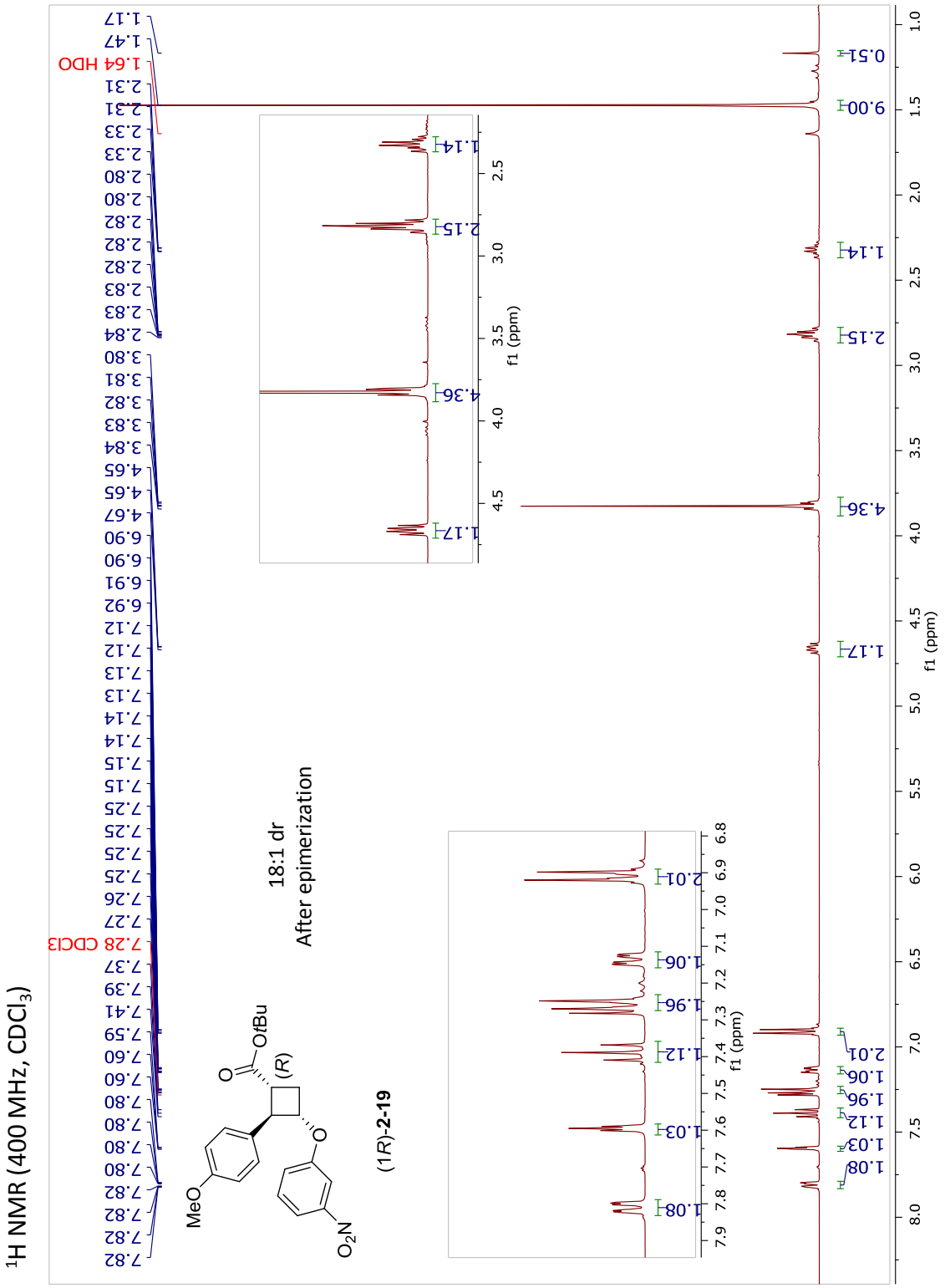
^{1}H NMR (400 MHz, $CDCl_3$)
18:1 dr
After epimerization
(1*R*)-**2-19**
MeO
O
OtBu
(*R*)
O_2N
f1 (ppm)

^{13}C NMR (100 MHz, $CDCl_3$)

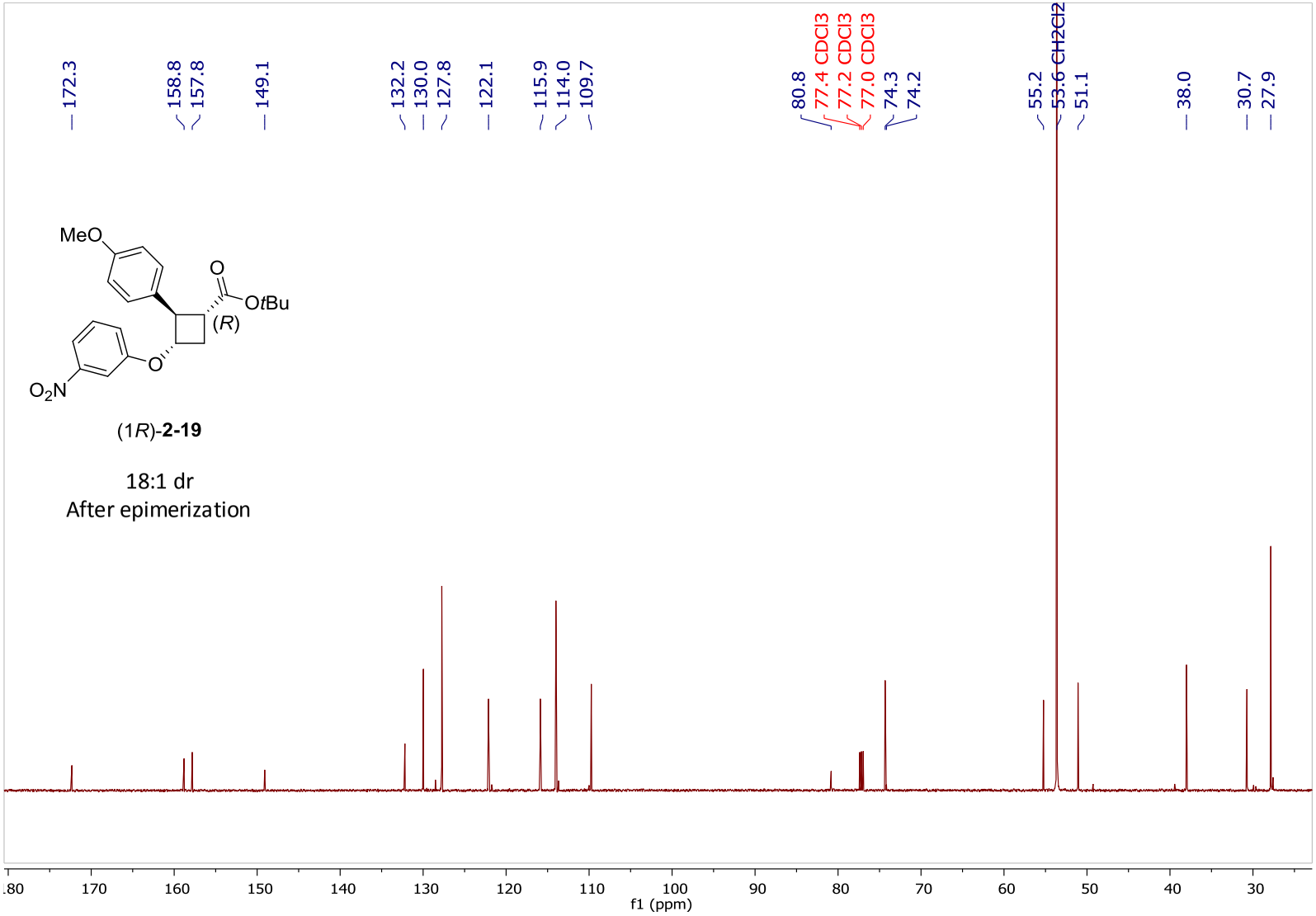

(1*R*)-**2-19**

18:1 dr
After epimerization

^{1}H NMR (400 MHz, $CDCl_3$); Purity is estimated to be 95% by ^{1}H NMR

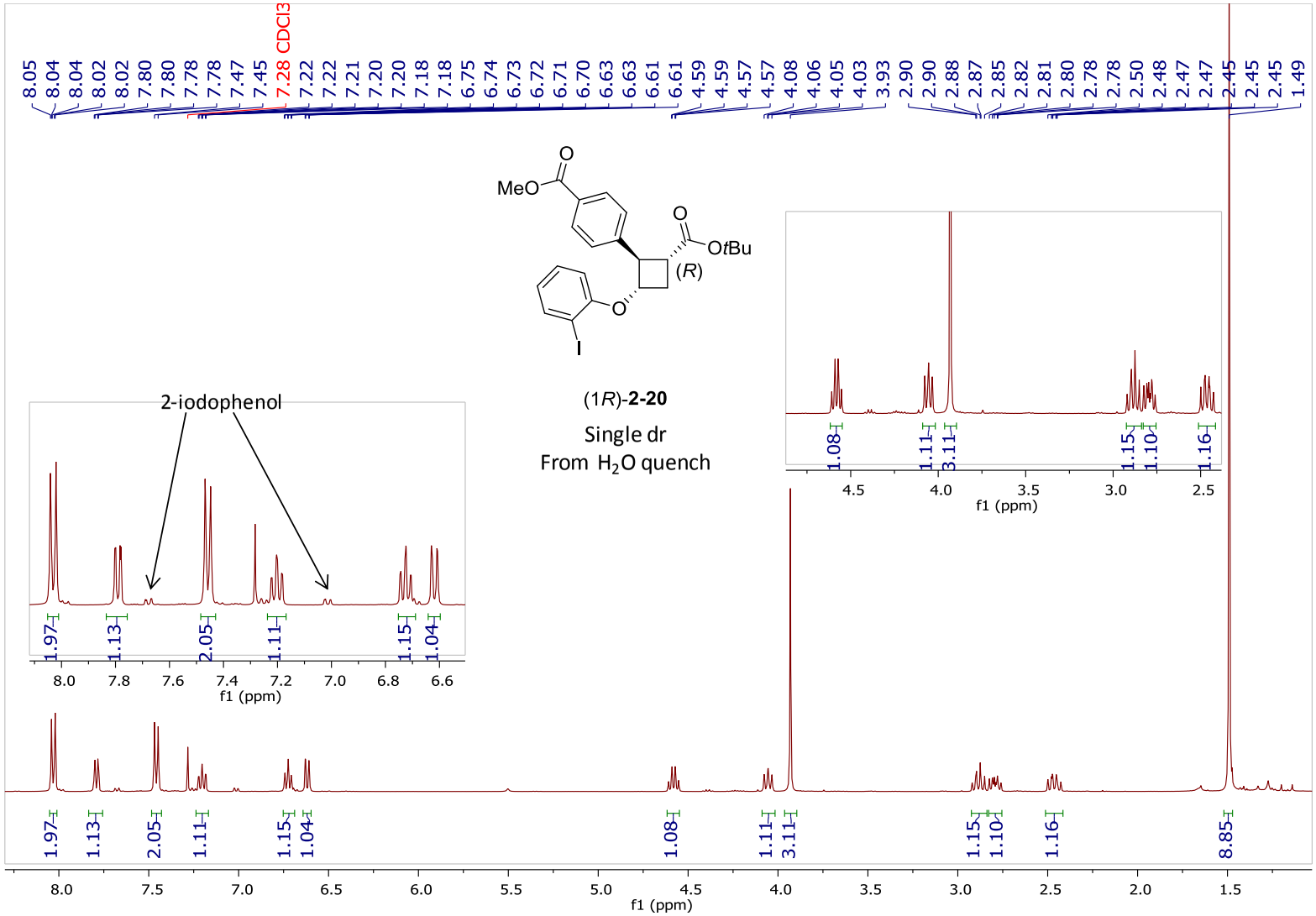

^{13}C NMR (100 MHz, $CDCl_3$)

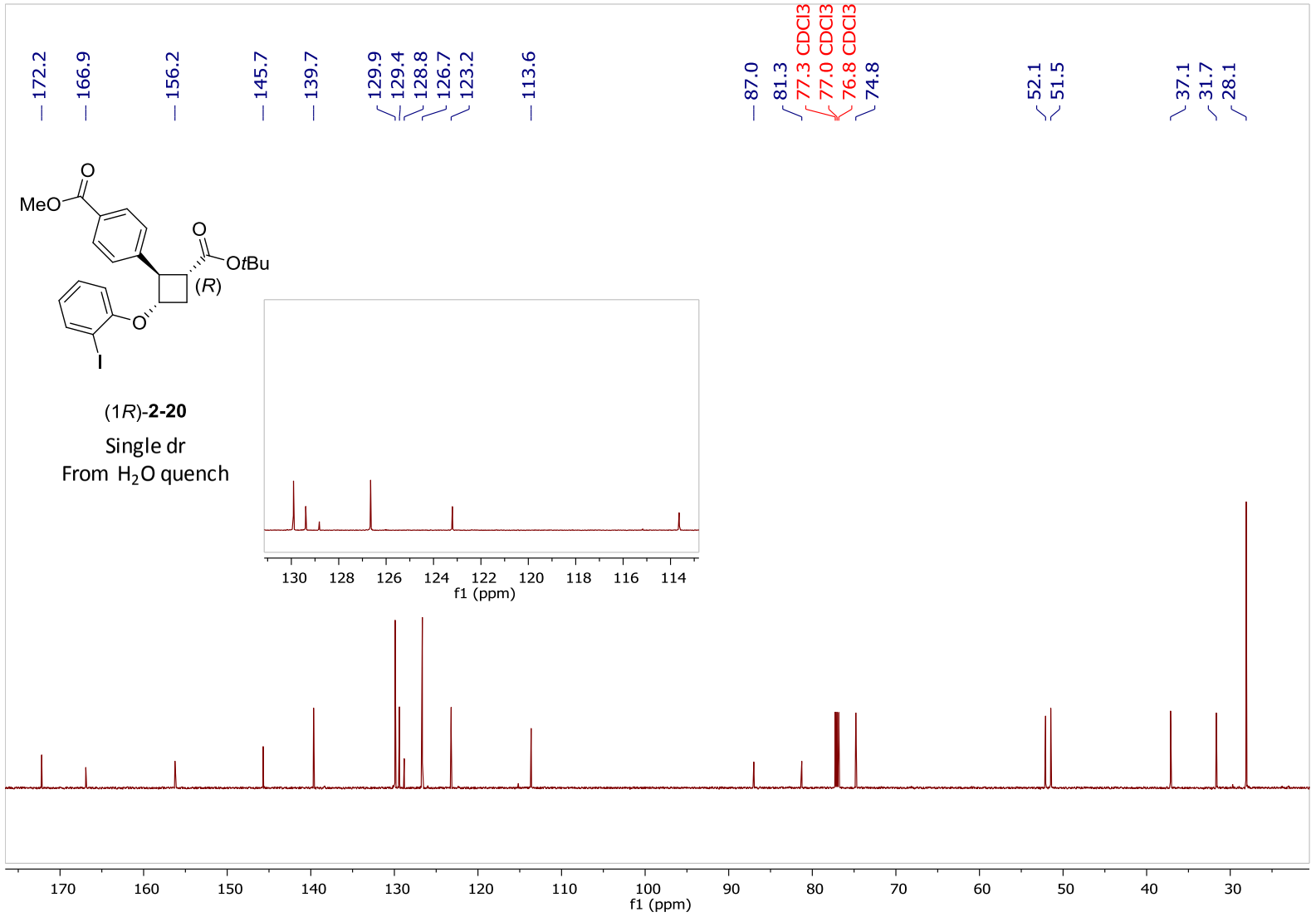

^{1}H NMR (400 MHz, $CDCl_3$)

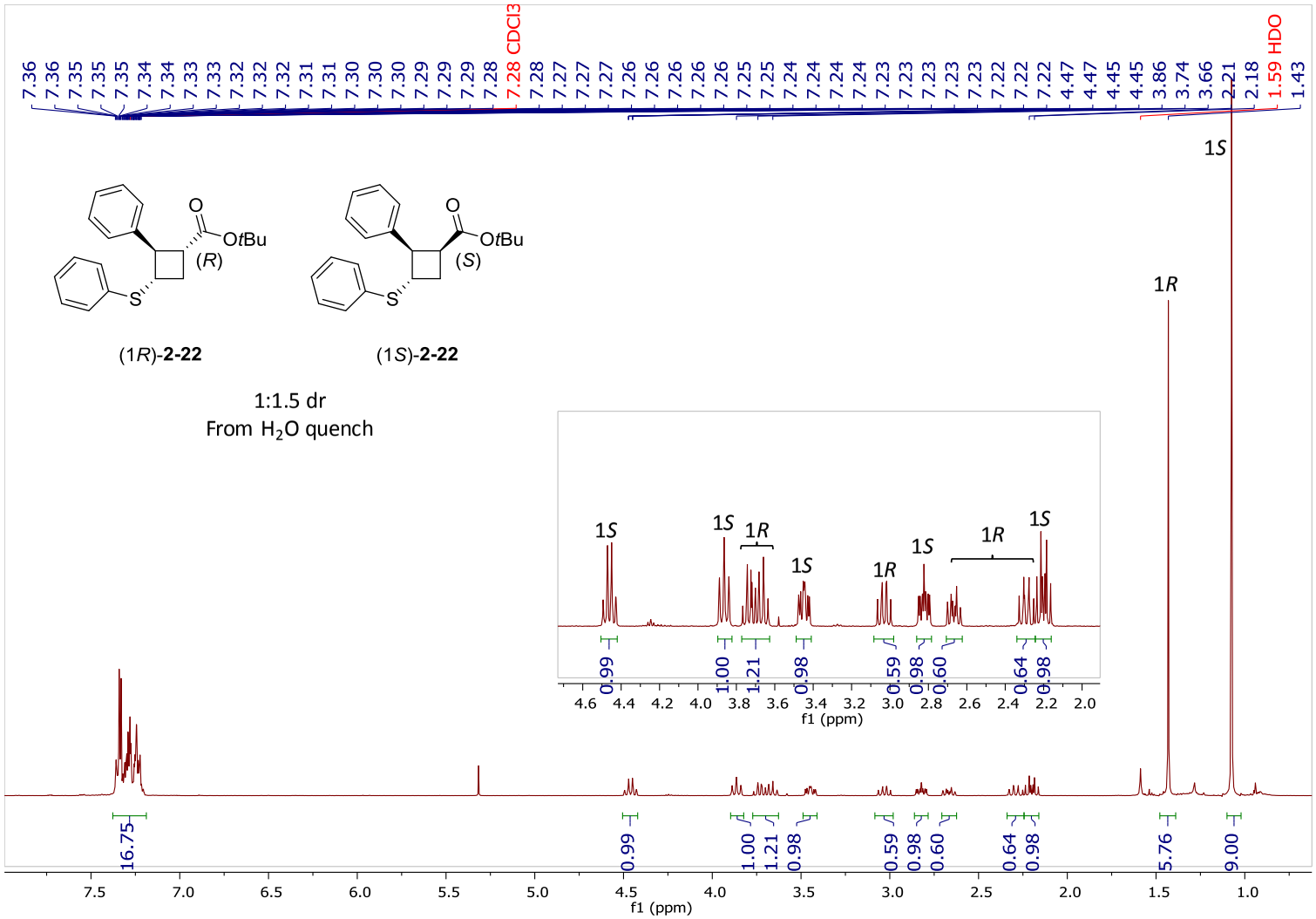

^{13}C NMR (100 MHz, $CDCl_3$)

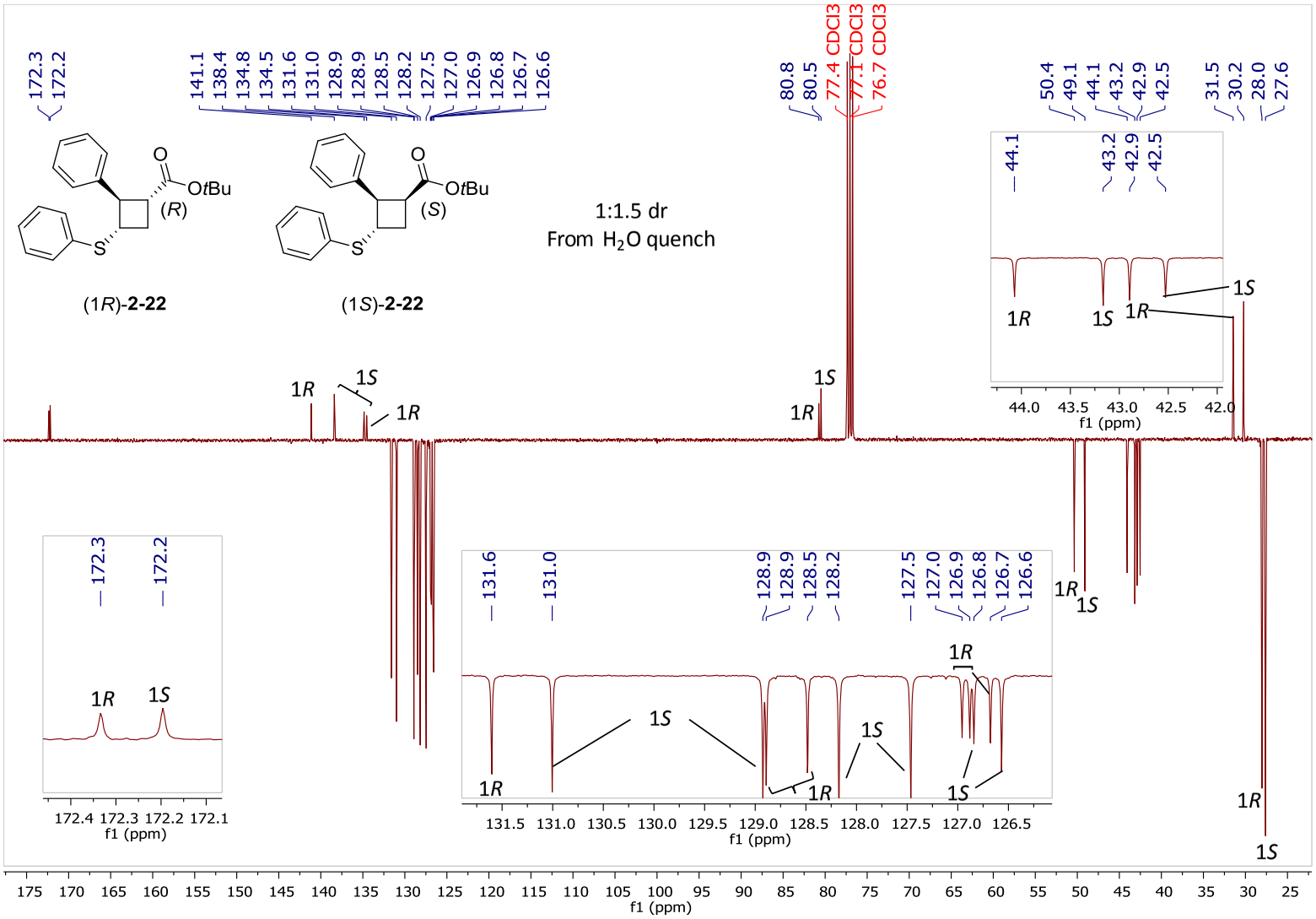

^{1}H NMR (600 MHz, $CDCl_3$)

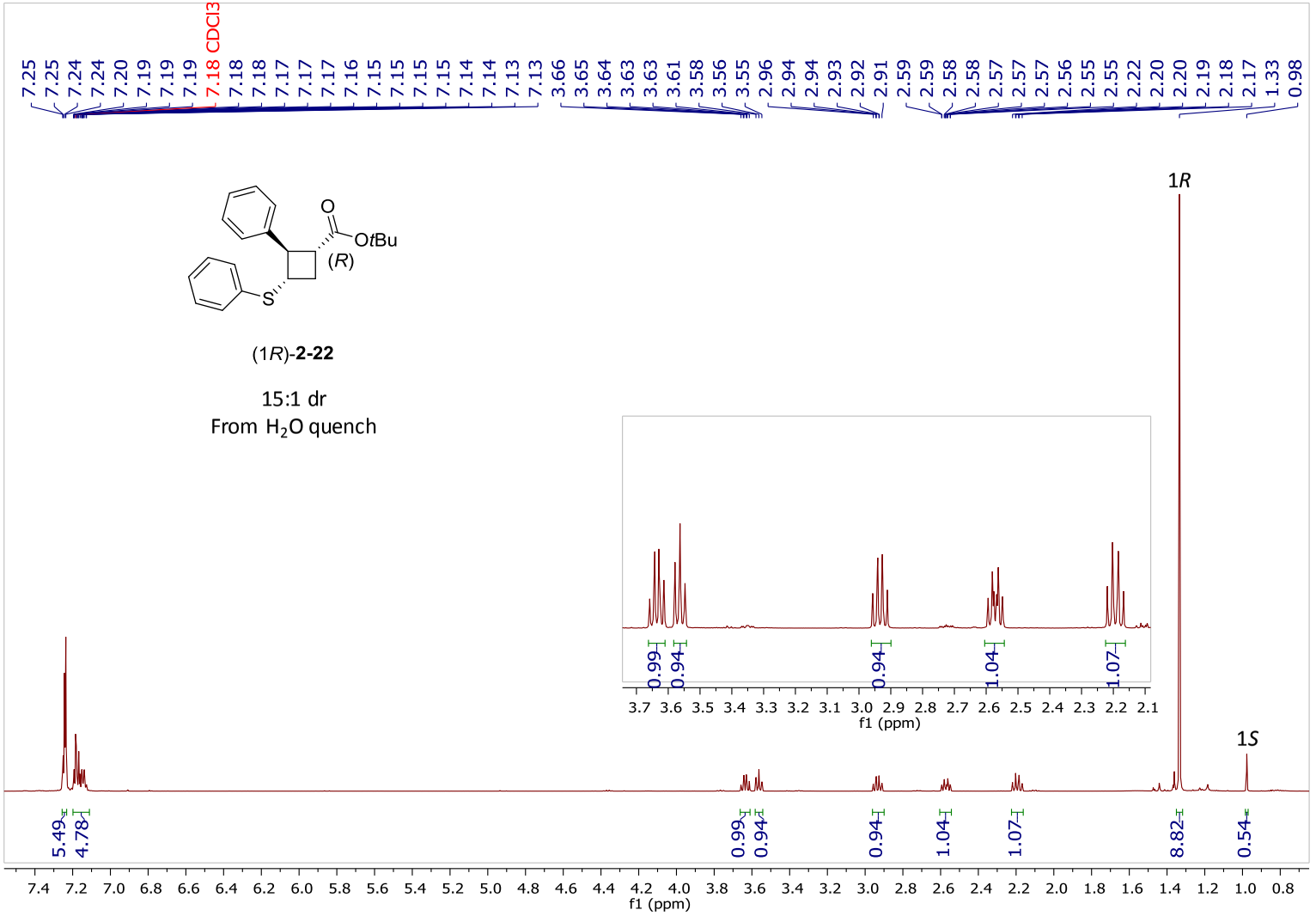

(1*R*)-**2-22**

15:1 dr

From H_2O quench

^{13}C NMR (150 MHz, $CDCl_3$)

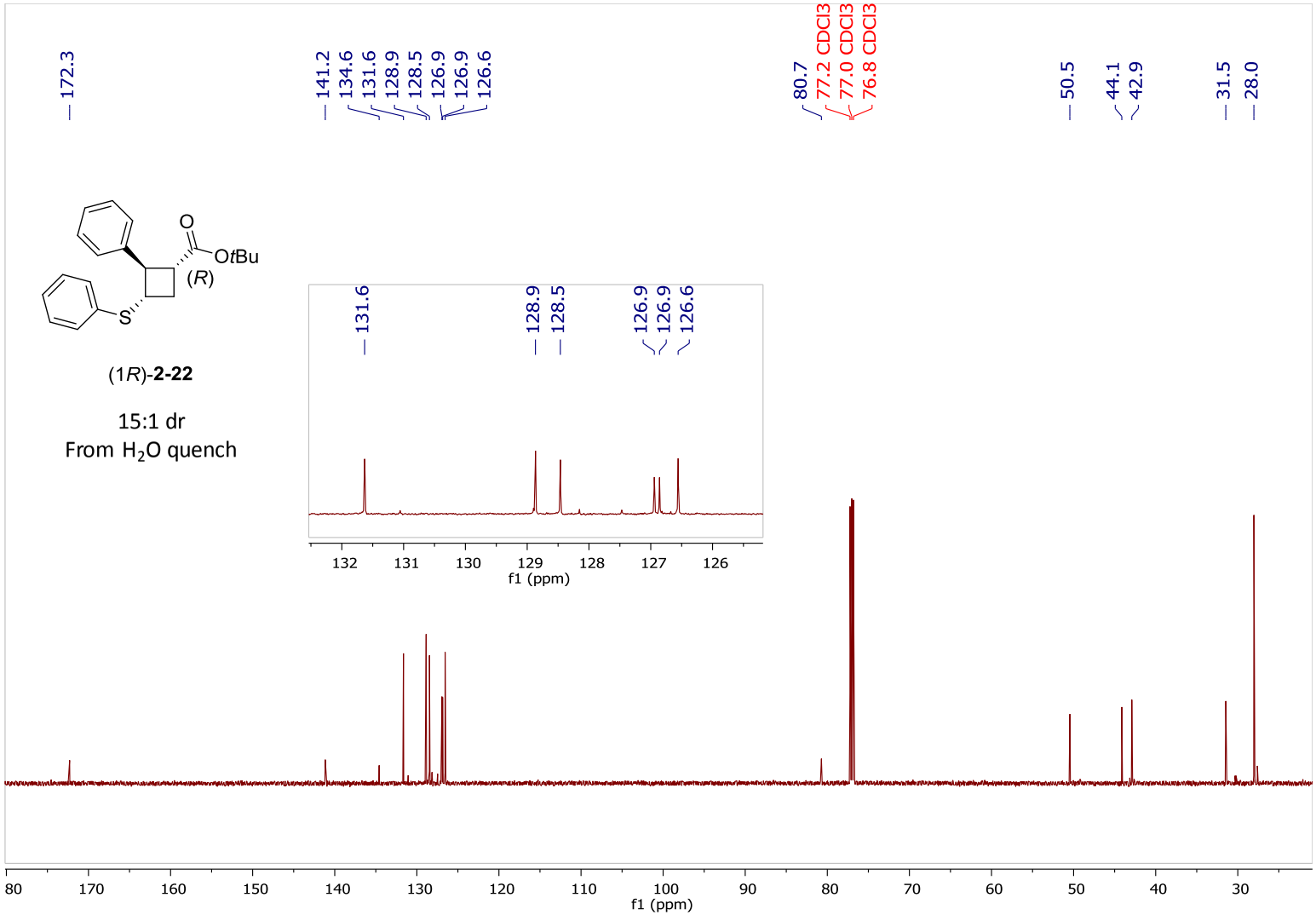

^{1}H NMR (400 MHz, $CDCl_3$)

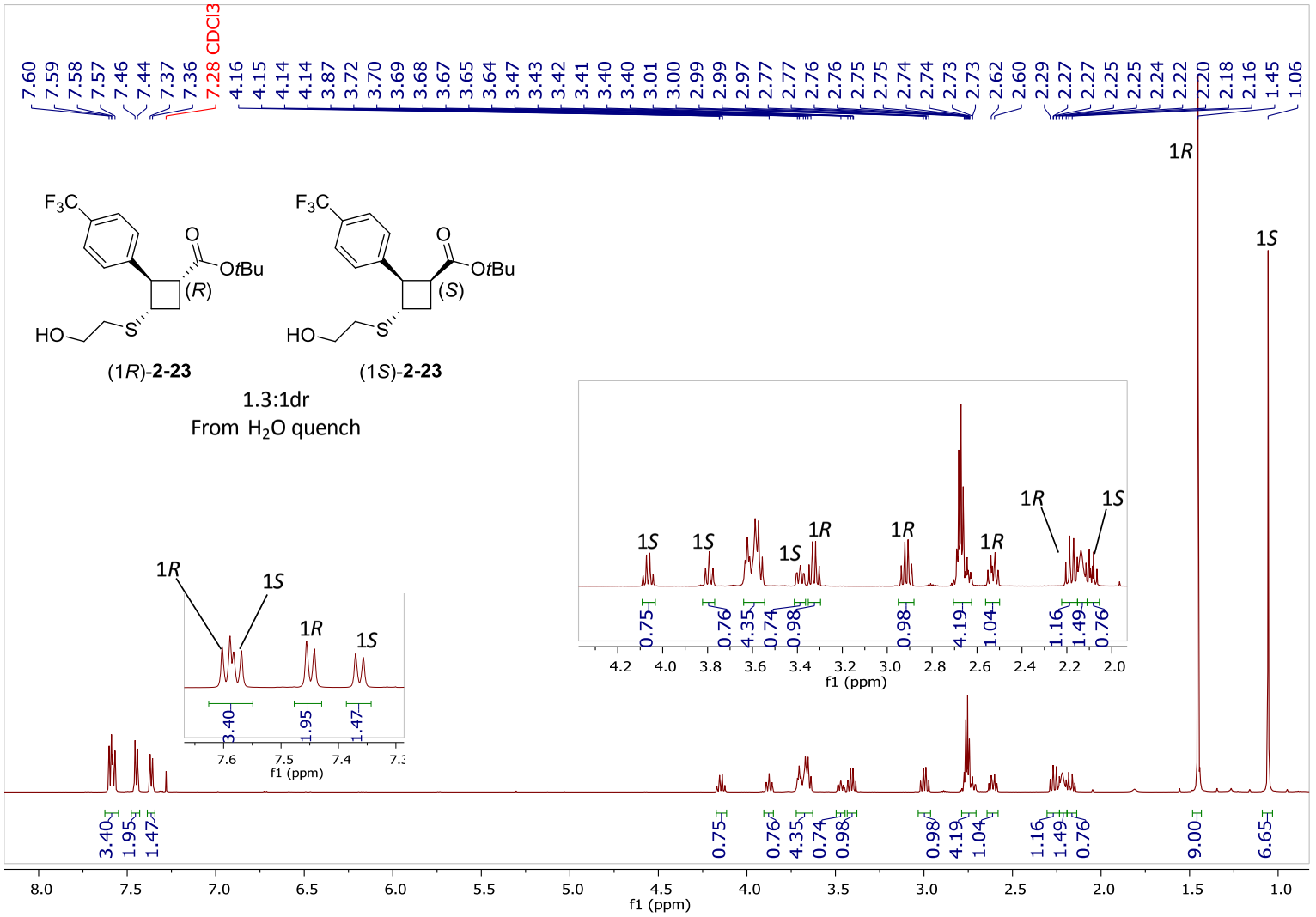

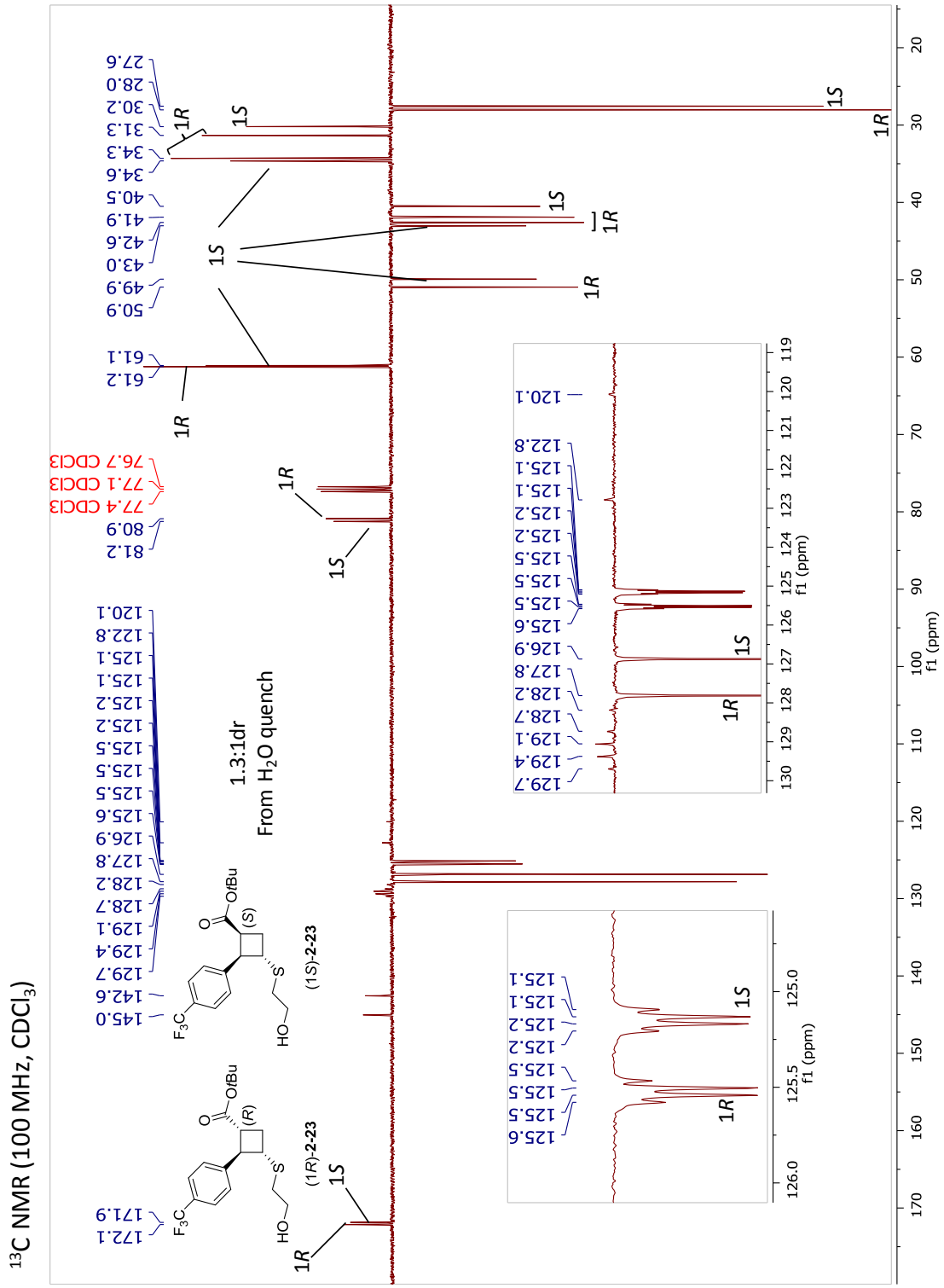
^{13}C NMR (100 MHz, CDCl$_3$)
1.3:1dr
From H$_2$O quench
(1R)-2-23
(1S)-2-23
1R
1S
f1 (ppm)

^{1}H NMR (400 MHz, $CDCl_3$)

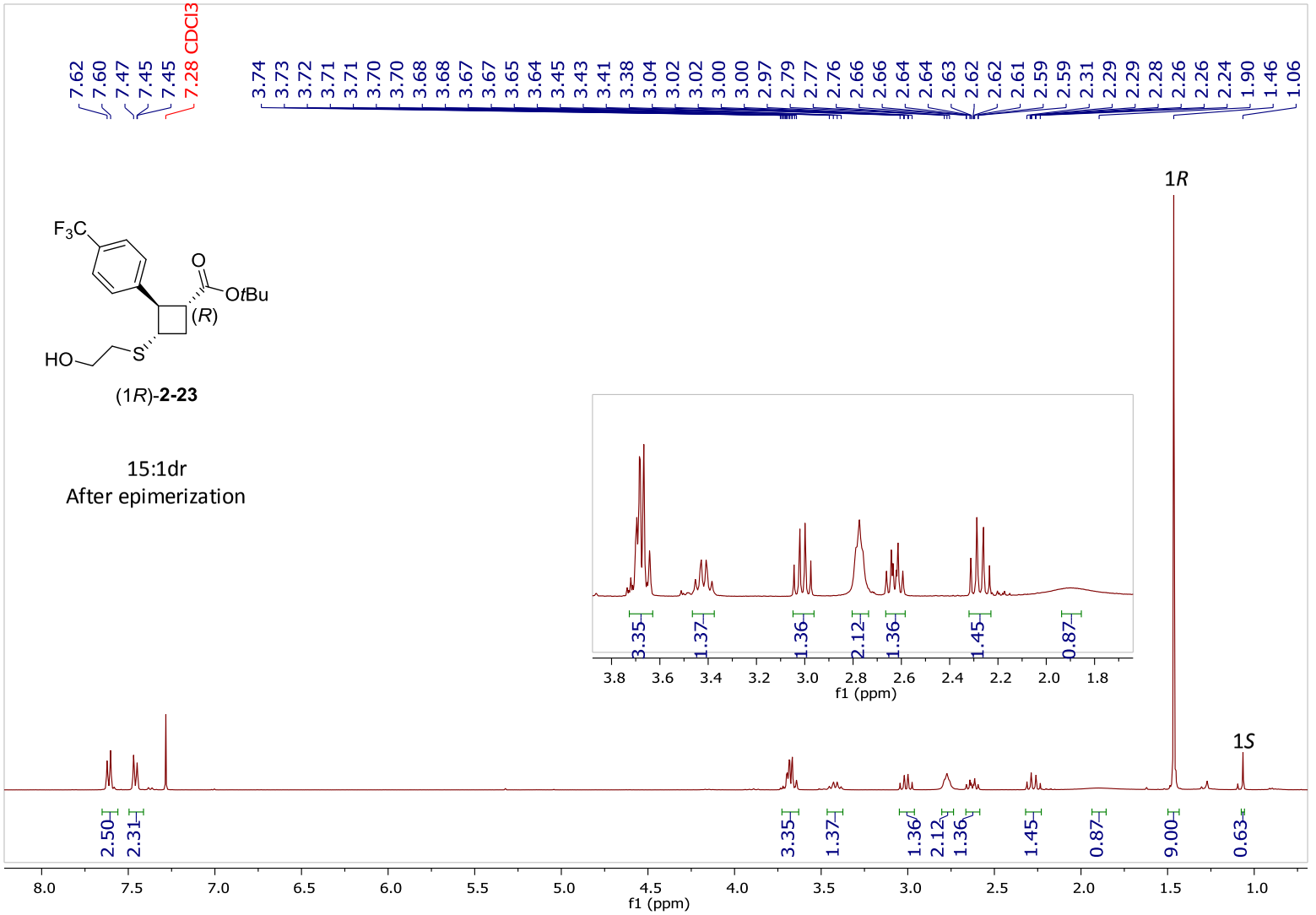

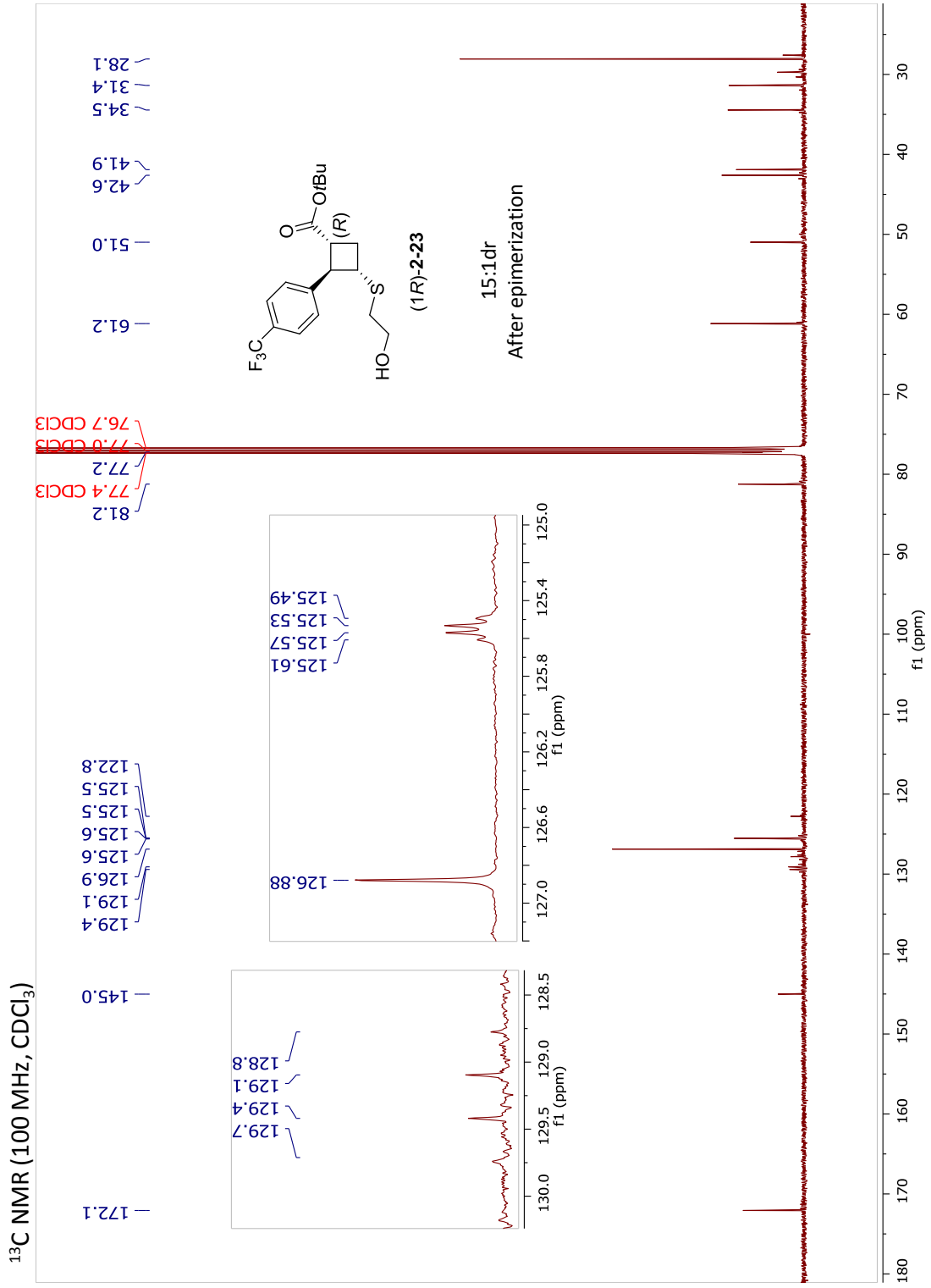
^{13}C NMR (100 MHz, $CDCl_3$)
172.1
145.0
129.4
129.1
126.9
125.6
125.6
125.5
125.5
122.8
81.2
77.4 CDCl3
77.2
76.7 CDCl3
61.2
51.0
42.6
41.9
34.5
31.4
28.1
126.88
125.61
125.57
125.53
125.49
129.7
129.4
129.1
128.8
f1 (ppm)
(1R)-2-23
15:1dr
After epimerization
OtBu
(R)
S
HO
F3C

^{19}F NMR (376 MHz, $CDCl_3$)

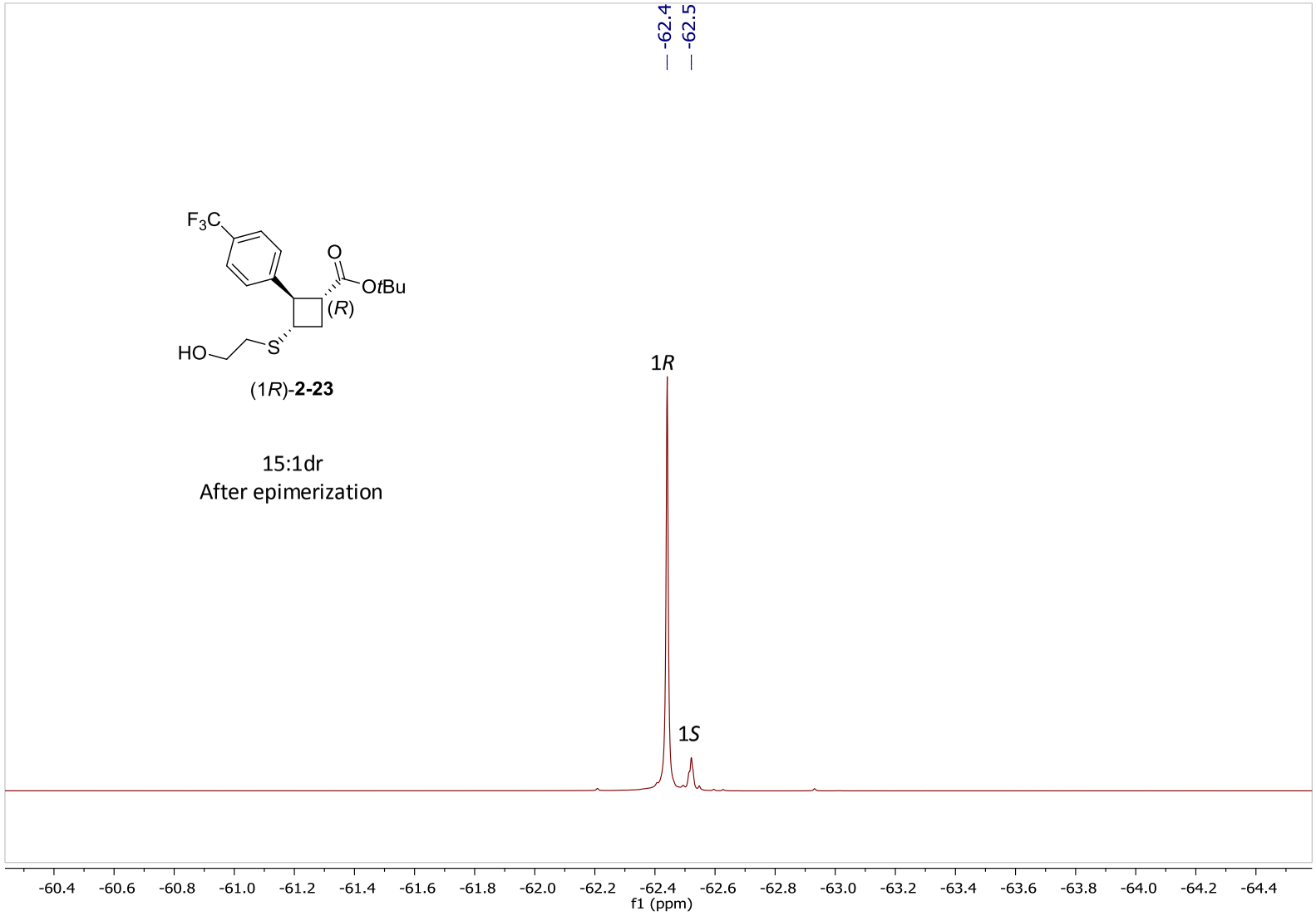

^{1}H NMR (400 MHz, $CDCl_3$)

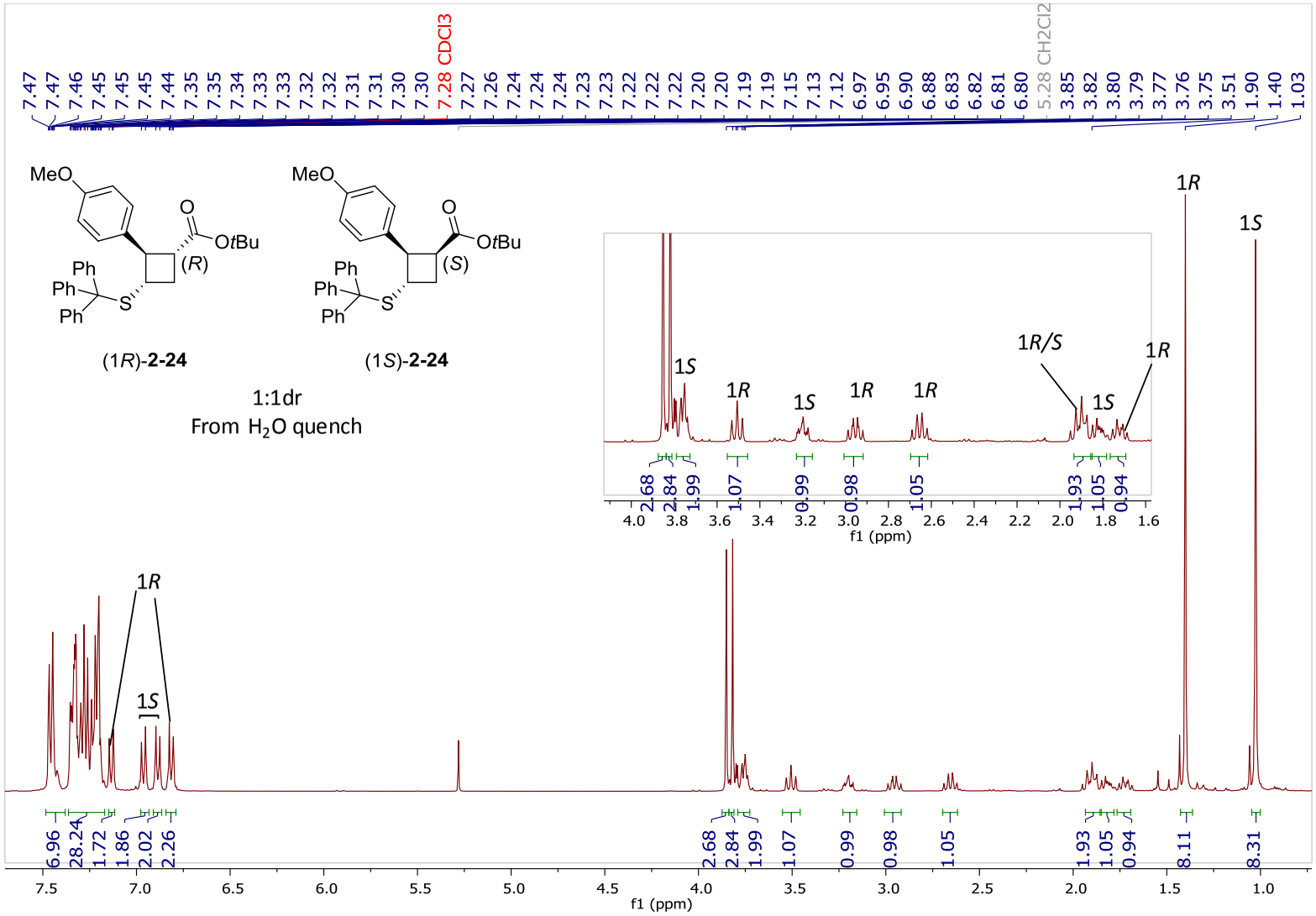

^{1}H NMR (400 MHz, $CDCl_3$)

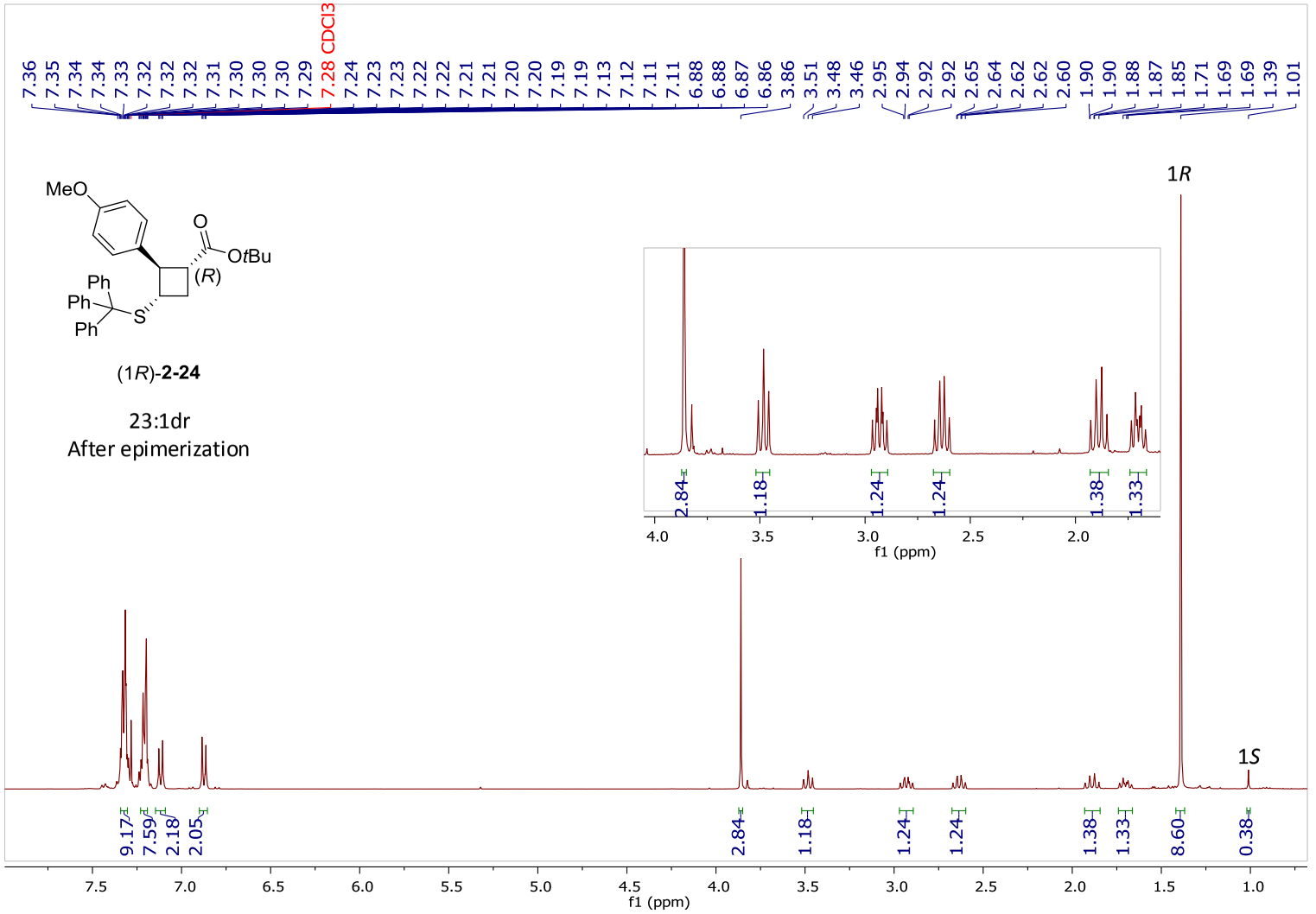

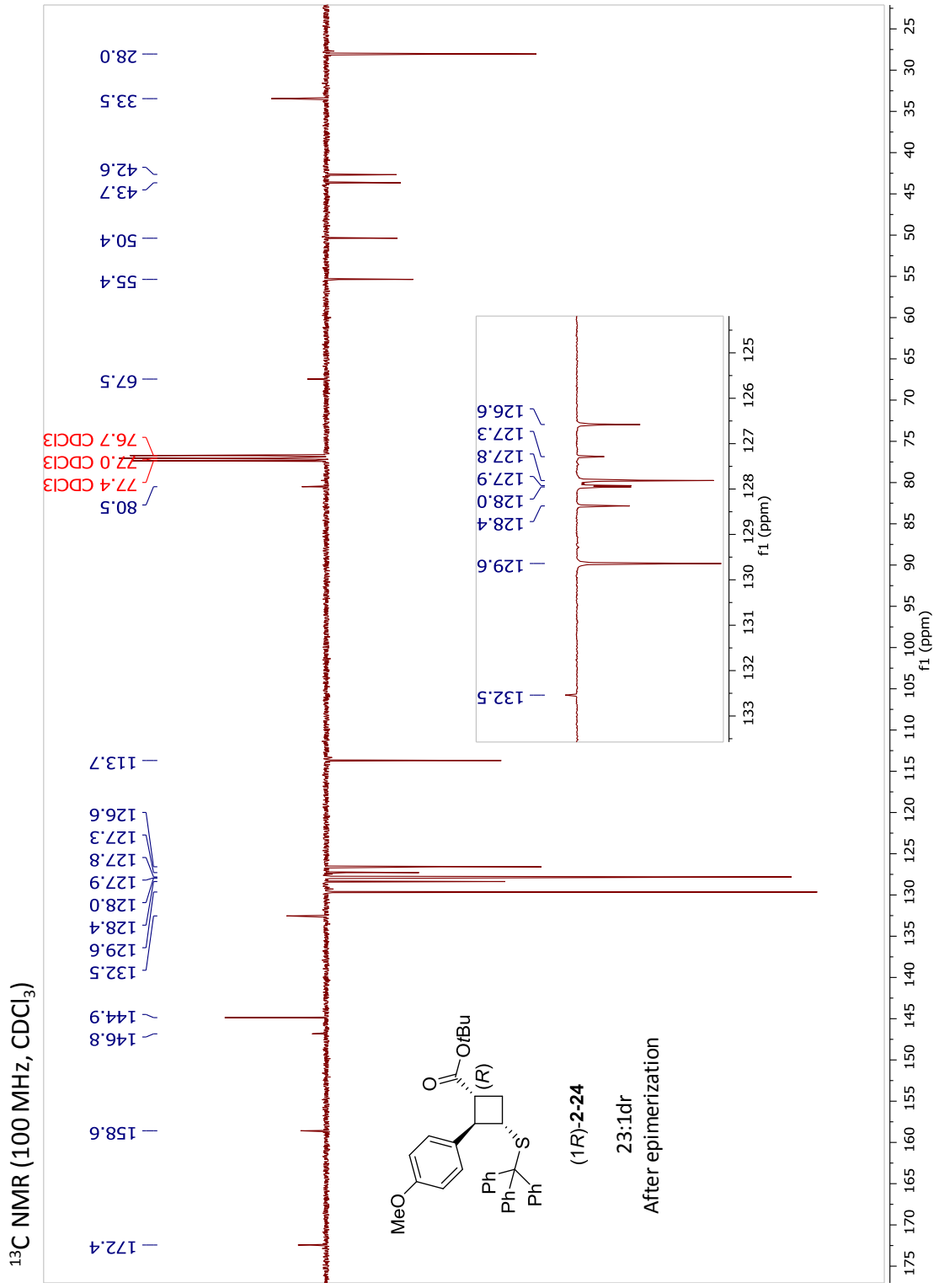
^{13}C NMR (100 MHz, $CDCl_3$)
172.4
158.6
146.8
144.9
132.5
129.6
128.4
128.0
127.9
127.8
127.3
126.6
113.7
80.5
77.4 CDCl3
77.0 CDCl3
76.7 CDCl3
67.5
55.4
50.4
43.7
42.6
33.5
28.0
MeO
Ph
Ph
Ph
S
(R)
O
OtBu
(1R)-2-24
23:1dr
After epimerization
f1 (ppm)

^{1}H NMR (400 MHz, $CDCl_3$)

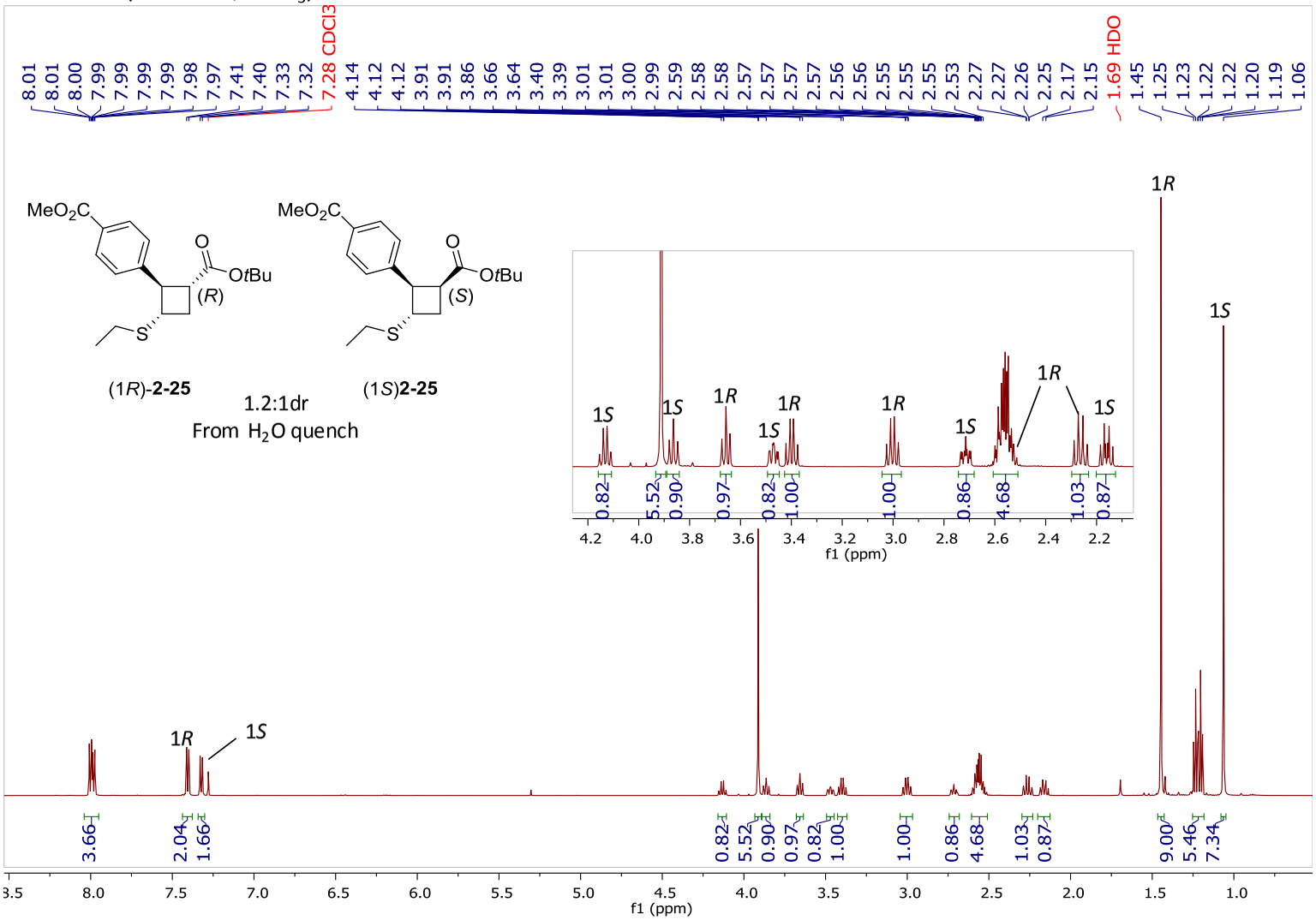

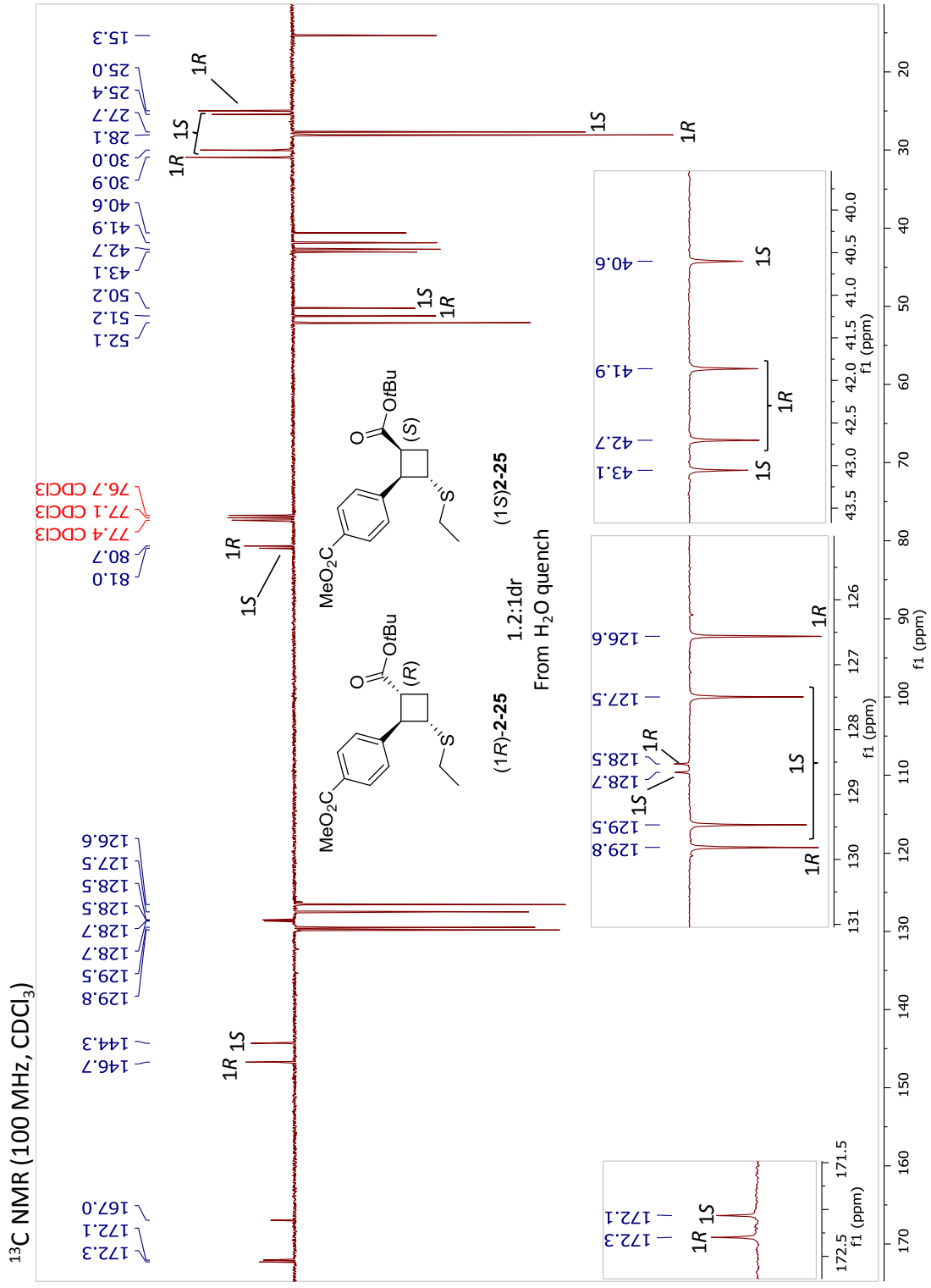
^{13}C NMR (100 MHz, $CDCl_3$)
172.3
172.1
167.0
146.7
144.3
129.8
129.5
128.7
128.7
128.5
128.5
127.5
126.6
81.0
80.7
77.4 CDCl3
77.1 CDCl3
76.7 CDCl3
52.1
51.2
50.2
43.1
42.7
41.9
40.6
30.9
30.0
28.1
27.7
25.4
25.0
15.3
1R
1S
MeO2C
OtBu
(S)
(R)
(1R)-2-25
1.2:1dr
From H2O quench
(1S)2-25
f1 (ppm)

^{1}H NMR (400 MHz, $CDCl_3$)

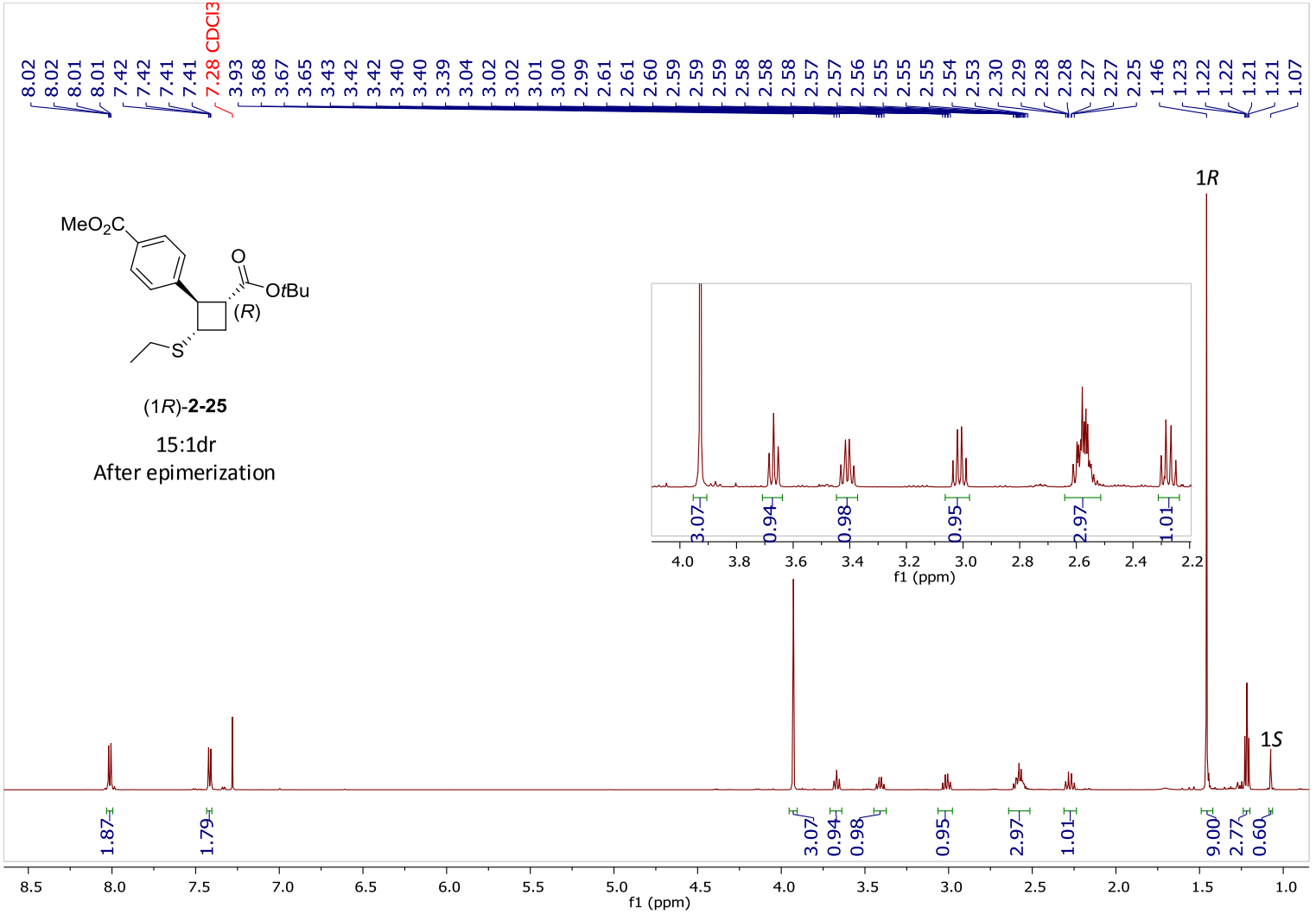

(1*R*)-**2-25**

15:1dr

After epimerization

^{13}C NMR (100 MHz, $CDCl_3$)

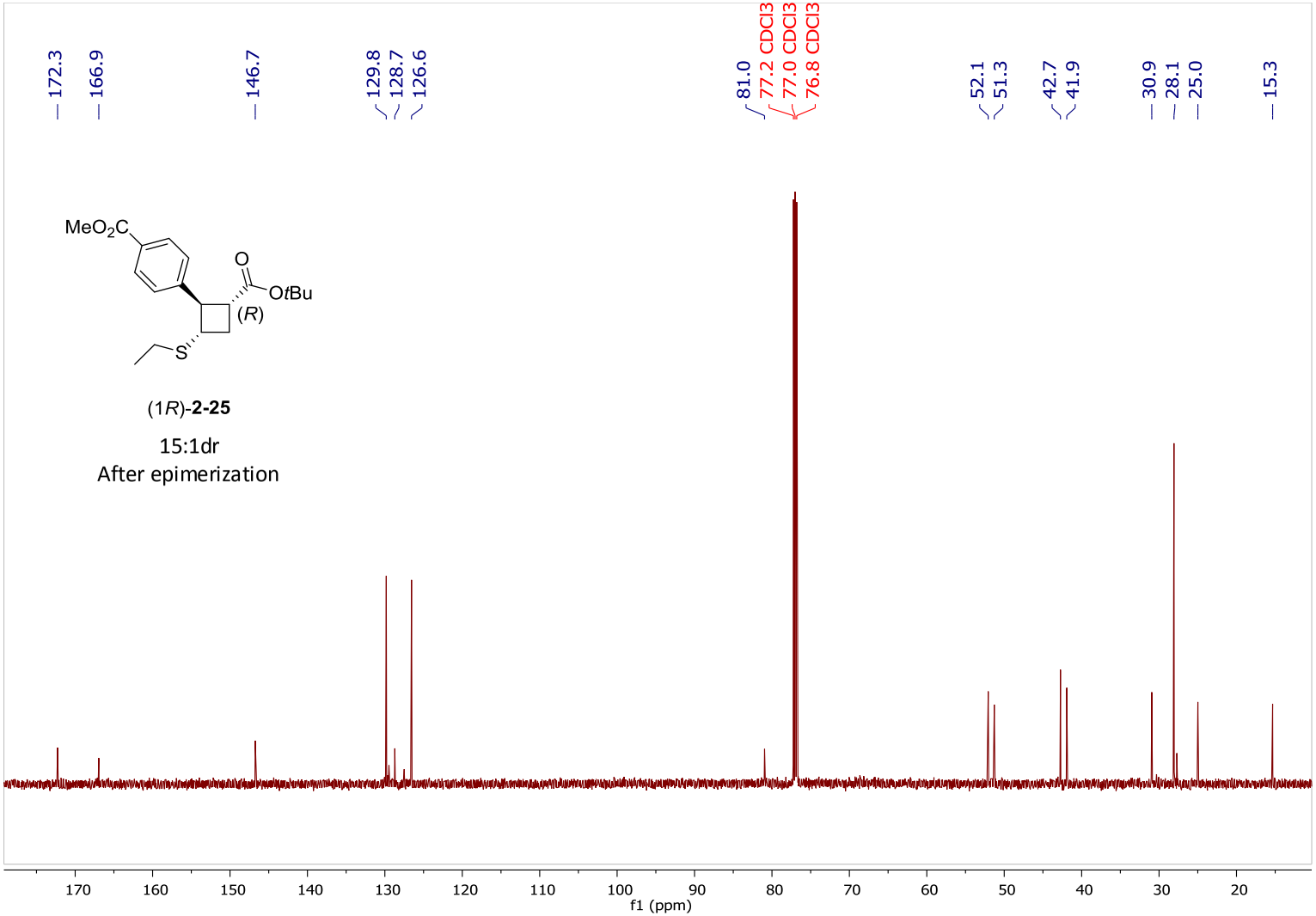

^{1}H NMR (400 MHz, $CDCl_3$)

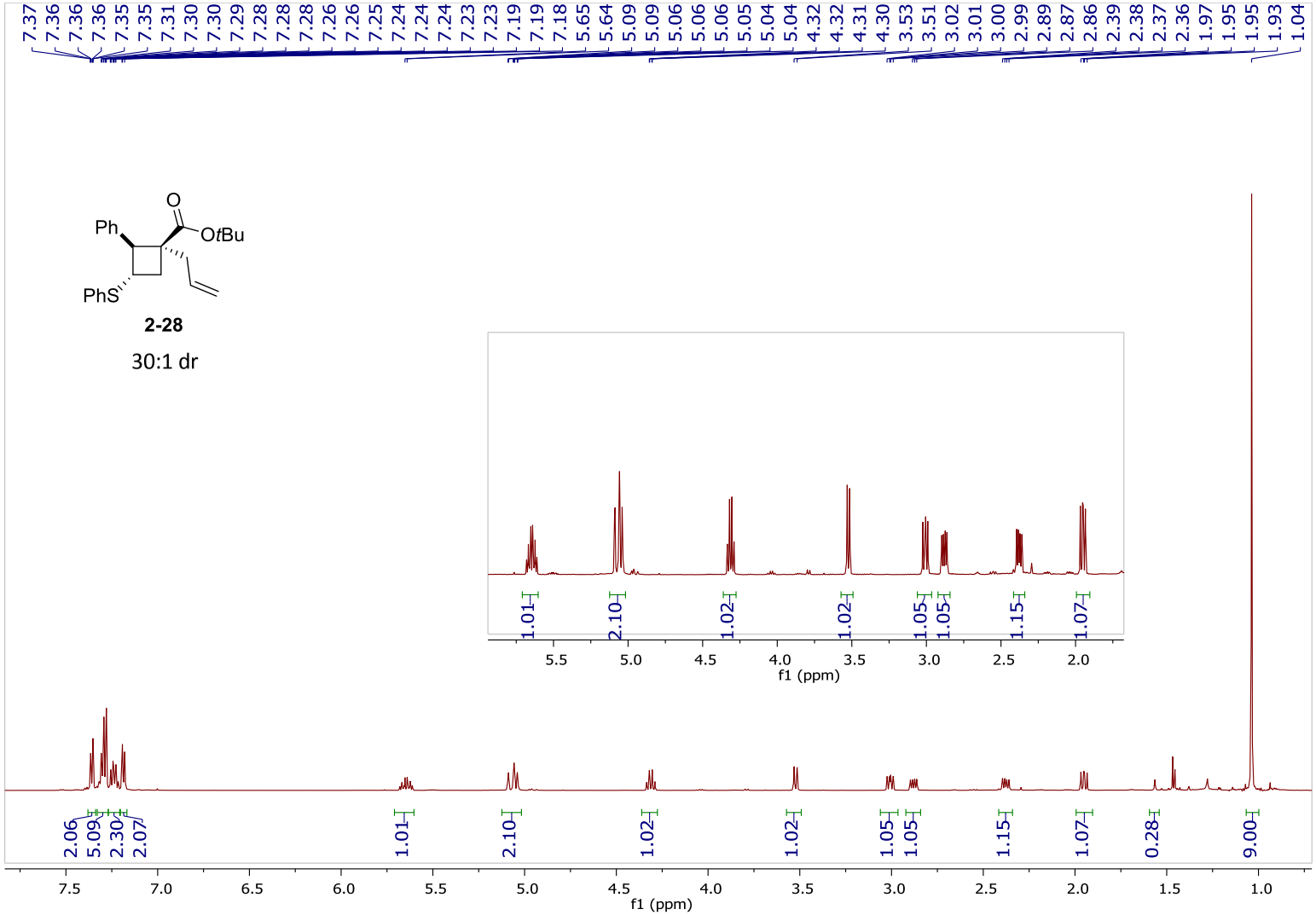

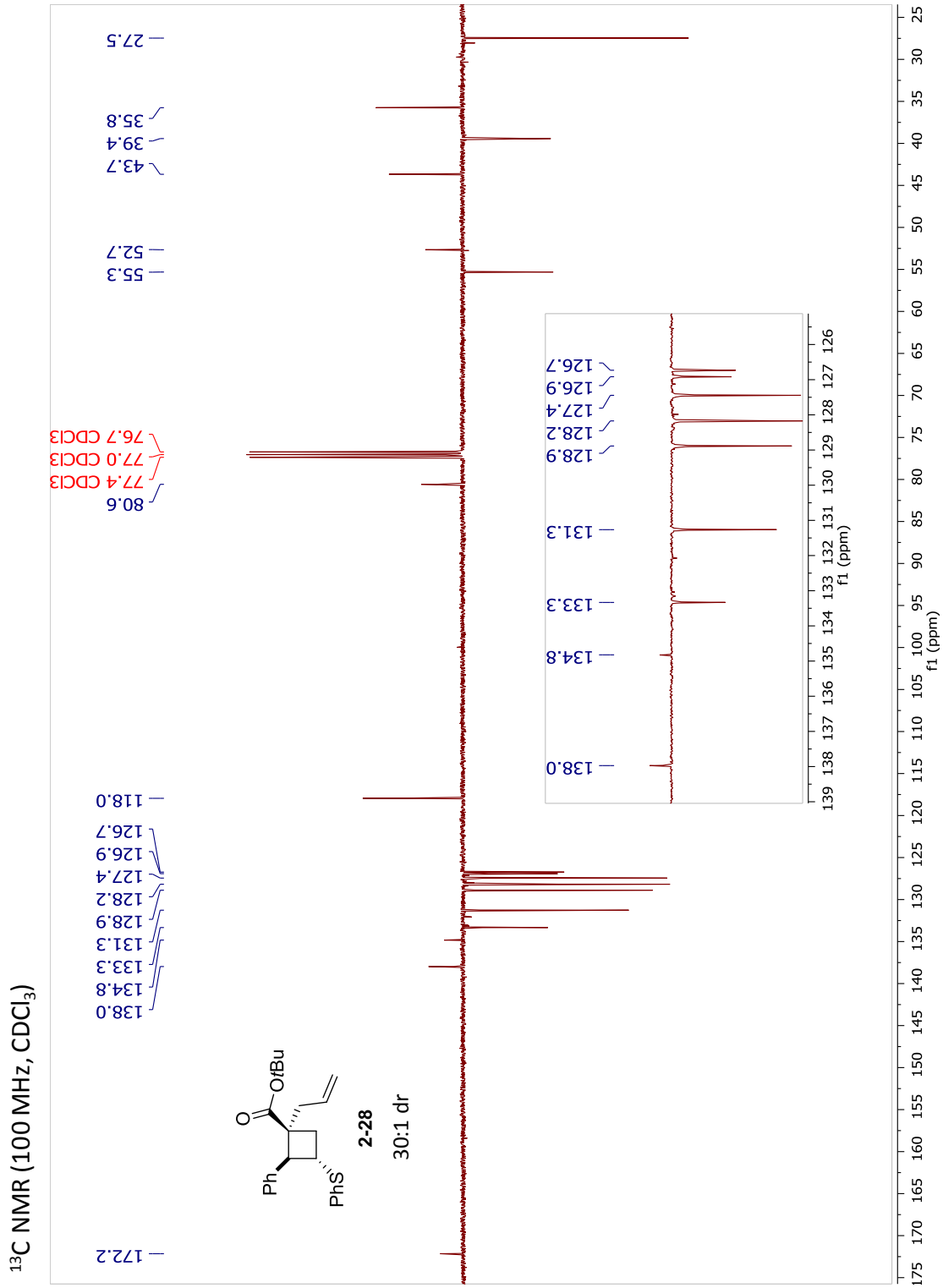
^{13}C NMR (100 MHz, $CDCl_3$)
172.2
138.0
134.8
133.3
131.3
128.9
128.2
127.4
126.9
126.7
118.0
80.6
77.4 CDCl3
77.0 CDCl3
76.7 CDCl3
55.3
52.7
43.7
39.4
35.8
27.5
O
OtBu
Ph
PhS
2-28
30:1 dr
f1 (ppm)

^{1}H NMR (400 MHz, $CDCl_3$)

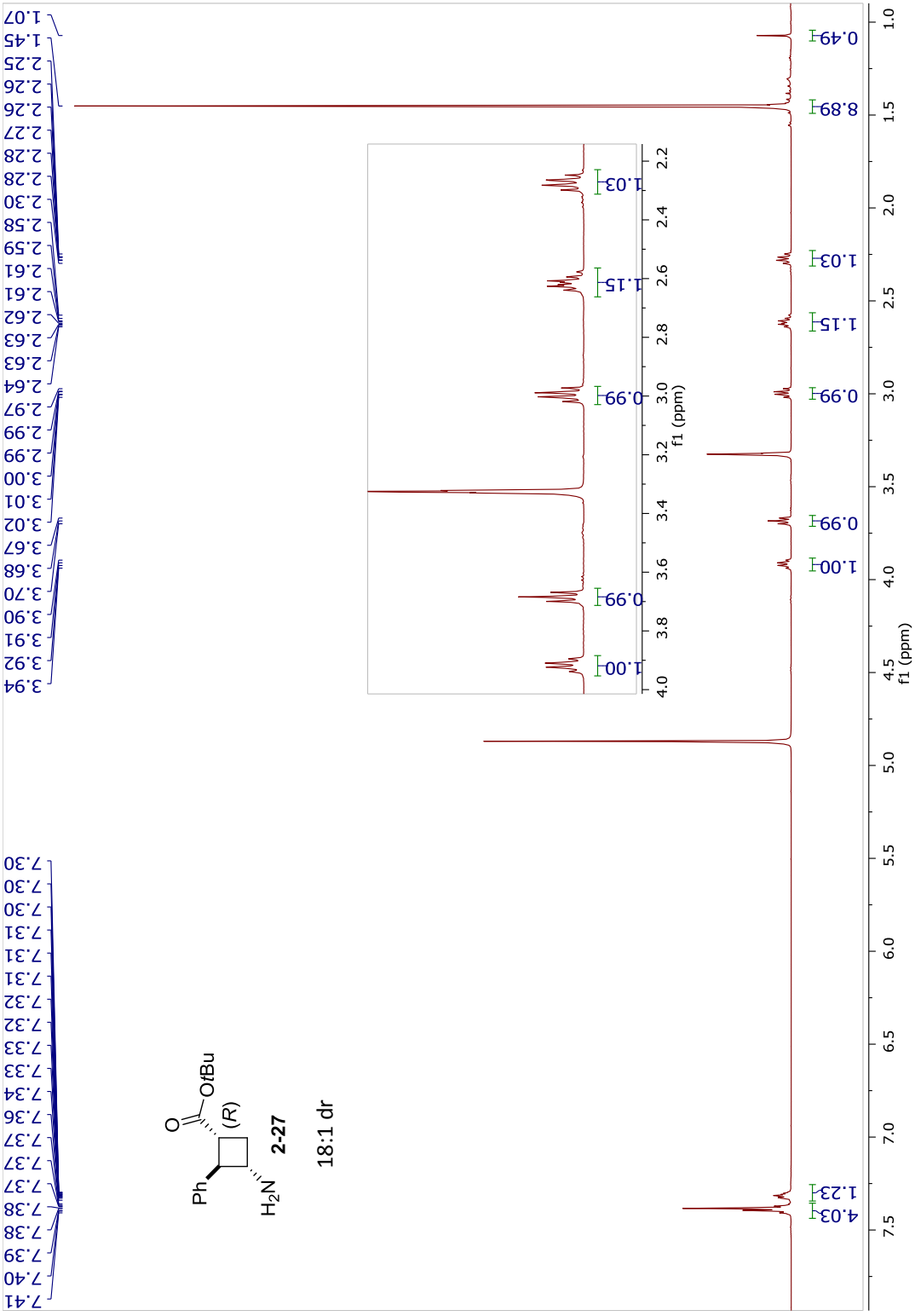

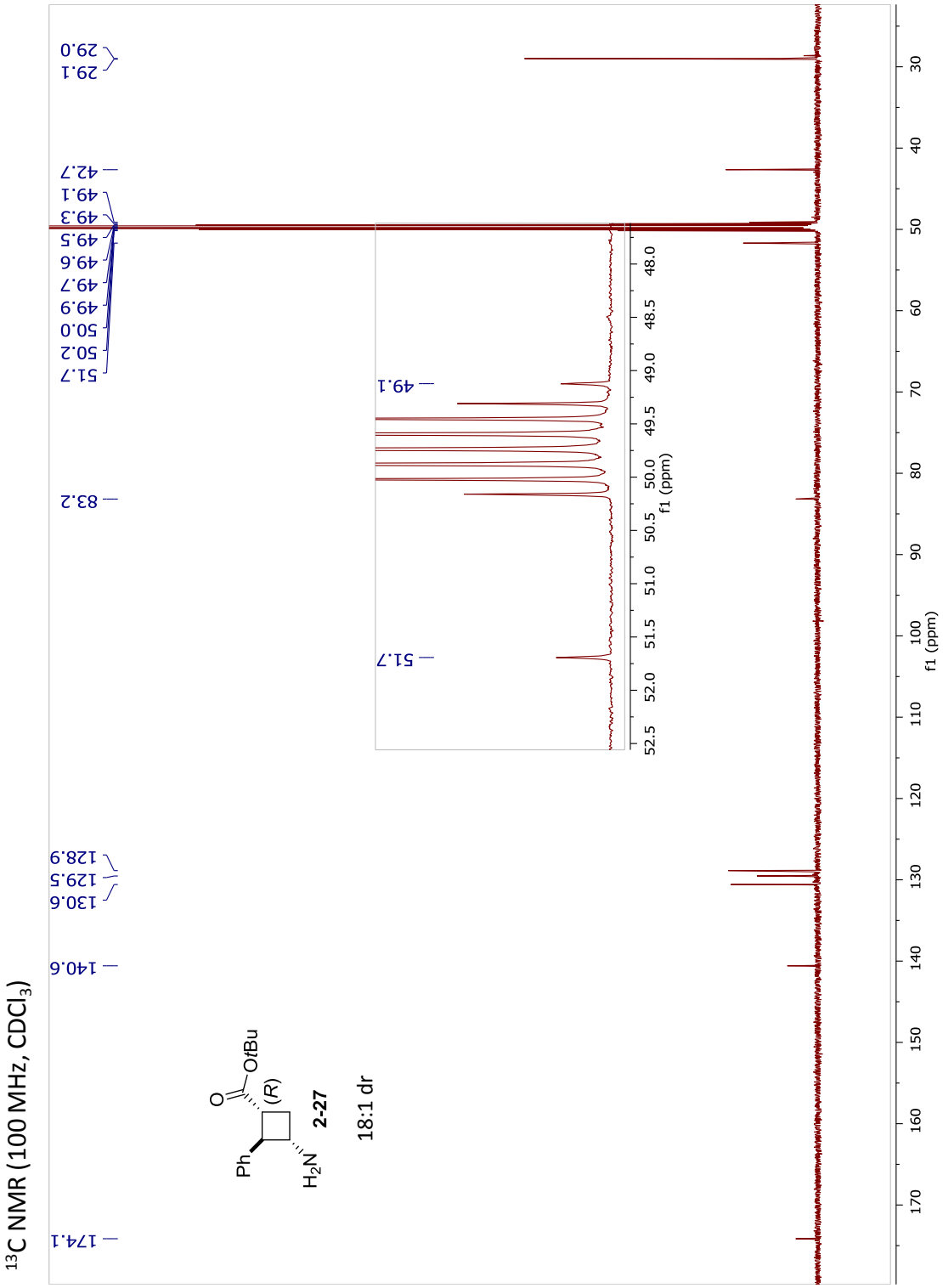
^{13}C NMR (100 MHz, CDCl$_3$)
174.1
140.6
130.6
129.5
128.9
83.2
51.7
50.2
50.0
49.9
49.7
49.6
49.5
49.3
49.1
42.7
29.1
29.0
49.1
51.7
f1 (ppm)
O
OtBu
(R)
Ph
H2N
2-27
18:1 dr

^{1}H NMR (400 MHz, $CDCl_3$)

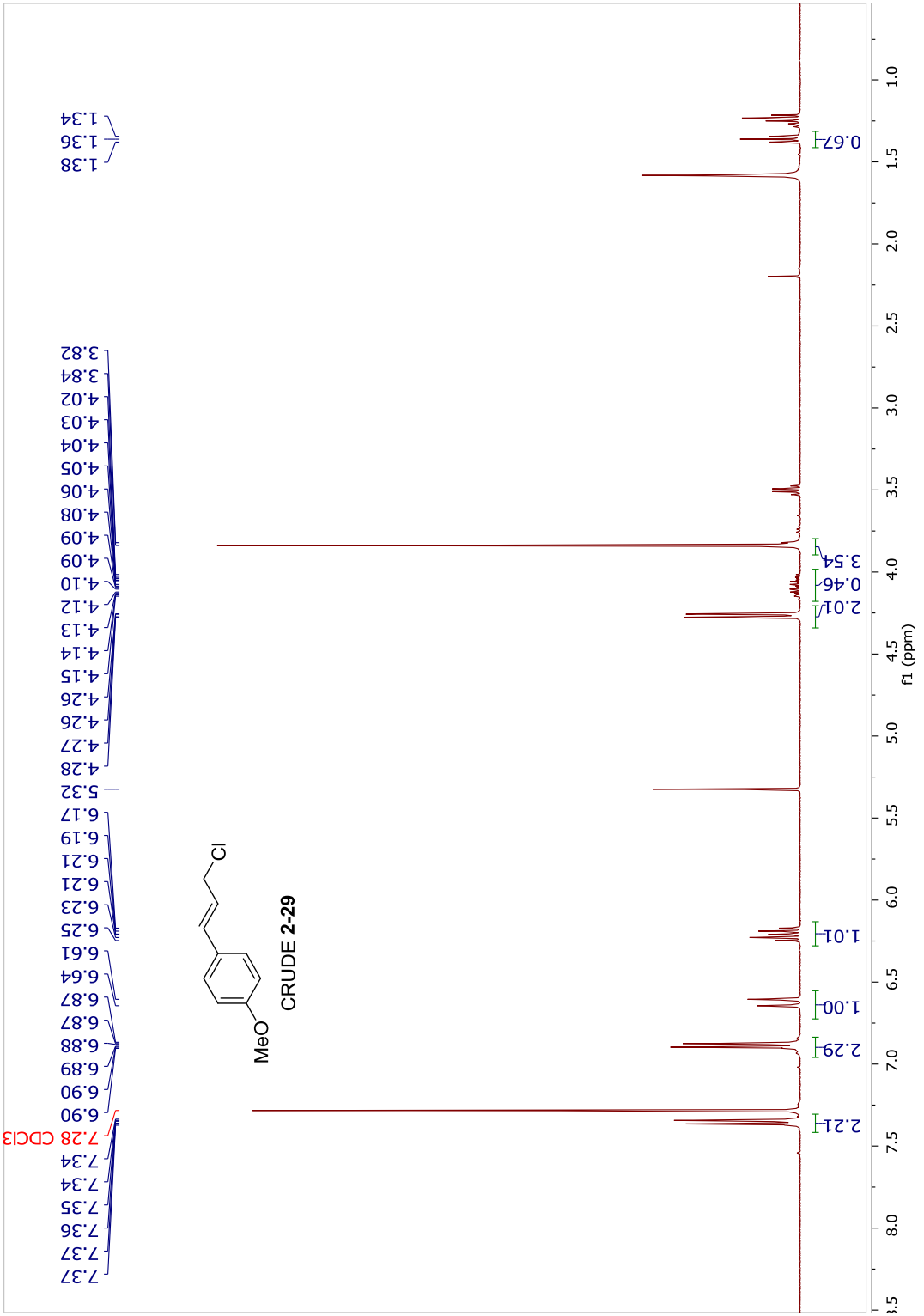

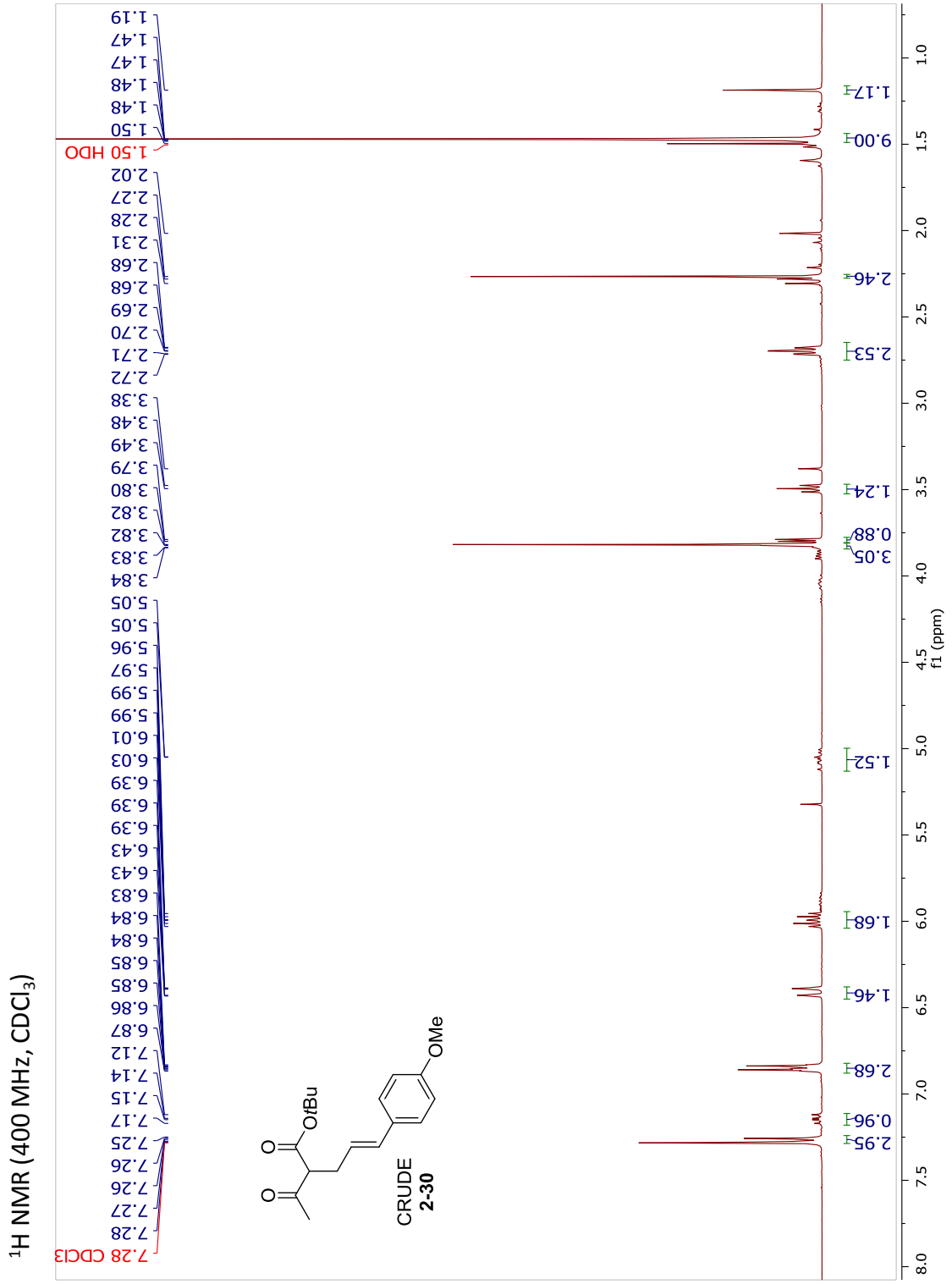
^{1}H NMR (400 MHz, $CDCl_3$)
CRUDE
2-30
OtBu
OMe
f1 (ppm)

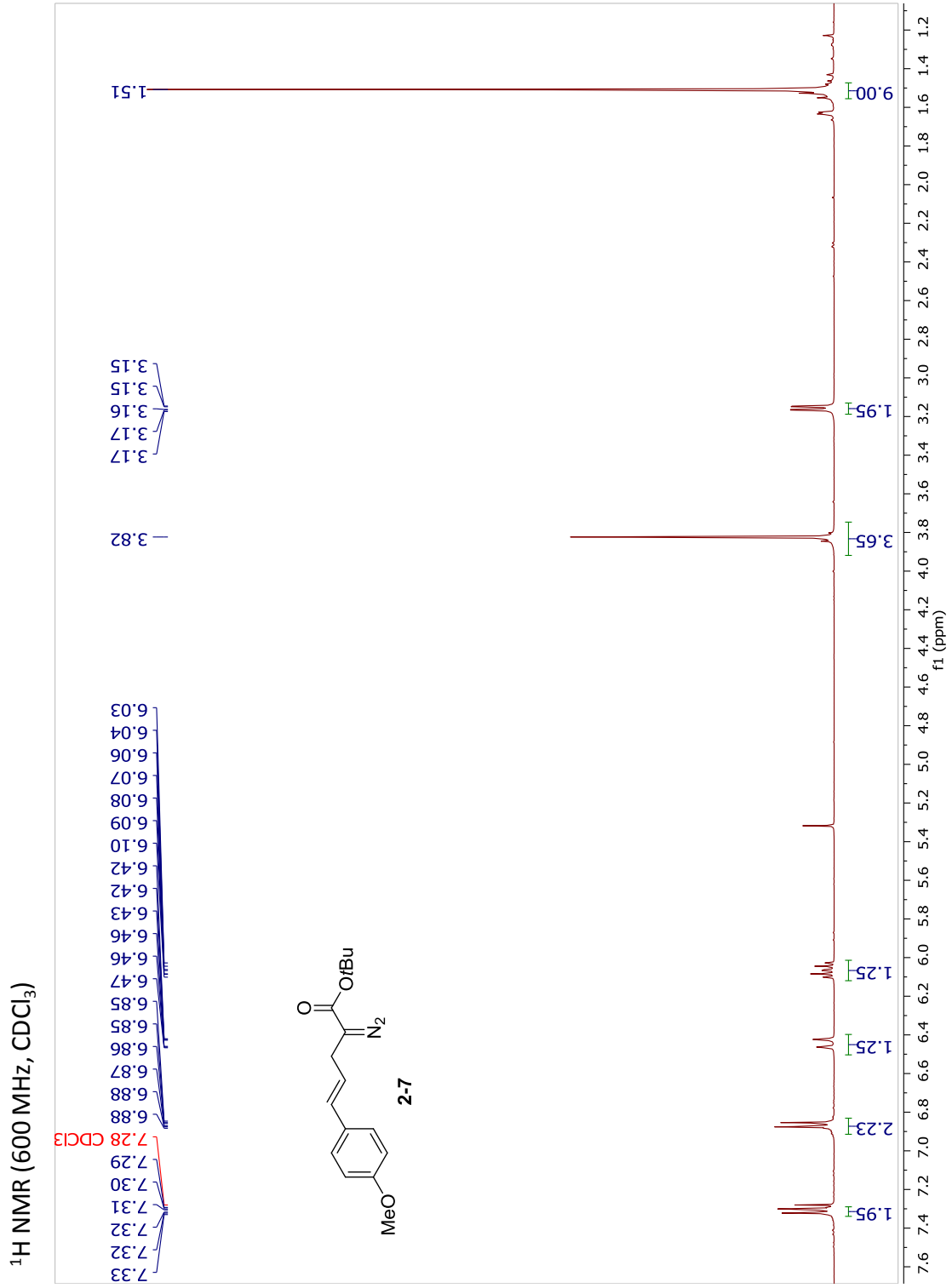
^{1}H NMR (600 MHz, $CDCl_3$)
7.33
7.32
7.32
7.31
7.30
7.29
7.28 CDCl3
6.88
6.88
6.87
6.86
6.85
6.85
6.47
6.46
6.46
6.43
6.42
6.42
6.10
6.09
6.08
6.07
6.06
6.04
6.03
3.82
3.17
3.17
3.16
3.15
3.15
1.51
O
OtBu
N2
MeO
2-7
9.00
1.95
3.65
1.95
1.25
1.25
2.23
1.95
f1 (ppm)

^{13}C NMR (100 MHz, $CDCl_3$)

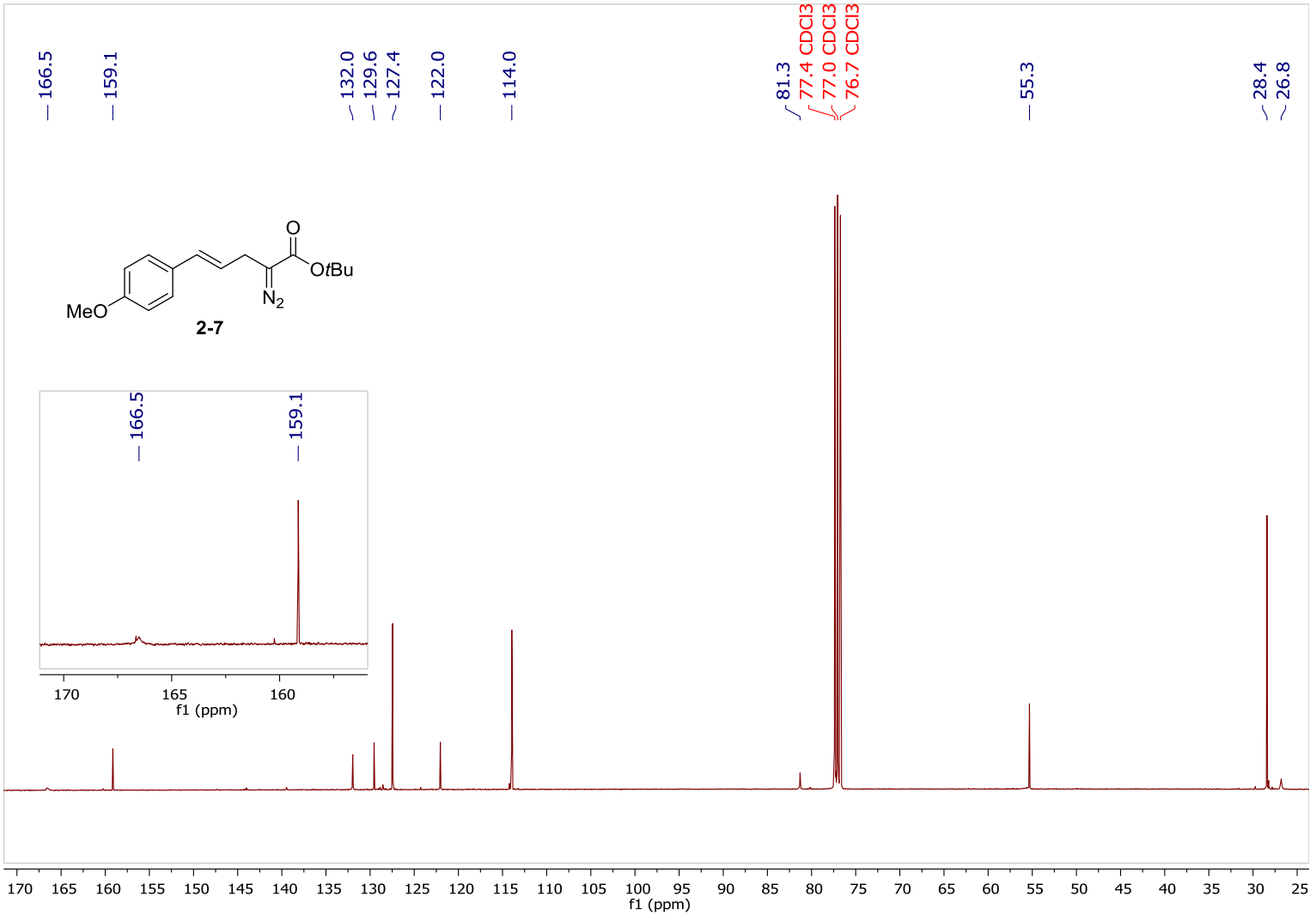

^{1}H NMR (600 MHz, $CDCl_3$)

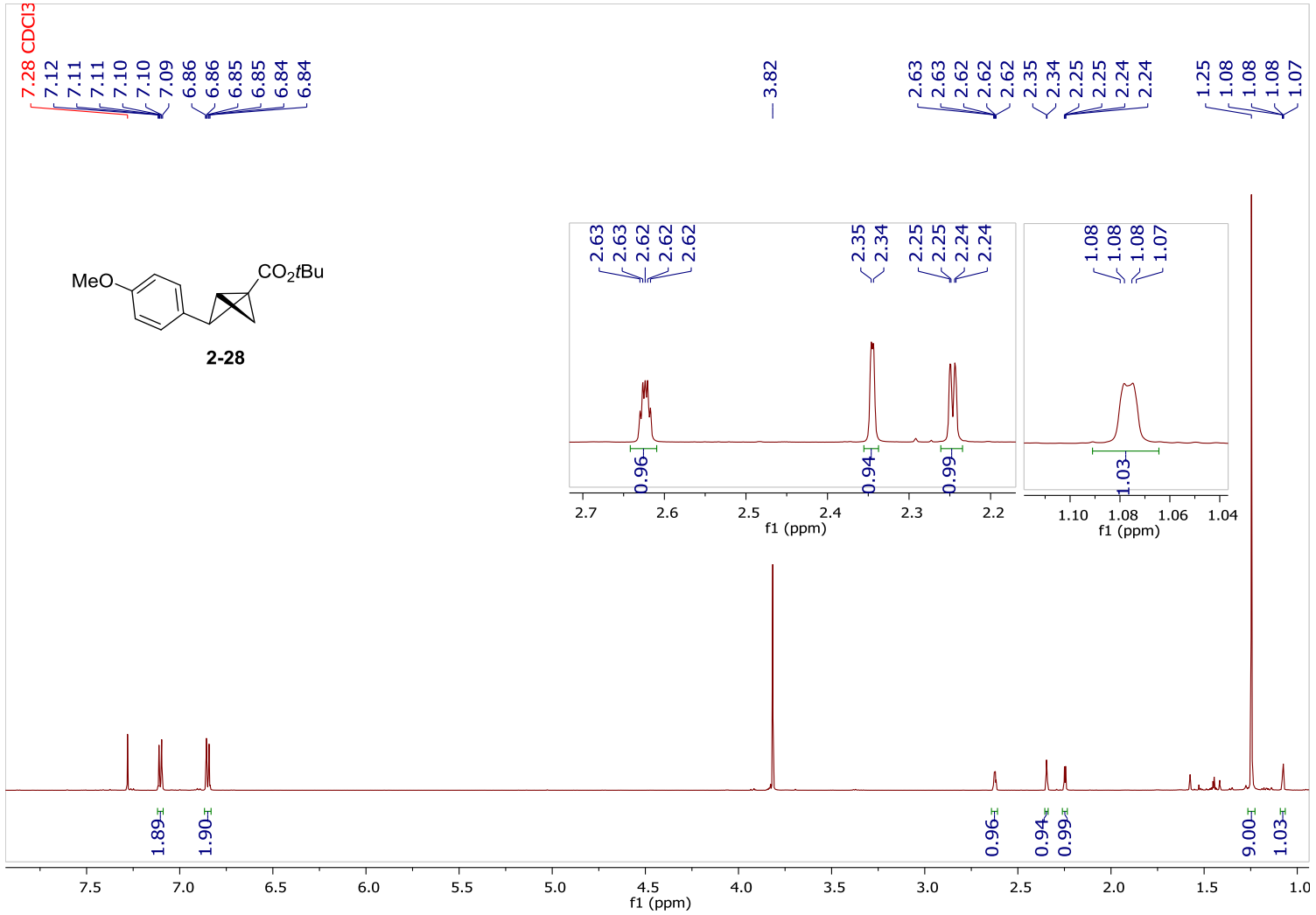

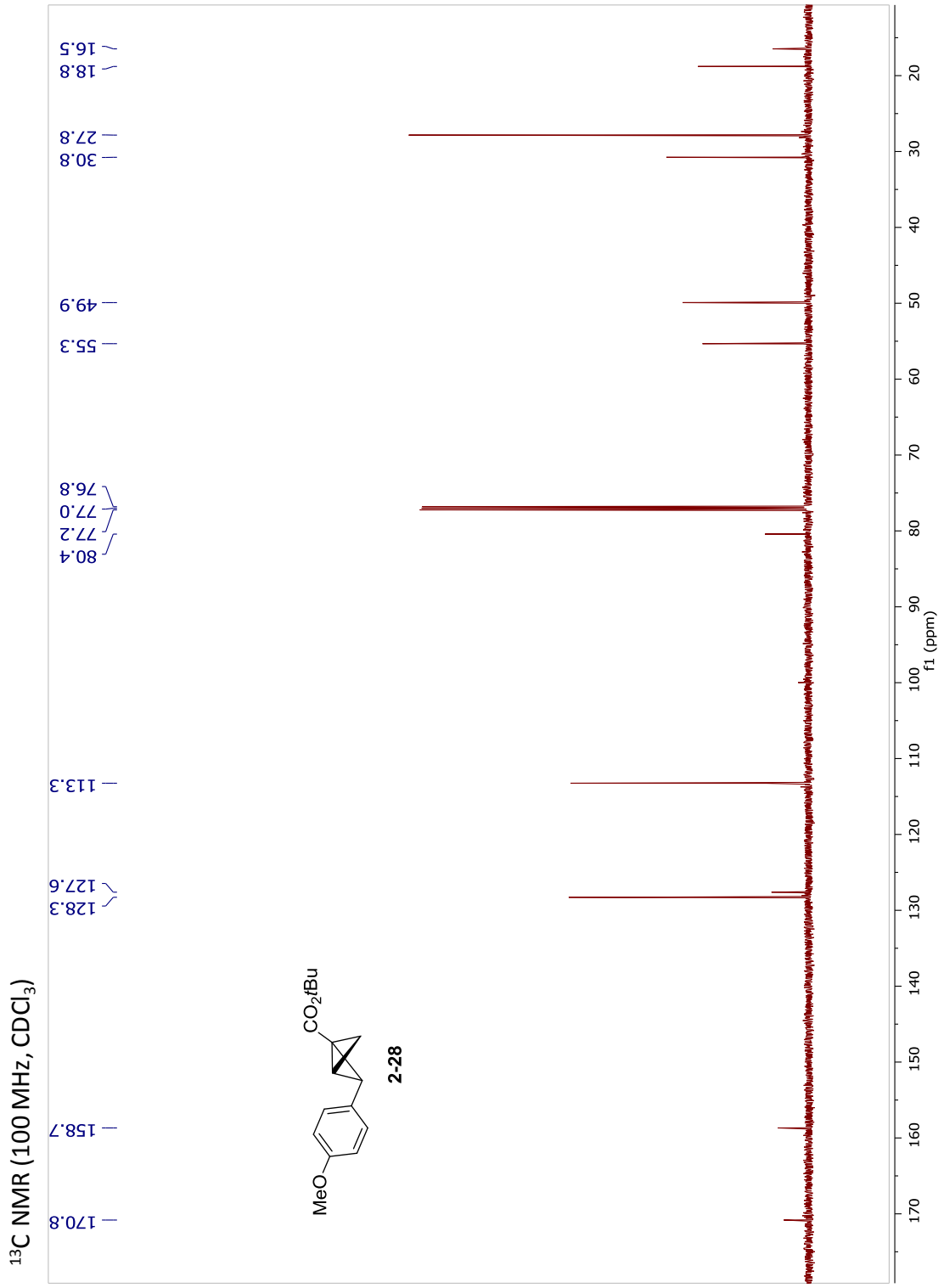
^{13}C NMR (100 MHz, CDCl$_3$)
170.8
158.7
128.3
127.6
113.3
80.4
77.2
77.0
76.8
55.3
49.9
30.8
27.8
18.8
16.5
MeO
CO$_2$tBu
2-28
f1 (ppm)

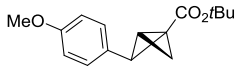

2-28

PDA Ch1 220 nm

Peak#	Ret. Time	Area	Area %
1	19.364	2930314	50.276
2	23.053	2898168	49.724
Total		5828482	100.000

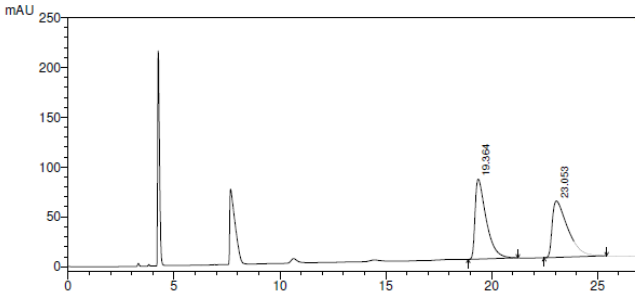

Peak#	Ret. Time	Area %
1	19.764	6.720
2	23.401	93.280
Total		100.000

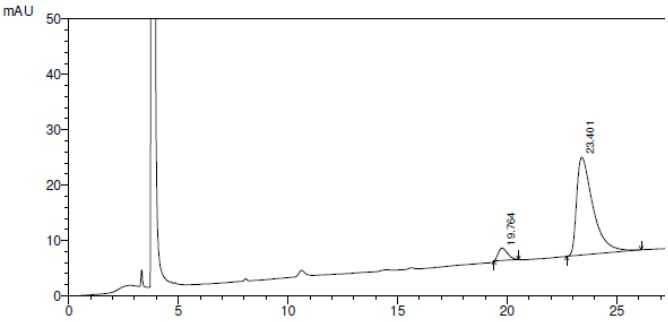

Appendix C

SPECTRAL DATA FOR CHAPTER 3

^{1}H NMR (600 MHz, $CDCl_3$)

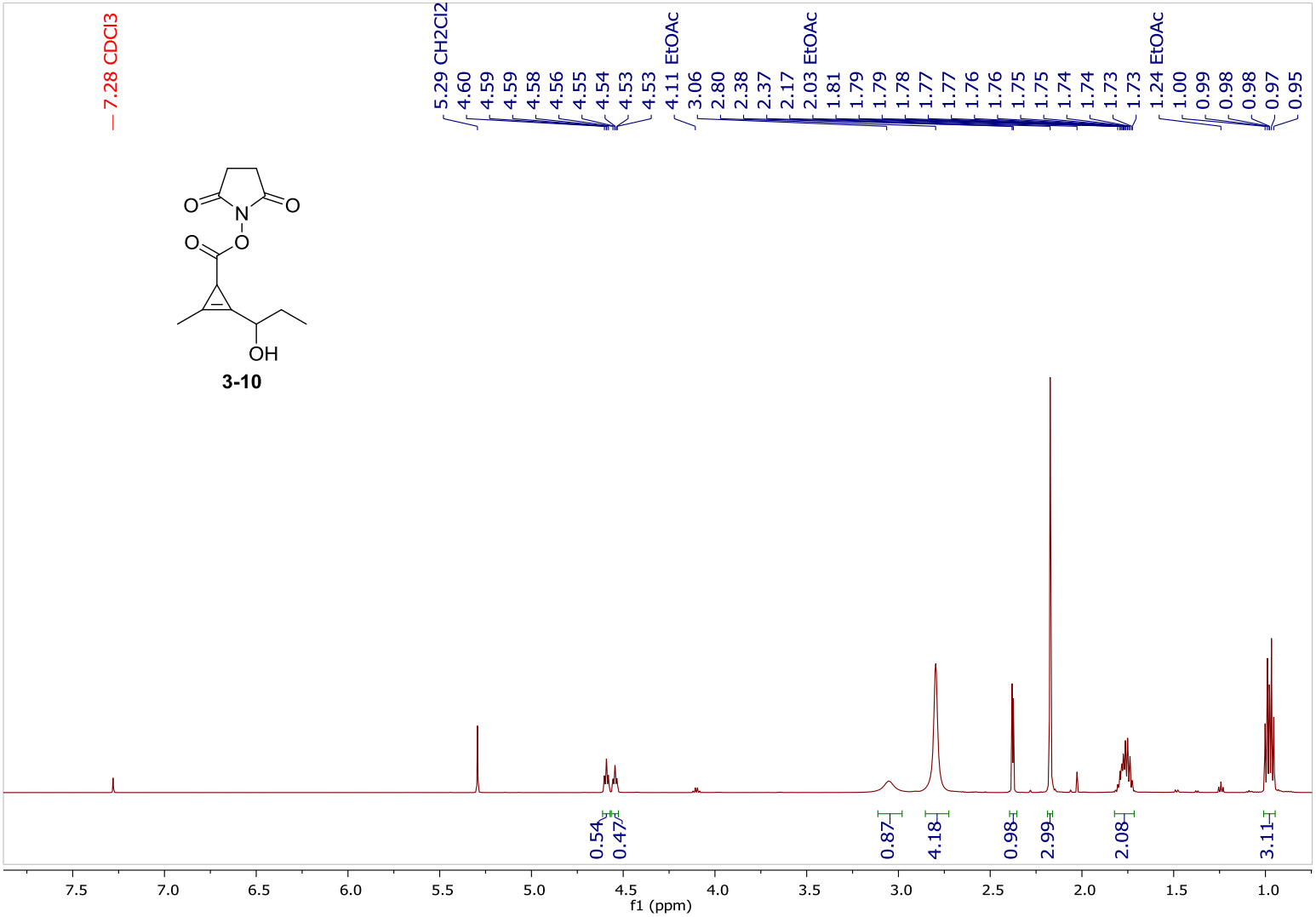

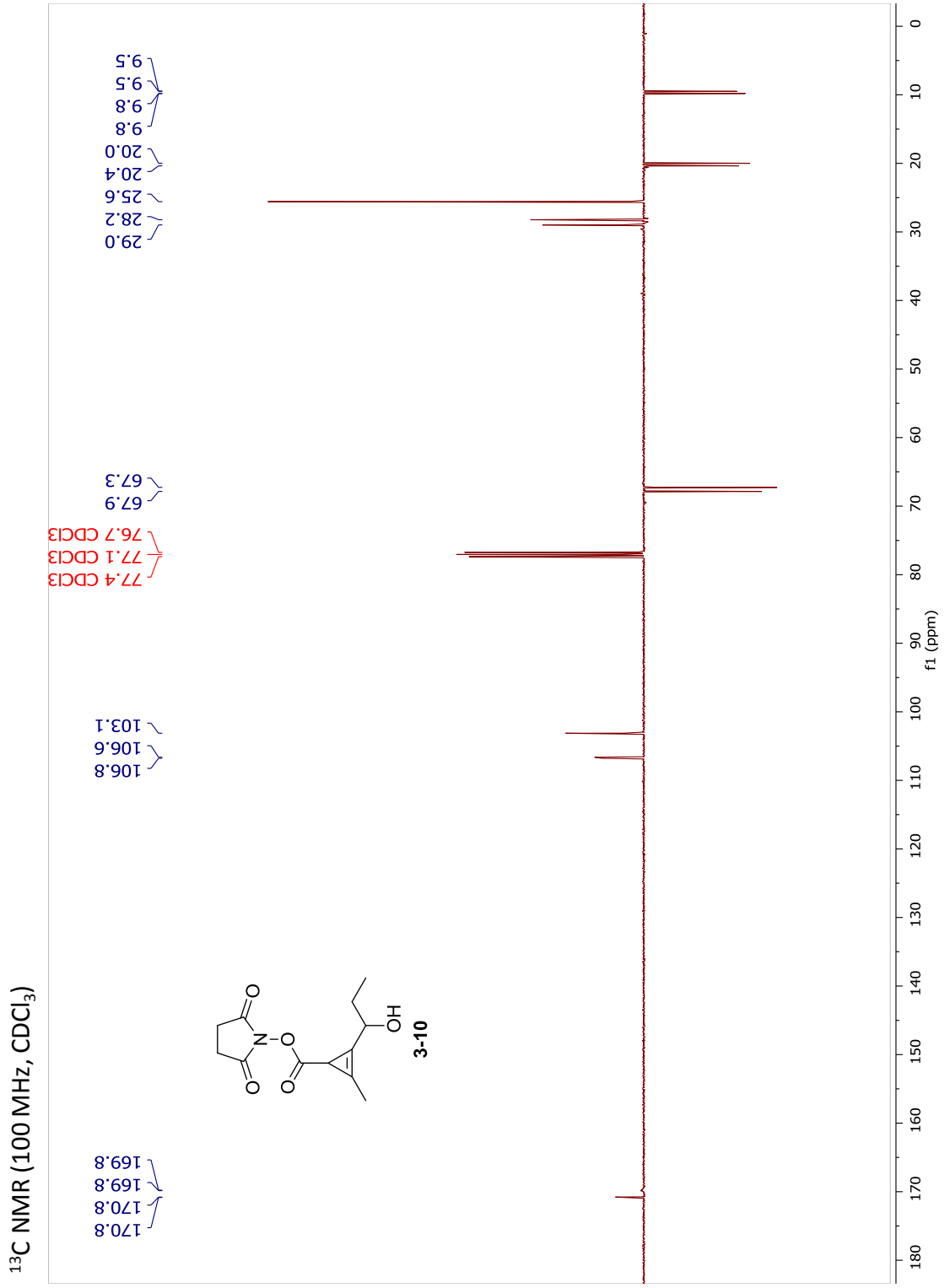
^{13}C NMR (100 MHz, $CDCl_3$)
170.8
170.8
169.8
169.8
106.8
106.6
103.1
77.4 CDCl3
77.1 CDCl3
76.7 CDCl3
67.9
67.3
29.0
28.2
25.6
20.4
20.0
9.8
9.8
9.5
9.5
3-10
f1 (ppm)

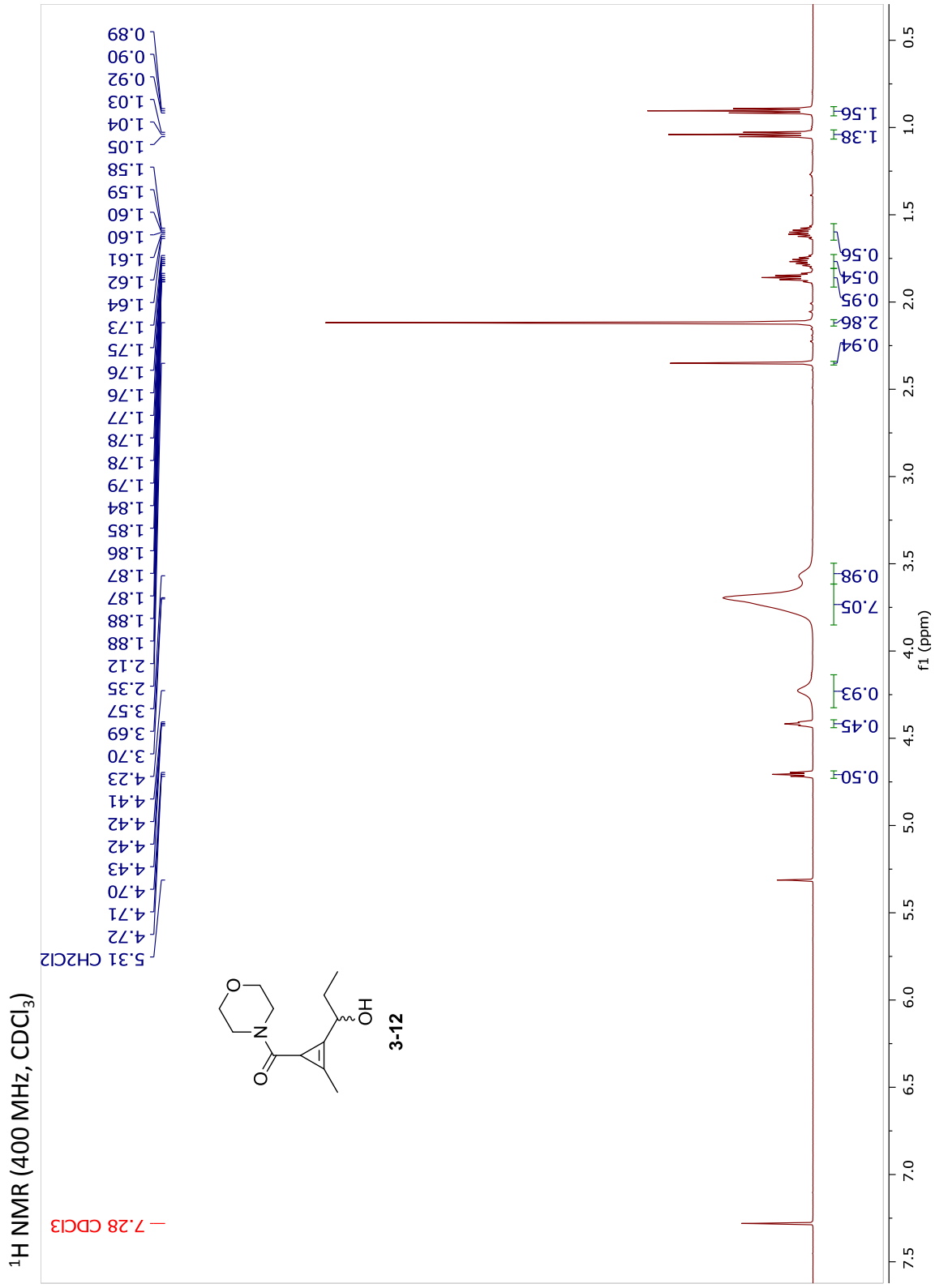
^{1}H NMR (400 MHz, CDCl$_3$)
7.28 CDCl3
5.31 CH2Cl2
4.72
4.71
4.70
4.43
4.42
4.42
4.41
4.23
3.70
3.69
3.57
2.35
2.12
1.88
1.88
1.87
1.87
1.86
1.85
1.84
1.79
1.78
1.78
1.77
1.76
1.76
1.75
1.73
1.64
1.62
1.61
1.60
1.60
1.59
1.58
1.05
1.04
1.03
0.92
0.90
0.89
O
N
O
OH
3-12
0.50
0.45
0.93
7.05
0.98
0.94
2.86
0.95
0.54
0.56
1.38
1.56
7.5
7.0
6.5
6.0
5.5
5.0
4.5
4.0
3.5
3.0
2.5
2.0
1.5
1.0
0.5
f1 (ppm)

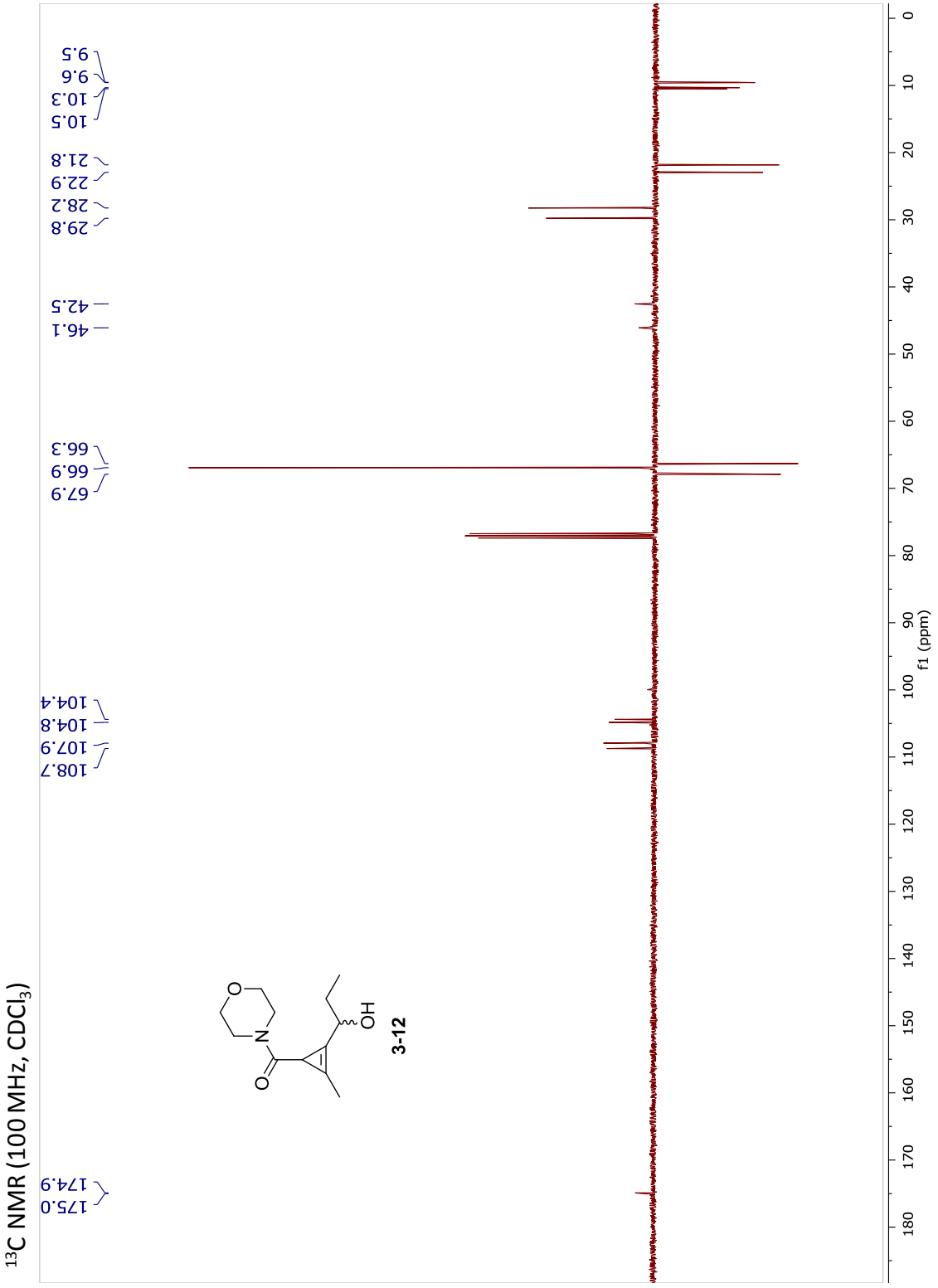
^{13}C NMR (100 MHz, $CDCl_3$)
175.0
174.9
108.7
107.9
104.8
104.4
67.9
66.9
66.3
46.1
42.5
29.8
28.2
22.9
21.8
10.5
10.3
9.6
9.5
O
N
O
OH
3-12
f1 (ppm)

^{1}H NMR (400 MHz, $CDCl_3$)

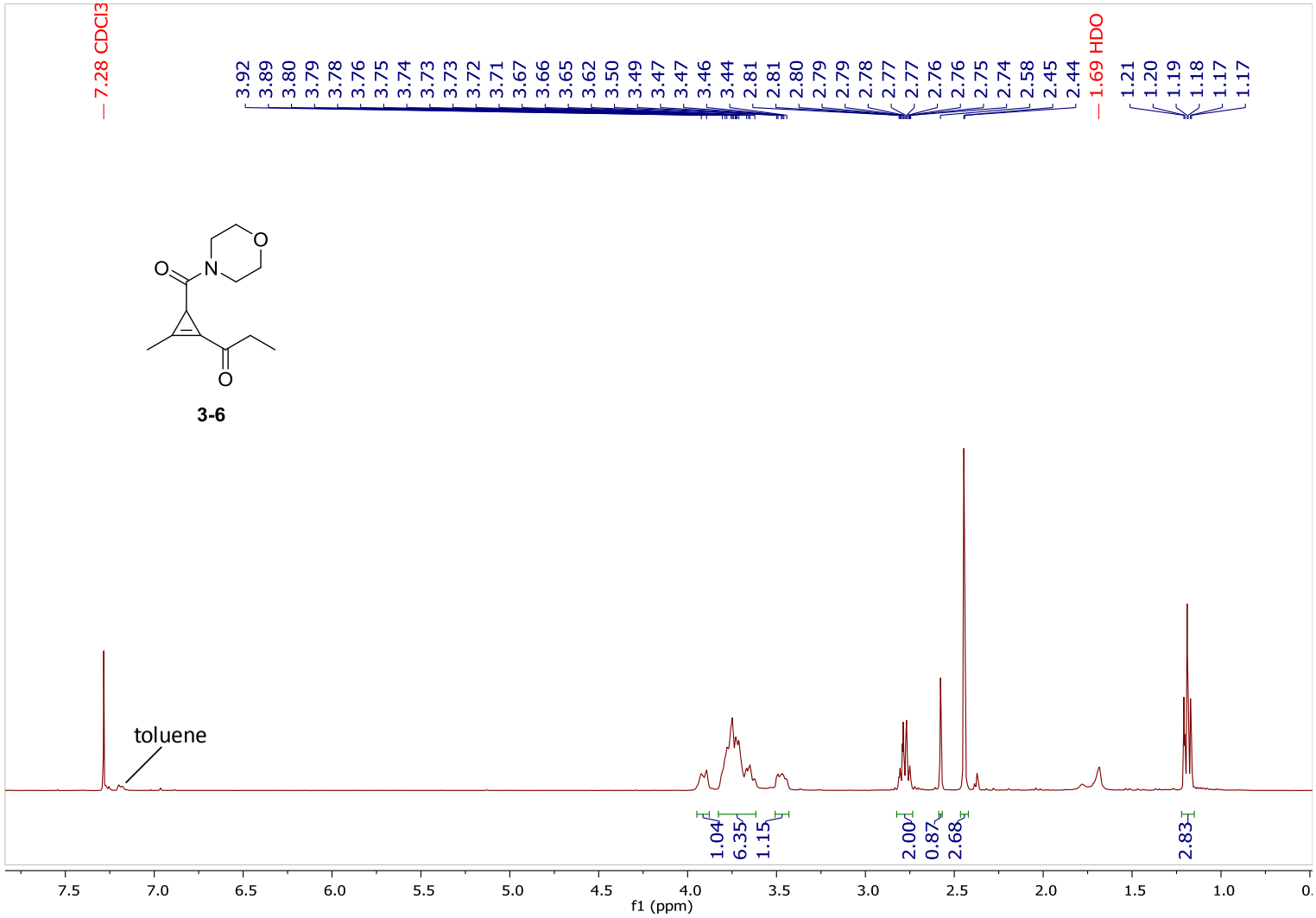

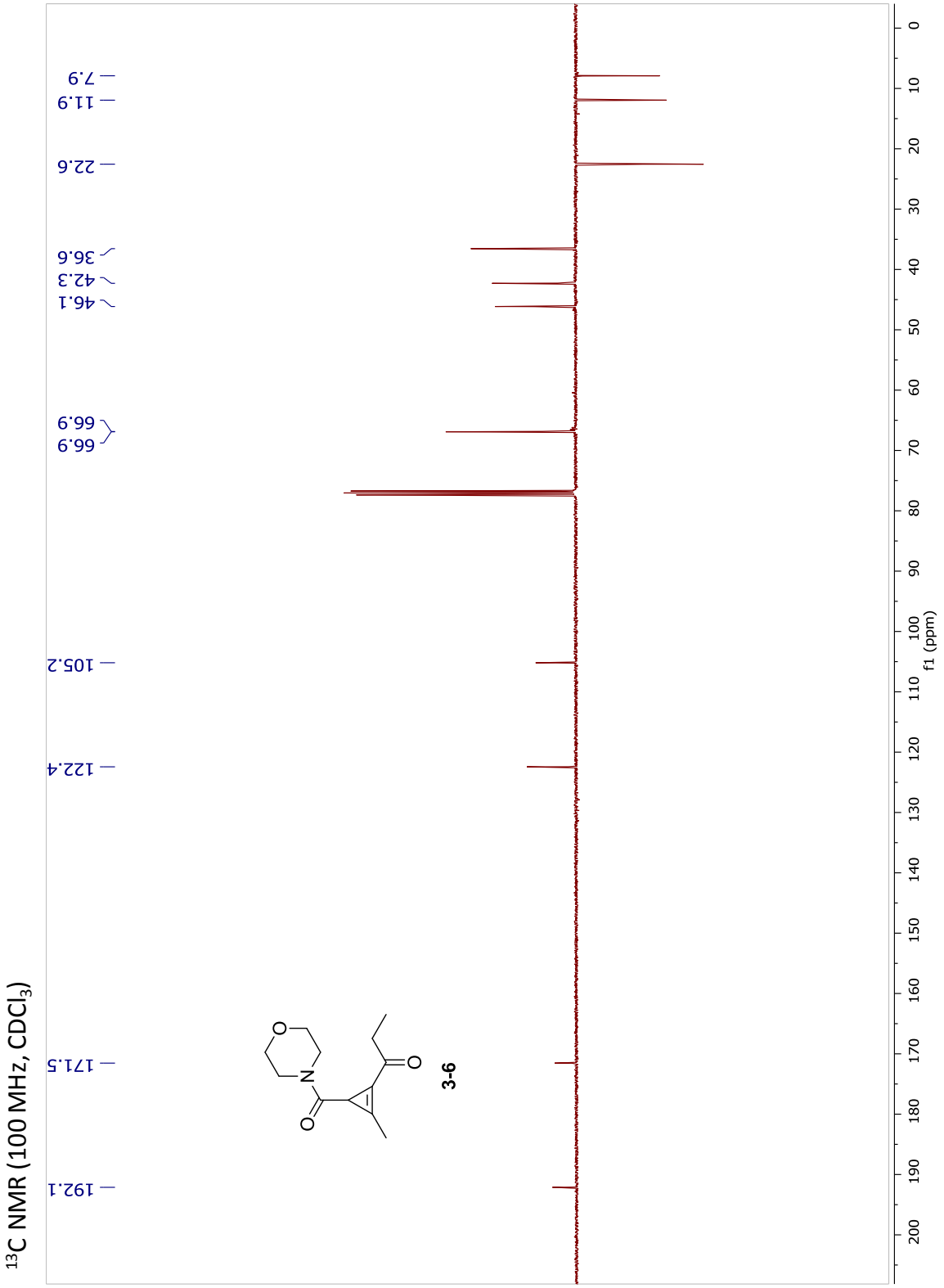
^{13}C NMR (100 MHz, $CDCl_3$)
192.1
171.5
122.4
105.2
66.9
66.9
46.1
42.3
36.6
22.6
11.9
7.9
3-6
f1 (ppm)

^{1}H NMR (400 MHz, $CDCl_3$)

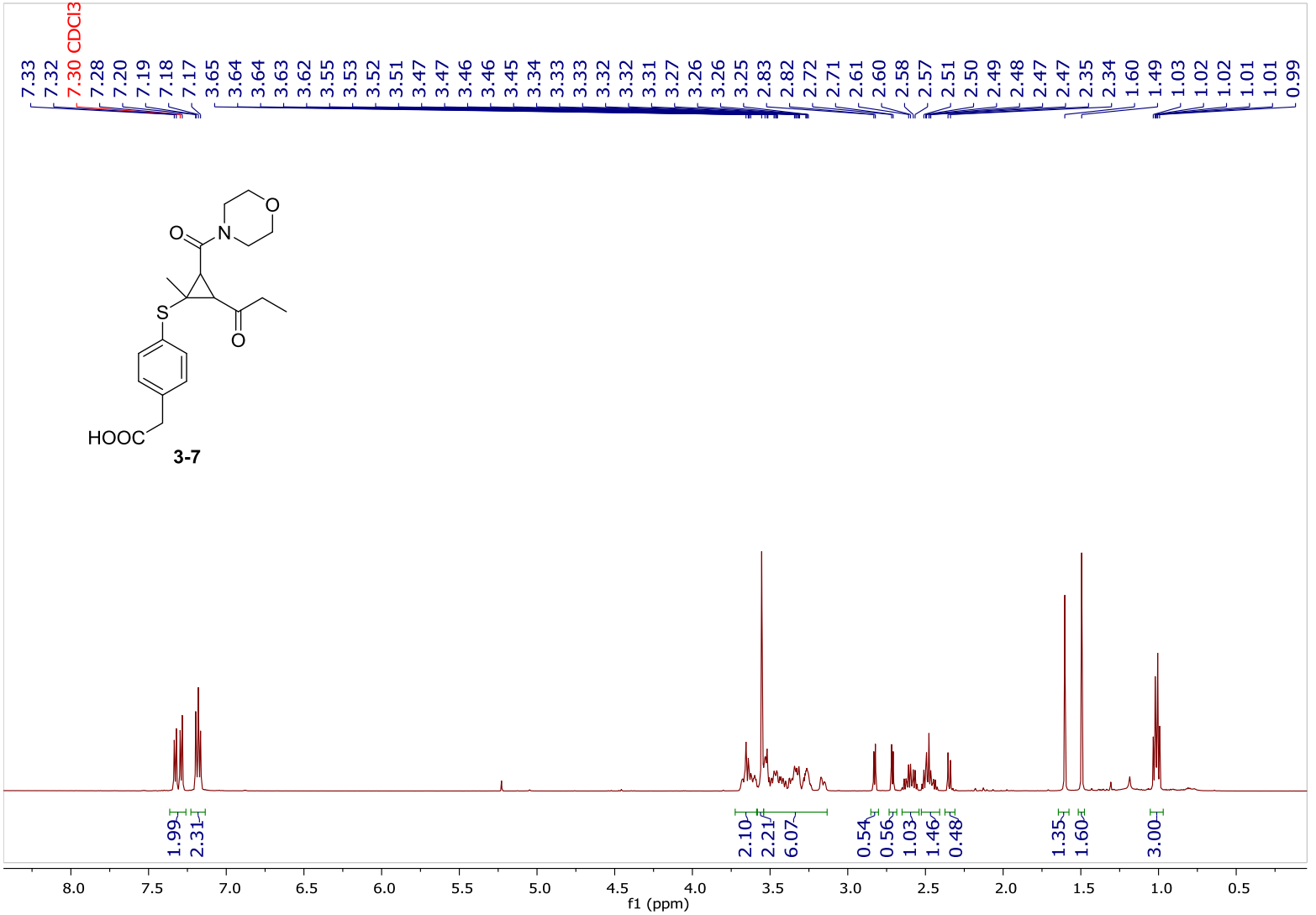

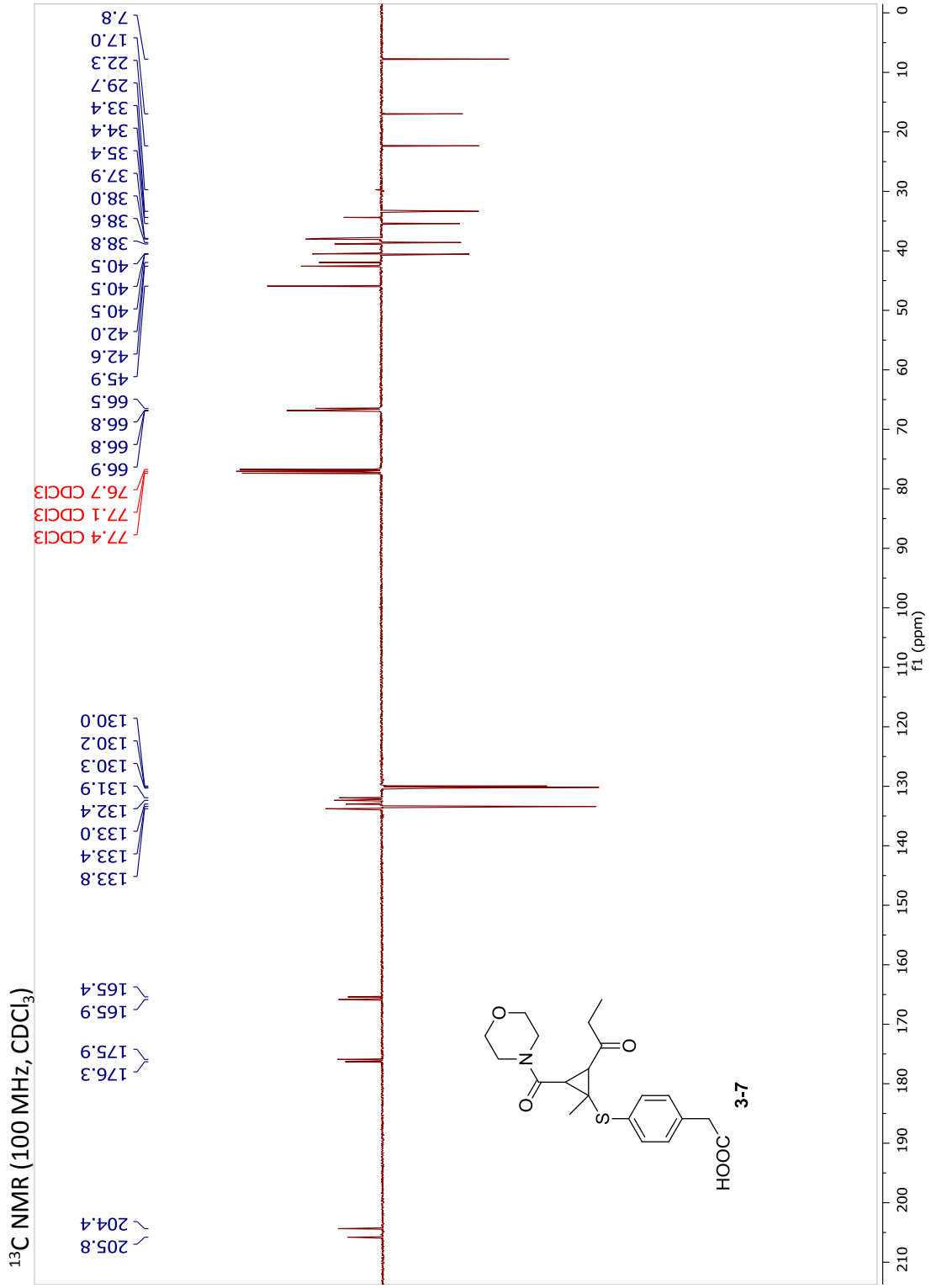
^{13}C NMR (100 MHz, CDCl$_3$)
205.8
204.4
176.3
175.9
165.9
165.4
133.8
133.4
133.0
132.4
131.9
130.3
130.2
130.0
77.4 CDCl3
77.1 CDCl3
76.7 CDCl3
66.9
66.8
66.8
66.5
45.9
42.6
42.0
40.5
40.5
40.5
38.8
38.6
38.0
37.9
35.4
34.4
33.4
29.7
22.3
17.0
7.8
f1 (ppm)
HOOC
3-7

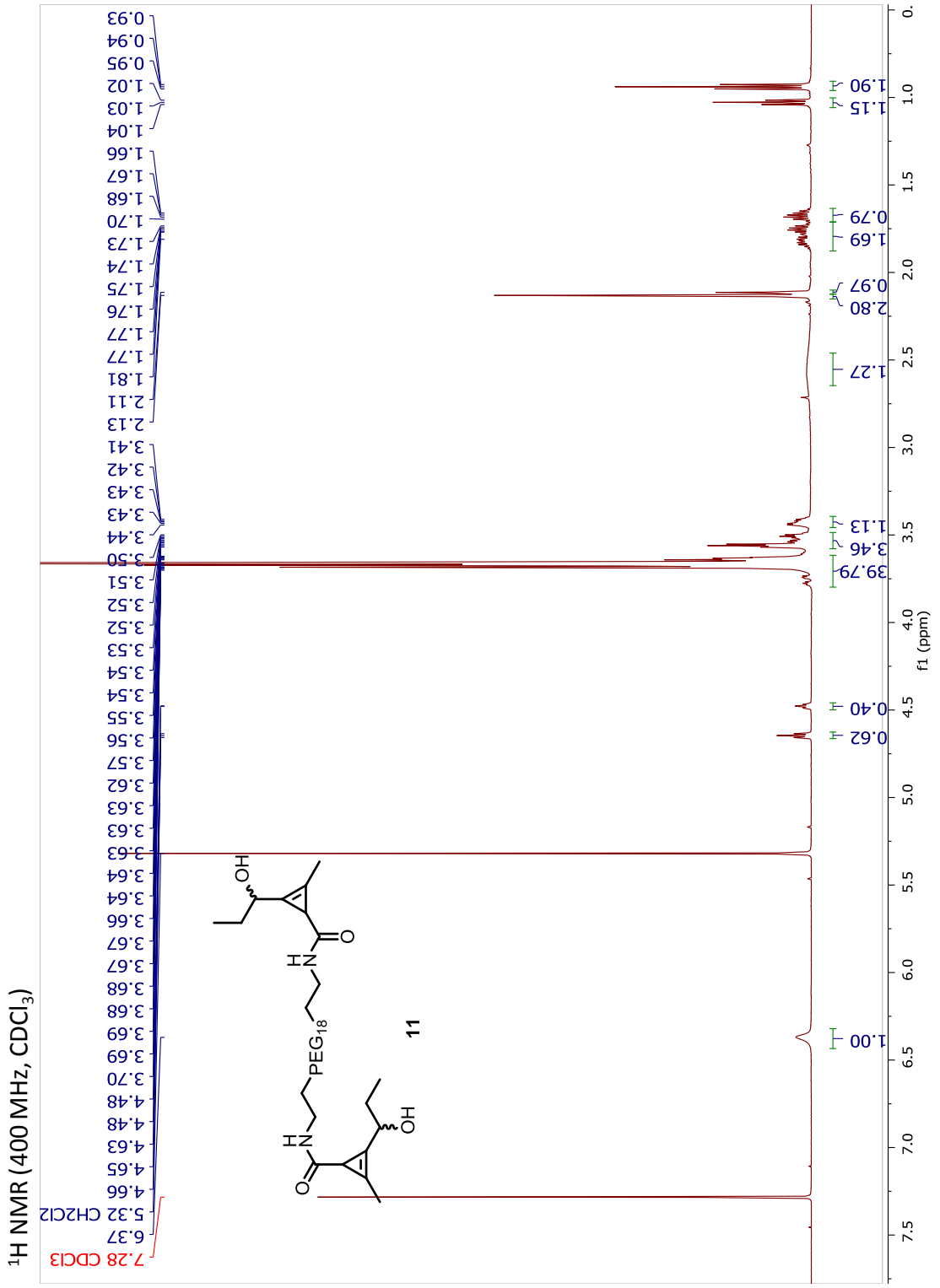
1H NMR (400 MHz, CDCl3)
7.28 CDCl3
5.32 CH2Cl2
PEG18
11
f1 (ppm)

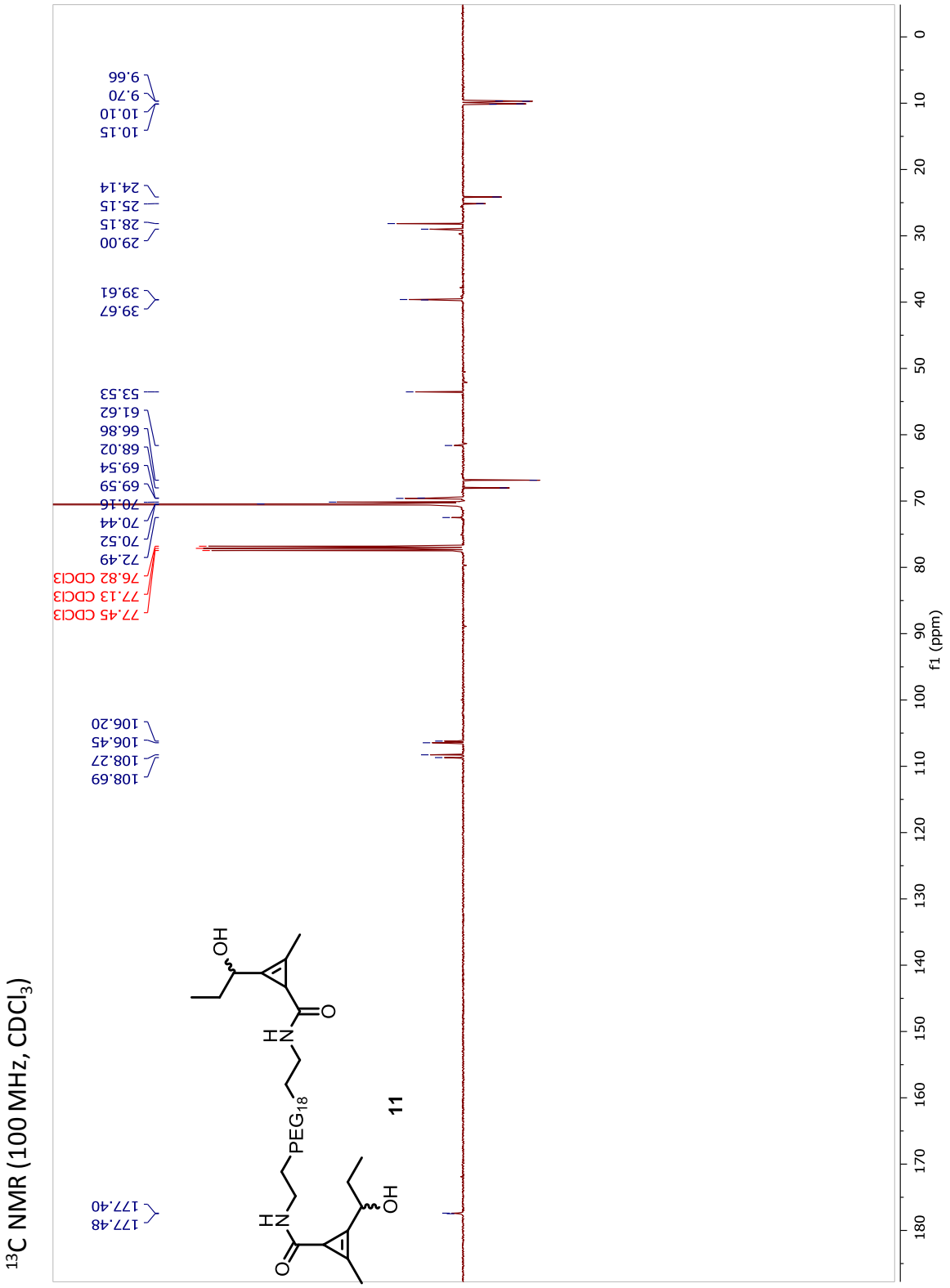
^{13}C NMR (100 MHz, $CDCl_3$)
177.48
177.40
108.69
108.27
106.45
106.20
77.45 CDCl3
77.13 CDCl3
76.82 CDCl3
72.49
70.52
70.44
70.16
69.59
69.54
68.02
66.86
61.62
53.53
39.67
39.61
29.00
28.15
25.15
24.14
10.15
10.10
9.70
9.66
PEG18
11
f1 (ppm)

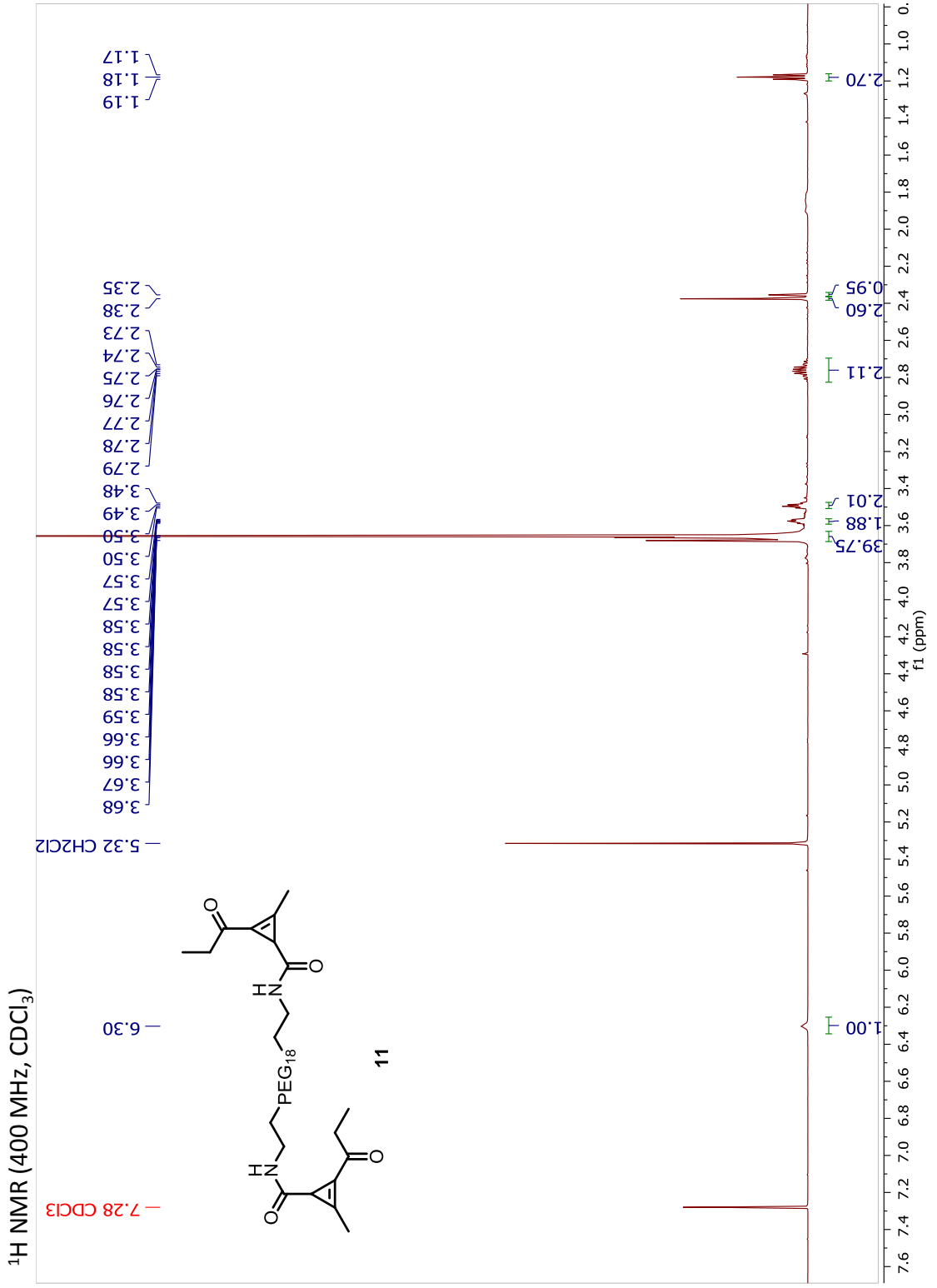
^{1}H NMR (400 MHz, CDCl$_3$)
7.28 CDCl3
6.30
5.32 CH2Cl2
3.68
3.67
3.66
3.66
3.59
3.58
3.58
3.58
3.58
3.57
3.57
3.50
3.50
3.49
3.48
2.79
2.78
2.77
2.76
2.75
2.74
2.73
2.38
2.35
1.19
1.18
1.17
PEG18
11
1.00
2.70
2.60
0.95
2.11
2.01
1.88
39.75
f1 (ppm)

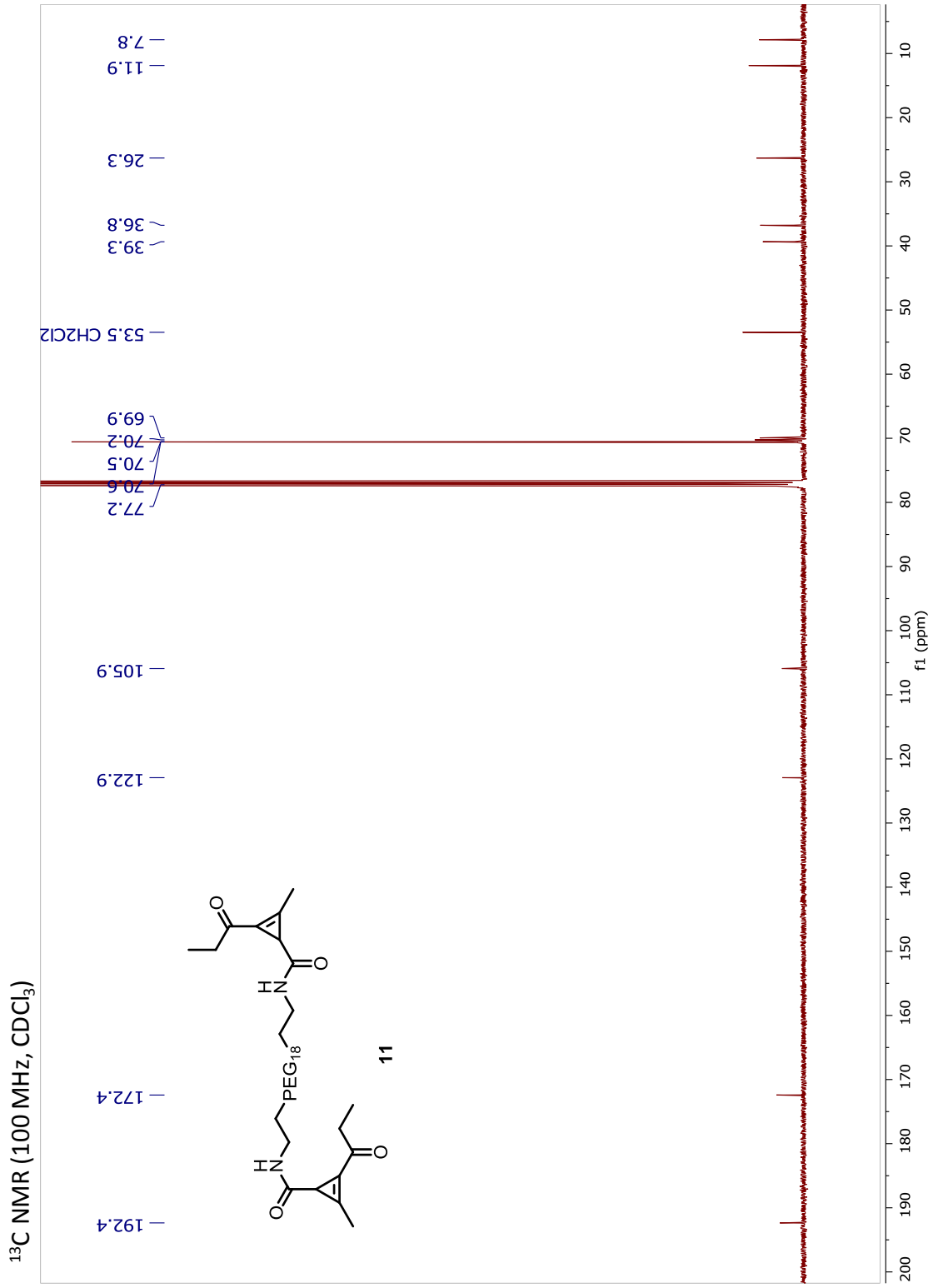
^{13}C NMR (100 MHz, $CDCl_3$)
192.4
172.4
122.9
105.9
77.2
70.6
70.5
70.2
69.9
53.5 CH_2Cl_2
39.3
36.8
26.3
11.9
7.8
PEG$_{18}$
11
f1 (ppm)

Appendix D

PERMISSION LETTERS